

Development, optimisation and application of  
*in vitro* and *in vivo* microdialysis methods  
contributing to characterise drug disposition processes

DISSERTATION

zur Erlangung des akademischen Grades

doctor rerum naturalium (Dr. rer. nat.)

vorgelegt der

Naturwissenschaftlichen Fakultät I  
Biowissenschaften

der Martin-Luther-Universität Halle-Wittenberg

von Frau Dipl. Pharm. Franziska Simmel  
geboren am 16.09.1981 in Magdeburg

Gutachter:

1. Prof. Dr. habil. Charlotte Kloft
2. Prof. Dr. habil. Dr. h. c. Reinhard Neubert
3. Prof. Dr. Markus Müller

Halle (Saale) im Juni 2010

verteidigt am 30.07.2010

Dipl. Pharm. Franziska Simmel

Development, optimisation and application of *in vitro* and *in vivo* microdialysis methods contributing to characterise drug disposition processes

Dissertation, 2010

Martin-Luther-Universität Halle-Wittenberg, Institute of Pharmacy,

Department of Pharmaceutical Chemistry and Clinical Pharmacy,

155 Pages, 56 Figures, 53 Tables

---

# TABLE OF CONTENTS

Table of Contents .....	III
List of Abbreviations and Symbols.....	VII
List of Tables .....	X
List of Figures .....	XII
<b>1 INTRODUCTION .....</b>	<b>1</b>
1.1 Optimisation of drug therapy.....	1
1.2 Microdialysis .....	3
1.2.1 Principle of microdialysis.....	4
1.2.2 Relative Recovery.....	5
1.2.3 Calibration of microdialysis catheters .....	5
1.2.4 Quantitative aspects of microdialysis sampling .....	7
1.2.5 Application of microdialysis.....	7
1.3 Invasive fungal infections.....	8
1.3.1 Trends in invasive fungal infections .....	8
1.3.2 Treatment of invasive fungal infections.....	9
1.4 Voriconazole .....	10
1.4.1 Pharmacodynamic properties and indication .....	10
1.4.2 Pharmacokinetic properties .....	12
1.4.3 Drug interactions and safety .....	13
1.5 Objectives .....	15
<b>2 MATERIALS, METHODS, PRE- AND CLINICAL STUDIES .....</b>	<b>17</b>
2.1 Chemicals, drug and pharmaceutical products.....	17
2.1.1 I – Bioanalytical methods for quantification of voriconazole .....	17
2.1.2 II – <i>In vitro</i> microdialysis of voriconazole .....	19
2.1.3 III – Influence of disease state on target site exposure.....	19
2.1.4 IV – Clinical long-term microdialysis pilot study with voriconazole in healthy volunteers .....	19
2.1.4.1 Clinical study.....	19
2.1.4.2 Genotype analysis .....	20
2.2 Laboratory and study equipment .....	21
2.2.1 I – Bioanalytical methods for quantification of voriconazole .....	21
2.2.2 II – <i>In vitro</i> and <i>in vivo</i> (III, IV) microdialysis of voriconazole .....	22
2.2.2.1 Microdialysis pumps and syringes .....	22
2.2.2.2 Microdialysis catheters and accessories.....	23
2.2.3 III – Influence of disease state on target site exposure.....	24
2.2.4 IV – Clinical long-term microdialysis pilot study with voriconazole in healthy volunteers .....	24
2.2.4.1 Clinical study.....	24
2.2.4.2 Genotype analysis .....	25

---

2.3	I – Bioanalytical methods for quantification of voriconazole.....	25
2.3.1	Quantification of voriconazole in microdialysate and plasma.....	26
2.3.1.1	Method development.....	26
2.3.1.2	Preparation of stock solutions, calibration samples and quality control samples.....	26
2.3.1.3	Voriconazole stability in microdialysate and plasma .....	27
2.3.1.4	Specificity of the analytical method .....	27
2.3.1.5	Accuracy and precision .....	28
2.3.1.6	Lower limit of quantification and assay linearity .....	28
2.3.1.7	Recovery of the analyte .....	28
2.3.1.8	Robustness and ruggedness .....	29
2.3.2	Determination of the unbound plasma concentration of voriconazole.....	29
2.3.3	Quantification of voriconazole in whole blood samples.....	30
2.3.4	Quantification of voriconazole in skin biopsy samples .....	30
2.4	II – <i>In vitro</i> microdialysis.....	31
2.4.1	Development of the <i>in vitro</i> microdialysis system (IVMS) .....	31
2.4.2	<i>In vitro</i> microdialysis investigations .....	34
2.4.2.1	Preparation of solutions used as perfusate or medium .....	34
2.4.2.2	Microdialysis settings .....	34
2.4.2.3	Dependencies of relative recovery .....	34
2.4.2.4	Steady state investigations .....	36
2.5	III – Influence of disease state on target site exposure.....	36
2.5.1	Study design and study procedure.....	36
2.5.1.1	Microdialysis procedure: catheter calibration and sample collection.....	37
2.5.1.2	Skin biopsy and blood specimen sampling .....	38
2.5.2	Dataset and pharmacokinetic analysis.....	38
2.6	IV – Clinical long-term microdialysis pilot study with voriconazole in healthy volunteers.....	39
2.6.1	Study design .....	39
2.6.2	<i>In vivo</i> long-term microdialysis study setting .....	41
2.6.3	Study procedure according to the clinical study protocol .....	42
2.6.4	Laboratory investigations .....	45
2.6.5	Documentation .....	45
2.6.6	Calibration procedure of microdialysis catheters.....	45
2.6.7	Sample collection and HPLC analysis of the samples .....	46
2.6.8	Analysis of genotype of Cytochrome P450 isoenzymes 2C9 and 2C19 .....	46
2.6.8.1	Preparation of genomic DNA from blood samples .....	46
2.6.8.2	Polymerase chain reaction.....	47
2.6.8.3	Pyrosequencing® for single nucleotide polymorphism analysis .....	47
2.6.9	Building the dataset and handling of missing values .....	48
2.6.10	Data(set) checkout .....	48
2.6.11	Data analysis.....	48

---

2.7	Descriptive and explorative statistics .....	50
2.8	Software.....	52
<b>3</b>	<b>RESULTS.....</b>	<b>53</b>
3.1	I – Bioanalytical methods for quantification of voriconazole .....	53
3.1.1	Quantification of voriconazole in microdialysate and plasma .....	53
3.1.1.1	Developed analytical method and system settings .....	53
3.1.1.2	Analyte stability in microdialysate and plasma.....	53
3.1.1.3	Specificity of the analytical method.....	54
3.1.1.4	Accuracy and precision.....	56
3.1.1.5	Lower limit of quantification and assay linearity.....	57
3.1.1.6	Recovery of the analyte .....	58
3.1.1.7	Robustness and ruggedness analysis .....	58
3.1.2	Determination of the unbound plasma concentration of voriconazole .....	59
3.1.3	Quantification of voriconazole in whole blood samples .....	60
3.1.4	Quantification of voriconazole in skin biopsy samples.....	60
3.2	II – <i>In vitro</i> microdialysis .....	61
3.2.1	Microdialysis equipment and system .....	61
3.2.1.1	Microdialysis pumps and syringes .....	61
3.2.1.2	<i>In vitro</i> microdialysis system (IVMS).....	62
3.2.2	<i>In vitro</i> microdialysis investigations.....	62
3.2.2.1	Flow rate dependence .....	62
3.2.2.2	Concentration dependence and influence of the drug product on RR.....	65
3.2.2.3	Steady state investigations .....	68
3.3	III – Influence of disease state on target site exposure .....	69
3.3.1	Applicability of microdialysis to inflamed subcutaneous adipose tissue .....	69
3.3.2	Dataset and concentration-time profiles of voriconazole .....	69
3.3.3	Pharmacokinetic analysis of the matrices.....	71
3.4	IV – Clinical long-term microdialysis pilot study with voriconazole in healthy volunteers .....	72
3.4.1	Feasibility of long-term application of clinical microdialysis .....	72
3.4.2	Bioanalysis of the study samples.....	74
3.4.3	Genotype analysis .....	74
3.4.4	<i>In vivo</i> relative recovery .....	75
3.4.5	Dataset and dataset checkout .....	78
3.4.6	Demographic data and genetic characteristics .....	79
3.4.7	Dose characteristics.....	80
3.4.8	Safety assessment during the clinical trial.....	81
3.4.9	Range of concentrations and individual concentration-time profiles of voriconazole.....	82
3.4.10	Pharmacokinetic parameters .....	88

<b>4</b>	<b>DISCUSSION .....</b>	<b>96</b>
4.1	I – Bioanalytical methods for quantification of voriconazole.....	96
4.2	II – <i>In vitro</i> microdialysis.....	100
4.2.1	<i>In vitro</i> microdialysis system .....	101
4.2.2	<i>In vitro</i> microdialysis investigations .....	101
4.3	III – Influence of disease state on target site exposure.....	106
4.3.1	Applicability of microdialysis to healthy and inflamed subcutaneous adipose tissue .....	107
4.3.2	Pharmacokinetics of voriconazole at the target site.....	107
4.4	IV – Clinical long-term microdialysis pilot study with voriconazole in healthy volunteers.....	111
4.4.1	Feasibility of long-term application of clinical microdialysis.....	112
4.4.2	Dataset, dataset checkout, demographic data and genetic characteristics ...	117
4.4.3	Target site pharmacokinetics of voriconazole assessed by microdialysis.....	120
<b>5</b>	<b>SUMMARY.....</b>	<b>134</b>
<b>6</b>	<b>REFERENCES.....</b>	<b>137</b>
<b>7</b>	<b>APPENDIX.....</b>	<b>i</b>
7.1	Tables .....	i
7.2	Figures .....	xii

---

## LIST OF ABBREVIATIONS AND SYMBOLS

ACN	Acetonitrile
ADR	Adverse drug reaction
AE	Adverse event
ALAT	Alanine aminotransferase [U/L]
AP	Alkaline phosphatase [U/L]
APS	Adenosine-5'-phosphosulphate
ASAT	Aspartate aminotransferase [U/L]
ATP	Adenosine triphosphate
AU	Arbitrary units
AUC	Area under the concentration-time curve
BP	Blood pressure [mmHg]
CD	Cyclodextrins
CI	Confidence interval
C <sub>ISF</sub>	Concentration in interstitial space fluid [µg/mL] obtained: - via concentric peripheral catheters (C <sub>ISF,c</sub> ), - via linear peripheral catheters (C <sub>ISF,l</sub> ), - from healthy skin (C <sub>ISF,H</sub> ), - from infected skin (C <sub>ISF,IN</sub> )
C <sub>max</sub>	Maximum concentration(s) [µg/mL]
C <sub>min</sub>	Minimum concentration(s) [µg/mL]
C <sub>nom</sub>	Nominal concentration(s) [µg/mL]
CRF	Case report form
C <sub>RP</sub>	Concentration in the retroperfusate (RP) [µg/mL]
CSF	Cerebrospinal fluid
C <sub>UF</sub>	Concentration of the unbound drug fraction in plasma (ultrafiltered) [µg/mL]
CV	Coefficient of variation in %
CYP	Cytochrome P450
dNTP	Deoxyribonucleotide triphosphate
ECG	Electrocardiogram
ELF	Epithelial lining fluid
EM	Extensive metaboliser (metabolism)
EMA	European Medicines Agency
ESS	Extensive sampling schedule
FDA	Food and Drug Administration
<i>g</i>	Local acceleration due to gravity (1 <i>g</i> ~ 9.81 m/s <sup>2</sup> )
γ-GTP	Gamma-glutamyltranspeptidase [U/L]
HepB, HepC	Hepatitis B, Hepatitis C
HIV	Human immunodeficiency virus
HPLC	High performance liquid chromatography
HR	Heart rate [1/min]
HSCT	Haematopoietic stem cell transplantation
HT	Height [cm]
ICH	International Conference on Harmonisation
ICU	Intensive care unit

ID	Individual identification number/individual
IFI	Invasive fungal infection(s)
INR	International normalised ratio
ISF	Interstitial space fluid: - accessed via concentric peripheral catheters (ISF <sub>c</sub> ), - accessed via linear peripheral catheters (ISF <sub>l</sub> ), - of healthy skin (ISF <sub>H</sub> ), - of infected skin (ISF <sub>IN</sub> )
iv	Intravenous
IVMS	<i>In vitro</i> microdialysis system
$\lambda_z$	Terminal elimination rate constant [1/h]
LDH	Lactate dehydrogenase [U/L]
LLOQ	Lower limit of quantification [ $\mu$ g/mL]
Max	Maximum
MIC	Concentration of an antiinfective in a given culture medium at which 90% of bacterial growth is inhibited, minimal inhibitory concentration
Min	Minimum
MLU	Martin-Luther-Universität Halle-Wittenberg
NCA	Non-compartmental analysis
PA	Polyamide
PAES	Polyarylethersulphone
PCR	Polymerase chain reaction
PD	Pharmacodynamic(s)
PG	Pharmacogenetic(s)
PK	Pharmacokinetic(s)
PM	Poor metaboliser (metabolism)
po	Per os
PPi	Di/Pyrophosphate
PU	Polyurethane
QC	Quality control
R	Range
RATE	Amount divided by infusion duration [mg/h]
RE	Relative error in %
RP	Retroperfusate
RR	Relative recovery(ies) in % - of concentric peripheral catheters (RR <sub>c</sub> ), - of linear peripheral catheters (RR <sub>l</sub> ), - for healthy areas (RR <sub>H</sub> ), - for inflamed areas (RR <sub>IN</sub> )
RSS	Reduced sampling schedule
RWCP	Research ward of the Department of Clinical Pharmacology, Medical University of Vienna
SB	Skin biopsy
SBECD	Sulphobutyl ether $\beta$ -cyclodextrin sodium
SD	Standard deviation
SE	Standard error
SNP	Single nucleotide polymorphism
$t_{1/2}$	Terminal elimination half-life [h]



$\tau$	Dosing interval
TDM	Therapeutic drug monitoring
$t_{\max}$	Time of maximum concentration [h]
$t_R$	Retention time [min]
Tris	Tris(hydroxymethyl)aminomethane
$T_x$	Sampling interval (point), with x from 0 min – 180 min
UF	Ultrafiltrate
UM	Ultra-rapid metaboliser (metabolism)
UV	Ultra violet
VISI	Study visit
WBC	Concentration of leukocytes/White blood count [1/L]
WT	Body weight [kg]
$\tilde{X}$	Median
$\bar{X}$	Arithmetic mean
$\bar{X}_{\text{geom}}$	Geometric mean

# LIST OF TABLES

Tab. 2-1:	Technical data of the catheters used in this thesis.....	23
Tab. 2-2:	Experimental settings to investigate the dependency of relative recovery (RR) on flow rate (0.4, 0.8, 1.0, 1.5, 2.0, 2.5, 5.0, 7.5, 10.0 $\mu\text{L}/\text{min}$ ) and on voriconazole concentration (1.0, 2.5, 5.0, 10.0, 20.0, 50.0 $\mu\text{g}/\text{mL}$ ) for CMA60 <sup>®</sup> and CMA66 <sup>®</sup> catheters. w/o: without.....	35
Tab. 2-3:	Schematic dosing and sampling schedule for single and multiple dose investigations (a visit involves one drug administration and all subsequent observations).....	40
Tab. 2-4:	Sampling time points (blood, red) and time intervals (microdialysate, blue).....	41
Tab. 2-5:	Statistical parameters.....	50
Tab. 2-6:	Statistical tests.....	51
Tab. 3-1:	Within-day and between-day precision (expressed as coefficient of variation, CV, %) and accuracy (as mean percentage deviation, RE, %) of determined voriconazole concentrations [ $\mu\text{g}/\text{mL}$ ] in microdialysate quality controls (QC).....	56
Tab. 3-2:	Within-day and between-day precision (expressed as coefficient of variation, CV, %) and accuracy (as mean percentage deviation, RE, %) of determined voriconazole concentrations [ $\mu\text{g}/\text{mL}$ ] in plasma quality controls (QC).....	57
Tab. 3-3:	Regression parameters and statistics of the calibration functions in microdialysate expressed as $\bar{x} \pm \text{SD}$ and precision as coefficient of variation, CV, %, AU: arbitrary units.....	57
Tab. 3-4:	Precision (between-day variability, CV, %) and accuracy (RE, %) of the quantitative assessment of voriconazole in microdialysate QC samples during study sample measurement.....	58
Tab. 3-5:	Precision (expressed as coefficient of variation, CV, %) and accuracy (as mean percentage deviation, RE, %) of determined voriconazole concentrations [ $\mu\text{g}/\text{mL}$ ] in microdialysate quality control samples from ruggedness experiments using a different analytical system, column lot, and analyst (method transfer).....	59
Tab. 3-6:	Flow rate dependence (CMA60 <sup>®</sup> , recovery experiment): mean relative recovery (RR) versus flow rate (0.4 $\mu\text{L}/\text{min}$ – 10.0 $\mu\text{L}/\text{min}$ , n=6).....	63
Tab. 3-7:	Flow rate dependence (CMA66 <sup>®</sup> , recovery, delivery experiment): mean relative recovery (RR) versus flow rate (1.0 $\mu\text{L}/\text{min}$ – 2.5 $\mu\text{L}/\text{min}$ , n=9).....	63
Tab. 3-8:	Dependency of relative recovery (RR) on voriconazole concentration (1.0 $\mu\text{g}/\text{mL}$ – 50.0 $\mu\text{g}/\text{mL}$ ) during recovery and delivery experiment: mean RR $\pm$ SD (CV, %) (n=9).....	66
Tab. 3-9:	Relative recoveries of voriconazole in healthy (RR <sub>H</sub> , %) and infected (RR <sub>IN</sub> , %) skin by CMA70 <sup>®</sup> catheters during low-concentration (RR <sub>low</sub> , %) and high-concentration (RR <sub>high</sub> , %) RR determination.....	69
Tab. 3-10:	PK parameters: C <sub>SS,max</sub> [ $\mu\text{g}/\text{mL}$ ], t <sub>SS,max</sub> [min], and partial AUC <sub>SS,0-3h</sub> [ $\mu\text{g}\cdot\text{h}/\text{mL}(\text{g})$ ] in the different matrices (n=3).....	71
Tab. 3-11:	Geometric mean, standard deviation, coefficient of variation, median, and range of AUC ratios of the matrices ISF <sub>H</sub> , ISF <sub>IN</sub> , blood, blood <sub>unbound(u)</sub> , and SB.....	71
Tab. 3-12:	Genotype results of pilot study individuals (n=3).....	75
Tab. 3-13:	Variability of relative recovery (RR <sub>c</sub> and RR <sub>i</sub> ) for RR samples 1 and 2 within one visit and one individual (n=2; n=1 for visit 3 ID 102 for RR <sub>c</sub> and visit 5 ID 103 for RR <sub>i</sub> ).....	77
Tab. 3-14:	Relative recovery (RR <sub>c</sub> and RR <sub>i</sub> ) for all study visits per individual during the whole study duration.....	77
Tab. 3-15:	Relative recovery (RR <sub>c</sub> and RR <sub>i</sub> ) for all study individuals at study visit 1, 3, 5, and 7.....	78
Tab. 3-16:	Overall relative recovery (RR): Mean RR for CMA60 <sup>®</sup> , CMA66 <sup>®</sup> , and both catheters for all RR samples obtained during the study.....	78
Tab. 3-17:	Distribution of the observations for the matrices studied (available samples at the end of the study).....	78

Tab. 3-18:	Individual characteristics: demographics and genetic variations for isoenzymes CYP2C9 and CYP2C19 within the individuals 101 – 103. ....	80
Tab. 3-19:	Dosing characteristics. ....	80
Tab. 3-20:	Adverse events (AEs) with certain, probable, or possible relationship to treatment. ....	82
Tab. 3-21:	Concentration characteristics of voriconazole in UF and ISF <sub>c,l</sub> during the entire study time. ....	82
Tab. 3-22:	Geometric mean [1/h], geometric SD [1/h], and geometric CV, % of terminal slope $\lambda_z$ . ....	89
Tab. 3-23:	Geometric mean [h] of terminal half-life $t_{1/2}$ . ....	89
Tab. 3-24:	Median [h] and range [h] of $t_{max}$ . ....	90
Tab. 3-25:	Geometric mean, geometric SD, and geometric CV, % of determined $C_{max}$ [ $\mu\text{g/mL}$ ] and dose-normalised $C_{max}$ [ $\text{ng/mL}$ ]. ....	92
Tab. 3-26:	Geometric mean, geometric SD, and geometric CV, % of determined partial AUC [ $\mu\text{g}\cdot\text{h/mL}$ ] and dose-normalised partial AUC [ $\text{ng}\cdot\text{h/mL}$ ]. ....	92
Tab. 3-27:	AUC ratios ( $\text{AUC}_{\text{ISF}}/\text{AUC}_{\text{UF}}$ ). ....	93
Tab. 3-28:	Drug accumulation factors ( $\text{AUC}_{\text{multiple dose}}/\text{AUC}_{\text{single dose}}$ ) ( $\text{AUC}_{\text{multiple dose}}$ of visit 5 and visit 7, $\text{AUC}_{\text{single dose}}$ of visit 1). ....	94
Tab. 4-1:	Relative recovery (RR) results presented in this thesis. ....	116
Tab. 4-2:	Nucleotide changes, effects, and resulting enzyme activity for isoenzymes CYP2C9*2, CYP2C9*3, and CYP2C19*2 (determined during the pilot study (see 2.6.8)). ....	119
Tab. 7-1:	Inclusion criteria, exclusion criteria, and reasons for withdrawal for study volunteers. ....	i
Tab. 7-2:	Lifestyle restrictions. ....	ii
Tab. 7-3:	Study schedule. ....	iii
Tab. 7-4:	Data items in the dataset. ....	iv
Tab. 7-5:	Within-day and between-day precision (expressed as coefficient of variation, CV, %) and accuracy (as mean percentage deviation, RE, %) of determined voriconazole concentrations [ $\mu\text{g/mL}$ ] in microdialysate calibrators. ....	v
Tab. 7-6:	Within-day and between-day precision (expressed as coefficient of variation, CV, %) and accuracy (as mean percentage deviation, RE, %) of determined voriconazole concentrations [ $\mu\text{g/mL}$ ] in plasma calibrators. ....	v
Tab. 7-7:	Calculation of recovery (n=3) of the method for the quantification of voriconazole in skin biopsy (SB) samples. ....	vi
Tab. 7-8:	Relative recoveries of concentric catheters ( $\text{RR}_c$ ): mean, standard deviation, and coefficient of variation. ....	vii
Tab. 7-9:	Relative recoveries of linear catheters ( $\text{RR}_l$ ): mean, standard deviation, and coefficient of variation. ....	viii
Tab. 7-10:	Interindividual variability among the amount of voriconazole given within the 6 mg/kg WT iv (visit 1, 2), 4 mg/kg WT iv (visit 3, 4), and 200 mg oral (visit 5, 6, 7) administration period. ....	viii
Tab. 7-11:	Interindividual variability among the duration of infusion. ....	ix
Tab. 7-12:	Intraindividual variability among the duration of infusion. ....	ix
Tab. 7-13:	Analysis of additionally obtained plasma samples at $C_{min}$ . ....	x
Tab. 7-14:	Terminal slope $\lambda_z$ [1/h] (data points involved in the analysis of $\lambda_z$ ). ....	x
Tab. 7-15:	Maximum concentration $C_{max}$ [ $\mu\text{g/mL}$ ] and related time $t_{max}$ (time after dose) [h]. ....	xi
Tab. 7-16:	Dose-normalised $C_{max}$ [ $\text{ng/mL}$ ]. ....	xi
Tab. 7-17:	Determined partial AUC [ $\mu\text{g}\cdot\text{h/mL}$ ] and dose-normalised partial AUC [ $\text{ng}\cdot\text{h/mL}$ ]. Visit 1: $\text{AUC}_{0-12\text{h}}$ , visit 5: $\text{AUC}_{48-60\text{h}}$ , visit 7: $\text{AUC}_{72-84\text{h}}$ . ....	xi

# LIST OF FIGURES

Fig. 1-1:	Schematic illustration of the principle of microdialysis. The analyte of interest mandatorily below the molecular mass cut-off value of the catheter membranes diffuses either into (recovery) or out of (delivery) the perfusate. The resulting (recovery) and remaining (delivery) amount can be quantified in the dialysate. ....	4
Fig. 1-2:	Chemical structure of voriconazole and fluconazole. ....	10
Fig. 1-3:	Mode of action of azoles (voriconazole) (modified from [73]). ....	11
Fig. 1-4:	Biosynthesis of ergosterol (modified from [74]). ....	11
Fig. 1-5:	Major metabolites of voriconazole in humans (as percentage of dose) following multiple administration of [ <sup>14</sup> C] voriconazole via a) fluoropyrimidine N-oxidation, b) fluoropyrimidine hydroxylation, c) methyl hydroxylation, d) loss of the fluoropyrimidine, e) defluorination and conjugation with glucuronic acid (modified from [86]). FMO: Flavin-containing monooxygenases. ....	13
Fig. 2-1:	Exemplary illustrations of linear and concentric catheters. Left panel: linear design (CMA66 <sup>®</sup> ), right panel: concentric design (CMA60 <sup>®</sup> ). ....	23
Fig. 2-2:	Outlet tubing guide channels with connection for microvials of 500 µL (top) and 1500 µL (bottom). ....	24
Fig. 2-3:	<i>In vitro</i> microdialysis system (without cover lid (No. 34)) in loading position. ....	32
Fig. 2-4:	Mounting parts of concentric (left, unit 'concentric catheter', No. 8 in Fig. 2-3) and linear (right, unit 'linear catheter', No. 15 in Fig. 2-3) microdialysis catheters as components of the <i>in vitro</i> microdialysis system. ....	33
Fig. 2-5:	Final position of the <i>in vitro</i> microdialysis system for <i>in vitro</i> microdialysis experiments with cover lid (No. 34) of the lowered platform (No. 4) into the thermoblock (No. 9) including the liquid (medium) containers (No. 21) and microdialysis catheters (Nos. 20, 32). ....	33
Fig. 2-6:	Time bar with study procedures and sample collection of both healthy (ISF <sub>H</sub> ) and infected (ISF <sub>I</sub> ) subcutaneous adipose tissue ISF, skin flank biopsy (SB), and whole blood. Microdialysis catheter perfusion flow rate: 1 µL/min. Bold arrows: Start and stop of RR <sub>low</sub> and RR <sub>high</sub> sampling intervals. RR <sub>low</sub> /RR <sub>high</sub> : 1 <sup>st</sup> /2 <sup>nd</sup> retrodialysate sample with low (RP <sub>low</sub> )/high (RP <sub>high</sub> ) voriconazole concentration retroperfusate. T <sub>x</sub> : sampling interval (point), with x from 0 min – 180 min. <sup>1</sup> Relative time elapsed from last step. For explanation of a-o see 2.5.1.1 and 2.5.1.2. ....	37
Fig. 2-7:	<i>In vivo</i> microdialysis setting for long-term sampling during the clinical pilot study in healthy volunteers. ....	42
Fig. 3-1:	Peak separation of voriconazole and an unknown endogenous substance or substance mixture in microdialysate samples (CMA60 <sup>®</sup> ) originating from a healthy volunteer (ID 102) (see 2.6 and 3.4): Chromatograms showing the interference (left) and the separation (right) in visit 1 (blue line), visit 2 (red line), and in visit 7 (black line). AU: arbitrary units. ....	55
Fig. 3-2:	Calibration curve of voriconazole microdialysate calibrators from ruggedness experiments using a different analytical system, column lot, and analyst (method transfer). AU: arbitrary units. ....	58
Fig. 3-3:	Dependence of relative recovery (RR) on flow rate (µL/min) of perfusate (Ringer's solution) during recovery experiment. Open symbols: individual results (n=3) of two CMA60 <sup>®</sup> catheters, filled circles: overall mean. Line: voriconazole showed a flow rate (F) dependency according to the equation $RR=100 \cdot (1-e^{-5.09/F})$ . ....	63
Fig. 3-4:	Dependence of relative recovery (RR) on flow rate (µL/min) of perfusate (Ringer's/ voriconazole solution) during recovery and delivery experiment. Open symbols: individual results (n=3) of three CMA66 <sup>®</sup> catheters, filled circles: overall mean. Line: voriconazole showed a flow rate (F) dependency according to the equation $RR=100 \cdot (1-e^{-5.18/F})$ . ....	63

Fig. 3-5:	Dependence of relative recovery (RR) of voriconazole on flow rate (F, $\mu\text{L}/\text{min}$ ) of perfusate according to the equation $RR=100 \cdot (1-e^{-r \cdot A/F})$ (r: mass transfer coefficient, A: membrane surface area) in concentric (solid line) and linear (dotted line) catheters (left panel). RR observed during investigations of dependency of RR on F ( $\mu\text{L}/\text{min}$ ) versus RR predicted via estimation of mass transfer coefficient r (right panel, open circles: concentric catheters, filled circles: linear catheters). Solid line reflects the line of identity. ....	64
Fig. 3-6:	Dependence of relative recovery (RR) of voriconazole (black solid and dotted line), linezolid (red dashed line), and daptomycin (blue dash-dotted line) on flow rate (F, $\mu\text{L}/\text{min}$ ) of perfusate according to the equation $RR=100 \cdot (1-e^{-r \cdot A/F})$ (r: mass transfer coefficient, A: membrane surface area) in concentric (black solid line) and linear catheters (left panel) and individual values of RR of linezolid and daptomycin (inset). RR observed during investigations of dependency of RR on F ( $\mu\text{L}/\text{min}$ ) versus RR predicted via estimation of r (right panel, open circles: voriconazole in concentric catheters (for comparison), filled circles: voriconazole in linear catheters (for comparison), rhombuses: linezolid in linear catheters, triangles: daptomycin in linear catheters). Solid line reflects the line of identity. ....	65
Fig. 3-7:	Peak areas of delivery versus recovery experiment (CMA60 <sup>®</sup> , flow rate 1.5 $\mu\text{L}/\text{min}$ ). Line: regression equation slope 0.028, intercept: 0.0023 AU, coefficient of determination: 0.9528). AU: arbitrary units. ....	66
Fig. 3-8:	Dependence of relative recovery (RR) on concentration ( $\mu\text{g}/\text{mL}$ ) of voriconazole during recovery and delivery experiment (3 CMA60 <sup>®</sup> each, 1.5 $\mu\text{L}/\text{min}$ flowrate, n=54), line: linear regression (left panel). Dependence of RR on concentration ( $\mu\text{g}/\text{mL}$ ) of voriconazole during recovery and delivery experiment (3 CMA66 <sup>®</sup> each, 2.0 $\mu\text{L}/\text{min}$ flow rate, n=36), line: linear regression (right panel). ....	67
Fig. 3-9:	Relative recovery (RR) (+SD) of voriconazole during delivery experiment (CMA60 <sup>®</sup> ; flow rate: 1.0 $\mu\text{L}/\text{min}$ ; n=3) using different perfusates (drug substance and drug product (Vfend <sup>®</sup> )). ....	68
Fig. 3-10:	Investigation of relative recovery (RR) (CMA60 <sup>®</sup> , delivery experiment) with varying voriconazole concentrations (perfusate: 50, 100, 150, 200 $\mu\text{g}/\text{mL}$ ) during simulated steady state conditions (medium 10 $\mu\text{g}/\text{mL}$ voriconazole, n=36). Line: regression equation (100, 150, 200 $\mu\text{g}/\text{mL}$ , slope: 0.0167%·mL/ $\mu\text{g}$ ). ....	68
Fig. 3-11:	Median (Min, Max) concentration-time profile of SB (black dashed line, black circles, in $\mu\text{g}/\text{g}$ , left and right panel), whole blood (red dashed-dotted line, red squares, in $\mu\text{g}/\text{mL}$ , right panel), unbound blood (blood <sub>u</sub> ) concentrations (red dotted line, red horizontal bars (calculated concentrations, see 3.3.2), red vertical bars (measured concentrations), in $\mu\text{g}/\text{mL}$ , right panel), ISF <sub>H</sub> (blue line, blue open triangles, in $\mu\text{g}/\text{mL}$ , right panel) and ISF <sub>IN</sub> (blue bold line, blue filled triangles, in $\mu\text{g}/\text{mL}$ , right panel) samples. ....	70
Fig. 3-12:	Geometric mean AUC (+SD) [ $\mu\text{g} \cdot \text{h}/\text{mL}/(\text{g})$ ] of the different matrices – blood, blood <sub>u</sub> , SB, ISF <sub>H</sub> , ISF <sub>IN</sub> – in guinea pigs. ....	71
Fig. 3-13:	Relative recoveries of concentric (RR <sub>c</sub> , blue symbols and lines) and linear catheters (RR <sub>l</sub> , red symbols and lines). Squares: ID 101, diamonds: ID 102, triangles: ID 103. Line: Overall median for catheter type; dotted line: $\pm 15\%$ of the median. ....	75
Fig. 3-14:	Unbound plasma (UF (red colour)) and interstitial space fluid (ISF <sub>c</sub> (blue colour), ISF <sub>l</sub> (black colour)) concentration-time profile of voriconazole in ID 101 (squares), ID 102 (diamonds), ID 103 (triangles). Mean dose amounts: green bars for infusion; green dots for tablets. Baseline and next two ISF samples excluded (see Fig. 3-17). ....	83
Fig. 3-15:	UF concentration-time profiles of voriconazole in ID 101 (squares), ID 102 (diamonds), and ID 103 (triangles) (left panel). Geometric mean (+SD) concentrations (black filled circles) (right panel). Mean amount of doses: green lines for infusion; green dots for tablets. ....	84
Fig. 3-16:	Minimal UF concentration-time profile (left panel) and dose-normalised profile (right panel) in ID 101 (crosses), ID 102 (circles), and ID 103 (triangles). Median values for tandem samples for visit 2-6. Geometric mean: blue bars. Mean amount of doses: green lines for infusion; green dots for tablets. ....	85

Fig. 3-17:	Early individual microdialysate concentration-time data (first, second, and third ISF samples (red symbols)) in ID 101 (squares), ID 102 (diamonds), and ID 103 (triangles). Open symbols: concentric catheters, filled symbols: linear catheters. ....	85
Fig. 3-18:	Concentration-time profiles of voriconazole in ISF of ID 101 (squares), ID 102 (diamonds), and ID 103 (triangles). Left panel: $C_{ISF_c}$ (open symbols). Right panel: $C_{ISF_l}$ (filled symbols). Mean amount of doses: green lines for infusion; green dots for tablets. ....	86
Fig. 3-19:	Geometric mean $ISF_c$ (+SD, open circles) and $ISF_l$ (+SD, filled circles) concentrations (left panel, mean amount of doses: green lines for infusion; green dots for tablets) and dose-normalised geometric mean $ISF_c$ (+SD, open circles) and $ISF_l$ (+SD, filled circles) concentrations (right panel). ....	87
Fig. 3-20:	Minimal $ISF_c$ (open symbols) and $ISF_l$ (filled symbols) concentration-time data for ID 101 (squares), ID 102 (diamonds), and ID 103 (triangles) including geometric mean of $ISF_c$ (dashed line) and $ISF_l$ (solid line) concentrations (left panel). Mean amount of doses: green lines for infusion; green dots for tablets. Right panel: dose-normalised data and geometric mean. ....	87
Fig. 3-21:	Geometric mean concentration-time profile of voriconazole in all matrices (UF (red triangles), $ISF_l$ (black circles), $ISF_c$ (blue squares) (left panel, mean amount of doses: green lines for infusion; green dots for tablets)). Dose-normalised geometric mean concentration-time profile of voriconazole in all matrices (right panel). ....	87
Fig. 3-22:	Semi-logarithmic geometric mean concentration (dose-normalised)-time plots of voriconazole in UF (red colour), $ISF_c$ (blue colour), and $ISF_l$ (black colour). Visit 1 (open squares), visit 2 (filled squares), visit 3 (crosses) (left panel). Right panel: spaghetti plot. ....	88
Fig. 3-23:	$\lambda_z$ after single (visit 1) and multiple dosing (visits 5, 7) in ID 101 (squares), ID 102 (diamonds), and ID 103 (triangles). UF (red colour), $ISF_c$ (blue colour), $ISF_l$ (black colour). Geometric means (bars). ....	89
Fig. 3-24:	Half-life $t_{1/2}$ after single (visit 1) and multiple dosing (visits 5, 7) in ID 101 (squares), ID 102 (diamonds), and ID 103 (triangles). UF (red colour), $ISF_c$ (blue colour), $ISF_l$ (black colour). Geometric means (bars). ....	89
Fig. 3-25:	$T_{max}$ after single (visit 1) and multiple dosing (visits 5, 7) in ID 101 (squares), ID 102 (diamonds), and ID 103 (triangles). UF (red colour), $ISF_c$ (blue colour), $ISF_l$ (black colour). Geometric means (bars). ....	90
Fig. 3-26:	$C_{max}$ and AUC after single (visit 1) and multiple dosing (visits 5, 7) in ID 101 (squares), ID 102 (diamonds), ID 103 (triangles). UF (red colour), $ISF_c$ (blue colour), $ISF_l$ (black colour). Determined parameters: left panel, dose-normalised parameters: right panel. Geometric means (bars). ....	91
Fig. 3-27:	AUC ratios ( $AUC_{ISF}/AUC_{UF}$ ) after single (visit 1) and multiple dosing (visits 5, 7) in ID 101 (squares), ID 102 (diamonds), and ID 103 (triangles). $ISF_c$ (blue, open symbols), $ISF_l$ (black, filled symbols). Geometric means ( $ISF_c$ : blue bars, $ISF_l$ : black bars, $ISF_c$ and $ISF_l$ : grey bars and line). ....	94
Fig. 3-28:	Drug accumulation factors ( $AUC_{multiple\ dose}/AUC_{single\ dose}$ ) ( $AUC_{multiple\ dose}$ of visit 5 and visit 7, $AUC_{single\ dose}$ of visit 1). ID 101 (squares), ID 102 (diamonds), ID 103 (triangles). UF (red colour), $ISF_c$ (blue colour), $ISF_l$ (black colour). Geometric means (bars). ....	94
Fig. 3-29:	AUC and AUC ratios in different genotypes. Single dose: visit 1 (open squares, blue colour); Multiple dose: visit 5 (filled squares, red colour) and visit 7 (crosses, red colour). Geometric means (bars). ....	95
Fig. 4-1:	Structure of sulphobutyl ether $\beta$ -cyclodextrin sodium (SBECD) ( $n=5$ , $R=(CH_2)_4SO_3Na$ or H, derivatives may have differing degrees of substitution on the 2, 3, and 6 positions). ....	106
Fig. 4-2:	Feasibility and PK approach of the clinical trial presented in this thesis. ....	112
Fig. 7-1:	Left panel: Chromatograms of microdialysate (left) and plasma (right): blank microdialysate and plasma (black lines), microdialysate (2.08 $\mu g/mL$ ) and plasma (2.04 $\mu g/mL$ ) calibrator (blue lines, retention time ( $t_R$ ) of voriconazole: 3.2 min), microdialysate and plasma calibrator with interfering co-eluting peak of ambroxol (red lines). Right panel: Peak sepa-	

	ration of voriconazole and ambroxol: Chromatograms of microdialysate (left) and plasma (right) calibrator ( $t_R$ of voriconazole: 8.7 min) and ambroxol ( $t_R$ : 7.3 min). AU: arbitrary units. ....	xii
Fig. 7-2:	Signal-time profile of the unknown endogenous substance or substance mixture in microdialysate (left panel) and retrodialysate (right panel) samples (CMA60 <sup>®</sup> , open symbols; CMA66 <sup>®</sup> , filled symbols) originating from healthy volunteers (ID 101, squares; ID 102, diamonds; ID 103, triangles) (see 2.6 and 3.4). AU: arbitrary units. ....	xii
Fig. 7-3:	Peak separation of voriconazole and an unknown endogenous substance or substance mixture in ultrafiltrate samples originating from a healthy volunteer (ID 102) (see 2.6 and 3.4): Chromatograms showing the interference (left) and the separation (right) in the baseline sample (blue line), visit 1 (red line), and in visit 7 (black line). AU: arbitrary units. ....	xiii
Fig. 7-4:	Calibration curve of voriconazole microdialysate calibrators (each n=6) from ruggedness experiments using different pH values of the mobile phase. Left panel: pH 5.4 (coefficient of determination: 0.997), right panel: pH 7.1 (coefficient of determination: 0.997). AU: arbitrary units. ....	xiii
Fig. 7-5:	Representative pyrogram <sup>®</sup> : Wild type for CYP2C19 (ID 101). X axis: chronologically dispensed nucleotides. Y axis: corresponding light signal. Highlighted area (yellow): polymorphic nucleotides. ....	xiii
Fig. 7-6:	Ratio of relative recoveries ( $RR_c$ and $RR_i$ ). Squares: ID 101, Diamonds: ID 102, Triangles: ID 103; Line: ratio=1. ....	xiv
Fig. 7-7:	Index plot of dependent variable DV (concentration). ....	xiv
Fig. 7-8:	Index plots for dosing related data items: amount (AMT), infusion rate (RATE), total dose within one individual (DOS1), and dose for each visit/occasion (DOS2). ....	xiv
Fig. 7-9:	Dose-normalised (left panel) and dose-, WT-normalised (right panel) concentration-time profile in UF in ID 101 (squares), ID 102 (diamonds), and ID 103 (triangles), geometric mean concentrations (filled circles). ....	xv
Fig. 7-10:	Minimal UF concentration-time profile showing tandem samples for visits 2-6 in ID 101 (crosses), in ID 102 (circles), and in ID 103 (triangles). Lines show the median of tandem samples per ID. ....	xv
Fig. 7-11:	Dose-normalised concentration-time profiles voriconazole in ISF of ID 101 (squares), ID 102 (diamonds), and ID 103 (triangles). Left panel: $C_{ISF,c}$ (open symbols). Right panel: $C_{ISF,i}$ (filled symbols). ....	xv
Fig. 7-12:	Concentration-time plots of voriconazole (left panels; semi-logarithmic (right panels)) after single and multiple intravenous and oral voriconazole administration for all matrices: UF (red colour), $ISF_c$ (blue colour), and $ISF_i$ (black colour). Visit 1 (open squares), visit 5 (filled squares), and visit 7 (crosses). ....	xvi
Fig. 7-13:	Concentration-time plots of voriconazole (left panels; semi-logarithmic (right panels)) after single and multiple intravenous and oral voriconazole administration for all individuals: ID 101 (red colour), ID 102 (blue colour), and ID 103 (black colour). Visit 1 (open squares), visit 5 (filled squares), and visit 7 (crosses). ....	xvii





---

# 1 INTRODUCTION

## 1.1 Optimisation of drug therapy

The search and development of new drug agents is an ongoing important process in many therapeutic areas. For instance, drugs targeted to specific genes involved in oncogenesis might lead to an improved outcome in the therapy of cancer patients [1]. New antiinfective agents broaden the armamentarium for the treatment of human pathogens not susceptible to currently available antibiotics [2] or antifungals [3]. But at least of the same importance is the rational use of currently available and emerging agents to exhaust and preserve their maximum therapeutic effectiveness.

In current drug therapy more than a few examples had demonstrated large interindividual variability in drug response and toxicity among patient populations: Once standard doses are administered a substantial proportion of patients do not respond, respond only partially, or experience adverse drug reactions (ADR). The major goal of individualised medicine is the optimisation of drug therapy involving the selection of the appropriate drug, dosing regimen, and drug combination, i.e., an optimal individual drug therapy should be tailored in order to minimise toxic side effects and to achieve the desired drug effect [4]. For several classes of drugs a direct pharmacodynamic (PD) marker has been established for the PD effect which enables adjustment of the dosing regimen immediately, e.g., anticoagulants (international normalised ratio, INR), antihypertensives (blood pressure), and insulin (blood glucose concentration). However, in many cases a convenient, routinely measurable PD marker is not available. In those cases the determination of pharmacokinetic (PK) parameters might guide the optimisation of therapy provided that the relationship between PK and PD has been established [4]. Most PK parameters are individually influenced. Exploring the factors contributing to the resulting PK variability (non-genetic factors, e.g., age, organ function, concomitant therapy, drug interactions, and the nature of disease; genetic factors) allow to reduce the PD variability and, hence, to maximise the therapeutic effect while minimising the occurrence of ADRs reflected by an improved outcome.

Adaptation of drug therapy is broadly practised in cancer chemotherapy by administering anticancer drugs primarily based on body size [1]. Despite this dose individualisation interindividual variability in cancer patient's outcome is still large and attributable to other sources of PK variability [5, 6]. Besides, the more rational approaches of drug dosing, e.g., based on renal function [7] and drug metabolising activity [8], recent advances in pharmacogenetics (PG) may lead to further optimisation of cancer therapy [1, 9].

PG aims to elucidate the inherited basis for interindividual differences in drug response by identifying differences in gene structure (polymorphism) that govern an individual's response to specific drugs via pharmacologic differences in drug metabolism, transport, or PD action [10]. Many of the genes encoding proteins responsible for the pharmacology of the drug

display genetic polymorphism. The latter may alter the functionality of the protein product and lead to remarkably phenotypic differences in response to medicines [11, 12]. Besides the non-genetic factors influencing the effect of medications genetics can account for up to 95% of variability in drug disposition and effects [13].

Several examples demonstrating the importance of PG are documented in the literature [11, 12, 14]: The influence of inherited differences in individual drug metabolising enzymes on the PK and, hence, PD of drugs is determined by the importance of these polymorphic enzymes for the activation or inactivation of drug substrates. The effect can be profound toxicity for agents with a narrow therapeutic index which are inactivated by a polymorphic enzyme (e.g., mercaptopurine, azathioprine) [15]. Thiopurine S-methyltransferase (TPMT) is a polymorphic phase II enzyme that catalyses the S-methylation of thiopurine medications in haematopoietic tissues [15]. In case of TPMT polymorphism, patients with two non-functional TPMT alleles will develop severe and life-threatening, dose-limiting haematopoietic toxicity at conventional dosages. Moreover, the potential seriousness of polymorphisms is further exemplified by irinotecan-induced gastrointestinal toxicity in patients with low activity of the phase II enzyme UGT1A1 (uridine diphosphate glucuronosyltransferase) responsible for glucuronidation of SN-38, the active metabolite of irinotecan [16, 17]. Additionally, several phase I enzymes exhibit functional genetic polymorphism leading to a deficiency of the enzyme activity associated with increased effects for medicines that are primarily inactivated by these enzymes, such as dihydropyrimidine dehydrogenase catalysing the reduction of 5-fluorouracil to inactive dihydrofluorouracil [9], cytochrome P450 (CYP)2D6 metabolising several tricyclic antidepressants [18] and antipsychotics [18], and CYP2C9 metabolising warfarin apart from VKORC 1 (Vitamin K Epoxide Reductase Complex) [19, 20]. Clinical studies have shown that patients with one or more variant CYP2C9 alleles (CYP2C9\*2 or CYP2C9\*3) require a significantly lower warfarin dose to maintain the target level of anticoagulation reflected by the INR. In fact, an optimisation of drug therapy is advisable for all drugs exhibiting any toxicity or merely subtherapeutic effects following standard dosing. The latter can be prevented by reaching therapeutically active drug concentrations at the site of action [21].

The measurement of concentrations in order to investigate the PK can be subjected to several misconceptions [22, 23]. Usually, the determinations of PK parameters are based on drug concentrations in plasma and urine albeit most drugs exert their effect in compartments (site of action) different from those considered for the determination of concentrations [22]. The distribution of the drug into the target tissue may result in substantial different concentrations compared to plasma concentrations [24]. Hence, conclusions drawn for plasma PK may be misleading while transferring them to target site PK [24]. In addition, mostly total drug concentrations are measured without differentiating between the unbound and bound drug fraction although it has been shown that only the unbound drug fraction exerts therapeutic activity [25-27] and has the ability to be distributed to the target site [22]. For infections, the majority is localised extracellularly, i.e., in the interstitial space fluid (ISF) [28]. Among the anti-infectives the concept of the unbound fraction at the site of action has been best

described for antibacterial agents but may be assumed for antifungal agents, too [22]. For the assessment whether sufficient anti-infective drug is available in the ISF a direct measurement of the unbound drug concentration is preferred and encouraged by regulatory agencies, such as the Food and Drug Administration (FDA) and the European Medicines Agency (EMA) [29, 30]. In addition, the establishment of the relationship of the unbound drug concentration and the *in vitro* susceptibility of the infecting organism is required if the dossier of a new anti-infective is submitted to regulatory authorities in the US.

Several experimental methods and techniques have been developed to gain access to the relevant spaces for drug action: i) Tissue drug concentrations have been measured from total biopsy specimens after sample homogenisation. These total concentrations may be misleading since a differentiation between plasma, intra- and extracellular components is impossible [22]. A possible overestimation of an anti-infective drug in a biopsy specimen disguising target site concentrations (ISF) below the minimal inhibitory concentration (MIC) might have a severe impact on the outcome of therapy [24] and the development of drug resistance [31]. ii) Cantharis- or suction-induced skin blisters enable the sampling of drug-containing blister fluid [32, 33]. The resulting concentrations are prone to artefacts due to differences in blister size, surface area-to-volume ratio, diffusion capacity across the blister basis [34], and to the inflammation as a result of the induction of the blisters [35]. Additionally, blister fluid provides no direct information on the unbound drug fraction attributable to considerable amounts of protein in the inflammatory exudate [33, 36]. Similar to biopsy sampling skin blister sampling is limited to one-point measurements. iii) Measurements in various surrogates, such as wound exudates or surface fluids, do not reflect the concentration at the target site and, hence, yield only limited information. More novel methods implement iv) imaging techniques within the study of drug distribution, e.g., positron emission tomography (PET) [37, 38]. Besides the enormous technical and financial expenditure, limitations include availability for only a small number of compounds, non-specific information regarding tissue compartments or signals not necessarily belonging to a measure of the intact drug [22]. Another technique capable of measuring drug distribution is v) microdialysis, a catheter-based sampling procedure applicable to a large variety of chemical entities and various tissues in many different clinical settings. The FDA and the EMA/Committee for Proprietary Medicinal Products (CPMP) acknowledged microdialysis as an attractive approach for the determination of the distribution of anti-infectives into the tissue [39-41].

## 1.2 Microdialysis

The microdialysis technique was originally developed in neuropharmacological sciences facilitating the measurement of neurotransmitters in rat brain in the 1980s [42]. Today, microdialysis is a relatively novel approach for the determination of unbound *in vivo* drug concentrations in virtually all tissues. The main advantage of this minimally invasive, catheter-based

sampling technique is that it reduces the burden on the study individual or patient, respectively, to a minimum since no tissue extraction is required also rendering the method easy to handle for the investigator. In addition, microdialysis allows continuous monitoring of target tissue drug concentrations over a defined time interval via a sampling series.

### 1.2.1 Principle of microdialysis

Microdialysis is based on sampling of analytes from the ISF by means of a semipermeable membrane. Typically, concentric microdialysis catheter (probe), consisting of a thin dialysis tubing and a membrane at the tip of the catheter, are employed (see Fig. 1-1). The more recently developed linear catheters have a simplified design as these catheters do not combine inlet and outlet tubing in one shaft as the concentric do (Fig. 1-1).

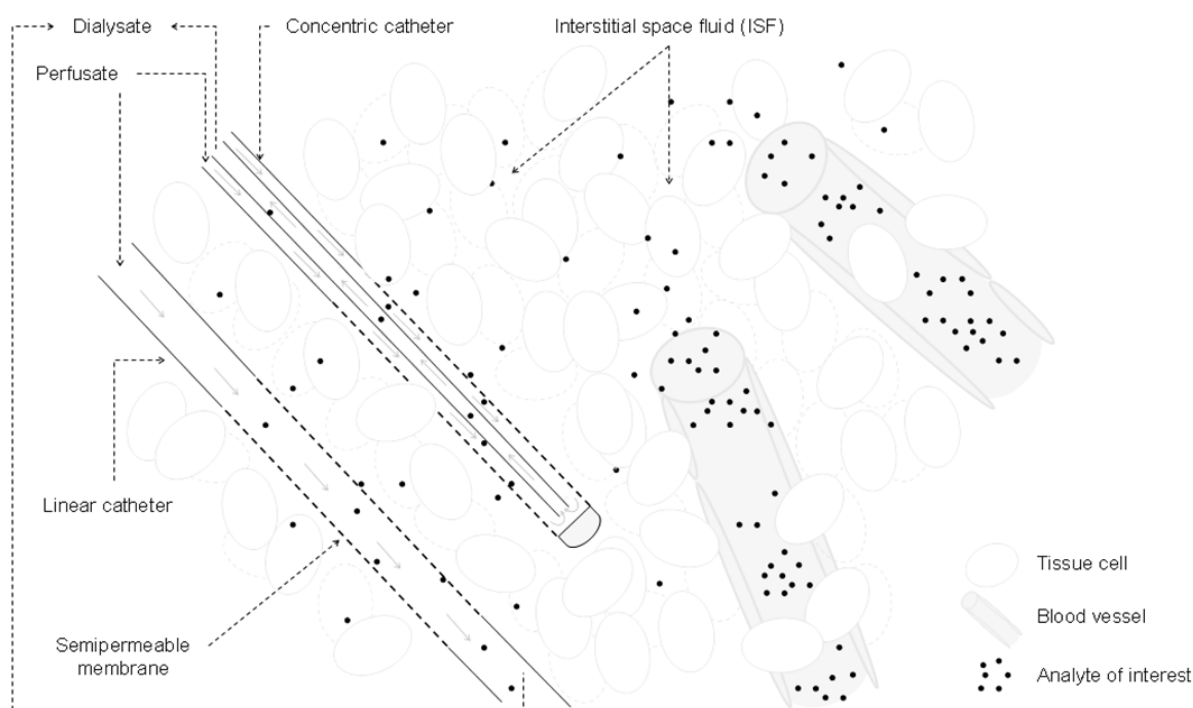


**Fig. 1-1:** Schematic illustration of the principle of microdialysis. The analyte of interest mandatorily below the molecular mass cut-off value of the catheter membranes diffuses either into (recovery) or out of (delivery) the perfusate. The resulting (recovery) and remaining (delivery) amount can be quantified in the dialysate.

Every microdialysis membrane has its own specific molecular mass cut-off reflected by its pore size usually ranging from 6 kDa to 100 kDa. Large molecules, e.g., proteins, are hampered in their passage over the, mostly inserted, 20 kDa membrane. Once the catheter is implanted into the tissue it is constantly perfused with a physiological solution (perfusate) at a constant flow rate (generally 0.5  $\mu\text{L}/\text{min}$  – 5  $\mu\text{L}/\text{min}$ ) using a high precision perfusion pump. Molecules up to a certain molecular mass present in the ISF in unknown concentration ( $C_{\text{ISF}}$ ) will move from the ISF into the catheter by diffusion (recovery), resulting in a certain concentration ( $C_{\text{dialysate}}$ ) in the perfusion medium (Fig. 1-1). Samples will be collected in microvials as

dialysate to be analysed. Besides analyte sampling, microdialysis can be used for delivering substances into the ISF (Fig. 1-1, delivery) since the diffusion process is directed by the concentration gradient [43]. Amongst others, this phenomenon is utilised for calibration purposes. Employing the microdialysis sampling technique involves the awareness and management of several challenges (see sections 1.2.2 to 1.2.4).

### 1.2.2 Relative Recovery

During microdialysis, a perfusate is delivered through the catheter, typically at a constant flow rate. Exchange of solutes occurs along the semipermeable membrane of the catheter, resulting in a dialysate solute concentration that is only a fraction of the actual ISF concentration. This fraction is called the relative recovery (RR). Hence, the measured concentrations in the dialysate do not reflect the true concentration in the ISF due to an incomplete equilibrium between the ISF and the catheter perfusing medium. For investigations examining changes in endogenous compound concentrations from their baseline values, it is usually not necessary to determine the RR provided that RR remains constant throughout the experiment. PK studies aim at providing information on absolute concentration-time profiles of drugs/metabolites in the ISF. For the quantification of the true ISF concentration of the analyte knowledge of RR becomes essential. Many factors affect RR including i) microdialysis (perfusion) flow rate, ii) temperature, iii) catheter membrane area and molecular mass cut-off, iv) tortuosity of the dialysed tissue, v) physicochemical properties of the analyte and composition of perfusate, vi) any other factors that alter the diffusion characteristics [23, 43, 44]. However, drug transfer across the semipermeable membrane is incomplete requiring catheter calibration *in vivo* for valid quantification of drug concentrations.

### 1.2.3 Calibration of microdialysis catheters

A number of different methods has been developed and used to calibrate the microdialysis catheters by estimating the RR *in vivo* including: i) the method of flow rate variation, ii) the method of no-net-flux, iii) the method of dynamic no-net-flux, iv) the usage of endogenous reference substances as well as v) internal standards (calibrators), and vi) the retrodialysis method [23, 43].

The drug of interest localised in the ISF is the initial situation for all procedures. The method of flow rate variation is accomplished by varying the perfusate flow rate, plotting it against the measured concentrations and extrapolating to zero flow yielding an estimate of the concentration at zero flow, i.e., the RR [45]. Long-sampling times for small flow rates and the necessity of extrapolation are the potential disadvantages of the method. The no-net-flux method schedules the addition of the compound to the perfusate in different concentrations and identifies the point of no net diffusion across the membrane by plotting the dialysate concentrations in relation to the perfusate against the different perfusate concentrations [46]. Due to the need of calibration with different concentrations and the necessity of steady state conditions the method is very time-consuming. The dynamic no-net-flux method accounts for

this disadvantage by the possibility to simultaneously perfuse several individuals with a single concentration and pool the data in order to estimate RR [47]. Investigators employing this method have to face larger variability and the requirement of more study individuals for calibration procedure due to the parallel design. These methods are typically performed prior to the actual microdialysis study. One approach using an endogenous substance as a reference, e.g., urea [48], offers a less time-consuming method for the determination of RR and does not require steady state conditions. However, further investigations have to be conducted before implementing that method in a clinical setting [43]. As indicated, the before mentioned types of calibration, except of the usage of an endogenous substance, are often not practical for most clinical PK studies.

In contrast, the method of retrodialysis is a less time-consuming technique proposed by STAHL et al. [49]. The setting is illustrated in Fig. 1-1. In the process, the catheter considered for calibration is perfused with a (retro)perfusate (RP), a solution spiked with the analyte of known concentration ( $C_{\text{perfusate}}$ ). The principle behind the retrodialysis method is based on the assumption that the diffusion process is quantitatively equal in both directions through the semipermeable membrane. Thus, prior to the initiation of *in vivo* studies it is important to investigate the behaviour of the substance of interest in an *in vitro* setting. During retrodialysis the diffusion (loss) of the drug from the perfusate ( $C_{\text{perfusate}}$ ) into the surrounding tissue/medium is taken as the (*in vivo*) RR which can be calculated using Eq. 1-1.

**Eq. 1-1:** Calculation of relative recovery (RR).

$$\text{RR, \%} = 100 \cdot \left( 1 - \frac{C_{\text{dialysate}}}{C_{\text{perfusate}}} \right)$$

$C_{\text{dialysate}}$  : Concentration in dialysate [ $\mu\text{g/mL}$ ]

$C_{\text{perfusate}}$  : Concentration in perfusate [ $\mu\text{g/mL}$ ]

Using RR, absolute (interstitial) concentrations can be determined by dividing  $C_{\text{dialysate}}$  by the RR value (Eq. 1-2).

**Eq. 1-2:** Calculation of  $C_{\text{ISF}}$ .

$$C_{\text{ISF,unbound}} [\mu\text{g/mL}] = 100 \cdot \frac{C_{\text{dialysate}}}{\text{RR, \%}}$$

In order to assess RR and, thus, for calculating valid absolute ISF concentrations reliable *in vivo* calibration of the microdialysis catheter has to be performed in each single microdialysis experiment. Due to the impact of tortuosity and limited volume fraction of the ISF the diffusibility of a substance in the living tissue fluid is hampered. The usage of *in vitro* RR values would definitely overestimate the *in vivo* RR value and, thus, underestimate the true ISF concentrations. Moreover, it should be taken into account that the diffusion process forced by

retrodialysis will resemble the later study situation only if the ISF does not already contain the analyte. Hence, ideally the calibration process should take place prior to the first drug administration. PK studies often aim at analysing the exposure of a drug at steady state. The management of that interest requires a concentration of the drug in the perfusate equal to or higher than tenfold of that in the ISF. Although an exact determination of RR is limited under these circumstances therewith a close approximation of true RR can be attained [43]. Intra-individual variability for the measurement of ISF concentration has been reported to range between 10% to 20% [44]. The perfusion with the analyte of interest could be circumvented by estimating its RR using a calibrator in a retrodialysis setting [50]. On condition that the calibrator is chemically and biologically similar to the analyte resulting in equal loss and recovery characteristics its loss could mirror the gain of the analyte. However, investigations have shown that even if *in vitro* RR of both the analyte and the calibrator are equal *in vivo* RR may differ [51]. In those cases, calibrators may serve as a quality control of the catheter functionality.

#### **1.2.4 Quantitative aspects of microdialysis sampling**

Dialysate samples derived from microdialysis can be characterised by a small sample volume or very low concentrations of the analyte of interest both depending on the flow rate. Limitations for microdialysis sampling experiments are often determined by the lower limit of quantification (LLOQ) of the analytical method or the feasibility of analysing small sample volumes. These limitations could be circumvented by employing long sampling intervals, low flow rates, or by pooling dialysates from several samples but would lead to a lower time resolution in return. The combination of microdialysis with analytical methods with low LLOQ values such as high performance liquid chromatography (HPLC), microbore/capillary LC methods, mass spectrometry and biosensors can overcome the analytical challenge [43, 44]. Due to the low-molecular mass cut-off of up to 20 kDa of typically employed microdialysis catheter membranes samples will be nearly free of protein not requiring labour-intensive sample cleanup and not subjected to enzymatic degradation of analytes collected.

#### **1.2.5 Application of microdialysis**

The most important fields where microdialysis technique has been applied besides the determination of neurotransmitter concentrations in brain are the monitoring of metabolism in several tissue fluids and measurement of anti-infective, predominantly antibiotic, drug concentrations in target tissues, respectively [24, 52]. Indeed, successful treatment of severe invasive fungal infections (IFI) with an antifungal agent relies on achieving adequate concentrations at the site of fungal infection as well.

## 1.3 Invasive fungal infections

### 1.3.1 Trends in invasive fungal infections

Since the early 1980s, fungal pathogens have emerged as major source of human disease, particularly among the immunocompromised such as haematological, solid organ transplant patients, and those ones hospitalised with serious underlying disease [53]. IFI in otherwise healthy patients are extremely rare, hence, all IFI can be regarded as opportunistic diseases. The annual number of cases of sepsis caused by fungal organisms increased by 207% between 1979 and 2000 in the USA [54]. Besides the gram-positive bacteria fungal organisms are increasingly common causes of sepsis. *Candida* species are the fourth leading cause of nosocomial bloodstream infection (BSI) in the USA, accounting for 8% to 10% of all BSIs acquired in the hospital [55]. In Germany, nearly 18% of severe sepsis are caused by mycoses on intensive care units (ICU) [56]. Nosocomial IFI are associated with high morbidity and mortality. Invasive aspergillosis-attributable mortality was approximately 50% in patients with leukemia and lymphoma and 87% in bone marrow transplant recipients [57]. Those attributed to candidiasis BSI amounts to approximately 40% [53]. Trends in mortality according to statistic data of the National Center for Health in the USA were published by MCNEIL et al. [58]: An increase in mortality due to mycoses was demonstrated by 2370 deaths in 1997 in comparison to 828 deaths in 1980 and an increase in multiple-cause mortality due to mycoses by 1557 deaths in 1980 to 6534 deaths in 1997, respectively. On that basis, of deaths in which an infectious disease was the underlying cause, those due to mycoses increased from the tenth most common in 1980 to the seventh most common in 1997. The pathogens primarily responsible for the fatal casualties included *Candida*, *Aspergillus*, and *Cryptococcus* species. Although invasive yeast infections, primarily invasive *Candida albicans* infections, have shown a slight decrease in North American centres during the past decade, the incidence of non-albicans *Candida* infections (*C. parapsilosis*, *C. tropicalis*, *C. glabrata*, *C. krusei*), and those caused by rare yeasts (*C. guilliermondii*, *C. kefyr*, *C. rugosa*, and *C. famata*) is relatively increasing [53, 55, 59, 60] with difficulties in their diagnosis and treatment. Mould infections, especially as a result of *Aspergillus* species (*A. fumigatus*, non-fumigatus species: *A. niger*, *A. terreus*, *A. flavus*), are still increasing [61]. However, apart from an expanding number of different Zygomycetes, previously uncommon hyaline filamentous fungi such as *Fusarium* species and *Scedosporium prolificans*, dematiaceous filamentous fungi, and yeast-like pathogens such as *Trichosporon* species, *Blastoschizomyces capitatus*, *Malassezia* species, *Rhodotorula rubra*, and others have increasingly emerged as clinically important pathogens often refractory to conventional therapies [62].

The factors predisposing to fungal infections are manifold headed by a growing immunocompromised population due to i) mucosal or cutaneous barrier disruption, ii) defects in the number and function (e.g., defective NADPH-oxidase) of neutrophils or in cell-mediated immunity, iii) solid organ transplants, iv) metabolic dysfunction, and v) extremes of age. Iron overload is considered to act through the increased availability of iron for fungal proliferation



and the negative effects of iron overload on the antimicrobial functions of neutrophils, monocytes and natural killer cells. In addition, host-related genetic factors such as single nucleotide polymorphism (SNP) in the interleukin-10 (IL-10) promoter associated with decreased IL-10 production, genetic differences in the tumour necrosis factor  $\alpha$  (TNF $\alpha$ ) receptor promoter or SNPs in Toll-like receptors resulting in defective production of inflammatory cytokines have shown to play a pivotal role in host susceptibility to invasive mould infections. Finally, invasive mould infections mostly occur in haematological diseases. Besides these factors, aggressive treatment regimens (e.g., neutropenia as a result of myeloablative therapy in acute leukaemia or allogeneic haematopoietic stem cell transplantation (HSCT)), resulting in prolonged periods of cytopenia and the use of high doses of corticosteroids are in relation to the incidence of mould infections. Even novel therapies (e.g., with alemtuzumab) that allow less intensive conditioning remain associated with IFIs. In addition, invasive candidiasis is often related to an indwelling catheter, prior abdominal surgery, prolonged ICU stay, total parenteral nutrition, and renal failure. Finally, the pharmacotherapy with broad-spectrum antibiotics over 14 days contributes to occurrence of fungal infections [53, 63-65].

Early clinical diagnosis of IFI is difficult due to the non-specific clinical picture and the overabundance of risk factors. The diagnosis of invasive aspergillosis and candidiasis should be made in accordance with the recently published revised consensus criteria of the European Organisation for Research and Treatment of Cancer and the Invasive Fungal Infections Cooperative Group and the National Institute of Allergy and Infectious Diseases Mycoses Study Group (EORTC/MSG) Consensus Group [66]. However, only a minority of all IFI can be proven ante mortem; reliable diagnostic methods are lacking. Early treatment initiation in patients with IFI by different treatment strategies, e.g., prophylaxis, empirical and pre-emptive treatment, as well as targeted treatment in response to a definite diagnosis of IFI has a profound impact on mortality rates.

### **1.3.2 Treatment of invasive fungal infections**

There is a limited number of evidence-based treatment options in invasive candidiasis and invasive aspergillosis. Moreover, acquired resistance to antifungal agents has been reported further complicating the management of patients with invasive fungal diseases [63].

Four classes are used to treat systemic fungal infections: polyenes (amphotericin B deoxycholate (D-AmB), lipid-based formulations of AmB (AmB lipid complex, ABLC), liposomal (L)-AmB), pyrimidines (5-flucytosin, of low importance), azoles (including fluconazole, itraconazole, voriconazole, posaconazole), and echinocandins (including caspofungin, micafungin, anidulafungin). Beginning with the 1990s, the former gold standard D-AmB has been displaced over the years by new antifungal agents with comparable efficacy but less toxicity. Recommendations on optimal timing and choice of antifungal agents are rather heterogeneous. Recently, recommendations of the Infectious Diseases Working Party (AGIHO) of the German Society of Hematology and Oncology (DGHO) for the treatment of IFI in cancer patients have been revised [67]. RUPING et al. recommend posaconazole as prophylaxis for

allogeneic HSCT recipients, patients receiving induction chemotherapy for acute leukaemia or myelodysplastic syndrome, and those undergoing immunosuppressive therapy for graft-versus-host disease after allogeneic HSCT [65]. Caspofungin is advised to be used for the empirical treatment of persistently febrile neutropenia. The prophylactic use of fluconazole for invasive candidiasis is to be reserved to high-risk ICU patients. For the diagnosis of invasive candidiasis the echinocandins should be considered as the first choice unless patients hold fluconazole susceptible *Candida* species. Voriconazole should preferentially be employed once an invasive aspergillosis has been diagnosed. L-AmB is intended as second line treatment [65]. Recently, it has now also been approved as first-line treatment for invasive candidiasis and invasive aspergillosis (expert information AmBisome<sup>®</sup>, Gilead, Germany, April 2009).

## 1.4 Voriconazole

At the end of the 1990s, treatment of fungal infections, particularly aspergillosis, highly demanded for antifungal agents with an enhanced antifungal spectrum [68]. The second generation triazole, voriconazole ((2R,3S)-2-(2,4-difluorophenyl)-3-(5-fluoropyrimidin-4-yl)-1-(1,2,4-triazol-1-yl)butan-2-ol has been developed via modification of fluconazole by substituting a 4-fluoropyrimidine ring for one of the triazole moieties, and adding an  $\alpha$ -methyl group (see Fig. 1-2) providing an enhanced fungicidal potency and spectrum [69].

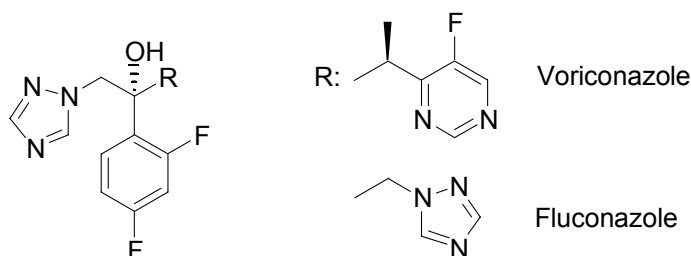


**Fig. 1-2:** Chemical structure of voriconazole and fluconazole.

The substitution accompanied a more lipophilic behaviour: The octanol:water partition coefficient increased from 3.5 (fluconazole, [70]) to 64.7 (voriconazole, [71]) and logP from 0.5 to 1.8, respectively. Voriconazole (molecular mass of 349.3 Da) is a weak base (pKa 1.76), and classified as a low solubility, high permeability compound (Class 2 compound according to the Biopharmaceutical Classification System (BCS)) [72].

### 1.4.1 Pharmacodynamic properties and indication

Similar to other azole antifungals, voriconazole acts by inhibiting the CYP-dependent lanosterol-14 $\alpha$ -demethylase (Fig. 1-3) which catalyses the removal of the methyl group on carbon 14 of lanosterol, an essential step for the biosynthesis of ergosterol in fungi (Fig. 1-4).

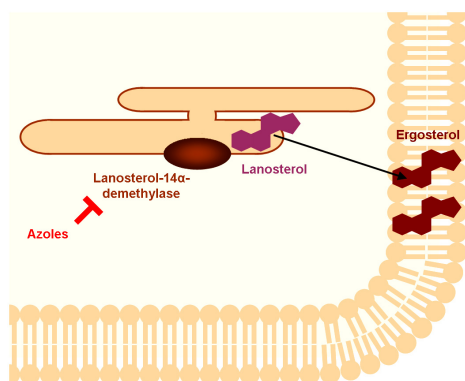


**Fig. 1-3:** Mode of action of azoles (voriconazole) (modified from [73]).

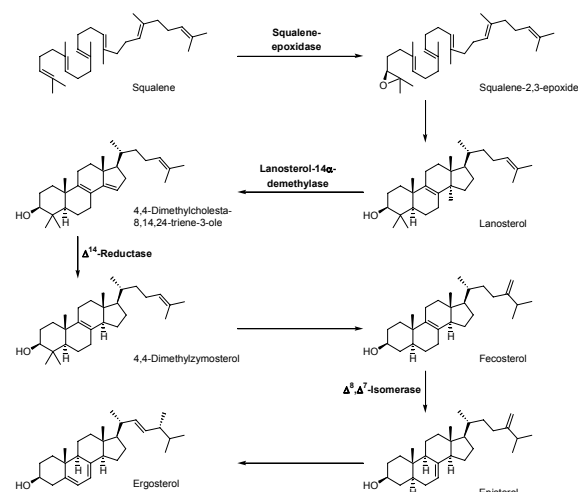


**Fig. 1-4:** Biosynthesis of ergosterol (modified from [74]).

In result, fungi treated with voriconazole are depleted of ergosterol and accumulate 14- $\alpha$ -methylated sterols, such as lanosterol, facilitating the disruption of the membrane structure and function and, finally, inhibiting fungal growth. In *Aspergillus* species and some other moulds this mechanism of action results in death of the organism as well [75-77]. Moreover, another effect of voriconazole, unrelated to the selective inhibition of CYP-dependent lanosterol-14 $\alpha$ -demethylase, has been discussed. VARANASI et al. suggest that the mechanism of action is due to direct or indirect effect on the formation of conidia of *Aspergillus* species. [78].

The mode of action related to lanosterol-14 $\alpha$ -demethylase is supported by the fact that the development of fungal resistance has most commonly been associated with alterations in *cyp51A*, the gene encoding the target enzyme of the azoles [79]. The contribution of other mechanisms, such as reduced intracellular concentration by efflux pumps and reduced uptake of the drug has been proposed. However, growing evidence suggests the role of multiple mechanisms contributing to the overall phenotype [79].

Voriconazole has broad-spectrum activity against pathogenic yeasts, dimorphic fungi and opportunistic moulds, including those that are most clinically relevant. In contrast to fluconazole, voriconazole demonstrated activity against *Aspergillus*, *Fusarium*, and *Scedosporium* species. Activity against Zygomycetes has not been observed [76, 77]. In Europe, voriconazole is approved by the EMA for the treatment of invasive aspergillosis, treatment of *Candida* infections in non-neutropenic patients, fluconazole-resistant serious invasive *Candida* infections (including *C. krusei*), and serious fungal infections caused by *Fusarium* and *Scedosporium* species. Voriconazole is intended for patients with worsening, possibly life-threatening, fungal infections [72]. The activity of the N-oxide metabolite of voriconazole against a range of fungal pathogens was 100-fold less than that of voriconazole [72] (see 1.4.2).

### 1.4.2 Pharmacokinetic properties

Voriconazole is available in both intravenous (iv) and oral (po) formulations. The iv formulation is solubilised in sulphobutyl ether  $\beta$ -cyclodextrin sodium (SBECD) and infused over 1 h to 2 h. The recommended iv (oral) regimen is a loading dose of 6 mg/kg (400 mg) every 12 h for two doses, followed by a maintenance dose of 4 mg/kg (200 mg) every 12 h [72]. The oral formulation of voriconazole should be administered either 1 h before or after a meal, since the high oral bioavailability (96%) will be reduced by (fat) food [75]. Voriconazole displays dose- and plasma concentration-independent protein binding of approximately 58%. The mean elimination half-life has been reported to be approximately about 6 h to 9 h [76] and it has a large volume of distribution at steady state of 2 L/kg – 4.6 L/kg [80]. Hence, the distribution outside the vascular space has been assumed to be extensive. Measurements in patients with invasive mycoses revealed large inter- and intraindividual variations of voriconazole plasma concentrations which may eventually have clinical implications and, therefore, high interindividual variability in the extent of distribution of voriconazole might rather be expected. So far, only a few reports on distribution studies of voriconazole in animal models or humans have been presented [81] such as investigations of synovial fluid [82], cerebrospinal fluid (CSF) [83, 84], brain tissue [84, 85], or cortical and medullar bone [82].

Voriconazole is predominantly cleared by hepatic metabolism, with less than 2% excretion unchanged in urine or faeces. The major pathways (Fig. 1-5, a-e) in humans involve fluoropyrimidine N-oxidation (a), fluoropyrimidine hydroxylation (b), and methyl hydroxylation (c). In addition, N-oxidation facilitated cleavage of the molecule, resulting in loss of the fluoropyrimidine moiety (d) and subsequent conjugation with glucuronic acid (e). The major circulating metabolite is the N-oxide of voriconazole (21%) [86]. The (quantitative) information about the entire enzymes involved in voriconazole metabolism is limited. Besides metabolic transformations catalysed by flavin-containing monooxygenases (FMO) (~25% of oxidative metabolism), voriconazole was shown to be metabolised by CYP2C19, CYP2C9, and CYP3A4 in *in vitro* studies using human liver microsomes [87-89] (Fig. 1-5).

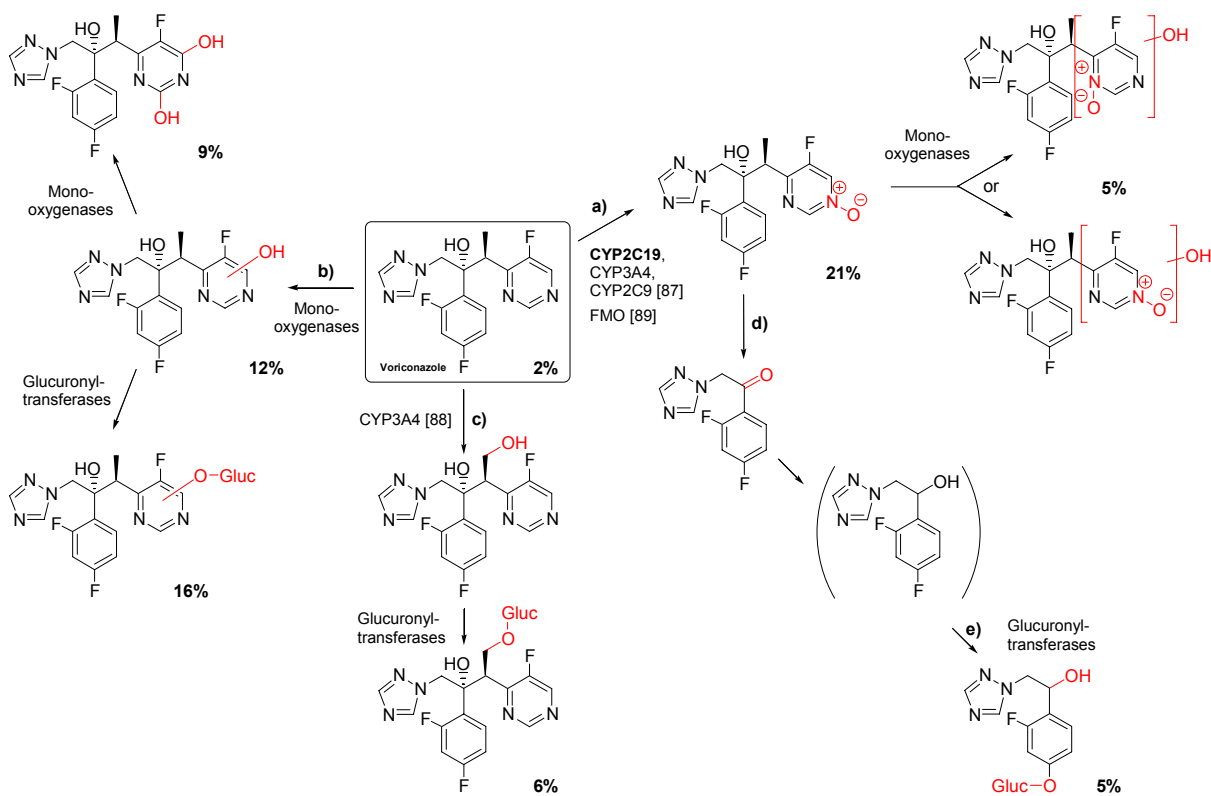


**Fig. 1-5:** Major metabolites of voriconazole in humans (as percentage of dose) following multiple administration of [ $^{14}\text{C}$ ] voriconazole via a) fluoropyrimidine N-oxidation, b) fluoropyrimidine hydroxylation, c) methyl hydroxylation, d) loss of the fluoropyrimidine, e) defluorination and conjugation with glucuronic acid (modified from [86]). FMO: Flavin-containing monooxygenases.

Results of YANNI et al. suggested that CYP-mediated metabolism accounted for ~75% of the total oxidative metabolism [89]. The genotype status for the metabolising CYP enzymes has been shown to influence voriconazole plasma concentrations [90]. However, dose adjustment based on genotype has not been recommended; the same applies for females and the elderly [75]. The most potential to affect the primary clearance of voriconazole and, hence, to largely affect voriconazole exposure is expected from chronic hepatic impairment. To limit overexposure of voriconazole dose adjustment is recommended [75]. Total clearance values of voriconazole ranged from 13 L/h to 36 L/h [81]. Due to the lack of influence of renal function on the clearance of voriconazole no dose adjustment is required for oral voriconazole in patients with renal dysfunction. However, the excipient SBEDC in the iv formulation was shown to accumulate in renal impairment and, therefore, voriconazole should be orally administered [75]. Nonlinearity has been described for voriconazole elimination and so far discussed to be attributed to saturation of metabolic clearance [81].

### 1.4.3 Drug interactions and safety

The potential for drug interactions with voriconazole is high due to its metabolism by CYP isoenzymes. Voriconazole can affect or be affected by other drugs metabolised by CYP2C19, CYP2C9, and CYP3A4. In consequence, voriconazole concentrations will be reduced (e.g.,

by rifampicin) or co-administered drugs will be elevated in their plasma concentrations (e.g., tacrolimus). Several drugs are contraindicated when using voriconazole (e.g., carbamazepine). For the clinical management of the interactions either dose adjustment of voriconazole, or dose adjustment of the interacting drug and/or its monitoring (or monitoring markers of its activity) are recommended [75, 81].

Voriconazole is generally well tolerated. Safety assessment in clinical trials demonstrates that voriconazole is associated with visual abnormalities, hepatic function abnormalities, and skin reactions [75]. The most frequent ADR is a transient and reversible disturbance of vision (photopsia) which occurs in approximately 30% of patients [81]. Visual disturbances include altered or enhanced visual perception, blurred vision, colour vision change, and photophobia. Symptoms tend to occur around 30 min after dose administration, spontaneously resolved within 1 h and were most common during the first week of therapy. No permanent damage to the retina has been noted and no visual ADR were assessed as severe. Elevations in hepatic enzymes were seen in approximately 13% of patients with voriconazole therapy. Most patients showed an asymptomatic elevation of these enzymes but some patients with severe life-threatening hepatitis and fulminant hepatic failure have been described. The risk of developing hepatitis appears to increase with increased serum voriconazole concentrations and resolves with discontinuation of treatment with the drug. Current recommendations include routine monitoring of hepatic enzymes during therapy [75]. Skin reactions occur in six percent of voriconazole recipients. Skin rashes were categorised as mild. However, severe reactions, including Stevens-Johnson syndrome, toxic epidermal necrolysis, and erythema multiforme, have been reported in a very small number of patients. Direct sunlight should be avoided, because of potential photosensitivity reactions [75]. Other less commonly noted ADR include headache, nausea and vomiting, diarrhea, abdominal pain, and visual hallucinations [91].

## 1.5 Objectives

Microdialysis is the method of choice to facilitate the direct access to the interstitium in order to determine local drug concentrations. In particular, this is reasonable for drugs which have their site of action in the ISF, such as antiinfectives. This effective approach requires several prerequisites for beneficial application. Therefore, the development and optimisation of methods enabling reproducible microdialysis investigations *in vitro* and *in vivo* were the central motivation of this work. In a second step, the application of the methods developed should investigate feasibility as well as tolerability in the *in vivo* situation allowing, in a third step, to comprehensively characterise the data and results obtained during the application in *in vitro* experiments and in *in vivo* studies from a statistical and pharmacokinetic point of view. These tasks were addressed in four projects all involving voriconazole:

- I A rapid and reliable bioanalytical assay for voriconazole should be developed permitting its quantification from small microdialysate sample volumes, from matrices additionally obtained in the pre-/clinical trials – whole blood, plasma, ultrafiltrate (UF), skin biopsy (SB) – and experimental solutions derived from the projects II-IV.
- II For thorough and reproducible microdialysis *in vitro* investigations a setting should be established by developing a robust and easy-to-handle stationary *in vitro* microdialysis system. Based on that system, extensive investigations with voriconazole should be performed in order to check for feasibility by characterising the permeation behaviour and to determine optimal conditions for microdialysis *in vivo*. Moreover, for investigating/defining specifications for the *in vitro* microdialysis system basic experiments were expanded to further antiinfective drugs (linezolid and daptomycin). Finally, investigations with the drug product of voriconazole (Vfend®) containing the solubilising excipient sulphobutyl ether  $\beta$ -cyclodextrin sodium should be performed since the drug product should be implemented in the projects III and IV.

Projects I and II were performed as prerequisite to conduct the pre-/clinical trials with voriconazole investigating its PK applying the microdialysis approach.

- III In a preclinical pilot study microdialysis was applied to both healthy and infected subcutaneous adipose tissue of guinea pigs after twelve days of multiple oral dosing of voriconazole. A potential influence of the disease state of the area under investigation should be elaborated by a comparison of the voriconazole disposition in healthy and inflamed skin. Additionally, the PK of voriconazole in the ISF was explored and compared to the results obtained for SB and whole blood specimens.
- IV The rationale for project IV derived from two important aspects: 1) Long-term application of microdialysis had scarcely been investigated in humans and 2) the

disposition characteristics of voriconazole, in particular the distribution to and the availability at the potential target site (ISF) in humans is yet unclear.

Therefore, the aim of this project was to design a prospective clinical trial in healthy volunteers during voriconazole sequence dosing. The trial should contain an observational pilot phase (part I) in order to comprehensively investigate the applicability and validity of the microdialysis technique over several days using linear as well as concentric microdialysis catheters for comparison and future selection, and a main phase (part II) considering the feasibility results of the pilot phase (long-term insertion, choice of catheter).

The pilot phase should be conducted requiring the development of a stable and reliable setting for a long-term application of microdialysis. Extensive longitudinal measurements of the relative recovery (RR) of voriconazole should be performed. The results of the RR should serve to determine the value of RR to be able to transform the concentration measured in the microdialysates into the “true” ISF concentrations. Moreover, these results should enlighten i) the intra- and ii) interindividual variability of the catheters over time, and iii) their consistency of recovery leading to conclusions concerning the long-time performance of the catheter. Besides, unbound voriconazole concentrations should be determined in plasma and in microdialysate of subcutaneous adipose tissue obtained via linear and concentric microdialysis catheters. Furthermore, the individual pharmacokinetic behaviour should be preliminarily explored leading to an initial characterisation of the availability and distribution of voriconazole independent of the complex situation in (critically ill) patients. Thereby, amongst others analyses should be focused on individual genotype.



---

## 2 MATERIALS, METHODS, PRE- AND CLINICAL STUDIES

### 2.1 Chemicals, drug and pharmaceutical products

#### 2.1.1 I – Bioanalytical methods for quantification of voriconazole

Acetonitrile (ACN) (HPLC grade)	Roth, Karlsruhe, Germany
Acetylcysteine (in ACC <sup>®</sup> injekt)	Hexal, Holzkirchen, Germany
Ambroxol	Sigma-Aldrich, St. Louis, USA
Ambroxol (in Mucosolvan <sup>®</sup> )	Boehringer Ingelheim, Ingelheim, Germany
Ammonia (30%)	Grüssing, Filsum, Germany
Ammonium dihydrogen phosphate	Fluka Chemie, Neu-Ulm, Germany
Ampicillin (in Ampicillin HEXAL <sup>®</sup> comp)	Hexal, Holzkirchen, Germany
Ceftriaxone (in Ceftriaxon-ratiopharm <sup>®</sup> )	Ratiopharm, Ulm, Germany
Cefuroxime (in Cefuroxim-ratiopharm <sup>®</sup> )	Ratiopharm, Ulm, Germany
Certoparin sodium (in Mono-Embolex <sup>®</sup> NM)	Novartis Pharma, Nuremberg, Germany
Ciprofloxacin (in Ciprobay <sup>®</sup> )	Bayer, Leverkusen, Germany
Clonidine hydrochloride (in Paracefan <sup>®</sup> )	Boehringer Ingelheim, Ingelheim, Germany
Digitoxin (in Digimerck <sup>®</sup> )	Merck, Darmstadt, Germany
Dobutamine (in Dobutamin Carino <sup>®</sup> )	Carinopharm, Gronau/Leine, Germany
Enoxaparin sodium (in Clexane multidose <sup>®</sup> )	Aventis Pharma/Hoechst Marion Roussel, Frankfurt/Main, Germany
Epinephrine hydrogen tartrate (in Adrenalin 1:1000 JENAPHARM <sup>®</sup> )	Mibe, Jena, Germany
Erythromycin (in Erythromycin STADA <sup>®</sup> )	STADA, Bad Vilbel, Germany
Esketamine hydrochloride (in Ketanest <sup>®</sup> S)	Parke-Davis, Karlsruhe, Germany
Furosemide (in Furosemid-ratiopharm <sup>®</sup> )	Ratiopharm, Ulm, Germany
Glyceryl trinitrate (in Trinitrosan <sup>®</sup> )	Merck, Darmstadt, Germany
Heparin sodium (in Heparin-Natrium Braun <sup>®</sup> )	Braun, Melsungen, Germany
Heparin sodium (in Liquemin <sup>®</sup> N)	Hoffmann-La Roche, Grenzach-Wyhlen, Germany
Hydrocortisone (in Hydrocortison 100-Rotexmedica <sup>®</sup> )	Rotexmedica, Trittau, Germany
Insulin human (in Berlinsulin <sup>®</sup> H)	Berlin-Chemie, Berlin, Germany
Isotonic sodium chloride solution	Serumwerk Bernburg, Bernburg, Germany
Metamizol sodium (in Novalgin <sup>®</sup> )	Aventis Pharma/Hoechst Marion Roussel, Frankfurt/Main, Germany
Metamizol sodium (in Novaminsulfon ratiopharm <sup>®</sup> )	Ratiopharm, Ulm, Germany

Methanol (HPLC grade)	Roth, Karlsruhe, Germany
Metoclopramide (iv and po formulation) (in Paspertin <sup>®</sup> )	Solvay, Hannover, Germany
Metoprolol (in Beloc-Zok <sup>®</sup> )	AstraZeneca, Wedel, Germany
Metronidazole (in Metronidazol Fresenius <sup>®</sup> )	Fresenius Kabi, Bad Homburg, Germany
Midazolam (in Dormicum <sup>®</sup> )	Hoffmann-La Roche, Grenzach-Wyhlen, Germany
Midazolam (in Midazolam-ratiopharm <sup>®</sup> )	Ratiopharm, Ulm, Germany
Multivitamin preparation (in Cernevit <sup>®</sup> ) Vitamin A, D, E, C, B1, B2, B5, B6, B12, Folic acid, Biotine, Nicotinamide	Baxter, Unterschleissheim, Germany
Norepinephrine (in Arterenol <sup>®</sup> )	Aventis Pharma/Hoechst Marion Roussel, Frankfurt/Main, Germany
Pantoprazole sodium (in Pantozol <sup>®</sup> )	Altana, Konstanz, Germany
Pantoprazole sodium (in Rifun <sup>®</sup> )	Schwarz Pharma, Monheim, Germany
Piperacillin (in Piperacillin 2 g DeltaSelect <sup>®</sup> )	DeltaSelect, Pfullingen, Germany
Propofol (in Disoprivan <sup>®</sup> )	AstraZeneca, Wedel, Germany
Pyridostigmine bromide (in Kalymin <sup>®</sup> )	Temmler Pharma, Marburg, Germany
Ranitidine hydrochloride (in Ranitidin-ratiopharm <sup>®</sup> )	Ratiopharm, Ulm, Germany
Ringer's solution B.Braun 147 mM Na <sup>+</sup> , 4 mM K <sup>+</sup> , 2.2 mM Ca <sup>2+</sup> , ~156 mM Cl <sup>-</sup> in 1 L WFI	Braun, Melsungen, Germany
Ringer's solution Bernburg 147 mM Na <sup>+</sup> , 4 mM K <sup>+</sup> , 2.25 mM Ca <sup>2+</sup> , ~156 mM Cl <sup>-</sup> in 1 L WFI	Serumwerk Bernburg, Bernburg, Germany
Sulbactam (in Ampicillin HEXAL <sup>®</sup> comp)	Hexal, Holzkirchen, Germany
Urapidil hydrochloride (in Ebrantil <sup>®</sup> )	Altana, Konstanz, Germany
Urapidil hydrochloride (in Urapidil-Pharmore <sup>®</sup> )	Helm Pharmaceuticals, Hamburg, Germany
Vancomycin (in Vanco-cell <sup>®</sup> )	Cell pharm, Hannover, Germany
Voriconazole LOT No. 052301-008-09, potency 98% [92]	Pfizer Global Research and Development, Sandwich, United Kingdom
Water, purified	Purelab Option, E80, ELGA LabWater, Celle, Germany

Analyte-free matrices for the development of the assays enabling the quantification of voriconazole in plasma (heparinised) or whole blood were provided by the blood transfusion service of the Medical Faculty, Martin-Luther-Universität Halle-Wittenberg (MLU) (reference number 0243385), or by blood donation of healthy volunteers (Department of Clinical Pharmacy, Institute of Pharmacy, MLU). For assay development for SB samples blank guinea pig SB samples were supplied by the University Clinic and Polyclinic for Otorhinolaryngology, Head and Neck Surgery, Medical Faculty, MLU.

**2.1.2 II – *In vitro* microdialysis of voriconazole**

Daptomycin LOT No. 360603F anhydrous potency 951 µg daptomycin/mg powder [93]	Cubist Pharmaceuticals, Lexington, USA, provided by Novartis, Nuremberg, Germany
Linezolid LOT No. 1000933645 potency 99.8% [94]	Pfizer Global Research and Development, Sandwich, United Kingdom
Methanol, Ringer's solution, Voriconazole, Water, purified	see 2.1.1
Vfend® (voriconazole) 200 mg powder for solution for infusion	Pfizer, Karlsruhe, Germany

**2.1.3 III – Influence of disease state on target site exposure**

Phosphate buffered saline (pH 7.4) containing 0.01% Tween 20	SSI Diagnostica, Hillerød, Denmark
Sabouraud glucose agar (SAB) with cycloheximide and chloramphenicol	SSI Diagnostica, Hillerød, Denmark
Combination anaesthetic: Torbugesic Vet® 10 mg/mL Butorphanol	Fort Dodge Veterinaria, Vall de Bianya, Spain
Xylazin Vet® 20 mg/mL Xylazin	Intervet International, Boxmeer, Netherlands
Zoletil 50 Vet® 125 mg Zolazepam, 125 mg Tiletamin	Virbac, Carros, France
Study drugs: Vfend® (voriconazole) 200 mg powder for oral suspension	Pfizer, Ballerup, Denmark
Vfend® (voriconazole) 200 mg powder for solution for infusion	Pfizer, Ballerup, Denmark

**2.1.4 IV – Clinical long-term microdialysis pilot study with voriconazole in healthy volunteers****2.1.4.1 Clinical study**

Aqua ad iniectabilia	Mayrhofer Pharmazeutika, Leonding, Austria
Isotonic physiological saline solution 154 mM Na <sup>+</sup> , Cl <sup>-</sup> in 1 L WFI	Mayrhofer Pharmazeutika, Leonding, Austria
Isozid®-H colourless, coloured	Gebro Pharma, Fieberbrunn, Austria
Ringer's solution ÖAB (Austrian pharmacopoeia) 154 mM Na <sup>+</sup> , 4 mM K <sup>+</sup> , 2.7 mM Ca <sup>2+</sup> , ~163.4 mM Cl <sup>-</sup> in 1 L WFI	Mayrhofer Pharmazeutika, Linz, Austria

## Study drugs:

Vfend® (voriconazole) 200 mg powder Pfizer, Vienna, Austria

for solution for infusion

Vfend® (voriconazole) 200 mg tablet Pfizer, Vienna, Austria

Preparation of the iv infusion solution: Prior to the administration one powder-containing vial was resuspended with 19 mL aqua ad iniectabilia (clear solution of 10 mg voriconazole/mL). The solution was further diluted with isotonic physiological saline solution to an iv infusion solution (max. concentration 5 mg voriconazole/mL).

Preparation of the retroperfusates 1 (RP1) and 2 (RP2) (see 1.2.3): Voriconazole (Vfend®) was added to the perfusion medium resulting in a concentration ( $C_{RP}$ ) of 20 µg/mL (RP1) or in  $C_{RP}$  of 200 µg/mL (RP2). All study preparations used during the trial were stored at the study site at room temperature and protected from light.

## 2.1.4.2 Genotype analysis

Adenosine-5'-phosphosulphate (APS)	Qiagen, Hilden, Germany
Adenosine triphosphate (ATP) sulfurylase	Qiagen, Hilden, Germany
Agarose	Biozym, Hessisch Oldendorf, Germany
Gel, 2%: consisting of agarose and TBE (Tris-(hydroxymethyl)aminomethane (Tris), boric acid and ethylenediaminetetraacetic acid (EDTA))	
Annealing-Buffer	Qiagen, Hilden, Germany
10 mM Tris/HCl, 20 mM Tris-Acetate, 2 mM Mg-acetate	
Apyrase	Qiagen, Hilden, Germany
Binding-Buffer	Qiagen, Hilden, Germany
2 mM NaCl, 1 mM EDTA, 0.1% Tween 20	
Boric acid	Sigma-Aldrich, Taufkirchen, Germany
Buffer	Invitrogen, Karlsruhe, Germany
200 mM Tris/HCl, pH 8.4, 500 mM KCl – without MgCl <sub>2</sub>	
Denaturation solution	Qiagen, Hilden, Germany
0.2 M NaOH	
Deoxyribonucleotide triphosphate (dNTP)	Biozym, Hessisch Oldendorf, Germany
Deoxyadenosine alfa-thio triphosphate (dATP $\alpha$ S) Deoxycytidine triphosphate (dCTP), Deoxyguanosine triphosphate (dGTP), Deoxythymidine triphosphate (dTTP)	
DNA polymerase	Qiagen, Hilden, Germany
EDTA	Sigma-Aldrich, Taufkirchen, Germany
Ethanol 70%	Roth, Karlsruhe, Germany
Ethanol 96%	Roth, Karlsruhe, Germany
Ethidium bromide	Sigma-Aldrich, Taufkirchen, Germany
Glycerol	Sigma-Aldrich, Taufkirchen, Germany
Highly purified water/WFI	DeltaSelect, Dreieich, Germany
Luciferase	Qiagen, Hilden, Germany

Luciferin	Qiagen, Hilden, Germany
MgCl <sub>2</sub>	Invitrogen, Karlsruhe, Germany
NucleoSpin <sup>®</sup> blood isolation kit	Macherey-Nagel, Düren, Germany
Lysis Buffer BQ1, Proteinase K (lyophilised), Proteinase Buffer PB, Wash Buffer BQ2, Elution Buffer BE (5 mM Tris/HCl, pH 8.5)	
Primer:	
CYP2C9*2 C430T	
CYP2C9_A2_F:	Invitrogen, Karlsruhe, Germany
5'-GTATTTTGGCCTGAAACCCATA-3'	
CYP2C9_A2_R:	Biomers, Ulm, Germany
5'-Biotin-CACCCTTGGTTTTCTCAACTC-3'	
Sequencing primer:	Invitrogen, Karlsruhe, Germany
5'-GGGAAGAGGAGCATTGAGGAC-3'	
CYP2C9*3 A1075C	
CYP2C9_A3_F:	Invitrogen, Karlsruhe, Germany
5'-Biotin-TGCACGAGGTCCAGAGAT-3'	
CYP2C9_A3_R:	Biomers, Ulm, Germany
5'-GATACTATGAATTTGGGACTTC-3'	
Sequencing primer:	Invitrogen, Karlsruhe, Germany
5'-TGGTGGGGAGAAGGTC-3'	
CYP2C19*2 G681A	
CYP2C19_A2_F:	Invitrogen, Karlsruhe, Germany
5'-Biotin-CAGAGCTTGGCATATTGTATC-3'	
CYP2C19_A2_R:	Biomers, Ulm, Germany
5'-GTAGTAAACACAAAAGTCAATG-3'	
Sequencing primer:	Invitrogen, Karlsruhe, Germany
5'-TTAAGTAATTTGTTATGGGT-3'	
Sterilised PCR water	Braun, Melsungen, Germany
Streptavidin coated Sepharose beads	GE Healthcare, Munich, Germany
Taq-Polymerase	Invitrogen, Karlsruhe, Germany
Tris (for gel and electrophoresis)	Roth, Karlsruhe, Germany
Washing buffer (10 mM Tris-Acetate)	Qiagen, Hilden, Germany

## 2.2 Laboratory and study equipment

### 2.2.1 I – Bioanalytical methods for quantification of voriconazole

Centrifree <sup>®</sup> Ultrafiltration devices	Millipore, Eschborn, Germany
Centrifuge 5417 R	Eppendorf, Hamburg, Germany
Helium pycnometer Pycnomatic ATC	Porotec, Hofheim/Ts, Germany
HPLC columns	
(sorbent, pore size [Å], type, modification, e (endcapped), particle size [µm], internal diameter × length [mm])	

LiChrospher®-100 RP-8, e, 5, 4.0 × 125 reversed phase column, functional group: C8	Merck, Darmstadt, Germany
LiChrospher®-100 RP-18, e, 5, 4.0 × 125 reversed phase column, functional group: C18	Merck, Darmstadt, Germany
LiChrospher®-100 RP-18, e, 5, 4.0 × 250	Merck, Darmstadt, Germany
Precolumn (integrated) LiChroCART® 4-4	Merck, Darmstadt, Germany
Spherisorb® ODS2, e, 5, 4.0 × 250 reversed phase column, functional group: C18	Waters Corporation, Milford, MA, USA
HPLC systems (modular)	JASCO, Gross-Umstadt, Germany
1 Controller LC-Net II/ ADC	
Pump (PU-2080 Plus)	
Peltier cooling and heating autosampler (AS-2051)	
Degasser module (DG-2080-53)	
Air-cooled Peltier element column Thermostat Jetstream Plus	
Ultraviolet (UV)/Visible (VIS) detector (UV-2075) using deuterium lamps (L2D2) (Hamamatsu Photonics K.K., Iwata city, Japan)	
2 Controller LC-Net II/ ADC	
Pump (PU-980)	
Autosampler (AS-1555)	
Degasser module (DG-980-50)	
UV/VIS detector (UV-975) using deuterium lamps (L2D2).	
Laboratory shaker S 421	MLW Prüfgeräte-Werk, Medingen, Germany
Membrane filters (0.22 µm)	Sartorius, Göttingen, Germany
Microshaker Type 326	Premed, Warsaw, Poland
pH meter pH315i (electrode SenTix®41)	WTW, Weilheim, Germany
Safe lock vials (0.5 – 1.5 mL)	Eppendorf, Hamburg, Germany
Sartorius analytic A200S	Sartorius, Göttingen, Germany
Speed-Vac® System Savant-AES1010	ThermoQuest, Egelsbach, Germany
Ultrasonic bath Sonorex RK 100 H	Bandelin Electronic, Berlin, Deutschland

### 2.2.2 II – *In vitro* and *in vivo* (III, IV) microdialysis of voriconazole

This section outlines the microdialysis equipment used in the *in vitro* microdialysis investigations (see 2.4), in the preclinical (see 2.5), or in the clinical studies (see 2.6). The development of the *in vitro* microdialysis system (IVMS), including the material processed, is described in section 2.4.1.

#### 2.2.2.1 Microdialysis pumps and syringes

CMA102® Pumps	CMA Microdialysis AB, Solna, Sweden
CMA107® Pumps	CMA Microdialysis AB, Solna, Sweden
CMA106® Syringes	CMA Microdialysis AB, Solna, Sweden
BD® Syringes 1mL Luer Lock®	BD, Heidelberg, Germany

All microdialysis pumps used during the experiments and studies were checked for accuracy and precision. For this purpose, microtubes were weighed before and after microdialysis with different flow rates ( $n=30$ : 1.5  $\mu\text{L}/\text{min}$ ,  $n=18$ : 2.0  $\mu\text{L}/\text{min}$  and  $n=30$ : 5.0  $\mu\text{L}/\text{min}$ ). Precision and accuracy of the volume obtained (accounted for density) were calculated.

### 2.2.2.2 Microdialysis catheters and accessories

All catheters used were CE marked according to the Medical Device Directive, 93/42/EEC, sterilised by  $\beta$ -radiation, stored according to the requirements in the product sheet (4 °C – 25 °C), were used once only except during the *in vitro* studies and were purchased from CMA Microdialysis AB, Solna, Sweden (Tab. 2-1).

**Tab. 2-1:** Technical data of the catheters used in this thesis.

Catheters		CMA60 <sup>®</sup> [95]	CMA70 <sup>®</sup> [96]	CMA66 <sup>®</sup> [97]
Design		Concentric	Concentric	Linear
Materials	Membrane	Polyamide (PA)	PA	Polyarylethersulphone (PAES)
	Inlet and outlet tubing	Polyurethane (PU)	PU	PU
Length [mm]	Membrane	30	10	30
	Inlet tube	400	600	400
	Outlet tube	105	220	100
Diameter [mm]	Membrane	0.6	0.6	0.5
	Inlet tube	0.15/1.0 (inner (ID)/outer (OD))	1.0	0.4
	Outlet tube	0.15/1.0 (ID/OD)	1.0	0.4
Membrane cut-off [kDa]		20	20	20
Membrane area [ $\text{mm}^2$ ] (length $\cdot$ $\pi$ $\cdot$ diameter)		56.55	18.85	47.12

An exemplary illustration of both a concentric and a linear catheter is shown in Fig. 2-1.

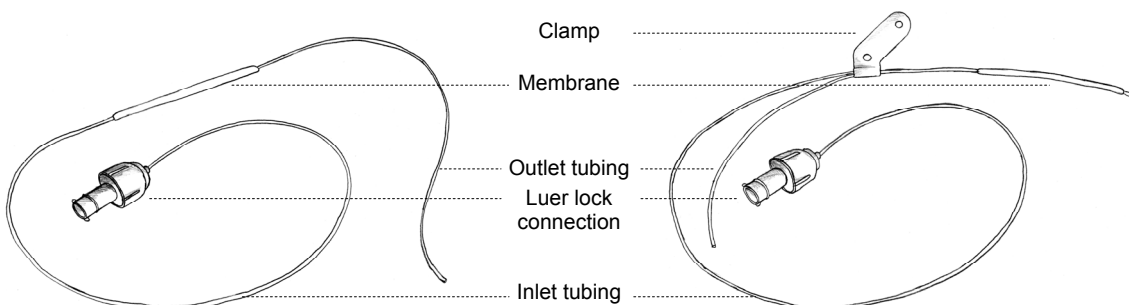


**Fig. 2-1:** Exemplary illustrations of linear and concentric catheters. Left panel: linear design (CMA66<sup>®</sup>), right panel: concentric design (CMA60<sup>®</sup>).

### 2.2.3 III – Influence of disease state on target site exposure

Biopsy punches	Produkte für die Medizin, Cologne, Germany
Cannula BD Microlance®	BD, Drogheda, Ireland
Nylon Net Filters, pore size 11 µm	Millipore, Carrigtwohill, Ireland
Razor Zorrik twin blades	Super-Max Ltd, Feltham, United Kingdom

### 2.2.4 IV – Clinical long-term microdialysis pilot study with voriconazole in healthy volunteers

#### 2.2.4.1 Clinical study

Combi-Stopper	Braun, Melsungen, Germany
Infusomat IP 85-2	Döring, Munich, Germany
Injekt Luer Solo	BD, Heidelberg, Austria
Injekt Luer Solo 2 mL	Braun, Melsungen, Germany
Luer adapter	Greiner Bio-one, Kremsmünster, Austria
Mini-Spike Plus®	Braun, Melsungen, Germany
Perifix®-Catheter Connector	Braun, Melsungen, Germany
Steristrip®	3M Health Care, Neuss, Germany
Tegaderm®	3M Health Care, Neuss, Germany
TriCath In®	Codan, Medizinische Geräte, Lensahn, Germany
Vacurette®/Vacurette®Premium	Greiner Bio-one, Kremsmünster, Austria

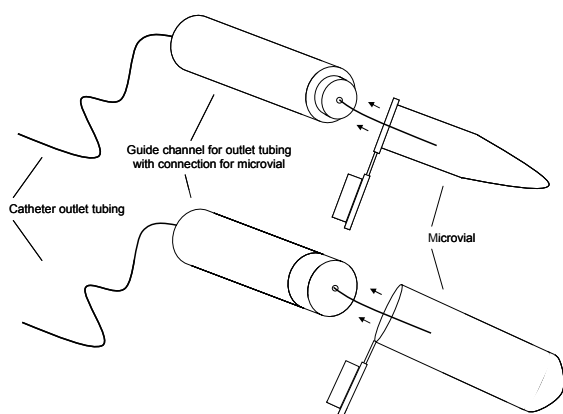


**Fig. 2-2:** Outlet tubing guide channels with connection for microvials of 500 µL (top) and 1500 µL (bottom).

Outlet tubing guide channels with connection for microvials (Technical laboratory at the Institute of Pharmacy, MLU, Germany) were developed to guide the outlet tubing of the microdialysis catheter directly into the microvial avoiding any loss of microdialysate (see Fig. 2-2). The lengths of the guide channels were different for linear (2 cm) and concentric (3 cm) catheters since the outlet tubing of the microdialysis catheter differed in length. The type of the connection for microvials depended on the volume sampled and the

type of the microvials used, respectively (see Fig. 2-2). The guide channels were elements of the *in vivo* long-term microdialysis setting (see 2.6.2).



#### 2.2.4.2 Genotype analysis

96-well PSQ <sup>®</sup> 96 plate	Qiagen, Hilden, Germany
96-well PCR plates for PCR product	Qiagen, Hilden, Germany
Collection tubes	Macherey-Nagel, Düren, Germany
Electrophoresis apparatus	Bio-Rad Laboratories, Hercules, USA
NucleoSpin <sup>®</sup> Blood QuickPure Columns	Macherey-Nagel, Düren, Germany
PyroMark Vacuum Prep Workstation <sup>®</sup>	Qiagen, Hilden, Germany
Pyrosequencer: PSQ <sup>®</sup> 96MA	Qiagen, Hilden, Germany
RT-PCR apparatus: iCycler <sup>®</sup>	Bio-Rad Laboratories, Hercules, USA
Spectrometer: Nanodrop <sup>®</sup> (ND-1000)	PEQLAB Biotechnologie, Erlangen, Germany

Pyrosequencing<sup>®</sup> is a non-electrophoretic method for DNA sequencing and analysis of SNPs, respectively. The method has already been reviewed in detail in the literature [98] and is briefly explained in this subsection. In a first step, a sequencing primer is hybridised to a single-stranded PCR (polymerase chain reaction) amplicon that serves as a template, and incubated with the enzymes DNA polymerase, ATP sulfurylase, luciferase, and apyrase as well as the substrates APS and luciferin. In a second step, the first dNTP is added to the reaction. DNA polymerase catalyses the incorporation of the dNTP into the DNA strand, if complementary to the base in the template strand. Each incorporation event is accompanied by the release of pyrophosphate (PPi) in a quantity which is equimolar to the amount of incorporated nucleotide. The enzymatic cascade is continued by a third step: ATP sulfurylase converts PPi to ATP in the presence of APS. ATP drives the luciferase-mediated conversion of luciferin to oxyluciferin generating visible light proportional to the amount of ATP. The light signal is detected by a charge coupled device chip and displayed as a peak in the raw data output (Pyrogram<sup>®</sup>). The height of each peak is proportional to the number of nucleotides incorporated. Finally, apyrase, a nucleotide-degrading enzyme, continuously degrades unincorporated nucleotides and ATP. After the degradation is complete, another nucleotide is added. The addition of dNTPs is performed sequentially. dATP $\alpha$ S is used as a substitute for the natural deoxyadenosine triphosphate since it is efficiently used by the DNA polymerase, but not recognised by the luciferase. As the process continues, the complementary DNA strand is built up and the nucleotide sequence is determined from the signal peaks in the Pyrogram<sup>®</sup>, chronological showing the dispensed nucleotides (x axis) and the corresponding light signal (y axis). The pyrosequencing<sup>®</sup> technology presents SNPs in the context of the surrounding sequence guaranteeing correctness of each individual analysis without the requirement of other controls (built-in quality control).

### 2.3 I – Bioanalytical methods for quantification of voriconazole

Prior to all *in vitro* and *in vivo* investigations bioanalytical assays for the quantification of voriconazole in different matrices (microdialysate, plasma, UF, whole blood, and SB) by means of HPLC with subsequent UV detection have been developed [99, 100] and validated

(microdialysate, plasma) [100] according to international guidelines for bioanalytical methods, including determination of stability of analyte, specificity, accuracy, precision, linearity (calibration function), recovery, robustness, and ruggedness of voriconazole [101-105].

### 2.3.1 Quantification of voriconazole in microdialysate and plasma

#### 2.3.1.1 Method development

Voriconazole spiked matrices (plasma and microdialysate) were added to ACN in percentages from 10% – 90%. In addition, a variety of sample preparation (evaporation), HPLC separation (LiChrospher®-100 RP-8, LiChrospher®-100 RP-18, Spherisorb® ODS-2), and injection modes (normal mode, zero-sample loss mode) were evaluated.

Due to the inherently small sample volume obtained from microdialysis sampling, the smallest volume of microdialysate required was determined using the zero-sample loss mode of AS-2051/AS-1555 (see 2.2.1) controlled by Chrompass® (see 2.8) where the sample was sandwiched between two zones of mobile phase solvent and the entire sample volume was drawn into the loop and injected without loss.

#### 2.3.1.2 Preparation of stock solutions, calibration samples and quality control samples

Four stock solutions were separately prepared for calibration and quality control (QC) samples, respectively, by dissolving two times 5.2 mg and 5.1 mg voriconazole, respectively, in methanol yielding concentrations of 1.04 mg/mL for the microdialysate calibration and QC stock solution and 1.02 mg/mL for the plasma calibration and QC stock solution. The microdialysate calibration stock solution was diluted with water to obtain working solutions of 1.56, 5.20, 10.40, 20.80, 62.40, and 104.00 µg/mL for microdialysate and the other one to obtain working solutions of 1.53, 5.10, 10.20, 20.40, 51.00, and 102.00 µg/mL for plasma calibration samples. Working solutions for microdialysate (plasma) QC samples were prepared by diluting the QC stock solutions with water to yield voriconazole concentrations of 1.56 (1.53), 15.60 (15.30), 41.60 (40.80), and 83.20 (81.60) µg/mL. Aliquots of stock and working solutions were frozen at -70 °C. Microdialysate calibration samples were prepared prior to each analytical run by mixing 5 µL of aqueous working solution with 45 µL analyte-free Ringer's solution, yielding voriconazole concentrations of 0.156, 0.520, 1.040, 2.080, 6.240, and 10.400 µg/mL. Analogously, plasma calibration samples resulted from mixing 10 µL of aqueous working solution with 90 µL blank human plasma to obtain the final voriconazole concentrations of 0.153, 0.510, 1.020, 2.040, 5.100, and 10.200 µg/mL. For pre-study validation and quality control during in-study analytical runs spiked matrix samples were immediately prepared from aqueous QC working solutions by dilution with either Ringer's solution or blank human plasma. QC samples of microdialysate (plasma) contained 0.156 (0.153), 1.56 (1.53), 4.16 (4.08), and 8.32 (8.16) µg/mL voriconazole. QC samples at the lower limit of quantification (LLOQ) were only used for pre-study validation. Aliquots of QC samples for pre- and in-study validation were stored at -20 °C until analysis.

### 2.3.1.3 Voriconazole stability in microdialysate and plasma

The freeze-thaw, short-term ambient temperature, stock solution, and post-preparative stability of voriconazole in spiked samples were determined. All stability tests in both matrices were performed using low (1.56 µg/mL, 1.53 µg/mL, see 2.3.1.2) and high (8.32 µg/mL, 8.16 µg/mL, see 2.3.1.2) QC concentrations, analysed in triplicate and evaluated by comparing analytical results (peak area) for stored samples with those for freshly prepared samples as reference (Eq. 2-1).

**Eq. 2-1:** Calculation of stability, %.

$$\text{Stability, \%} = \frac{\text{Peak area}_{\text{stored sample}}}{\text{Peak area}_{\text{freshly prepared sample}}} \cdot 100$$

For the determination of the freeze-thaw stability of voriconazole, three sets of QC samples were analysed after one, two, or three freeze and thaw cycles (freezing at -20 °C for 24 h, completely thawing unassisted at room temperature, then refreezing for 24 h) and compared to freshly prepared samples by calculating the ratio between the peak area of the stored sample and the peak area of the freshly prepared sample (Eq. 2-1).

For the determination of stability at room temperature, QC samples were thawed at ambient temperature and kept at this temperature for 4 h or 24 h, chromatographically analysed (3.1.1.1), and evaluated as described above.

For the determination of stock solution stability, aliquots of the stock solution were thawed at room temperature and kept under these conditions for 6 h, chromatographically analysed (3.1.1.1), and evaluated as described above.

To determine the stability of processed samples at room temperature over time, a set of QC samples was prepared as described below (3.1.1.1). One part was stored at room temperature the other at -20 °C, in each case for 7 h. These results were compared with those from QC samples measured immediately after preparation and stability was calculated as mentioned above. One-way ANOVA and the Welch test, if homoscedasticity was not provided, were applied to compare means.

### 2.3.1.4 Specificity of the analytical method

Peak interference with that of voriconazole was investigated analysing voriconazole-free matrices, microdialysate, and plasma, from six different human sources, and a broad variety of drugs possibly co-administered with voriconazole at ICUs, in each matrix. For this purpose, aqueous solutions of the drug products were diluted with either blank plasma or Ringer's solution, to yield the following final concentrations which were at least in the clinically relevant range: acetylcysteine (5 mg/L), ambroxol (3 mg/L), clonidine hydrochloride (0.1 mg/L), ceftriaxone (0.15 mg/L), cefuroxime (500 mg/L), certoparin (10 U/mL), ciprofloxacin (5 mg/L), digitoxin (0.1 mg/L), dobutamine (0.6 mg/mL), enoxaparin (10 U/mL),

epinephrine hydrogen tartrate (1 mg/L), erythromycin (0.1 mg/mL), esketamine hydrochloride (0.5 mg/L), furosemide (1 mg/L), glyceryl trinitrate (0.1 mg/L), heparin sodium (5 U/mL), hydrocortisone (20 mg/L), insulin (100 U/L), metamizol sodium (80 mg/L), metoclopramide (1.5 mg/L), metoprolol (0.2 mg/L), metronidazole (50 mg/L), midazolam (0.2 mg/L), pantoprazole sodium (3 mg/L), piperacillin (0.5 mg/L), propofol (2.5 mg/mL), pyridostigmine bromide (0.1 mg/L), ranitidine hydrochloride (1 mg/L), sulbactam (70 mg/L), urapidil hydrochloride (5 mg/L), vancomycin (65 mg/L), vitamin supplement (1:100 dilution). Samples underwent preparation and HPLC analysis as described below (see 3.1.1.1). Investigations regarding the interference of voriconazole with an unknown endogenous substance (or substance mixture) during analysis of microdialysate samples originating from healthy volunteers (see 2.6 and 3.4) are presented in section 3.1.1.3.

#### 2.3.1.5 Accuracy and precision

Within- and between-day accuracy (or, more precisely, inaccuracy) and precision (or, more precisely, imprecision) were evaluated from the back-calculated concentrations of the calibration samples used to generate three different calibration curves. For pre-study validation six QC samples per concentration (covering the whole concentration range) and matrix were analysed on three days. Accuracy was calculated as the percentage deviation (relative error, RE) of measured concentration ( $C_{\text{calc}}$ ) of QC samples from their nominal concentration ( $C_{\text{nom}}$ ) (Eq. 2-2) and precision as the coefficient of variation (CV) from multiple determinations.

**Eq. 2-2:** Calculation of percentage deviation/relative error (RE), %.

$$\text{RE, \%} = \frac{C_{\text{calc}} - C_{\text{nom}}}{C_{\text{nom}}} \cdot 100$$

#### 2.3.1.6 Lower limit of quantification and assay linearity

LLOQ was assessed by comparing the chromatograms of blank matrix with those obtained from five spiked matrix samples at each concentration. For this purpose, voriconazole working solution was added to blank microdialysate (Ringer's solution) and plasma yielding concentrations from 0.05 µg/mL to 0.20 µg/mL. The lowest concentration of voriconazole which could be analysed with acceptable accuracy and precision ( $\pm 20\%$  RE and CV, respectively) was defined as LLOQ for each matrix. Calibration curves consisting of six calibrator concentrations were analysed by weighted linear regression. Linearity was evaluated in a concentration range from 0.15 µg/mL – 10 µg/mL for microdialysate and plasma samples (n=3 on day 1 and n=1 on days 2 and 3, respectively).

#### 2.3.1.7 Recovery of the analyte

For recovery determinations peak area data of at least five spiked matrix samples at three separate QC concentrations were compared to the results of three diluted aqueous solutions

of the same  $C_{nom}$  as the spiked matrix samples. The recovery was calculated according to Eq. 2-3.

**Eq. 2-3:** Calculation of recovery, %.

$$\text{Recovery, \%} = \frac{\text{Peak area}_{\text{processed sample}}}{\text{Peak area}_{\text{non-processed sample}}} \cdot 100$$

### 2.3.1.8 Robustness and ruggedness

After method development and validation according to the FDA guideline [101] the following aspects of robustness and ruggedness were investigated [102, 104, 105]:

1. accuracy (expressed as RE, %) and precision (expressed as CV, %) of determinations of plasma QC samples during long-term application and of measurement of microdialysate calibration and QC samples after longer periods, both during in-study validation;
2. the effect of a different analytical system, a different column batch, and analyst replacement (method transfer) on method accuracy, expressed as RE, %, and precision, expressed as CV, %, by evaluating microdialysate calibration and QC samples; and
3. the effect of different mobile phase pH on method accuracy and precision (expressed as RE, % and CV, %, respectively) using microdialysate calibration and QC samples.

Linearity of calibration curves, obtained during the investigation of the aspects 1 – 3, was analysed and expressed as coefficients of determination.

### 2.3.2 Determination of the unbound plasma concentration of voriconazole

For direct comparison of the (unbound) concentration of voriconazole in the interstitium, accessible by microdialysis (see 1.2), with the unbound fraction ( $f_u$ ) in plasma a separation of the protein-bound fraction of voriconazole had to be achieved. For this purpose, 1 mL plasma was transferred to an ultrafiltration device consisting of a sample reservoir (styrene acrylonitrile), a low-adsorptive hydrophilic membrane (Ultracel<sup>®</sup>, regenerated cellulose, nominal molecular mass limit: 30 kDa), an o-ring without plasticizer (ethylene propylene diene monomer rubber), a membrane support base (polycarbonate), and a filtrate cup (polyethylene). Devices were centrifuged at room temperature and 2,000 g for 20 min. Protein became selectively partitioned into a fraction of the sample volume (retentate), while free voriconazole passed unhindered through the membrane along with solvent, the so called ultrafiltrate (UF). To ensure suitability of the system for the intended application preliminary adsorption and retention studies were conducted. To investigate whether voriconazole interacted with any component of the ultrafiltration device aqueous solutions of voriconazole covering the concentrations of the calibration curve (0.156, 0.52, 1.04, 2.08, 6.24, and 10.4 µg/mL) were aliquoted in two samples for each concentration. One aliquot was subjected to ultrafiltration applying the same conditions as for plasma samples. RE of the ultrafiltered sample from the nominal value of the non-ultrafiltered sample was calculated in analogy to Eq. 2-2.

For quantification purposes, calibration samples are usually prepared using the same, but analyte-free matrix from which the quantification is desired. Since analyte-free UF was not sufficiently available for the preparation of calibration and QC samples, analytical results of voriconazole in microdialysate and UF were compared in order to evaluate whether the use of microdialysate calibration and QC samples for UF quantification is appropriate. Therefore, a calibrator with  $C_{\text{nom}}$  of 6.24  $\mu\text{g/mL}$  was prepared using analyte-free UF instead of Ringer's solution for microdialysate. To investigate the influence of a possibly incomplete protein separation during ultrafiltration, samples were centrifuged at 13,500  $g$  for 15 min ( $n=3$ ) or processed without an additional centrifugation step ( $n=3$ ). Subsequent to that, samples were assayed together with a microdialysate sample in Ringer's solution of the same concentration ( $n=3$ ). RE of the sample, made of analyte-free UF, from the result of the sample, made of Ringer's solution, was calculated in analogy to Eq. 2-2.

### 2.3.3 Quantification of voriconazole in whole blood samples

Calibration (0.2, 0.5, 1.0, 2.0, 5.0, 7.5  $\mu\text{g/mL}$ ) and QC (0.5, 1.0, 2.0  $\mu\text{g/mL}$ ) samples were identically prepared to plasma calibration and QC samples using analyte-free whole blood. Different modifications of the method for the quantification of voriconazole in plasma samples (sample volume, weighing of samples) were applied in order to account for possible preparation limits of whole blood. Method accuracy and precision were determined by means of RE and CV, respectively, of multiple determinations.

### 2.3.4 Quantification of voriconazole in skin biopsy samples

Blank guinea pig SB samples ( $n=3$ , 2.2 mg – 3.7 mg) were used for method development for the quantification of voriconazole in skin biopsies. The same biopsy punches involved in preclinical experiments (see 2.2.3 and 2.5.1.2, [99]) were used for the blank biopsy samples in order to obtain pieces of skin in the dimension comparable to the study specimens. After separating the subcutaneous fat tissue, blank samples were weighed (mass 1) and spiked with voriconazole by shaking them in a voriconazole solution ('spike-sol', e.g., with  $C_{\text{spike-sol } 1}$  5  $\mu\text{g/mL}$  of voriconazole in isotonic sodium chloride solution,  $m_{\text{spike-sol } 1}$  0.5  $\mu\text{g}$  voriconazole,  $V_{\text{spike-sol } 1}$  100  $\mu\text{L}$ ) overnight for approximately 16 h. Spiked skin biopsies were removed from the spike-sol solution reservoir by a pincer, slightly wrung out, weighed (mass 2) and the residual volume calculated ( $v_{\text{spike-sol } 2}$ ). The voriconazole concentration/mass of the spike-sol solution after the spiking procedure,  $C_{\text{spike-sol } 2}$  and  $m_{\text{spike-sol } 2}$ , were determined via HPLC with calibration samples (0.2, 0.5, 1.0, 2.0, 5.0, 7.5  $\mu\text{g/mL}$ ) identically prepared to microdialysate calibration samples using analyte-free isotonic sodium chloride solution. The preparation procedure was analogous to the one for microdialysate and plasma samples, i.e., samples were vortex mixed with ACN at a ratio of 40 to 60 (v/v), centrifuged at 13,500  $g$  for 10 min intended for 1) precipitation of proteins dissolved by the spiking procedure, 2) dilution, and 3) direct injection of the supernatant (30  $\mu\text{L}$ ) onto the HPLC system. HPLC system and assay conditions were consistent with the ones for the determinations in plasma.

## 2.4 II – *In vitro* microdialysis

Before microdialysis can validly be applied in preclinical or clinical settings (see 2.5 and 2.6) it is essential to comprehensively study the characteristics of the drug under investigation, i.e., voriconazole, *in vitro* with regards to the scheduled catheters. Moreover, the employment of the clinically approved drug product of voriconazole for calibration purposes was evaluated. All experiments were performed on a prior developed robust *in vitro* microdialysis system (IVMS). Finally, the *in vitro* results for voriconazole were compared with other antiinfectives.

### 2.4.1 Development of the *in vitro* microdialysis system (IVMS)

The prior method usually used at the Department to evaluate the suitability of microdialysis of a drug [48, 106, 107] was thoroughly revised. The final IVMS is displayed in Fig. 2-3, Fig. 2-4, and Fig. 2-5.

A base frame (No. 11, see legend for Fig. 2-3, Fig. 2-4 and Fig. 2-5) assured the fixation of all components. A rearward directed platform (No. 2) for the safe positioning of the microdialysis pumps (Nos. 12, 13) was mounted at the top. In the developed dimension (20.5 cm × 31 cm), two stationary pumps (e.g., CMA102<sup>®</sup>) (No. 13) and two portable pumps (e.g., CMA107<sup>®</sup>) (No. 12) together or up to six portable pumps (e.g., CMA107<sup>®</sup>) (No. 12) could be parallel stored. The platform (No. 2) was widthwise and lengthwise expandable enabling the positioning of further pumps (Nos. 12, 13). Microsyringes (e.g., CMA107<sup>®</sup>), filled with perfusate, were deposited in the pumps and fixed. Moreover, a forward directed thermoblock, 7 cm high and 10 cm in diameter (No. 9), manufactured from an aluminium alloy, was mounted at the base frame (No. 11). Beakers typically implemented in the former *in vitro* method were replaced by low-volume liquid (medium) containers (Fiolax, height 80 mm, Paschold Werner Glaswarenfabrik, Bamberg, Germany) (No. 21) placed in precisely fitting wells arranged in a circle inside the thermoblock (No. 9). A rack (No. 1) stuck out of the thermoblock (No. 9) providing the support for the stepless height adjustable multifunctional hardware adapter platform (No. 4). The latter incorporated the (embedded) mounting parts (Nos. 5-7, 29, 30, 33) for the catheters (Nos. 20, 32), the liquid (medium) containers (No. 21), and the cavities (No. 3) for the dialysate collection vials (0.5 mL – 2.5 mL) (No. 26). In contrast to concentric catheters (No. 20) which could be fixed directly (Nos. 19, 6) within the platform (No. 4) a special fitting, guide lug (No. 33) and guide cap (No. 29), had been developed for safely mounting linear catheters (No. 32) accounting for the bilateral design and the lack of a direct mount at the catheter itself. The complete hardware adapter platform (No. 4) could be covered by a transparent lid (No. 34). The thermoblock (No. 9) was directly connected to a programmable thermoblock temperature control module (No. 17) with digital display, mounted to the base frame (No. 11), facilitating precise and stepless temperature regulation during the experiments. Below the thermoblock a magnetic stirrer (RH basic 2, IKA, Staufen, Germany) (No. 10) provided the impulse for rotation of the magnetic stir bar (No. 25) inside the liquid (medium) containers (No. 21) and, hence, the agitation of the medium during the experiments.

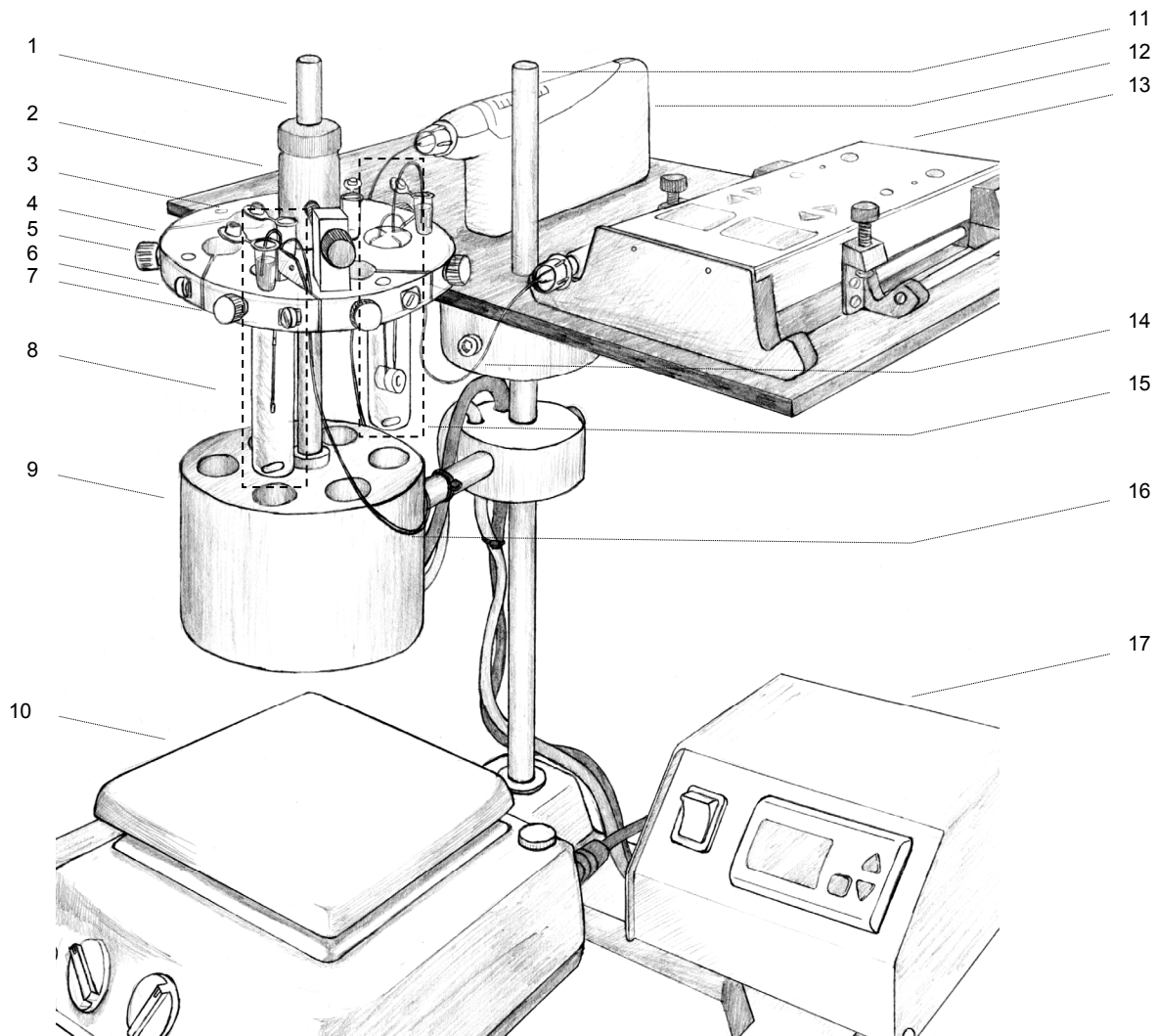


**Fig. 2-3:** *In vitro* microdialysis system (without cover lid (No. 34)) in loading position.

Legend for Fig. 2-3, Fig. 2-4 and Fig. 2-5 (for explanations see text)

- |  |  |
|--|--|
| 1 Rack   | 18 Outlet tubing of concentric catheter with dialysate |
| 2 Platform for microdialysis pumps                       | 19 Clamp of concentric catheter                        |
| 3 Cavity for dialysate collection vial                   | 20 Concentric catheter, e.g., CMA60®                   |
| 4 Multifunctional hardware adapter platform              | 21 Medium container                                    |
| 5 Mounting screw   | 22 Semipermeable membrane of concentric catheter       |
| 6 Embedded mounting screw                                | 23 Synthetic tip of concentric catheter                |
| 7 Trench for mounting concentric catheter                | 24 Liquid (medium)                                     |
| <b>8 Unit 'concentric catheter' (see Fig. 2-4, left)</b> | 25 Magnetic stir bar                                   |
| 9 Thermoblock with wells                                 | 26 Dialysate collection vial                           |
| 10 Magnetic stirrer                                      | 27 Dialysate   |
| 11 Base frame  | 28 Outlet tubing of linear catheter with dialysate     |
| 12 Portable pump, e.g., CMA107®, with syringe            | 29 Guide cap for linear catheter                       |
| 13 Stationary pump, e.g., CMA102®, with syringe          | 30 Trench for mounting linear catheter                 |
| 14 Inlet tubing of linear catheter with perfusate        | 31 Semipermeable membrane of linear catheter           |
| <b>15 Unit 'linear catheter' (see Fig. 2-4, right)</b>   | 32 Linear catheter, e.g., CMA66®                       |
| 16 Inlet tubing of concentric catheter with perfusate    | 33 Guide lug for linear catheter                       |
| 17 Thermoblock temperature control module                | 34 Cover lid   |



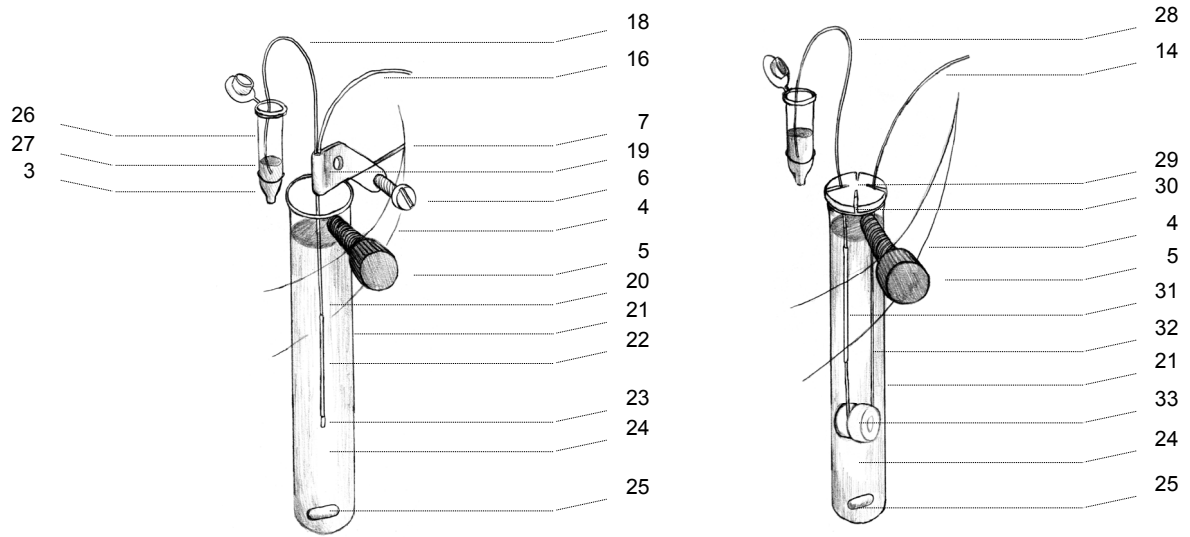


**Fig. 2-4:** Mounting parts of concentric (left, unit 'concentric catheter', No. 8 in Fig. 2-3) and linear (right, unit 'linear catheter', No. 15 in Fig. 2-3) microdialysis catheters as components of the *in vitro* microdialysis system.

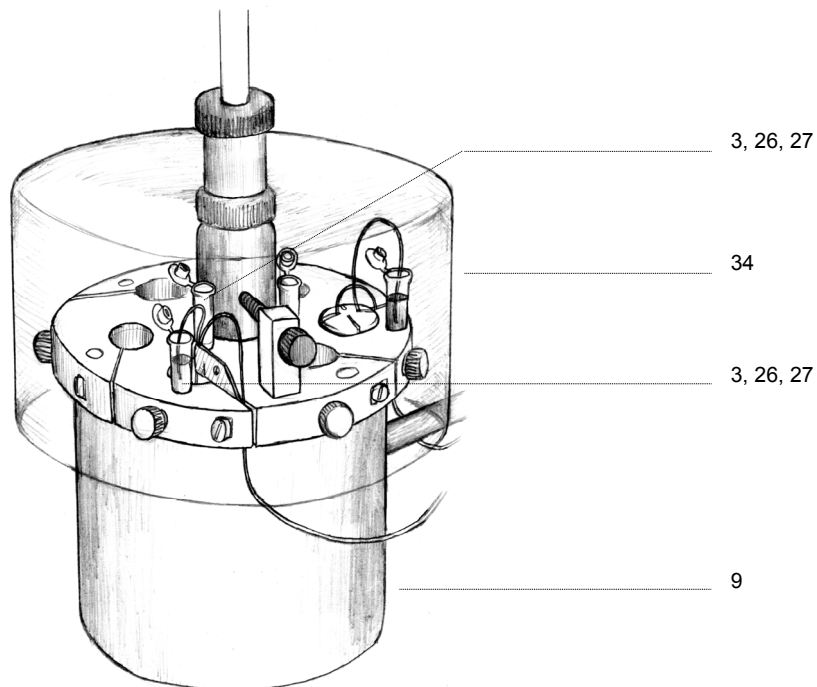


**Fig. 2-5:** Final position of the *in vitro* microdialysis system for *in vitro* microdialysis experiments with cover lid (No. 34) of the lowered platform (No. 4) into the thermoblock (No. 9) including the liquid (medium) containers (No. 21) and microdialysis catheters (Nos. 20, 32).

A preliminary model resulted from the model development process. This model integrated most of the components described for the final IVMS but lacks for constant temperature maintenance, compactness in alignment, and simple coverage option. For long-term storage of catheter once used those drawbacks were not of relevance and, hence, the preliminary model could offer its function as a depot.

## 2.4.2 *In vitro* microdialysis investigations

### 2.4.2.1 Preparation of solutions used as perfusate or medium

Solutions of voriconazole were prepared by dissolving the drug substance in methanol obtaining the stock solution of 0.2 g/mL. The stock solution was diluted with Ringer's solution yielding eight different final concentrations (1.0, 2.5, 5.0, 10.0, 20.0, 50.0, 100.0, 150.0 µg/mL). For Vfend<sup>®</sup> solution one powder-containing vial was resuspended with 19.0 mL water (10 mg voriconazole/mL). 50 µL of this solution were filled up with Ringer's solution resulting in a concentration of 5.0 µg/mL.

Solutions of linezolid or daptomycin were prepared by diluting already prepared stock solutions (linezolid: 1 mg/mL, daptomycin: 2 mg/mL, Department Clinical Pharmacy) with Ringer's solution yielding a final concentration of 5.0 µg/mL or 60.0 µg/mL, respectively.

### 2.4.2.2 Microdialysis settings

CMA60<sup>®</sup> and CMA66<sup>®</sup> microdialysis catheters and a high-precision pump CMA102<sup>®</sup> delivering perfusates at different flow rates were used for microdialysis investigations *in vitro*. The catheters were constantly perfused with physiological Ringer's solution without or with different amounts of voriconazole, Vfend<sup>®</sup> solution, linezolid, or daptomycin (perfusate), respectively.

For all *in vitro* experiments medium samples were stirred (600 1/min) and investigated at body temperature (37 °C) employing the developed IVMS (see 2.4.1). The peak areas of perfusates and dialysates (see 2.3.1) of the experiments were used for the calculations of RR (Eq. 1-1 for delivery experiment; Eq. 1-2 for recovery experiment with  $C_{\text{medium}}$  equivalent to  $C_{\text{ISF, unbound}}$ ) and further statistical evaluations.

Stability of voriconazole in Ringer's solution in the microdialysis system under the *in vitro* experimental conditions at 37 °C was measured over a period of 10 h (10 µg/mL, n=3). The peak areas of the voriconazole samples (see 2.3.1) were compared with the peak area of the voriconazole solution samples measured at the beginning of the experiment and set to 100%. Deviations in a random pattern of less than ±15% were considered to indicate stability.

### 2.4.2.3 Dependencies of relative recovery

In order to assess the dependency of RR of voriconazole on flow rate and concentration three microdialysis catheters perfused with either Ringer's solution at different voriconazole concentrations (delivery experiment; retrodialysis) or analyte-free Ringer's solution (recovery

experiment) were placed in medium with either analyte-free Ringer's solution (delivery experiment; retrodialysis) or Ringer's solution at different voriconazole concentrations (recovery experiment). For experimental details and direct comparison, the settings are listed in Tab. 2-2.

**Tab. 2-2:** Experimental settings to investigate the dependency of relative recovery (RR) on flow rate (0.4, 0.8, 1.0, 1.5, 2.0, 2.5, 5.0, 7.5, 10.0  $\mu\text{L}/\text{min}$ ) and on voriconazole concentration (1.0, 2.5, 5.0, 10.0, 20.0, 50.0  $\mu\text{g}/\text{mL}$ ) for CMA60<sup>®</sup> and CMA66<sup>®</sup> catheters. w/o: without.

Experimental arrangement	Recovery experiment - on flow rate -	Delivery experiment	Recovery experiment - on concentration -	Delivery experiment
Temperature [ $^{\circ}\text{C}$ ]	-----		37	-----
Stirring velocity [1/min]	-----		moderate (600)	-----
<i>CMA60<sup>®</sup> catheters (n=3)</i>				
Flow rate [ $\mu\text{L}/\text{min}$ ]	0.4 – 10	-	1.5	1.5
Perfusate [ $\mu\text{g}/\text{mL}$ ]	Ringer's w/o drug	-	Ringer's w/o drug	1.0 – 50.0
Medium [ $\mu\text{g}/\text{mL}$ ]	10.0	-	1.0 – 50.0	Ringer's w/o drug
Dialysate [ $\mu\text{g}/\text{mL}$ ]	-----		to be measured	-----
<i>CMA66<sup>®</sup> catheters (n=3)</i>				
Flow rate [ $\mu\text{L}/\text{min}$ ]	1.0 – 2.5	1.0 – 2.5	2.0	2.0
Perfusate [ $\mu\text{g}/\text{mL}$ ]	Ringer's w/o drug	5.0	Ringer's w/o drug	1.0 – 10.0
Medium [ $\mu\text{g}/\text{mL}$ ]	5.0	Ringer's w/o drug	1.0 – 10.0	Ringer's w/o drug
Dialysate [ $\mu\text{g}/\text{mL}$ ]	-----		to be measured	-----

RR of voriconazole was assessed performing the recovery and retrodialysis method described by STAHLÉ et al. [49] at nine flow rates of 0.4, 0.8, 1.0, 1.5, 2.0, 2.5, 5.0, 7.5, and 10.0  $\mu\text{L}/\text{min}$  to determine an optimal flow rate for subsequent *in vitro* and *in vivo* experiments and for estimating the mass transfer coefficient. Samples (n=3) were collected at different intervals (2 min – 50 min) considering the actual flow rate and minimal sample volume required for HPLC analysis and analysed (see 3.1.1).

To investigate the dependence of RR of voriconazole from the concentration (1.0, 2.5, 5.0, 10.0, 20.0, 50.0  $\mu\text{g}/\text{mL}$  of voriconazole) of perfusate three catheters were perfused with Ringer's solution at a flow rate of 1.5  $\mu\text{L}/\text{min}$  or 2.0  $\mu\text{L}/\text{min}$ . Samples were taken every 13 min or 10 min (n=3 each), respectively, and analysed (see 3.1.1).

To explore whether the clinically approved drug product Vfend<sup>®</sup> can be employed for calibration purposes a microdialysis catheter (CMA60<sup>®</sup>) was perfused with either a solution (Ringer's solution) of voriconazole drug substance or the drug product Vfend<sup>®</sup> at a concentration of voriconazole of 5.0  $\mu\text{g}/\text{mL}$  during a delivery experiment. Analysis was performed in triplicate and the chosen flow rate of the respective perfusate was 1.0  $\mu\text{L}/\text{min}$ . Samples were taken every 20 min and analysed (see 3.1.1).

To estimate the mass transfer coefficient, RR of linezolid (one catheter in 5  $\mu\text{g}/\text{mL}$ ) and daptomycin (three catheters in 60  $\mu\text{g}/\text{mL}$ ) were assessed performing microdialysis at flow rates of 1.0, 1.5, 2.0, 2.5, 5.0, 7.5, and 10.0  $\mu\text{L}/\text{min}$  and 0.2, 1.0, 1.5, 2.0, 2.5, 5.0, 7.5, and 10.0  $\mu\text{L}/\text{min}$ , respectively. Samples (n=3 for each flow rate and each catheter) were collected at different intervals (2 min – 14 min and 4 min – 200 min, respectively) with respect to the

actual flow rate and minimal sample volume required for HPLC analysis. The preparation procedure and bioanalytical assay specifications for the analysis of the dialysates containing linezolid were performed as developed at the Department of Clinical Pharmacy at the Freie Universität in Berlin prior to the investigation [106]. For the samples with daptomycin a previously at the Department of Clinical Pharmacy, MLU developed analytical HPLC assay for the determination of daptomycin from Mueller-Hinton broth provided the basis for the sample preparation procedure and assay conditions for the dialysates. Due to the lack of proteins every *in vitro* sample (20 µL) was directly injected into the HPLC system 1 (see 2.2.1). The mobile phase consisting of an ACN/ammonium phosphate buffer (pH 4.5; 40 mM; 44/66, v/v) was used under isocratic conditions at a flow rate of 1 mL/min. All samples were separated on a LiChrospher®-100 RP-18 (e, 5, 4.0 × 250) with an integrated precolumn as the stationary phase. The column temperature was maintained at 25 °C. Monitoring of daptomycin was realised with UV detection at a wavelength of 225 nm. Repeated measurements of the daptomycin solution (60 µg/mL, n=5) resulted in a CV of 2.7%. Hence, the method was evaluated as precise also relying upon the validation results obtained for Mueller-Hinton broth (internal communication; overall RE Range (R): -10.2% – +11.2% (n=18) and overall CV R: 1.4% – 8.3% (n=18), respectively).

#### 2.4.2.4 Steady state investigations

If the retrodialysis method was to be used for *in vivo* catheter calibration after multiple dosing at steady state, the calibration solution should be high enough to ensure that voriconazole diffuses from the catheter into the ISF as voriconazole is already present in the tissue fluid. Voriconazole solutions of 50, 100, 150, and 200 µg/mL were investigated as perfusate flowing through a catheter (CMA60®) with a surrounding medium of 10 µg/mL voriconazole. Dialysate samples of three catheters were collected in triplicate at intervals of 10 min and analysed (see 3.1.1).

## 2.5 III – Influence of disease state on target site exposure

This exploratory preclinical study was carried out in cooperation with the Unit of Mycology and Parasitology, Statens Serum Institut, Copenhagen, Denmark. The experiments were approved by the Animal Experiments Inspectorate under the Danish Ministry of Justice (2003/561-868). All experimental procedures were carried out under biosafety level 3 conditions owing to the risk of transmission of infection by *Microsporium* spores.

### 2.5.1 Study design and study procedure

Three of 18 included female guinea pigs (Harlan Netherlands, Horst, The Netherlands, 418 g to 482 g) were subjected to a PK analysis of voriconazole concentrations after twelve days of multiple dosing in a) both healthy (ISF<sub>H</sub>, neck) and infected (ISF<sub>IN</sub>, flank) subcutaneous adipose tissue ISF, b) SB, and c) whole blood specimens. Study procedures are summarised



fusate (Fig. 2-6, b). In order to let the tissue recover from insertion trauma an equilibration period of 30 min was allowed prior to the start of the experiment (Fig. 2-6, b→c). Prior to voriconazole administration, *in vivo* RR of voriconazole was determined in each of the guinea pigs by means of retrodialysis [49]. For calibration, two perfusates containing different concentrations of voriconazole ( $C_{RP}$ :  $RP_{low}$  5  $\mu\text{g/mL}$  and  $RP_{high}$  10  $\mu\text{g/mL}$ ) were used (Fig. 2-6, c, e) applying a flow rate of 1  $\mu\text{L/min}$ . The first *in vivo* catheter calibration procedure was carried out starting with an equilibration period of 15 min with  $RP_{low}$  (Fig. 2-6, c→d) followed by retrodialysate sampling (interval of 30 min,  $RR_{low}$ ) (Fig. 2-6, d→e). The second *in vivo* catheter calibration procedure started with an equilibration period of 30 min with  $RP_{high}$  (Fig. 2-6, e→f) as perfusate followed by retrodialysate sampling (interval of 30 min,  $RR_{high}$ ) (Fig. 2-6, f→g). Afterwards, a washout period, initiated by changing the RP to sodium chloride (Fig. 2-6, g), of 30 min (Fig. 2-6, g→h) was performed and, then, a baseline microdialysate sample ( $T_0$ ) of 30 min (Fig. 2-6, h→i) was taken.

The *in vivo* RR ( $RR_H$  for healthy and  $RR_{IN}$  for inflamed areas) were calculated according to Eq. 1-1 (see 1.2.3). Beginning with the end of the administration of voriconazole (twelfth dose) six dialysates were collected every 30 min over a period of 3 h (Fig. 2-6, i→j ( $T_{30}$ ), j→k ( $T_{60}$ ), k→l ( $T_{90}$ ), l→m ( $T_{120}$ ), m→n ( $T_{150}$ ), n→o ( $T_{180}$ )). Samples were analysed employing the developed analytical assay (see 3.1.1).

#### 2.5.1.2 Skin biopsy and blood specimen sampling

After the twelfth dose of voriconazole full-thickness SB specimens (diameter: 3 mm) were punched and subsequently cut off with a knife from the margin of the inoculated areas every hour according to Fig. 2-6 (k, m, o) for 3 h. No adherence of the biopsies to fat or muscles was recorded. Blood samples were obtained from the eye vein and collected hourly starting with a baseline sample before the twelfth administration and continuing hourly after voriconazole administration (Fig. 2-6, i, k, m, o) for 3 h. Blood and therefrom obtained unbound blood ( $\text{blood}_u$ ) samples were analysed using the developed assay (2.3.2, 2.3.3, 3.1.2, and 3.1.3). For the analysis of the study biopsy specimens sample masses ( $n=12$ ) were determined and the extraction was performed as described for the method development of the quantification of voriconazole in SB samples (2.3.4 and 3.1.4, [99]). After measurement and data processing concentrations were transformed by means of method recovery.

### 2.5.2 Dataset and pharmacokinetic analysis

One dataset for all subjects was built including information about dosing, sampling time points, and measured concentrations in the five different matrices investigated. Voriconazole concentration values below the LLOQ were set to zero if they have been obtained for samples before the first quantifiable value after drug administration, if after these values were defined as missing values. Apparent concentrations in the microdialysates were transformed into the final ISF concentrations ( $C_{ISF,H}$ ,  $C_{ISF,IN}$ ) while accounting for the recovery results according to Eq. 1-2 (see 1.2.3).

The PK of voriconazole in ISF, SB, and whole blood was examined in the software Excel and WinNonlin® (see 2.8) applying the non-compartmental approach (NCA) which is explained in section 0. For each matrix the steady state (index: SS) parameters  $t_{SS,max}$ ,  $C_{SS,max}$ , and partial  $AUC_{SS,0-3h}$  (linear trapezoidal rule) were estimated and in order to quantify the extent of voriconazole distribution in the different matrices AUC ratios were calculated (SB/blood, SB/blood<sub>u</sub>, ISF<sub>H</sub>/blood, ISF<sub>H</sub>/blood<sub>u</sub>, ISF<sub>IN</sub>/blood, ISF<sub>IN</sub>/blood<sub>u</sub>, ISF<sub>IN</sub>/ISF<sub>H</sub>) where the AUC corresponded to the area under the concentration-time curve for matrix concentration data from 0 h – 3 h. Apart from  $t_{SS,max}$ , given as median and range, parameters will be presented as geometric mean values (see 1.1).

## 2.6 IV – Clinical long-term microdialysis pilot study with voriconazole in healthy volunteers

The study was approved by the Ethics Committee of the Medical University of Vienna, Austria, and was conducted in cooperation with the Department of Clinical Pharmacology, Medical University of Vienna, Austria, in accordance with the Declaration of Helsinki, as amended in Seoul 2008 [108].

### 2.6.1 Study design

The investigation was designed as a prospective, sequential, two part, open-labelled, uncontrolled trial. For this exploratory study no blinding procedure was performed. As this was the first human study of voriconazole employing the microdialysis technique determining the target site concentrations over several days (single and multiple dosing) the trial has been divided into two subsequent parts:

Part I: Pilot study with two microdialysis catheters (linear CMA66® and concentric CMA60® design) and an extensive sampling schedule (ESS) (Tab. 2-3) in three healthy volunteers to determine the feasibility of the long-term *in vivo* microdialysis catheter insertion and entire sampling schedule for single and multiple dose investigations. If infeasible, a reduced sampling schedule (RSS) (Tab. 2-3) was to be chosen for part II, i.e., the RSS will be employed if the long-term insertion of the catheters emerged being not feasible and the catheters will have to be displaced after a certain time.

Part II: Main study with the sampling schedule selected from part I, i.e., ESS with one long-term insertion of the selected catheter or RSS with two short-term insertions of the catheters (15 h) and sparse sampling (see Tab. 2-3).

**Tab. 2-3:** Schematic dosing and sampling schedule for single and multiple dose investigations (a visit involves one drug administration and all subsequent observations).

<b>Study days</b>						
----- 1 -----		----- 2 -----		----- 3 -----		----- 4 -----
<b>Study visits</b>						
1	2	3	4	5	6	7
<b>Time [h]</b>						
0 - 12	12 - 24	24 - 36	36 - 48	48 - 60	60 - 72	72 - 84
<b>Sequence dosing schedule</b>						
iv (6 mg/kg WT)	iv (6 mg/kg WT)	iv (4 mg/kg WT)	iv (4 mg/kg WT)	po (200 mg)	po (200 mg)	po (200 mg)
<b>Extensive sampling schedule (ESS)</b>						
<i>Insertion of microdialysis catheter</i>						
x <sup>a</sup> -----						
<i>Microdialysate sampling (ISF<sub>c</sub> and ISF<sub>f</sub>)<sup>c,d</sup></i>						
intensive	sparse	sparse	sparse	intensive	-	intensive
<i>Plasma sampling<sup>c,d</sup></i>						
intensive	sparse	sparse	sparse	intensive	sparse	intensive
<b>Reduced sampling schedule (RSS)</b>						
<i>Insertion of microdialysis catheter</i>						
x <sup>b</sup> -----			----- x <sup>b</sup> -----			
<i>Microdialysate sampling (ISF<sub>c</sub> and ISF<sub>f</sub>)<sup>c,d</sup></i>						
intensive	sparse	-	-	-	-	intensive
<i>Plasma sampling<sup>c,d</sup></i>						
intensive	sparse	sparse	sparse	sparse	sparse	intensive

<sup>a</sup>For ~87 h.<sup>b</sup>For ~15 h.<sup>c</sup>Intensive sampling: 15-16 samples per study visit (see Tab. 2-4).<sup>d</sup>Sparse sampling: 2-6 samples per study visit (see Tab. 2-4).

Nine male healthy volunteers were planned to be enrolled into the entire two-part study with three allocated to part I (pilot study). This thesis deals with the conduction and evaluation of the pilot study. In case of proven feasibility of the new approach investigated in the pilot phase further six individuals were planned to be allocated to part II (main study).

Inclusion and exclusion criteria as well as reasons for withdrawal for healthy volunteers are summarised in Tab. 7-1. Lifestyle restrictions during the study are listed in Tab. 7-2. Microdialysis catheters resided in the tissue according to the ESS or RSS. Throughout the period during which catheters were inserted, individuals were not allowed to take a bath and obligatorily had to cover the catheter with a plastic wrap and the pump with a plastic bag in order to avoid wetting when taking a shower. In addition, the investigator instructed the individuals to refrain from intensive sports or activities to avoid premature dislocation of the catheters.



Voriconazole was administered as sequence dosing, i.e., as an iv infusion of 6 mg per kg body weight (WT) over 2 h (initial two loading doses on day 1, dosing interval  $\tau=12$  h) and 4 mg per kg WT over 1.3 h (following two doses on day 2,  $\tau=12$  h). Subsequent doses of 200 mg voriconazole tablets were swallowed in intervals of 12 h for 1.5 days (see 2.6.3). Blood and microdialysis samples were taken according to the ESS (see Tab. 2-4). In the case of failed feasibility of the long-term insertion of the catheter in a volunteer leading to a discontinuation of microdialysate sampling samples would have been taken according to the RSS (see Tab. 2-4).

**Tab. 2-4:** Sampling time points (blood, red) and time intervals (microdialysate, blue).

Extensive sampling schedule (ESS) <sup>1</sup>	Reduced sampling schedule (RSS) <sup>2</sup>
<b>Visit 1<sup>a</sup></b> 0, 0.5, 1, 1.5, 1.75, 2, 2.25, 2.5, 3.25, 4.5, 6, 8, 9, 10, 11, 12 h 0-0.5, 0.5-1, 1-1.5, 1.5-2, 2-2.5, 2.5-3, 3-3.5, 3.5-4, 4-5, 5-6, 6-7, 7-8, 8-9, 9-10, 10-11, 11-12 h	<b>Visit 1<sup>a</sup></b> 0, 0.5, 1, 1.5, 1.75, 2, 2.25, 2.5, 3.25, 4.5, 6, 8, 9, 10, 11, 12 h 0-0.5, 0.5-1, 1-1.5, 1.5-2, 2-2.5, 2.5-3, 3-3.5, 3.5-4, 4-5, 5-6, 6-7, 7-8, 8-9, 9-10, 10-11, 11-12 h
<b>Visit 2<sup>b,c</sup></b> 2 h, 2 x 12 h <sup>d</sup> 0-20, 20-40, 40-60, 60-80, 80-100, 100-120 min	<b>Visit 2<sup>b</sup></b> 2 h, 2 x 12 h <sup>d</sup> 0-20, 20-40, 40-60, 60-80, 80-100, 100-120 min
<b>Visit 3<sup>b,c</sup></b> 80 min, 2 x 12 h <sup>d</sup> 0-20, 20-40, 40-60, 60-80 min	<b>Visit 3<sup>b</sup></b> 80 min, 2 x 12 h <sup>d</sup>
<b>Visit 4<sup>b,c</sup></b> 80 min, 2 x 12 h <sup>d</sup> 0-20, 20-40, 40-60, 60-80 min	<b>Visit 4<sup>b</sup></b> 80 min, 2 x 12 h <sup>d</sup>
<b>Visit 5<sup>a</sup></b> 0.5, 1, 1.5, 1.75, 2, 2.25, 2.5, 3.25, 4.5, 6, 8, 9, 10, 11h, 2 x 12 h <sup>d</sup> 0-0.5, 0.5-1, 1-1.5, 1.5-2, 2-2.5, 2.5-3, 3-3.5, 3.5-4, 4-5, 5-6, 6-7, 7-8, 8-9, 9-10, 10-11,3 h	<b>Visit 5<sup>b</sup></b> 2 x 12 h <sup>d</sup>
<b>Visit 6<sup>b</sup></b> 2 x 12 h <sup>d</sup>	<b>Visit 6<sup>b</sup></b> 2 x 12 h <sup>d</sup>
<b>Visit 7<sup>a</sup></b> 0.5, 1, 1.5, 1.75, 2, 2.25, 2.5, 3.25, 4.5, 6, 8, 9, 10, 11, 12 h 0-0.5, 0.5-1, 1-1.5, 1.5-2, 2-2.5, 2.5-3, 3-3.5, 3.5-4, 4-5, 5-6, 6-7, 7-8, 8-9, 9-10, 10-11, 11-12 h	<b>Visit 7<sup>a</sup></b> 0.5, 1, 1.5, 1.75, 2, 2.25, 2.5, 3.25, 4.5, 6, 8, 9, 10, 11, 12 h 0-0.5, 0.5-1, 1-1.5, 1.5-2, 2-2.5, 2.5-3, 3-3.5, 3.5-4, 4-5, 5-6, 6-7, 7-8, 8-9, 9-10, 10-11, 11-12 h

<sup>1</sup>Sampling from one microdialysis catheter over the entire period of 84 h.

<sup>2</sup>Sampling from two microdialysis catheters (14 h (visit 1+2) and 12 h (visit 7)).

<sup>a</sup>Intensive blood and microdialysate sampling.

<sup>b</sup>Sparse blood sampling.

<sup>c</sup>Sparse microdialysate sampling.

<sup>d</sup>Tandem: two blood samples were taken instead of one.

## 2.6.2 *In vivo* long-term microdialysis study setting

The *in vivo* microdialysis pilot study setting is illustrated in Fig. 2-7. For the safe protection of the microdialysis pumps during the entire study duration, particularly at night, a modified medicinal belt (Lohmann & Rauscher, Vienna, Austria) was employed which allowed to cover and to fix the pump directly at the human body and at the same time avoiding the direct contact to the skin. Moreover, the bags of the belts allowed for an easy and fast change of the syringes in the pumps. Both microdialysis catheters were fixed and protected by a transparent adhesive tape. Safe microdialysate sampling as well as the easy and fast change of the microvials were guaranteed by outlet tubing guide channels with a precisely tailored fitting connection for the microvials (see Fig. 2-2). A disposable common medicinal skirt

protected the pumps from water when a shower was taken. For additional protection during the night a fastened medicinal cuff was applied on an optional basis.

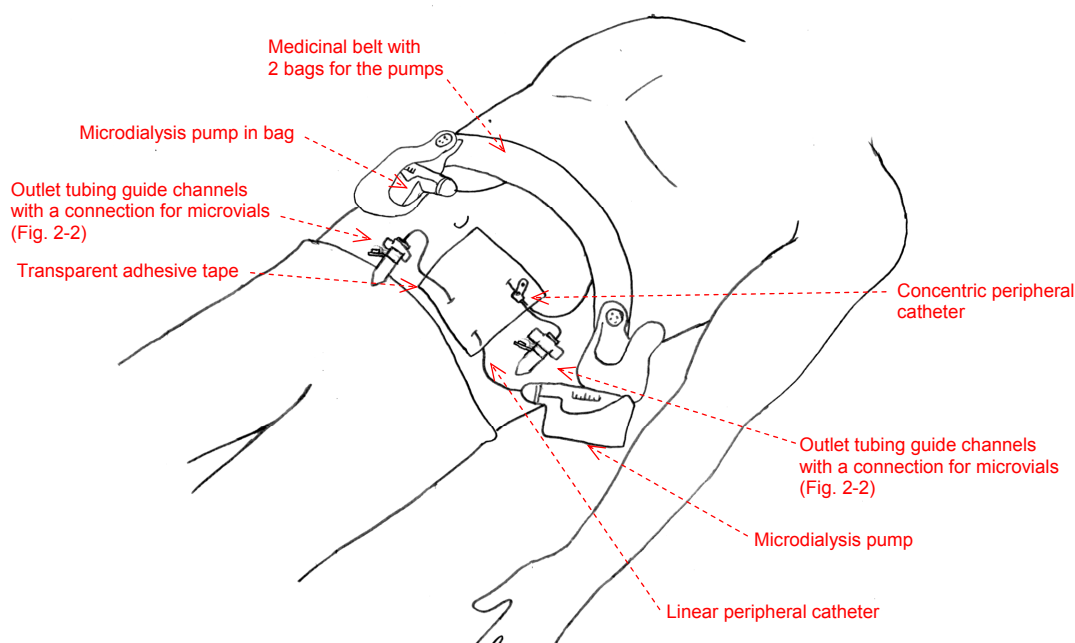


**Fig. 2-7:** *In vivo* microdialysis setting for long-term sampling during the clinical pilot study in healthy volunteers.

### 2.6.3 Study procedure according to the clinical study protocol

First, the volunteers had to take part in one screening visit. Seven study visits had to be completed according to the ESS. A visit was defined as the time span between the start of a drug administration and the start of the next administration. At all study visits vital signs were determined, AEs, food intake within 2 h prior to oral administration and concomitant drugs were recorded, and at study visit 1 the drug history of the last 14 days was documented. During the study procedures, the volunteers were mostly in a resting position and were recommended to continue in this resting position at home. The iv administration of voriconazole was performed using an automatic infusion apparatus with a maximum infusion rate of 3 mg voriconazole/kg WT per h for 2 h (6 mg/kg) or 1.3 h (4 mg/kg), respectively. On completion of infusion, about 50 mL isotonic physiological saline solution were infused via the infusion tubing to rinse and to guarantee that the complete dosage has been administered (infusion rate: same as for voriconazole infusion). Voriconazole tablets were swallowed with ~200 mL water.

#### Screening visit

Each recruited healthy volunteer was scheduled to undergo a general physical examination by a physician, including, e.g., an anamnesis, determination of BMI, drawing of blood for

laboratory screening tests and virology, vital signs recording (blood pressure (BP) and heart rate (HR) measured after 5 min rest in supine position) according to the study schedule (Tab. 7-3).

In addition, an electrocardiogram (ECG) was performed and an ophthalmological examination took place to ensure the absence of abnormalities. For genotyping, one whole blood sample (~4 mL) was drawn. Furthermore, drug screening in urine and urinalysis were performed. The screening visit took place within three weeks before study day 1. Prior to inclusion volunteers were informed about the nature, scope and the procedures of the study, and about the risks involved. Upon signature of the informed consent form and provided that volunteers fulfilled the inclusion but not the exclusion criteria, volunteers were enrolled into the study. At screening, each individual screened was identified by a given consecutive screening individual number and his initials (the first letter of the first name and the first letter of the surname). At the end of screening each finally enrolled individual was identified by a given consecutive individual number and his initials (the first letter of the first name and the first letter of the surname).

#### *Study day 1 - Study visit 1*

In the morning (~6 a.m.) of study day 1, the volunteers were admitted to the clinical research ward of the Department of Clinical Pharmacology, Medical University of Vienna (RWCP). HR, BP, and WT were recorded. An indwelling catheter was inserted, into the antecubital vein for the administration of voriconazole. A second indwelling catheter with a switch-valve was inserted into the contralateral arm vein, into the antecubital vein, to monitor plasma concentrations of voriconazole. To monitor ISF concentrations of voriconazole two microdialysis catheters were inserted (CMA60<sup>®</sup> and CMA66<sup>®</sup>, see 2.2.2.2 and 2.6.2). The skin of the periumbilical abdomen was cleaned and disinfected at the site of the microdialysis catheter insertion (see 2.1.4) and then horizontally punctured by a steel guidance cannula without anaesthesia. Using this guidance cannula, the microdialysis catheters were placed into the subcutaneous tissue. The microdialysis system was connected and perfused with Ringer's solution at a flow rate of 2.0  $\mu\text{L}/\text{min}$  provided by a microinfusion pump (CMA107<sup>®</sup>, see 2.2.2.1). After insertion of the catheter an equilibration period of 30 min and the *in vivo* catheter calibration procedure (40 min) (see 2.6.6) were performed. Next, 6 mg voriconazole per kg WT was administered iv over a period of 120 min. At pre-defined time intervals – according to the ESS (Tab. 2-4) – blood (~4 mL each) and microdialysis (~60  $\mu\text{L}$  to ~120  $\mu\text{L}$  each, depending on the interval) samples were taken.

#### *Study day 1 - Study visit 2*

Study visit 2 started with the second iv administration of 6 mg voriconazole per kg WT within 120 min 12 h after the first iv administration. During administration, blood (~4 mL each) and microdialysis (~40  $\mu\text{L}$  each) samples were taken according to the ESS (Tab. 2-4). The volunteers stayed at the RWCP for the night. Flow rates of the microdialysis pumps were adjusted to 0.5  $\mu\text{L}/\text{min}$  during the night until next study visit.

*Study day 2 - Study visit 3*

Study visit 3 started with the first iv administration of the maintenance dose of 4 mg voriconazole per kg WT 12 h after last administration. During administration, blood (~4 mL each) and microdialysis (~40 µL each) samples were taken according to the ESS (Tab. 2-4). After the sampling, retrodialysis was performed (see 2.6.6). Flow rates of the microdialysis pumps were adjusted to 0.5 µL/min until next study visit. After a short time under supervision (~ up to 0.5 h) the volunteers left the RWCP.

*Study day 2 - Study visit 4*

Study visit 4 was identical to study visit 3 except that no retrodialysis was conducted. The volunteers left the RWCP for the night.

*Study day 3 - Study visit 5*

Study visit 5 started with the determination of WT and the first oral administration of 200 mg voriconazole 12 h after last administration. Before and after administration, blood (~4 mL each) and microdialysis (~60 µL to ~160 µL each, depending on the interval) samples were taken according to the ESS (Tab. 2-4). Afterwards, a retrodialysis was performed (see 2.6.6). Flow rates of the microdialysis pumps were adjusted to 0.5 µL/min until study visit 7. After a short time under supervision (~ up to 0.5 h) the volunteers left the RWCP for the night.

*Study day 3 - Study visit 6*

Study visit 6 started with the second oral administration of 200 mg voriconazole 12 h after last administration. Before administration, blood (~4 mL each) samples were taken according to the ESS (Tab. 2-4). After a short time under supervision (~ up to 0.5 h) the volunteers left the RWCP for the night.

*Study day 4 - Study visit 7*

Study visit 7 started with the third oral administration of 200 mg voriconazole 12 h after last administration. Before administration, blood (~4 mL each) samples were taken according to the ESS (Tab. 2-4). After administration, blood (~4 mL each) and microdialysis (~60 µL to ~120 µL each, depending on the interval) samples were taken according to the ESS (Tab. 2-4). Afterwards a retrodialysis was performed (see 2.6.6). After a short time under supervision (~ up to 0.5 h) the volunteers left the RWCP.

*Final examination*

At least one day, but not longer than seven days, after the last drug administration, a final examination for safety was performed by a physician. The evaluation included vital signs, a physical examination (including clinical chemistry, haematology, urinalysis, WT, ECG, and ophthalmological examination as at screening visit except for drug screening and virology), and AE monitoring.

The study procedures according to the ESS described in this section was analogous to the study procedure according to the RSS. However, a reduced number of samples would have been taken according to Tab. 2-4.

#### 2.6.4 Laboratory investigations

Besides the medical history, physical examination, and an ECG the participants were ascertained to be healthy by laboratory screening:

Haematology – erythrocytes concentration, WBC, haemoglobin, mean corpuscular volume, mean corpuscular haemoglobin, mean corpuscular haemoglobin concentration, haematocrit, thrombocytes concentration.

Clinical chemistry – Total bilirubin, AP, ASAT, ALAT,  $\gamma$ -GTP, LDH, creatinine.

Virology – HIV, HepB antigen and HepC antibody only at screening.

Urinalysis – Stix<sup>®</sup> Test and drug screening for amphetamines, barbiturates, opiates, cocaine, methadone were performed only at screening.

Coagulation test – Activated partial thromboplastin time, normotest.

Genotype – genotype of the CYP isoenzymes 2C9, 2C19 by pyrosequencing (see 2.6.8).

Measurement of Visual Acuity – Distance best-corrected visual acuity (BCVA) was measured using the standard Early Treatment Diabetic Retinopathy Study charts at screening and the final examination. In addition, near BCVA was measured with Jaeger reading charts at distances of 20 cm or 40 cm. All tests for visual activity were performed by qualified ophthalmologists.

#### 2.6.5 Documentation

All findings during the monitoring of the volunteers throughout the course of the trial were recorded in the case report forms (CRFs). The records included the study number, the written informed consent, visit dates of the individual, records of vital signs, medical history or examinations, laboratory results, concomitant treatment and sample collection times for diagnostic as well as PK samples, any AE encountered, and other notes as appropriate. A physician assessed the severity according to the predefined criteria on the AE page. Clinical laboratory and haematology parameters were provided as print-outs which were signed and dated by the investigator. Comments on all clinically significant abnormal values were given by the investigator.

#### 2.6.6 Calibration procedure of microdialysis catheters

The calibration procedure of the microdialysis catheters was repeatedly performed by retrodialysis (see 1.2.3) covering the entire study duration. The first *in vivo* catheter calibration procedure was carried out prior to the first voriconazole administration at study visit 1 starting with an equilibration period of 10 min with RP1 (see 2.1.4.1) followed by retrodialysate sampling (two intervals of 15 min). Afterwards a washout period of 30 min was performed and then a baseline microdialysate sample of 15 min was taken. For microdialysis catheter calibration during voriconazole administration after ~25 h, ~59 h, and ~84 h (i.e., at the end of the sampling period of study visit 3, 5, and 7), the procedure started with an equilibration period of 10 min with RP2 (see 2.1.4.1) as the perfusate, followed by retrodialysate sampling (two intervals of 15 min).

### 2.6.7 Sample collection and HPLC analysis of the samples

For the measurement of voriconazole plasma concentrations approximately 4 mL venous blood was drawn and collected into citrate tubes. The venous catheter was rinsed after each sampling with physiological saline solution. Microdialysate was collected into microvials (see 2.6.2). Each sample was clearly and unequivocally identified with a label, i.e., resistant to the storage temperature with the following information: Study name (VOR-Target-Site), individual number, matrix, relative time elapsed since last dose, study visit. Blood samples were kept in an ice bath for a maximum of 60 min and were centrifuged at approximately 4 °C and 3,720 g for 5 min, cells were discharged and plasma was obtained. Microdialysate samples were kept in an ice bath for a maximum of 60 min. Thereafter, all plasma and microdialysate samples were shock frozen at approximately -20 °C and stored at approximately -80 °C until transport to the Department Clinical Pharmacy, MLU and analysis. HPLC analysis was performed according to the developed methods for the quantification of voriconazole from UF and microdialysate (double analysis due to specificity aspect) (see 3.1.1). The pH values of selected microdialysis samples were measured with pH measuring sticks.

### 2.6.8 Analysis of genotype of Cytochrome P450 isoenzymes 2C9 and 2C19

The genotype analysis of blood samples of the pilot study individuals (see 2.6.1) with regard to the CYP isoenzymes 2C9 and 2C19 (CYP2C9\*2/\*3- and CYP2C19\*2-alleles) was carried out in cooperation with the Institute of Pharmacology, Medical Faculty, Ernst Moritz Arndt Universität Greifswald. The analysis involved three steps: DNA preparation and purification, amplification of the purified DNA, and pyrosequencing.

#### 2.6.8.1 Preparation of genomic DNA from blood samples

The DNA purification procedure was supported by the NucleoSpin® Blood isolation kit providing the reaction solutions and NucleoSpin® Blood QuickPure Columns. Cell lysis was achieved by incubation of 200 µL whole blood sample in BQ1, containing large amounts of chaotropic ions, in presence of 25 µL Proteinase K and PB at 70 °C for 10 to 15 min leading to denaturation of proteins. The addition of 200 µL ethanol offered appropriate conditions of specific (reversible) binding of DNA to the silica membrane of the column in which the sample was transferred and centrifuged (1 min at 11,000 g). In order to remove contaminations, two wash steps were further applied using 350 µL BQ2 each time followed by a centrifugation for 3 min at 11,000 g enabling fast purification. Washing liquids were eluted in collection tubes which were removed after centrifugation. The drying of the column was performed by a 3 min centrifugation at 11,000 g. The elution of DNA was achieved under low ionic strength conditions provided by a slightly alkaline elution buffer (BE, 50 µL) which was prewarmed to 70 °C. After the incubation for 1 min at room temperature the column was centrifuged for 1 min at 11,000 g and, finally, pure DNA was collected into a microcentrifuge tube. In order to control the purification process the concentration of the eluted DNA was determined by spectrometric analysis ( $\lambda=220\text{ nm} - 750\text{ nm}$ ) of 1.5 µL of the elution buffer obtained.

### 2.6.8.2 Polymerase chain reaction

The amplification of the purified DNA (see 2.6.8.1) was achieved using PCR. Two mixtures (CYP2C9/CYP2C19), each containing buffer without  $MgCl_2$  (6  $\mu$ L/5  $\mu$ L), 10 mM dNTPs (1.2  $\mu$ L/1.0  $\mu$ L), 50 mM  $MgCl_2$  (1.8  $\mu$ L/1.5  $\mu$ L), biotinylated oligonucleotide primer F (duplex (two alleles) approach for CYP2C9: A2, A3; simplex (one allele) approach for CYP2C19: A2) (1.2  $\mu$ L/1.0  $\mu$ L), biotinylated oligonucleotide primer R (duplex approach for CYP2C9: A2, A3; simplex approach for CYP2C19: A2) (1.2  $\mu$ L/1.0  $\mu$ L), 5 U/ $\mu$ L Polymerase (0.30  $\mu$ L/0.25  $\mu$ L), sterilised PCR water (44.70  $\mu$ L/39.25  $\mu$ L) were prepared. Afterwards, 2  $\mu$ L of the genomic DNA were transferred to 48  $\mu$ L of each of the mixtures. Optimal cyclers conditions for real time PCR (15 min at 95 °C; 45 cycles: 45 sec at 95 °C, 45 sec at 55 °C, 45 sec at 72 °C; 5 min at 72 °C; final temperature: 4 °C) were adjusted enabling 1) denaturation (separation of the DNA strands), 2) annealing (primer attachment), and 3) extension (elongation of chains). To control the PCR process and to detect the PCR product, respectively, electrophoresis was carried out using a 2% agarose gel. Both the PCR product and a tracker mixture, containing Tris, EDTA, and glycerol, accounting for sample density, were applied to the gel cavities. Electrophoresis was conducted with the intercalating fluorescent tag ethidium bromide for 60 min at 400 V and 120 mA.

### 2.6.8.3 Pyrosequencing<sup>®</sup> for single nucleotide polymorphism analysis

Previous to the pyrosequencing<sup>®</sup> procedure, single-stranded DNA had to be prepared. For this purpose, the PCR product was processed using the Vacuum Prep Tool<sup>®</sup>: Streptavidin coated Sepharose beads (5  $\mu$ L per well) and Binding-Buffer (35  $\mu$ L per well) were added to the PCR plate containing the biotinylated PCR product (40  $\mu$ L per well), and the mixture was agitated for 5 min at room temperature. Vacuum was applied and the beads with immobilised PCR product were picked up by the Vacuum Prep Tool<sup>®</sup> from the PCR plate and moved to a separate trough, where 70% ethanol was aspirated through the filter probes for 5 sec. After that, the Vacuum Prep Tool was placed in a trough of sodium hydroxide (0.2 M) for 5 sec, still with the vacuum pressure switched on, to denature the DNA and to filter out the released single-stranded DNA, while the 5'-biotinylated strand remained immobilised on the beads. Finally, the tool was placed in a trough of wash buffer and highly purified water each for 5 sec where the strands were rinsed by aspiration. The single-stranded templates were then transferred to a previously prepared PSQ<sup>®</sup> plate containing annealing buffer (37  $\mu$ L per well) and sequencing primer (3  $\mu$ L per well). With the vacuum pressure switched off, a slight shake of the Vacuum Prep Tool<sup>®</sup> released the beads with attached templates into the 96-well PSQ<sup>®</sup> plate. After annealing of the sequencing primer on a prewarmed heater for 2 min, the plate was ready for analysis using a Pyrosequencing<sup>®</sup> System following the correct charging of the cartridges with enzymes (165  $\mu$ L pyrosequencing<sup>®</sup> enzyme mixture), substrates (165  $\mu$ L pyrosequencing<sup>®</sup> substrate mixture), and dNTPs (71  $\mu$ L dTTP, 64  $\mu$ L dGTP, 59  $\mu$ L dCTP, 62  $\mu$ L dATP $\alpha$ S).

### 2.6.9 Building the dataset and handling of missing values

The pilot character of the study implied – in case of proven feasibility – a continuation of data acquisition during a main part of the study planned. Therefore, the building of the dataset should meet the demands for datasets readable by the most common and also more specialised PK software (e.g., WinNonlin®, NONMEM™) to facilitate further completion and evaluation of the data, respectively. For all three individuals and all studied matrices one single analysis dataset was manually created in Excel (see 2.8) including information about the individual, sampling time points and corresponding unbound voriconazole concentrations of the respective matrices prior accounting for RR results for microdialysates. To be coherent with the structure for datasets specified for NONMEM™ by Beal and Sheiner [109], the items listed in Tab. 7-4 were integrated in the dataset.

The calculations for selected data items (e.g., BMI) were performed in Excel (see 2.8). Missing data values were coded as -99 but not considered in data analysis.

#### 2.6.10 Data(set) checkout

After building the dataset a systematic dataset checkout procedure was performed in order to check for completeness, correctness, and plausibility. First, single columns were inspected for their minimum (Min) and maximum (Max) values to check overall plausibility of the values. A subsequent cross-column check should identify consequential combinations within one row. The column check was carried out using the filter function in Excel (see 2.8). To illustrate the data, index plots were generated by plotting every item of the dataset against the individual identification number (ID) in R-based Xpose (see 2.8).

#### 2.6.11 Data analysis

PK analysis was performed using non-compartmental data analysis (NCA). This approach describes the PK characteristics without assuming the existence of specific kinetic compartments and applies to first-order (linear) kinetics [110] being the prerequisite for the validity of the calculated parameters. The method of NCA used here involved application of the trapezoidal rule for determinations of the area under the concentration-time curve (AUC), estimation of the terminal elimination rate constant  $\lambda_z$  and terminal half-life  $t_{1/2}$ . The minimum and maximum concentration ( $C_{min}$ ,  $C_{max}$ ) and time of  $C_{max}$  ( $t_{max}$ ) were directly taken from the non-logarithmic concentration-time plots.

The AUC from start of administration until the last measurable concentration was estimated by means of the linear trapezoidal rule for ascending or equal and of the log-linear one for the descending concentrations in order to keep under- or over estimation as low as possible (Linear Up/Log Down Method, Eq. 2-4) [110-112].



**Eq. 2-4:** Calculation of AUC (top), linear trapezoidal rule (middle) and log-linear trapezoidal rule (bottom).

$$AUC_{\tau} = \int_{t_{i-1}}^{t_i} C(t)dt = \sum_{i=2}^n \int_{t_{i-1}}^{t_i} C(t)dt = \sum_{i=2}^n AUC(t_{i-1} - t_i)$$

$$AUC(t_{i-1} - t_i) = \frac{1}{2}(t_i - t_{i-1}) \cdot (C_{i-1} + C_i)$$

$$AUC(t_{i-1} - t_i) = (t_i - t_{i-1}) \frac{C_{i-1} - C_i}{\ln(C_{i-1}/C_i)} \quad (C_i \text{ or } C_{i-1} \neq 0)$$

$\tau$  = dosing interval with  $C_i=C(t_i)$  concentration measured at times  $t_i$ ,  $i=2, \dots, n$ , with  $t_1=0$ .

The terminal slopes ( $\lambda_z$ ) were estimated by the unweighted log-linear regression technique using a semi-logarithmic presentation of measured drug concentrations versus time (Eq. 2-5) [112]. For this purpose, the data of the terminal portion were examined in order to best identify the mono-exponential terminal phase [112-114], i.e., to find the appropriate number of concentration-time points ( $n$ ) to be included in the log-linear regression. To reliably identify the mono-exponential terminal phase, the two times  $t_{\max}$  method (TTT method) was applied when a monophasic shape in the semi-logarithmic plot after reaching the  $C_{\max}$  was visible [114]. Otherwise, if the semi-logarithmic concentration-time profile after  $C_{\max}$  showed a biphasic shape, the crossing of the imaginary first and second disposition phase lines in the profile was used as 'visual marker' for the beginning of the mono-exponential terminal phase [114]. For all estimations, the use of at least four terminal concentration-time points should be and has been involved [115]. Next,  $\lambda_z$  was used for calculating the terminal half-life according to Eq. 2-6 [112].

**Eq. 2-5 and Eq. 2-6:** Determination of  $\lambda_z$  (top) and  $t_{1/2}$  (bottom).

$$\text{Eq. 2-5} \quad \lambda_z = \frac{\sum t_i \cdot \sum \ln(C_i) - n \cdot \sum t_i \cdot \ln(C_i)}{n \cdot \sum t_i^2 - (\sum t_i)^2}$$

$$\text{Eq. 2-6} \quad t_{1/2} = \frac{\ln 2}{\lambda_z}$$

$n$ : number of data points used in the regression analysis,  $t_i$ : respective times,  $\ln(C_i)$  natural logarithm of the corresponding drug concentrations,  $i=1, \dots, n$ .

The maximum unbound plasma (UF), ISF<sub>c</sub>, and ISF<sub>i</sub> concentration,  $C_{\max}$ , as well as the AUC were used to estimate and to assess the extent of exposure of the drug investigated [110] and to compare the results within the matrices. AUC ratios were calculated to analyse penetration into the tissue (ISF) by dividing the AUC in the ISF by the AUC in plasma.

Comparison was drawn between the IDs, the matrices, the catheters, the dosing, and the administration routes. Drug accumulation was calculated via the accumulation factor using the following equation (Eq. 2-7):

**Eq. 2-7:** Determination of the accumulation factor.

$$\text{Accumulation factor} = \frac{\text{AUC}_{\text{SS},\tau}(\text{multiple dose})}{\text{AUC}_{0-\tau}(\text{single dose})}$$

## 2.7 Descriptive and explorative statistics

Statistical analysis and evaluation were carried out according to standard procedures [116] using appropriate software programs (see 2.8).

The localisation and dispersion parameters listed in Tab. 2-5 were used to characterise the data as well as the results of the data analysis in this thesis.

**Tab. 2-5:** Statistical parameters.

Parameter	Symbol
<i>Localisation parameters (continuous data)</i>	
Arithmetic mean	$\bar{X}$
Median	$\tilde{X}$
Geometric mean	$\bar{X}_{\text{geom}}$
<i>Dispersion parameters (continuous data)</i>	
Standard deviation	SD
Range (Minimum - Maximum)	R (Min – Max)
Geometric standard deviation	$\text{SD}_{\text{geom}}$
Coefficient of variation	CV
Geometric coefficient of variation	$\text{CV}_{\text{geom}}$

The confidence interval (CI) was utilised as an interval estimate of a parameter in which the parameter is likely included. The calculation of the standard error (SE) was applied to estimate the standard deviation (SD) of a series of measurements over all possible samples. Geometric mean parameters were used as statistical measures for the centre of the data for most PK parameters ( $C_{\text{max}}$ ,  $\lambda_z$ , AUC). Geometric mean, SD, and CV were calculated according Eq. 2-8 – Eq. 2-10 and [112].  $T_{\text{max}}$  values were given as median.

**Eq. 2-8, Eq. 2-9, Eq. 2-10:** Calculation of geometric mean (top), geometric standard deviation (middle), and geometric coefficient of variation (bottom).

$$\text{Eq. 2-8} \quad \bar{X}_{\text{geom}} = \sqrt[n]{x_1 \cdot x_2 \cdot \dots \cdot x_n} = e^{\frac{1}{n} \sum_{i=1}^n \ln(x_i)}$$

$$\text{Eq. 2-9} \quad \text{SD}_{\text{geom}} = e^{\sqrt{\frac{\sum_{i=1}^n \ln(x_i)^2 - \frac{1}{n} \left( \sum_{i=1}^n \ln(x_i) \right)^2}{n-1}}}$$

$$\text{Eq. 2-10} \quad \text{CV}_{\text{geom}, \%} = 100 \cdot \sqrt{e^{\left[ \ln(\text{SD}_{\text{geom}}) \right]^2} - 1}$$

Explorative statistical analysis was carried out applying appropriate statistical tests (see Tab. 2-6). Selection of a test depended on the problem, the distribution of the data, the homogeneity of variance of the parameter and the sample size (n). The level of significance  $\alpha$  was set to 0.05, i.e., probability values (p) less than 5% ( $p < 0.05$ ) were considered to indicate statistically significant differences (rejection of null hypothesis).

**Tab. 2-6:** Statistical tests.

Statistical test	Description
<i>Test on normal distribution</i>	
Kolmogorov-Smirnov test (K-S test)	Test of normality of the data
<i>Test on homogeneity of variance</i>	
F test	Test of homogeneity of two variances
Levene's test	Test of homogeneity of variances of more than two groups
<i>Parametric test (applied for normally distributed data and homogeneous variances)</i>	
Student's t-test	Test of the significance of the difference between two sample means (two independent samples)
Student's paired t-test	Test of the significance of the difference between two sample means (two dependent samples)
One-way ANOVA (analysis of variance)	Test to compare the means of more than two groups (independent samples)
<i>Parametric test (applied for normally distributed data and heterogeneous variances)</i>	
Welch test	Test of the significance of the difference between two sample means (two independent samples)
<i>Non-parametric test (applied for not normally distributed data)</i>	
Wilcoxon test	Rank test to compare two samples (two dependent samples)
Kruskal-Wallis test	One-way analysis of variance by ranks to compare multiple independent samples

Regression analysis was carried out to analyse numerical data consisting of values of a dependent variable (response variable,  $y$ ) and of one or more independent variables (explanatory variables,  $x_i$ ). A regression equation  $y=f(x,\beta)$  modelled the dependent variable (outcome of a measurement,  $y$ ) as a function of the independent variables  $x$ , the unknown parameters  $\beta$ , and corresponding parameters (constants). Parameters were estimated to give the best fit to the data which was evaluated by using the least squares method, i.e., minimising the distance between the measured and predicted values of the dependent variable  $y$ . The linear regression implied that the dependent variable  $y$  was in a linear relation to the parameters in the linear equation  $y=a \cdot x+b$ . To characterise and confirm the goodness of fit of the model the coefficient of determination  $R^2$  ( $0 \leq R^2 \leq 1$ ) was calculated using the observed as well as the predicted  $y$  values. Goodness of fit plots (observed versus predicted values) were generated to graphically demonstrate goodness of fit.

## 2.8 Software

Datasets were generated by Microsoft® Office Excel (Microsoft Corporation, Munich, Germany, Version 11.0, SP-3, 2003). Statistical analysis was performed using SPSS Statistics® (SPSS Inc., Chicago, Illinois, USA, Versions 15.0.1, 2007; 17.0, 2008; and 18.0, 2009) and Microsoft® Office Excel. HPLC system control, data acquisition, and processing (integration of HPLC signals) were carried out with Chrompass® (JASCO ChromPass Chromatography Data System (developed in France), Gross-Umstadt, Germany, Version 1.8.6.1, 2004) and Borwin® (JMBS Developments, Le Fontanil, France, Version 2.1). PyroMark Q96 ID software was used for pyrosequencing procedure and analysis. For NCA (see 0) all parameters and for the *in vitro* microdialysis investigation the mass transfer coefficient  $r$  were estimated with WinNonlin® Professional (Pharsight Corporation, Mountain View, USA, Versions 5.2, 2007 and 5.2.1, 2008). For the coefficient the following specifications were set: user defined ASCII model, number of functions: 1, number of primary parameters: 1 (i.e.,  $r$ ); the membrane surface area ( $A$ ) was defined as a constant and the flow rate ( $F$ ) as temporary variable. Uniform weighting and Gauss-Newton (Levenberg and Hartley) method were used (convergence criteria of 0.0001 used during minimisation process). Data check-out and graphical analysis including index plots were performed using NONMEM™ (Globomax L, San Francisco, Ca, USA, Version V, Level 1.1, 1998) combined with the software management program PROPHET™ (Version V 1.0.1 – 05.05.2004), Xpose (R-based, open-sourced, The R Foundation for Statistical Computing, Version 2.6.1, 2007) (Niclas Jonsson and Mats Karlsson, Version 4\_4.0-6.1 [117]), and Microsoft® Office Excel.

---

## 3 RESULTS

### 3.1 I – Bioanalytical methods for quantification of voriconazole

#### 3.1.1 Quantification of voriconazole in microdialysate and plasma

##### 3.1.1.1 Developed analytical method and system settings

For microdialysate, due to the lack of proteins a simple one-step dilution preparation procedure was developed. Every microdialysate sample (flow rate-dependent volume; minimum 20  $\mu\text{L}$ ) was mixed with ACN (40/60, v/v), vortex mixed for 10 s, and directly injected. The final plasma sample preparation was a two-in-one step procedure: Precipitation of proteins and dilution were performed by mixing a 50  $\mu\text{L}$  aliquot with 75  $\mu\text{L}$  ACN. The mixture was vortex mixed (10 s), centrifuged at 13,500  $g$  for 15 min and the clear supernatant was taken for direct injection.

All samples were maintained at 10  $^{\circ}\text{C}$  in the autosampler prior to injection. A volume of 20  $\mu\text{L}$  of each sample was directly injected into the HPLC system. For a fast, reliable, and high-throughput assay direct sampling via needle puncture through the sample vial was achieved by sample rack modifications. Only briefly stored micro-tubes guaranteed reproducible puncture of the sample vial and led to fully automatic sample injection. Microdialysates underwent the zero-sample loss mode; plasma samples were injected in the normal mode. The mobile phase consisting of an ammonium phosphate buffer/ACN (pH 6.0; 40 mM; 50/50, v/v) was used under isocratic conditions at a flow rate of 1 mL/min. All samples were separated on a LiChrospher<sup>®</sup>-100 RP-18 column with an integrated precolumn as the stationary phase. The column temperature was maintained at 25  $^{\circ}\text{C}$ . Monitoring of voriconazole was realised with UV detection at a wavelength of 254 nm. Peak areas of unknown concentrations were back-calculated by use of the calibration function obtained by weighted linear regression (weight:  $1/\text{concentration}^2$ ). The weighting factor yielded a higher weight for lower concentrations and, hence, leveled the different absolute SDs, which increased with rising concentration of the calibrators [118].

##### 3.1.1.2 Analyte stability in microdialysate and plasma

Different storage conditions during freeze-thaw, short-term ambient temperature, stock solution, and post-preparative stability investigations (see 2.3.1.3) revealed no degradation or enrichment tendency of voriconazole in spiked microdialysis or plasma samples.

Stability of voriconazole in microdialysate and plasma after one to three freeze-thaw cycles ranged from 108.9% (CV: 2.3%) to 116.5% (CV: 1.7%) and 86.0% (CV: 5.9%) to 111.1% (CV: 16.2%), respectively. No statistically significant difference was shown for voriconazole microdialysis samples at low and high concentration as well as voriconazole plasma samples at low and high concentration (low and high QC of microdialysate: with  $p=0.111$  ( $n=11$ ) and

$p=0.138$  ( $n=12$ ); low and high QC of plasma: with  $p=0.073$  ( $n=11$ ) and  $p=0.070$  ( $n=12$ ), see 2.3.1.3 and 1.1).

Storage of microdialysate and plasma samples at room temperature for 4 h or 24 h had no influence on degradation processes. Average results from evaluation of stability in microdialysate and plasma were 103.2% (CV: 6.2%) to 114.6% (CV: 5.2%) and 99.7% (CV: 1.7%) to 102.0% (CV: 0.5%), respectively, compared with freshly prepared QC samples. Results from voriconazole microdialysate and plasma samples at low and high concentrations stored at room temperature for 4 h and 24 h were statistically not significantly different and the samples proved to be stable (low and high QC of microdialysate: with  $p=0.179$  ( $n=9$ ) and  $p=0.161$  ( $n=9$ ); low and high QC of plasma: with  $p=0.996$  ( $n=9$ ) and  $p=0.110$  ( $n=8$ ), see 2.3.1.3 and 1.1).

Voriconazole was also stable after sample preparation in which one set of QC samples was frozen after preparation for at least 7 h and another set was stored in the sample tray of the autosampler at room temperature for 7 h. Average stability for microdialysate and plasma varied between 97.2% (CV: 7.6%) and 112.1% (CV: 1.0%) and between 94.4% (CV: 4.7%) and 100.9% (CV: 1.6%), respectively. No sample was statistically significantly different from QC samples measured immediately after preparation (low and high QC of microdialysate: with  $p=0.723$  ( $n=9$ ) and  $p=0.130$  ( $n=9$ ); low and high QC of plasma: with  $p=0.280$  ( $n=9$ ) and with  $p=0.252$  ( $n=9$ ), see 2.3.1.3 and 1.1).

Based on these results, voriconazole was considered to be stable in microdialysate and plasma in all the circumstances investigated.

#### 3.1.1.3 Specificity of the analytical method

Voriconazole-free microdialysate and plasma samples did not show any interference with the voriconazole signal (Fig. 7-1, left panel).

None of the 36 drug products predominantly administered at ICUs (see 2.3.1.4), and therefore possibly co-administered with voriconazole, interfered with the peak of the analyte, owing to different retention times ( $t_R$ ), the sample preparation procedure resulting in low recoveries, or the particular wavelength required for voriconazole, except for ambroxol (in Mucosolvan<sup>®</sup>) (Fig. 7-1, left panel). Ambroxol, frequently used as bronchial expectorant in continuous therapy, interfered with the signal of voriconazole. In consequence, ambroxol drug substance was utilised to identify this peak overlapping with that of voriconazole at  $t_R$  of 3.2 min. In case of ambroxol co-administration in patients during clinical studies the bioanalytical assay used for voriconazole quantification was modified and shifted to later  $t_R$  values by using another column (LiChrospher<sup>®</sup>-100 RP-18, e, 5, 4.0 × 250) and adding ammonium phosphate buffer (pH 6.0; 40 mM; 55/45, v/v) to the mobile phase resulting in peak separation (Fig. 7-1, right panel).

During analysis of microdialysate samples originating from healthy volunteers (see 2.6 and 3.4), an unknown endogenous substance or substance mixture showed full interference with voriconazole (see Fig. 3-1, left chromatograms).

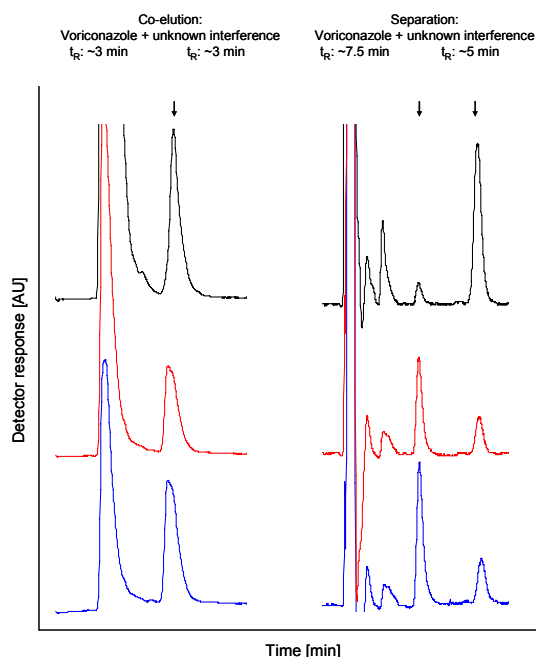


**Fig. 3-1:** Peak separation of voriconazole and an unknown endogenous substance or substance mixture in microdialysate samples (CMA60<sup>®</sup>) originating from a healthy volunteer (ID 102) (see 2.6 and 3.4): Chromatograms showing the interference (left) and the separation (right) in visit 1 (blue line), visit 2 (red line), and in visit 7 (black line). AU: arbitrary units.

The strategy already applied for the interference with ambroxol was appropriate for peak separation in these samples, too. Later  $t_R$  values of voriconazole (~7.5 min) were achieved by adding ammonium phosphate buffer (pH 6.0; 40 mM; 65/35, v/v) to the mobile phase resulting in adequate peak separation (see Fig. 3-1, right chromatograms) independent of the varying extent of the interference.

The extent of the unknown interfering substance (or substance mixture) was different among the samples analysed. Since the samples originated from healthy volunteers during continuous dialysis by a microdialysis catheter (CMA60<sup>®</sup>, CMA66<sup>®</sup>), signals of the interference have been longitudinally represented in Fig. 7-2 (left panel) and analysed: On average, the signal of the interference decreased (exponentially-like) starting with the baseline sample (visit 1, 0 h) until the last study sample (visit 7, 83.5 h) by 88.4% (n=3) for CMA60<sup>®</sup> and 66.1% (n=3) for CMA66<sup>®</sup>, respectively. This difference (i.e., steeper decrease for CMA60<sup>®</sup>) was explained by the higher extent of the interference in early samples (until visit 4) obtained via CMA60<sup>®</sup> (baseline samples of CMA60<sup>®</sup> (0.34 AU  $\pm$  0.065 AU, 19.1% CV, n=3) and CMA66<sup>®</sup> (0.12 AU  $\pm$  0.011 AU, 9.5% CV, n=3): 0.23 AU  $\pm$  0.129 AU, 56.0% CV, n=6). Later samples (from visit 5 on) contained a highly comparable amount of the interfering substance (last study samples of CMA60<sup>®</sup>: 0.04 AU  $\pm$  0.012 AU, 30.3% CV, n=3, CMA66<sup>®</sup>: 0.04 AU  $\pm$  0.008 AU, 20.3% CV, n=3, and both catheters: 0.04 AU  $\pm$  0.009 AU, 23.0% CV, n=6). In case of a co-elution, a considerable impact of the interference on the signal of voriconazole could be expected: For CMA60<sup>®</sup> samples the percentage of the co-eluting substance ranged from 6.3% to 87.4% of the sum whereas CMA66<sup>®</sup> samples would have been overestimated with an additional percentage of 1.9% to 79.4%. An impact on retrodialysis

samples, predominantly of visit 1, was detected as well (Fig. 7-2, right panel) definitely leading to an influence on RR determination of voriconazole (i.e., RR would have been underestimated) in both catheters. UF samples were much less influenced by this interference (e.g., ID 103, median: 9.6%, R: 4.6% – 40.4%) than the microdialysate samples (see Fig. 7-3). Baseline samples (samples taken before voriconazole administration) of the healthy volunteers showed no interfering peak at the  $t_R$  of voriconazole when applying the method leading to co-elution of voriconazole and the unknown substance in microdialysate (see Fig. 7-3, left panel). Additionally, when peak separation was achieved baseline samples did not show the interfering peak as well (see Fig. 7-3, right panel). The PK samples (samples taken after voriconazole administration) exhibited a peak comparable to the range of  $t_R$  of the interfering peak in microdialysates but without variation (increase or decrease) over time. Structure determination should be focused on in future investigations.

#### 3.1.1.4 Accuracy and precision

Within- and between-day accuracy and precision studies (see 2.3.1.5) revealed that for microdialysate and plasma CVs and REs ranged between 0.5% and 6.1% as well as between -3.3% and +7.0%, respectively, and, thus, were below  $\pm 20\%$  at LLOQ and below  $\pm 15\%$  for low, medium, and high concentrations of the QC samples (see Tab. 3-1 and Tab. 3-2). Tab. 7-5 and Tab. 7-6 show CVs and REs for the calibration samples used during the three days of validation. In conclusion, CV and RE data obtained for voriconazole were within acceptable limits stated for bioanalytical method validation [101].

**Tab. 3-1:** Within-day and between-day precision (expressed as coefficient of variation, CV, %) and accuracy (as mean percentage deviation, RE, %) of determined voriconazole concentrations [ $\mu\text{g/mL}$ ] in microdialysate quality controls (QC).

$C_{\text{nom}}$ [ $\mu\text{g/mL}$ ]	$\bar{x}$ [ $\mu\text{g/mL}$ ] $\pm$ SD [ $\mu\text{g/mL}$ ]	CV, %	RE, %
<i>Within-day variability (n=6)</i>			
0.156	0.158 $\pm$ 0.001	0.5	+1.4
1.560	1.508 $\pm$ 0.010	0.6	-3.3
4.160	4.090 $\pm$ 0.030	0.7	-1.7
8.320	8.215 $\pm$ 0.085	1.0	-1.3
<i>Between-day variability (n=18)</i>			
0.156	0.160 $\pm$ 0.002	1.2	+2.3
1.560	1.522 $\pm$ 0.029	1.9	-2.4
4.160	4.093 $\pm$ 0.084	2.1	-1.6
8.320	8.294 $\pm$ 0.226	2.7	-0.3



**Tab. 3-2:** Within-day and between-day precision (expressed as coefficient of variation, CV, %) and accuracy (as mean percentage deviation, RE, %) of determined voriconazole concentrations [ $\mu\text{g/mL}$ ] in plasma quality controls (QC).

$C_{\text{nom}}$ [ $\mu\text{g/mL}$ ]	$\bar{x}$ [ $\mu\text{g/mL}$ ] $\pm$ SD [ $\mu\text{g/mL}$ ]	CV, %	RE, %
<i>Within-day variability (n=6)</i>			
0.153	0.154 $\pm$ 0.005	3.0	+0.6
1.530	1.488 $\pm$ 0.058	3.9	-2.8
4.080	4.129 $\pm$ 0.036	0.9	+1.2
8.160	8.348 $\pm$ 0.102	1.2	+2.3
<i>Between-day variability (n=18)</i>			
0.153	0.160 $\pm$ 0.010	6.1	+4.8
1.530	1.549 $\pm$ 0.062	4.0	+1.2
4.080	4.280 $\pm$ 0.160	3.7	+4.9
8.160	8.731 $\pm$ 0.299	3.4	+7.0

### 3.1.1.5 Lower limit of quantification and assay linearity

The LLOQ was 0.15  $\mu\text{g/mL}$  for both microdialysate and plasma. Values lower than this concentration exceeded the acceptable limits for accuracy and precision ( $\pm 20\%$  RE and CV, respectively). The back-calculated concentrations were determined with precision and accuracy expressed as CV and RE of 1.4% and +0.5% (n=6) for microdialysate, and 3.6% and +3.0% (n=6) for plasma. Assay linearity was determined using weighted (weighting factor:  $1/\text{concentration}^2$ ) linear regression analysis of the peak areas versus voriconazole concentrations in microdialysate and plasma [118]. Calibration functions for both matrices (n=6 calibrator concentrations each) showed good linearity across the investigated concentration range (0.15  $\mu\text{g/mL}$  – 10.0  $\mu\text{g/mL}$ ) indicated by coefficients of determination  $\geq 0.992$  for all functions (n=10). Mean calibration functions for microdialysate and plasma were determined on three consecutive validation days. Detailed results for linearity parameters for microdialysate are listed in Tab. 3-3. Means and CVs for slope (72705 AU $\cdot\text{mL}/\mu\text{g}$ , 8.2%), intercept (-4910 AU, 13.0%) and coefficient of determination (0.999, 0.1%) for plasma were calculated.

**Tab. 3-3:** Regression parameters and statistics of the calibration functions in microdialysate expressed as  $\bar{x} \pm \text{SD}$  and precision as coefficient of variation, CV, %, AU: arbitrary units.

Day	n	Slope [AU $\cdot\text{mL}/\mu\text{g}$ ]	Intercept [AU]	Coefficient of determination
1	3	0.063	-0.0067	0.997
		0.063	-0.0066	0.997
		0.063	-0.0067	0.997
2	1	0.064	-0.0066	0.999
3	1	0.065	-0.0068	0.999
$\bar{x} \pm \text{SD}$ (CV, %)	5	0.064 $\pm$ 1.0E-03 (0.9)	-0.0067 $\pm$ 6.0E-05 (1.6)	0.998 $\pm$ 1.0E-03 (0.1)

Microdialysate and plasma samples containing voriconazole concentrations potentially higher than the upper limit of quantification (10.0  $\mu\text{g/mL}$ ) were diluted with the corresponding matrix in the proportion 1+2 (v/v). The back-calculated concentrations for microdialysate and plas-

ma resulted in precision and accuracy expressed as CV and RE of 1.1% and +6.0% (n=6), and 3.0% and -5.3% (n=5), respectively.

### 3.1.1.6 Recovery of the analyte

The recovery of spiked microdialysate samples was 112.6% (CV: 3.2%, n=27) on average. The comparison between peak area data obtained from spiked plasma and aqueous solution resulted in a mean recovery of 136.6% (CV: 5.7%, n=18).

### 3.1.1.7 Robustness and ruggedness analysis

In-study QC validation samples (n=156) measured over a period of nine months within 26 runs performed according to the developed method indicated the overall robustness of the method for voriconazole plasma samples demonstrated by overall imprecision ranging from 4.6% to 11.2% CV. Overall, 90% of all inaccuracy values were between -8.0% and +13.7% RE.

In-study validation samples measured within nine runs over a period of six weeks performed according to the developed method indicated the overall robustness of the method for voriconazole microdialysate samples expressed by the results for accuracy and interday precision of the QC samples summarised in Tab. 3-4. Between-day precision was between 0.6% and 9.4% CV and between-day accuracy between -15.3% and 12.7% RE. Coefficients of determination of the calibration functions were between 0.996 and 0.999 (0.1% CV, n=9).

**Tab. 3-4:** Precision (between-day variability, CV, %) and accuracy (RE, %) of the quantitative assessment of voriconazole in microdialysate QC samples during study sample measurement.

n	C <sub>nom</sub> [µg/mL]	C <sub>calc</sub> [µg/mL] $\bar{x} \pm SD$	CV, %	Min CV, %	Max CV, %	RE, %	Min RE, %	Max RE, %
27	1.56	1.46 ± 0.109	7.4	1.6	11.1	-6.3	-15.3	+11.8
27	4.16	4.16 ± 0.304	7.3	1.4	8.1	-0.1	-12.5	+12.7
27	8.32	8.63 ± 0.353	4.1	0.5	3.8	+3.7	-4.3	+11.4

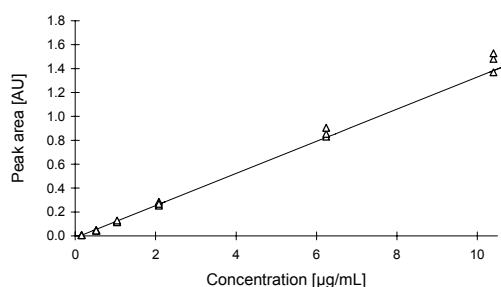


**Fig. 3-2:** Calibration curve of voriconazole microdialysate calibrators from ruggedness experiments using a different analytical system, column lot, and analyst (method transfer). AU: arbitrary units.

In addition, the complete assay developed was transferred to another HPLC system consisting of an autosampler with fully automatic sample injection but without a Peltier cooling element. An air-cooled Peltier element column oven for temperature control was not available for this system. Moreover, measurement was performed by another analyst and the column used was from different lot from that used during the main validation. The calibration function

(six calibrator concentrations, n=3) showed good linearity across the investigated concentration range, indicated by a coefficient of determination of  $0.996 \pm 0.001$  (0.1% CV) (Fig. 3-2).

Accuracy and precision studies revealed that CVs and REs ranged between 1.1% and 12.5% and between -3.4% and +15.3%, respectively, and, thus, were below  $\pm 20\%$  at the LLOQ (n=3) and less than  $\pm 15\%$  for QC samples of low, medium, and high concentrations (n=3) (Tab. 3-5).

**Tab. 3-5:** Precision (expressed as coefficient of variation, CV, %) and accuracy (as mean percentage deviation, RE, %) of determined voriconazole concentrations [ $\mu\text{g/mL}$ ] in microdialysate quality control samples from ruggedness experiments using a different analytical system, column lot, and analyst (method transfer).

$C_{\text{nom}}$ [ $\mu\text{g/mL}$ ]	n	$\bar{x}$ [ $\mu\text{g/mL}$ ] $\pm$ SD [ $\mu\text{g/mL}$ ]	CV, %	RE, %
0.156	3	$0.180 \pm 0.005$	2.7	+15.3
1.560	3	$1.512 \pm 0.017$	1.1	-3.1
4.160	3	$4.020 \pm 0.504$	12.5	-3.4
8.320	3	$8.529 \pm 0.481$	5.6	+2.5

Finally, investigation of the effect of mobile phase pH (5.4 and 7.1) was performed. The calibration function (six calibrator concentrations (n=3)) showed good linearity across the investigated concentration range (Fig. 7-4). Accuracy and precision evaluation revealed CVs and REs between 2.6% and 5.9% and between -11.2% and +4.5%, respectively, for both pH values investigated (n=6 for each QC). The results showed robustness of the developed bioanalytical method in the pH range of 5.4 to 7.1. However, values above the pH of the method developed (>pH 6 = validated method pH) had an effect on peak shape, hence, the actual method pH was preferable.

In summary, all experiments confirmed the ruggedness of the method over a variety of method conditions (e.g., different system, column lot, and analyst), demonstrated its capacity to remain unaffected by small but deliberate variations in method conditions, and provided an indication of its reliability during routine usage [102, 105]. Overall, the method proved robust and rugged over the course of 785 injections of microdialysate and protein-precipitated plasma samples performed during pre-study and in-study validation.

### 3.1.2 Determination of the unbound plasma concentration of voriconazole

For the determination of a possible adsorption of voriconazole to the ultrafiltration device the deviations of the peak areas of aqueous ultrafiltered solutions from equally concentrated aqueous non-ultrafiltered solutions were calculated (see 2.3.2). The mean relative percentage deviations ranged from +0.01% to +10.2% and were well in accordance with the REs obtained during the pre-study validation of the method. From these results the conclusion derived that the peak areas of the aqueous ultrafiltered solutions were consistent with the ones of the non-ultrafiltered solutions and, thus, voriconazole did not adsorb to any component of the ultrafiltration device.

To examine whether the validation results obtained for microdialysate could be transferred to UF a microdialysate calibrator with  $C_{nom}$  of 6.24  $\mu\text{g/mL}$  was prepared using analyt-free UF and assayed together with a microdialysate sample of the same concentration ( $n=3$ ) (see 2.3.2). UF calibrators deviated from the nominal peak area by +1.2% (R: +0.3% – +1.8%) for centrifuged samples and by -2.5% (R: -5.9% – +1.6%) for non-centrifuged samples. Those deviations were in the range of the REs of the microdialysate calibrators (all: -10.6% – +5.1%,  $C_{nom}$  of 6.24  $\mu\text{g/mL}$ : +4.0%). Hence, the calibrators in UF and in microdialysate were in concordance. It was hence accepted that the results of the pre-study validation for microdialysate could be transferred to the matrix UF. Thus, the calibration function for microdialysate and QCs were implemented in the analysis of UF samples within the clinical study (see 2.6). A final centrifugation step introduced within the sample preparation accounted for the higher accuracy within the centrifuged sample batch and the influence of a possibly incomplete protein separation during ultrafiltration.

### 3.1.3 Quantification of voriconazole in whole blood samples

Since whole blood consists of blood cells and plasma whole blood samples were prepared and assayed almost equally to the analytical procedure for plasma samples [99, 100] (see 3.1.1.1). Due to probable preparation limits of whole blood study specimens, all necessary volumes (average density of whole blood: average 1.0595  $\text{g/cm}^3$  at 25 °C [119]) of all samples processed were higher than for plasma and weighed (target weight: 100 mg). A volume of 30  $\mu\text{L}$  of the prepared samples was taken for direct injection onto the HPLC system with assay conditions consistent with the ones for the determinations in plasma. After measurement and data processing concentrations were normalised to the target weight by multiplying the concentration by the target weight and dividing by the exact net weight. The LLOQ could be defined as 0.2  $\mu\text{g/mL}$ . The application of the method for the quantification of voriconazole in blood samples yielded a mean coefficient of determination of 0.998 and an acceptable within-day variability demonstrated by REs (calibration samples: mean RE: +0.2%, R: -9.1% – +8.2%; QC samples: mean RE: +2.8%, R: -11.4% – +14.7%) and CVs (calibration samples: mean CV: 4.1%, R: 2.6% – 7.7%; QC samples: mean CV: 5.2%, R: 1.2% – 12.1%) below  $\pm 15\%$  and  $\pm 20\%$ , respectively, as specified in the FDA guideline [101].

### 3.1.4 Quantification of voriconazole in skin biopsy samples

Voriconazole spiked skin biopsies (see 2.3.4) during method development or study specimens, respectively, were extracted (~6 h at room temperature) by transferring them into extraction agent (ammonium phosphate buffer/ACN (pH 6.0; 40 mM; 40/60, v/v)) providing solubilising conditions for voriconazole. Moreover, precipitation of solubilised protein was achieved with this step. During the first hour of extraction under continuous shaking five freeze-thaw cycles were performed in order to damage skin cells forcing the extraction. Skin biopsies in the extraction tube were shock-frozen by shortly maintaining the tube in liquid nitrogen and subsequently thawing by maintaining the tube in water (20 °C). Extraction

samples were centrifuged at 13,500 *g* for 10 min in order to separate precipitated protein which might have been emerged during the extraction procedure and the supernatants were directly injected onto the HPLC system. Calibration samples (0.2, 0.5, 1.0, 2.0, 4.0, and 8.0  $\mu\text{g/mL}$ ) were identically prepared to microdialysate calibration samples using analyte-free ammonium phosphate buffer (pH 6.0; 40 mM) and processed identically to microdialysate, i.e., vortex mixed with ACN at a ratio of 40 to 60 (v/v) for 10 sec and directly injected onto the HPLC system. HPLC system and assay conditions were consistent with the ones for the determinations in microdialysate. After measuring the concentration of voriconazole in the extract samples ( $C_{\text{meas extract}}$ ) and mass of voriconazole ( $m_{\text{meas extract 1}}$ ), respectively, the recovery of the method developed resulted from the ratio  $m_{\text{meas extract 2}}/m_{\text{nom extract 2}}$  multiplied by 100 – with the nominal mass of voriconazole ( $m_{\text{nom extract 1}}$ ) as well as the measured mass of voriconazole ( $m_{\text{meas extract 1}}$ ) referring to the mass of the biopsy (mass 1) before ( $m_{\text{nom extract 2}}$ ,  $m_{\text{meas extract 2}}$ ).

The method developed for SB samples recovered 50.6% (CV: 11.9%,  $n=3$ ) of the spiked voriconazole (Tab. 7-7). The coefficients of determination of the calibration functions used for analysing the spiked solution or extracts were above or equal to 0.991. While applying the method to study specimens, within-day variability, demonstrated by REs and CVs, was in the FDA limits [101] (CV R: 0.9% – 9.4%; RE R: -6.7% – +4.5%) with a coefficient of determination of  $0.999 \pm 0.001$  (0.1% CV,  $n=3$ ).

An estimation of SB density by means of water displacement ( $\sim 1.15 \text{ g/cm}^3$ , i.e., 1.15 g displace approximately 1 mL water) could be supported by the measurement of  $1.05 \text{ g/cm}^3$  by the helium pycnometer.

## 3.2 II – *In vitro* microdialysis

### 3.2.1 Microdialysis equipment and system

#### 3.2.1.1 Microdialysis pumps and syringes

Stationary *in vitro* pumps CMA102<sup>®</sup> revealed high precision and accuracy even while using disposable syringes not directly intended for the systems (low flow rate of 1.5  $\mu\text{L/min}$ : RE: -3.0%, CV: 4.0%, high flow rate of 5.0  $\mu\text{L/min}$ : RE: +0.1%, CV: 2.9%) (see 2.2.2.1). All portable *in vivo* pumps CMA107<sup>®</sup> worked reproducibly but led to systematically less dialysate volume (flow rate of 2  $\mu\text{L/min}$ : RE: -11.0%, CV: 6.6%). However, since sufficient dialysate volume was obtained for HPLC analysis no adaptation of sampling time was made.

### 3.2.1.2 *In vitro* microdialysis system (IVMS)

An apparatus (see 2.4.1) for the conduction of *in vitro* microdialysis investigations was developed which guaranteed conditions mimicking the *in vivo* situation via an integrated temperature and stirring module and allowed for easy and clean handling. The practical employment of the system demonstrated its reliability and compactness combining all essential components for various experiments in multiple (up to six) parallel determinations. The final space-saving design, partly extendable, permits its application in any laboratory performing *in vitro* microdialysis investigations in basic or applied research. The system enables the exploration of commercially available catheters for the preclinical or clinical use. The standardised (physiological-like) conditions ensure an absolute congruent arrangement of setting expressed by reproducible results and low intra-catheter variability, respectively (see 3.2.2.1, 3.2.2.2, and 3.2.2.3). Additionally, the liquid (medium) containers can be replaced without changing the position or mounting of the catheter owing to the stepless height adjustable multifunctional hardware adapter platform. The mountings of the catheters provide the fit on the one hand and an easy removal on the other. Due to this fit the membrane is constantly maintained in the centre of the medium container avoiding the contact with its sides. Moreover, the distance of the catheters to the bottom of the medium container prevents the accidental contact with the magnetic stir bar and, hence, the potential damage of the catheter. Two cavities are provided on the platform per sampling unit which enable a quick and exact switch of the outlet tube into the next sampling vial. The transparent lid avoids any external contamination of the liquids or catheters with, e.g., dust or bacteria and enables to pursue the experiment at the same time.

## 3.2.2 *In vitro* microdialysis investigations

As a prerequisite (see 2.4.2.2), stability of voriconazole (mean $\pm$ SD: 102.5% $\pm$ 3.7%, CV: 3.6%, RE: +2.5%) was demonstrated over the entire experimental period of 10 h at 37 °C ranging from 95.6% (RE: -4.4%) to 109.9% (RE: +9.9%).

### 3.2.2.1 Flow rate dependence

Results of the investigations on the dependence of RR of voriconazole on different flow rates (see 2.4.2.3) revealed measurable dialysate concentrations for all settings and for CMA60<sup>®</sup> catheters shown in Tab. 3-6 and Fig. 3-3 including all individual results.

**Tab. 3-6:** Flow rate dependence (CMA60<sup>®</sup>, recovery experiment): mean relative recovery (RR) versus flow rate (0.4  $\mu\text{L}/\text{min}$  – 10.0  $\mu\text{L}/\text{min}$ , n=6).

Flow rate [ $\mu\text{L}/\text{min}$ ]	Mean RR, % $\pm$ SD	CV, %
0.4	98.4 $\pm$ 0.5	0.5
0.8	97.0 $\pm$ 4.2	4.4
1.0	98.9 $\pm$ 0.3	0.3
1.5	97.0 $\pm$ 3.2	3.3
2.0	91.5 $\pm$ 1.7	1.8
2.5	86.4 $\pm$ 0.9	1.1
5.0	64.1 $\pm$ 6.8	10.6
7.5	50.4 $\pm$ 5.8	11.6
10.0	40.2 $\pm$ 0.04	0.1

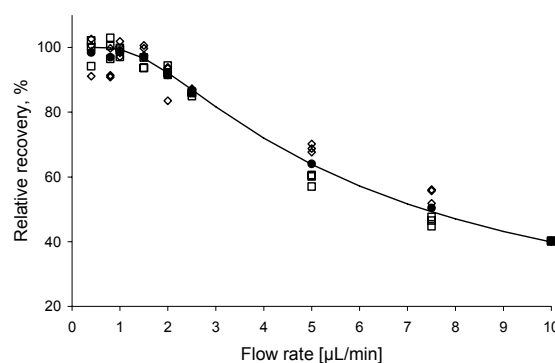


**Fig. 3-3:** Dependence of relative recovery (RR) on flow rate ( $\mu\text{L}/\text{min}$ ) of perfusate (Ringer's solution) during recovery experiment. Open symbols: individual results (n=3) of two CMA60<sup>®</sup> catheters, filled circles: overall mean. Line: voriconazole showed a flow rate (F) dependency according to the equation  $RR=100 \cdot (1 - e^{-5.09/F})$ .

RR in the recovery experiments increased from 40.2% (CV: 0.1%) to 98.4% (CV: 0.5%) while reducing the flow rate from 10.0  $\mu\text{L}/\text{min}$  to 0.4  $\mu\text{L}/\text{min}$ . Significant differences in the recovery resulted from an increase of flow rate starting at 2.5  $\mu\text{L}/\text{min}$ . This lower flow rate range was thus investigated with the recently approved CMA66<sup>®</sup> catheters (Tab. 3-7 and Fig. 3-4).

**Tab. 3-7:** Flow rate dependence (CMA66<sup>®</sup>, recovery, delivery experiment): mean relative recovery (RR) versus flow rate (1.0  $\mu\text{L}/\text{min}$  – 2.5  $\mu\text{L}/\text{min}$ , n=9).

Flow rate [ $\mu\text{L}/\text{min}$ ]	Mean RR, % $\pm$ SD	CV, %
<i>Recovery experiment</i>		
1.0	100.9 $\pm$ 2.2	2.1
1.5	98.7 $\pm$ 1.2	1.2
2.0	90.8 $\pm$ 4.2	4.6
2.5	89.1 $\pm$ 2.2	2.5
<i>Delivery experiment</i>		
1.0	97.1 $\pm$ 1.3	1.3
1.5	94.8 $\pm$ 0.8	0.8
2.0	91.7 $\pm$ 1.1	1.2
2.5	87.2 $\pm$ 1.8	2.1

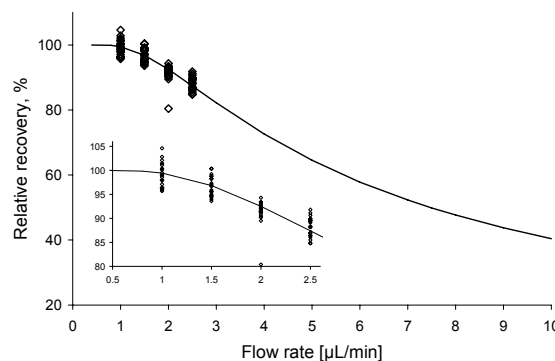


**Fig. 3-4:** Dependence of relative recovery (RR) on flow rate ( $\mu\text{L}/\text{min}$ ) of perfusate (Ringer's/voriconazole solution) during recovery and delivery experiment. Open symbols: individual results (n=3) of three CMA66<sup>®</sup> catheters, filled circles: overall mean. Line: voriconazole showed a flow rate (F) dependency according to the equation  $RR=100 \cdot (1 - e^{-5.18/F})$ .

Similar RR without statistically significant differences up to 2.0  $\mu\text{L}/\text{min}$  were obtained for CMA66<sup>®</sup> (at 2.5  $\mu\text{L}/\text{min}$ : p=0.02, ANOVA). For clinical applications it is therefore advisable to choose flow rates below or even better equal to 2.0  $\mu\text{L}/\text{min}$  in order to retain adequate recoveries as well as sufficient sample volumes for HPLC analysis.

The recoveries followed a typical behaviour describable by an exponential equation (see Fig. 3-3, Fig. 3-4). Curve fitting was performed using WinNonlin<sup>™</sup> with the mass transfer

coefficient  $r$  as the parameter to be estimated. The function for estimation was as follows:  $RR=100 \cdot (1 - \exp(-r \cdot A / F))$  with  $F$  as the flow rate and  $A$  surface area of the microdialysis membrane  $A$  of  $56.55 \text{ mm}^2$  for concentric catheters and  $47.12 \text{ mm}^2$  for linear catheters and, hence, the equations emerged as:  $RR=100 \cdot (1 - e^{-5.09/F})$  and  $RR=100 \cdot (1 - e^{-5.18/F})$ , respectively. The mass transfer coefficient  $r$  was estimated to be  $0.09 \text{ mm/min}$  for CMA60<sup>®</sup> catheters with a SE of  $0.002 \text{ mm/min}$  and a CV of 1.9%. For linear CMA66<sup>®</sup> catheters  $r$  amounted to  $0.11 \text{ mm/min}$  (SE:  $0.002 \text{ mm/min}$ , CV: 1.7%). Plotting the simulated (predicted) data from the CMA60<sup>®</sup> and CMA66<sup>®</sup> simultaneously, revealed a highly comparable shape of the curve (see Fig. 3-5, left panel).

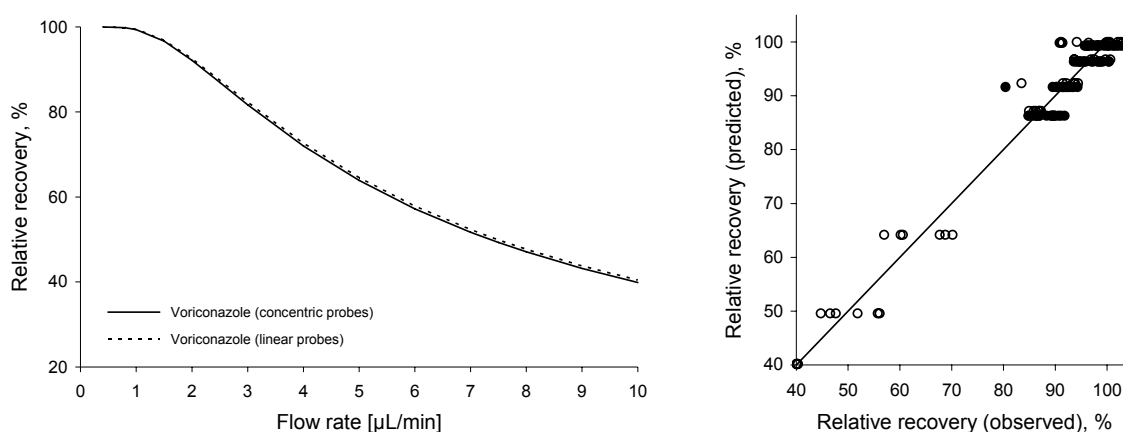


**Fig. 3-5:** Dependence of relative recovery (RR) of voriconazole on flow rate ( $F$ ,  $\mu\text{L/min}$ ) of perfusate according to the equation  $RR=100 \cdot (1 - e^{-r \cdot A / F})$  ( $r$ : mass transfer coefficient,  $A$ : membrane surface area) in concentric (solid line) and linear (dotted line) catheters (left panel). RR observed during investigations of dependency of RR on  $F$  ( $\mu\text{L/min}$ ) versus RR predicted via estimation of mass transfer coefficient  $r$  (right panel, open circles: concentric catheters, filled circles: linear catheters). Solid line reflects the line of identity.

The goodness of fit plot of model-predicted versus observed RR (Fig. 3-5, right panel) showed slopes of approximately 1 (1.00 for concentric catheters and 1.20 for linear catheters, respectively) and a coefficient of determination of 0.973 for concentric catheters and 0.739 for linear catheters, respectively. In summary, increasing the flow rate decreased RR according to the determined relations that adequately described the data. The behaviour was consistent in both concentric as well as linear catheters and supported application of both catheters in different matrices in one individual.

The experiments on flow rate dependence of RR with CMA66<sup>®</sup> were expanded to two other anti-infectives (see 2.4.2.3). The experimental proceeding and data processing was equal to the investigations on linear catheters with voriconazole. Linezolid showed a nearly analogous behaviour to voriconazole describable as  $RR=100 \cdot (1 - e^{-4.71/F})$  with an estimated mass transfer coefficient  $r$  of  $0.10 \text{ mm/min}$  (SE:  $0.006 \text{ mm/min}$ , CV: 5.9%) (Fig. 3-6, left panel; the inset shows individual values). The curve of daptomycin ( $RR=100 \cdot (1 - e^{-3.30/F})$ ) showed a steeper decline for RR with increasing flow rate than voriconazole or linezolid ( $r$ :  $0.07 \text{ mm/min}$ , SE:  $0.002 \text{ mm/min}$ , CV: 2.4%) (Fig. 3-6, left panel; inset: individual values). The goodness of fit



plot of model-predicted versus observed RR (Fig. 3-6, right panel) showed slopes of approximately 1 (0.92 for linezolid and 1.07 for daptomycin, respectively) and a coefficient of determination of 0.916 for linezolid and 0.962 for daptomycin, respectively.

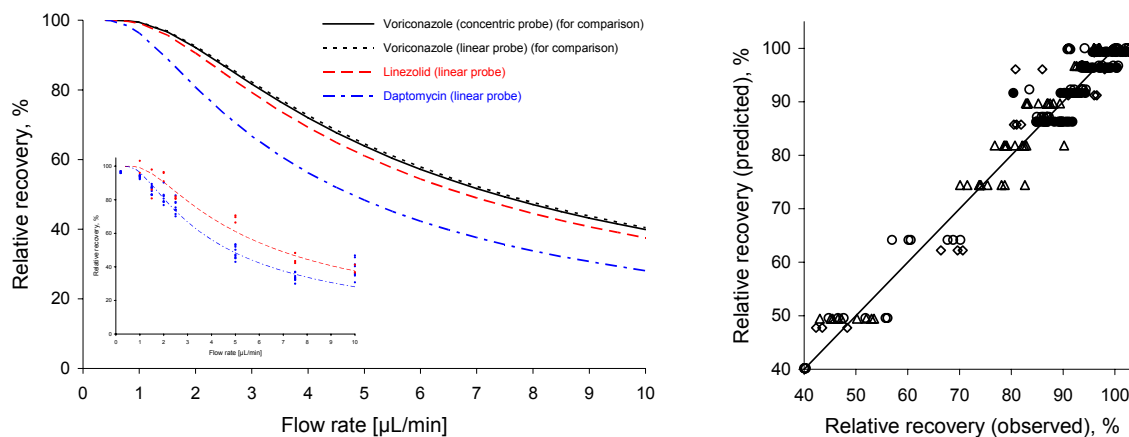


**Fig. 3-6:** Dependence of relative recovery (RR) of voriconazole (black solid and dotted line), linezolid (red dashed line), and daptomycin (blue dash-dotted line) on flow rate ( $F$ ,  $\mu\text{L}/\text{min}$ ) of perfusate according to the equation  $RR=100 \cdot (1 - e^{-r \cdot A/F})$  ( $r$ : mass transfer coefficient,  $A$ : membrane surface area) in concentric (black solid line) and linear catheters (left panel) and individual values of RR of linezolid and daptomycin (inset). RR observed during investigations of dependency of RR on  $F$  ( $\mu\text{L}/\text{min}$ ) versus RR predicted via estimation of  $r$  (right panel, open circles: voriconazole in concentric catheters (for comparison), filled circles: voriconazole in linear catheters (for comparison), rhombuses: linezolid in linear catheters, triangles: daptomycin in linear catheters). Solid line reflects the line of identity.

### 3.2.2.2 Concentration dependence and influence of the drug product on RR

Varying concentrations of voriconazole in the medium or perfusate (see 2.4.2.3) did not affect RR: For CMA60<sup>®</sup> catheters, individual RR in delivery experiments was high and ranged from 96.0% to 97.8% with an overall mean RR of 97.1% (CV: 0.5%) whereas RR in recovery experiments varied from 93.8% to 100.2% with an overall mean RR of 96.7% (CV: 1.7%) covering a concentration range between 1  $\mu\text{g}/\text{mL}$  and 50  $\mu\text{g}/\text{mL}$  of voriconazole (Tab. 3-8).

**Tab. 3-8:** Dependency of relative recovery (RR) on voriconazole concentration (1.0 µg/mL – 50.0 µg/mL) during recovery and delivery experiment: mean RR ± SD (CV, %) (n=9).

----- Recovery experiment -----			----- Delivery experiment -----		
Concentration [µg/mL]	Mean RR ± SD, %	CV, %	Concentration [µg/mL]	Mean RR ± SD, %	CV, %
<i>Concentric catheters (flow rate: 1.5 µL/min)</i>					
1.0	99.4 ± 0.9	0.9	1.0	96.9 ± 0.9	0.9
2.5	95.3 ± 1.3	1.4	2.5	96.7 ± 0.4	0.5
5.0	97.3 ± 0.7	0.8	5.0	97.0 ± 0.3	0.3
10.0	96.0 ± 1.1	1.1	10.0	97.2 ± 0.5	0.5
20.0	96.1 ± 1.2	1.2	20.0	97.4 ± 0.4	0.4
50.0	96.3 ± 1.4	1.5	50.0	97.4 ± 0.5	0.6
<i>Linear catheters (flow rate: 2.0 µL/min)</i>					
1.0	92.1 ± 7.5	8.1	1.0	95.0 ± 6.1	6.4
2.5	89.6 ± 3.3	3.7	2.5	95.7 ± 2.3	2.4
5.0	88.5 ± 3.9	4.4	5.0	95.7 ± 2.1	2.2
10.0	91.4 ± 2.3	2.6	10.0	95.7 ± 2.3	2.4

The results were comparable within one catheter as well as among catheters and results corresponded very well with the data obtained from the investigations on the dependency of recovery on flow rate (at 1.5 µL/min 97.0% (CV: 3.3%) (Tab. 3-6)).

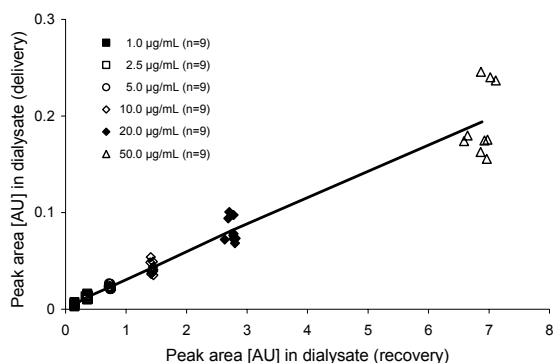
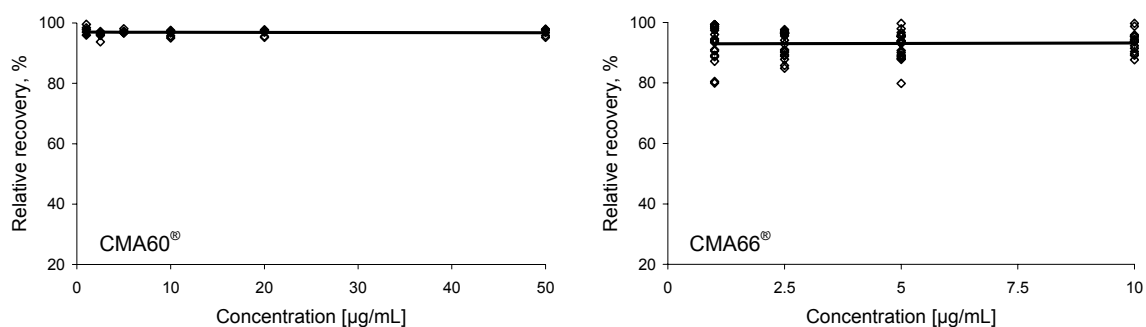
**Fig. 3-7:** Peak areas of delivery versus recovery experiment (CMA60®, flow rate 1.5 µL/min). Line: regression equation slope 0.028, intercept: 0.0023 AU, coefficient of determination: 0.9528). AU: arbitrary units.

Fig. 3-7 reflects the change in peak area dimension between the two different settings under corresponding conditions. Inherently, loss of voriconazole from the perfusate was much higher considering the RR during delivery experiment. Consequently, the peak area of the dialysate samples achieved was very small. By contrast, gain from the medium during recovery experiment was correspondingly high resulting in high peak area dimensions. The linear correlation in Fig. 3-7 confirmed the assumption that the permeation process was quantitatively equal in both directions through the semipermeable membrane.

In total, differences in RR between the results of the recovery and the delivery experiment were statistically not significant ( $p=0.34$ , ANOVA).

Moreover, statistical evaluation between RR and concentration of surrounding and perfusing medium yielded a regression line with a slope of  $-0.005\% \cdot \text{mL}/\mu\text{g}$  (SE:  $0.010\% \cdot \text{mL}/\mu\text{g}$ ) and an intercept of 97% (SE: 0.220%). The line was demonstrated to run parallel to the x-axis because the 95% CI of slope included zero ( $-0.025\% \cdot \text{mL}/\mu\text{g} - +0.014\% \cdot \text{mL}/\mu\text{g}$ ) (Fig. 3-8, left panel).



**Fig. 3-8:** Dependence of relative recovery (RR) on concentration ( $\mu\text{g/mL}$ ) of voriconazole during recovery and delivery experiment (3 CMA60<sup>®</sup> each, 1.5  $\mu\text{L/min}$  flowrate,  $n=54$ ), line: linear regression (left panel). Dependence of RR on concentration ( $\mu\text{g/mL}$ ) of voriconazole during recovery and delivery experiment (3 CMA66<sup>®</sup> each, 2.0  $\mu\text{L/min}$  flow rate,  $n=36$ ), line: linear regression (right panel).

In summary, from these results it can be concluded that RR was not influenced by the voriconazole concentrations investigated and that the permeation process was quantitatively equal in both directions through the semipermeable membrane. Therefore, retrodialysis is suitable for catheter calibration in future *in vivo* microdialysis studies. Confirmatory and highly comparable results were found for linear CMA66<sup>®</sup> catheters (Tab. 3-8, Fig. 3-8 right panel). RR in delivery experiments ranged from 80.4% to 99.7% with a mean recovery of 95.5% (CV: 2.2%) whereas RR in recovery experiments varied from 79.8% to 103.7% with a mean recovery of 90.5% (CV: 3.7%) covering a concentration range between 1  $\mu\text{g/mL}$  and 10  $\mu\text{g/mL}$ . The intra- and intercatheter variability was comparable and the results were well in line with the data from the investigations on flow rate dependence (at 2.0  $\mu\text{L/min}$  90.8% (CV: 4.6%) recovery experiment; 91.7% (CV: 1.2%) delivery experiment (Tab. 3-7)). The statistical evaluation between RR and concentration of surrounding and perfusing medium revealed a regression line with a slope of  $-0.016\% \cdot \text{mL}/\mu\text{g}$  (SE:  $0.214\% \cdot \text{mL}/\mu\text{g}$ ) and an intercept of 93% (SE: 0.954%). Analogously to concentric catheters, the line was demonstrated to run parallel to the x-axis since the 95% CI of slope included zero ( $-0.443\% \cdot \text{mL}/\mu\text{g}$  to  $+0.410\% \cdot \text{mL}/\mu\text{g}$ ) (Fig. 3-8). Analysis of the RR of the recovery and the delivery experiment did not show statistically significant differences ( $p=0.09$ , ANOVA).

The experiments on the question whether the clinically approved drug product of voriconazole (Vfend®) can be employed instead of the drug substance in clinical studies, e.g., for calibration purposes (see 2.4.2.3), revealed no significant differences between RR of voriconazole in the two solutions ( $p=0.986$ , Student's t-test). RR obtained for voriconazole ( $98.6\% \pm 0.38\%$ ) or Vfend® ( $98.6\% \pm 0.67\%$ ) solution (see Fig. 3-9) were well in correspondence to both the values elaborated during the delivery and the recovery experiments with voriconazole in concentric and linear catheters (see 3.2.2.1, Tab. 3-6, Tab. 3-7).

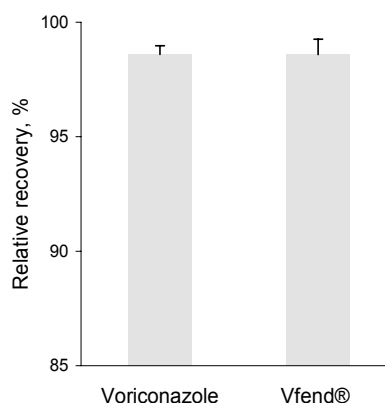


**Fig. 3-9:** Relative recovery (RR) (+SD) of voriconazole during delivery experiment (CMA60®; flow rate: 1.0  $\mu\text{L}/\text{min}$ ;  $n=3$ ) using different perfusates (drug substance and drug product (Vfend®)).

### 3.2.2.3 Steady state investigations

Steady state investigations were performed with increasing perfusate concentrations and microdialysis catheters (CMA60®) placed in a voriconazole solution of 10  $\mu\text{g}/\text{mL}$  imitating exaggerated steady state conditions after multiple dosing in humans. RR increased from 78.1% (CV: 12.3%) at a perfusate concentration of 50  $\mu\text{g}/\text{mL}$  voriconazole to 89.8% (CV: 3.8%) at 100  $\mu\text{g}/\text{mL}$  voriconazole (Fig. 3-10). RR of 150  $\mu\text{g}/\text{mL}$  and 200  $\mu\text{g}/\text{mL}$  catheter surrounding medium averaged at 87.3% (CV: 5.2%) and 91.4% (CV: 2.8%), respectively. Although the differences of RR obtained from the three explored perfusate concentrations (100  $\mu\text{g}/\text{mL}$  – 200  $\mu\text{g}/\text{mL}$ ) were statistically significant ( $p=0.033$ ), concentrations higher than 200  $\mu\text{g}/\text{mL}$  were not examined since higher concentrations in the perfusate used for retrodialysis may have a relevant influence on the 'true' interstitial concentration during subsequent PK sampling. Therefore a concentration of voriconazole equal to or higher than 100  $\mu\text{g}/\text{mL}$  but less than 200  $\mu\text{g}/\text{mL}$  is recommended for the *in vivo* calibration solution.

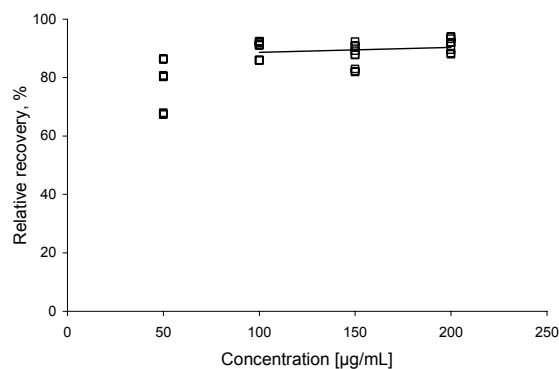


**Fig. 3-10:** Investigation of relative recovery (RR) (CMA60®, delivery experiment) with varying voriconazole concentrations (perfusate: 50, 100, 150, 200  $\mu\text{g}/\text{mL}$ ) during simulated steady state conditions (medium 10  $\mu\text{g}/\text{mL}$  voriconazole,  $n=36$ ). Line: regression equation (100, 150, 200  $\mu\text{g}/\text{mL}$ , slope: 0.0167%·mL/ $\mu\text{g}$ ).

### 3.3 III – Influence of disease state on target site exposure

#### 3.3.1 Applicability of microdialysis to inflamed subcutaneous adipose tissue

Microdialysates were successfully obtained from skin in two different states: infected and not infected. A calibration of each inserted catheter was performed with low and high concentration of voriconazole. The RR values are presented in Tab. 3-9. The mean *in vivo* RR of voriconazole was 71.0% (R: 62.1% – 84.5%, n=6) for RR<sub>H</sub> and 73.9% (R: 66.1% – 84.3%, n=6) for RR<sub>IN</sub>. Overall, the RR was similar within one individual for both concentrations and both conditions except for one guinea pig (No. 2) which showed a little difference in the infected area during the calibration with RP<sub>low</sub> (Tab. 3-9). Intraindividual variability of RR was low ranging from 0.1% to 2.6% (11.0% for guinea pig No. 2). The variability of RR was higher in the inflamed area (CV: 1.8% – 2.6% (11.0% for guinea pig No. 2)) than in the healthy one (CV: 0.1% – 0.5%). Overall mean RR for all determinations was 72.4% with a low CV of 12.5%. Despite the low inter-catheter variability individual mean RR values obtained for each animal and each area were used for conversion of the apparent microdialysate concentrations into the true ISF concentrations.

**Tab. 3-9:** Relative recoveries of voriconazole in healthy (RR<sub>H</sub>, %) and infected (RR<sub>IN</sub>, %) skin by CMA70<sup>®</sup> catheters during low-concentration (RR<sub>low</sub>, %) and high-concentration (RR<sub>high</sub>, %) RR determination.

Guinea pig No.	----- Healthy skin (H) -----			----- Infected skin (IN) -----		
	RR <sub>low</sub> <sup>1</sup>	RR <sub>high</sub> <sup>2</sup>	$\bar{x}$ RR <sub>H</sub> ± SD (CV, %)	RR <sub>low</sub> <sup>1</sup>	RR <sub>high</sub> <sup>2</sup>	$\bar{x}$ RR <sub>IN</sub> ± SD (CV, %)
1	84.5	83.9	84.2 ± 0.43 (0.5)	81.3	84.3	82.8 ± 2.12 (2.6)
2	67.0	66.5	66.8 ± 0.34 (0.5)	77.5	66.3	71.9 ± 7.94 (11.0)
3	62.1	62.2	62.1 ± 0.08 (0.1)	67.7	66.1	66.9 ± 1.19 (1.8)
$\bar{x}$ RR ± SD (CV, %)			72.4 ± 9.05 (12.5)			

<sup>1</sup>Mean C<sub>RP,low</sub> used for the low-concentration RR determination: 6.18 µg/mL (8.2% CV).

<sup>2</sup>Mean C<sub>RP,high</sub> used for the high-concentration RR determination: 11.66 µg/mL (4.8% CV).

#### 3.3.2 Dataset and concentration-time profiles of voriconazole

In total, 82 matrix samples, divided into 42 ISF samples, twelve RR samples, nine SB samples, twelve whole blood samples, and seven blood<sub>u</sub> samples, of the three guinea pigs were available from study sampling and the corresponding concentrations were included in the data set. Microdialysates were measured once with double injection, SB samples and blood<sub>u</sub> samples were measured once and whole blood samples were determined in duplicate with double injection. Due to clotting, ultrafiltration of the blood samples was feasible in only seven of twelve samples. Three samples (all at T<sub>0</sub>) were below the LLOQ and, hence, four samples enabled calculation of the fraction unbound (f<sub>u</sub>) in blood samples: guinea pig No. 1 T60 24.0%; guinea pig No. 2 T180 16.0%; guinea pig No. 3 T120 23.9% and T180 28.6%. The mean f<sub>u</sub> was 23.1% (CV: 22.6%). To provide unbound blood concentrations for all blood samples, blood<sub>u</sub> concentrations were obtained by transformation of all blood concentrations

by means of  $f_u$ . Five of the 82 samples were below the LLOQ. All of them resulted from blood (two) and blood<sub>u</sub> (three, see above) samples, respectively, taken prior to the last administered dose ( $T_0$ ). For evaluation and calculation of the AUCs of all matrices the concentration values at  $T_0$  were set to zero despite multiple dosing.

The median and individual concentration-time profile for ISF, SB, whole blood, and blood<sub>u</sub> during the 3 h sampling period presented in Fig. 3-11 revealed one general result: All graphs for ISF, SB, whole blood, or blood<sub>u</sub> of the guinea pigs were in comparable ranges within one matrix and they all followed very similar trends supported by the minor fluctuation. In addition, geometric CVs of the concentrations in the guinea pigs for each time point and each matrix ranged from 11.2% – 26.2% for ISF<sub>H</sub> and from 10.7% – 25.9% for ISF<sub>IN</sub>, from 20.0% – 42.0% for SB and from 1.2% – 18.4% for whole blood and blood<sub>u</sub>, respectively, indicating a low to moderate interindividual variability of voriconazole in guinea pigs. The concentrations of the ISF samples ranged between 0.9 µg/mL and 2.0 µg/mL for healthy skin and between 0.9 µg/mL and 1.7 µg/mL for infected skin, respectively. For both inflammation states concentrations did not vary largely during the sample period. The graphs of the ISF concentrations clearly indicated (Fig. 3-11) a strong similarity of the unbound concentrations of voriconazole in both infected and healthy skin. A statistical comparison of ISF<sub>H</sub> and ISF<sub>IN</sub> supported this result since a significant difference could not be ascertained ( $0.078 \leq p \leq 0.673$ , Wilcoxon test). This finding demonstrated that the unbound concentrations of voriconazole in ISF were not influenced by inflammation. Wider concentration ranges were found for SB and whole blood samples, 9.1 µg/g to 35.9 µg/g and 4.0 µg/mL to 7.7 µg/mL, respectively. Blood<sub>u</sub> concentrations ranged between 0.9 µg/mL and 1.8 µg/mL definitely comparable to the ISF concentrations.

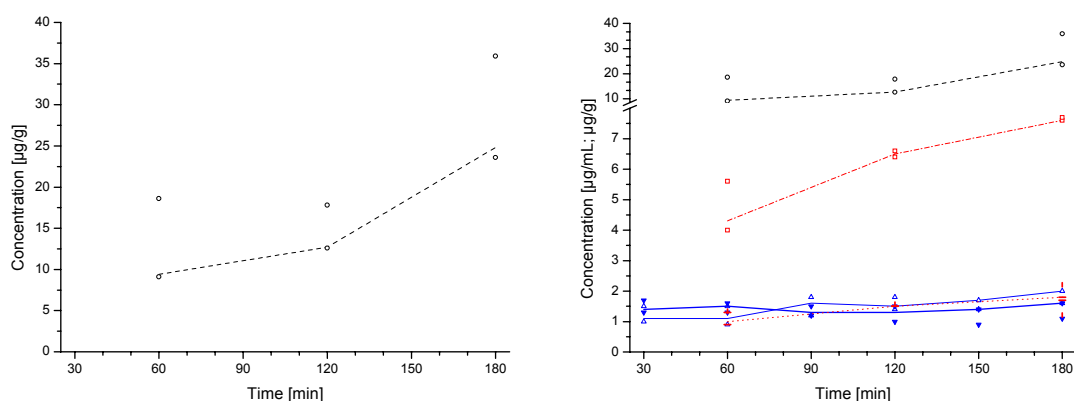


**Fig. 3-11:** Median (Min, Max) concentration-time profile of SB (black dashed line, black circles, in µg/g, left and right panel), whole blood (red dashed-dotted line, red squares, in µg/mL, right panel), unbound blood (blood<sub>u</sub>) concentrations (red dotted line, red horizontal bars (calculated concentrations, see 3.3.2), red vertical bars (measured concentrations), in µg/mL, right panel), ISF<sub>H</sub> (blue line, blue open triangles, in µg/mL, right panel) and ISF<sub>IN</sub> (blue bold line, blue filled triangles, in µg/mL, right panel) samples.

### 3.3.3 Pharmacokinetic analysis of the matrices

The geometric mean or median PK parameters and corresponding CVs are summarised in Tab. 3-10.

**Tab. 3-10:** PK parameters:  $C_{SS,max}$  [ $\mu\text{g/mL}$ ],  $t_{SS,max}$  [min], and partial  $AUC_{SS,0-3h}$  [ $\mu\text{g}\cdot\text{h/mL}(\text{g})$ ] in the different matrices (n=3).

Matrix	$C_{SS,max}$ $\bar{x}_{geom} \pm SD_{geom}$ ( $CV_{geom}$ , %)	$t_{SS,max}$ $\tilde{x}$ (R)	Partial $AUC_{SS,0-3h}$ $\bar{x}_{geom} \pm SD_{geom}$ ( $CV_{geom}$ , %)
SB	27.6 $\pm$ 1.26 (23.3)	180 (180-180)	39.7 $\pm$ 1.31 (27.7)
Blood	7.6 $\pm$ 1.01 (1.2)	180 (180-180)	14.6 $\pm$ 1.06 (5.4)
Blood <sub>u</sub>	1.8 $\pm$ 1.01 (1.2)	180 (180-180)	3.4 $\pm$ 1.06 (5.4)
ISF <sub>H</sub>	1.9 $\pm$ 1.06 (6.1)	180 (90-180)	4.0 $\pm$ 1.10 (9.5)
ISF <sub>IN</sub>	1.6 $\pm$ 1.04 (3.5)	60 (30-180)	3.7 $\pm$ 1.05 (5.2)

In ISF<sub>H</sub> and ISF<sub>IN</sub>, voriconazole reached a geometric mean  $C_{SS,max}$  of 1.9  $\mu\text{g/mL}$  and 1.6  $\mu\text{g/mL}$ , respectively, after a time period ranging from 30 min to 180 min (see Tab. 3-10).

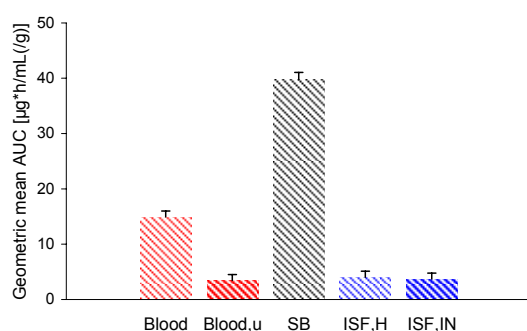


**Fig. 3-12:** Geometric mean AUC (+SD) [ $\mu\text{g}\cdot\text{h/mL}(\text{g})$ ] of the different matrices – blood, blood<sub>u</sub>, SB, ISF<sub>H</sub>, ISF<sub>IN</sub> – in guinea pigs.

**Tab. 3-11:** Geometric mean, standard deviation, coefficient of variation, median, and range of AUC ratios of the matrices ISF<sub>H</sub>, ISF<sub>IN</sub>, blood, blood<sub>unbound(u)</sub>, and SB.

Ratio	$\bar{x}_{geom} \pm SD_{geom}$ ( $CV_{geom}$ , %)	$\tilde{x}$ (R)
ISF <sub>IN</sub> /ISF <sub>H</sub>	0.9 $\pm$ 1.15 (14.2)	0.9 (0.8-1.1)
ISF <sub>H</sub> /blood	0.3 $\pm$ 1.05 (4.8)	0.3 (0.3-0.3)
ISF <sub>H</sub> /blood <sub>u</sub>	1.2 $\pm$ 1.05 (5.0)	1.2 (1.1-1.2)
ISF <sub>IN</sub> /blood	0.2 $\pm$ 1.10 (9.5)	0.2 (0.2-0.3)
ISF <sub>IN</sub> /blood <sub>u</sub>	1.1 $\pm$ 1.10 (9.4)	1.1 (1.0-1.2)
SB/blood	2.7 $\pm$ 1.24 (22.1)	2.3 (2.3-3.4)
SB/blood <sub>u</sub>	11.5 $\pm$ 1.24 (22.1)	10.2 (10.2-14.8)

The  $AUC_{SS,0-3h}$  was calculated to be 4.0  $\mu\text{g}\cdot\text{h/mL}$  for ISF<sub>H</sub> and 3.7  $\mu\text{g}\cdot\text{h/mL}$  for ISF<sub>IN</sub> (see Tab. 3-10, Fig. 3-12).

PK parameters for ISF substantiated the general analysis of the concentrations and concentration-time profiles, respectively. Both sites investigated yielded highly comparable results for  $C_{SS,max}$  and  $t_{SS,max}$  and, hence, the shapes of the profiles were comparable as well. An overall geometric mean AUC value was calculated to be 3.9  $\mu\text{g}\cdot\text{h/mL}$  with a low CV of 7.9% confirming the low variability in this matrix.

The geometric mean ratio  $AUC_{ISF,IN}/AUC_{ISF,H}$  of 0.9 (CV: 14.2%, R: 0.8 – 1.1, see Tab. 3-11) supported the hypothesis that the distribution in these two matrices was almost equal. Thus, a dependence of exposure on an inflammation cannot be anticipated.

A notably high concentration was achieved in the entire skin (geometric mean  $C_{SS,max}$  27.6  $\mu\text{g/g}$ , CV: 23.3%). An intensive and fast increase (permeation and distribution) of voriconazole in the tissue was found

during the entire sample period (Fig. 3-11, left panel). The tendency that the increase in SB lagged behind the blood, i.e., the slope of the concentration increase was smaller between the  $T_{60}$  and the  $T_{120}$  sample compared to blood, has been observed in all animals. The geometric mean partial  $AUC_{SS,0-3h}$  amounted to  $39.7 \mu\text{g}\cdot\text{h}/\text{g}$ , CV: 27.7% (see Tab. 3-10, Fig. 3-12). In order to enable a comparison of SB results to the other matrices density measurements of SB were carried out with a blank biopsy sample ( $\sim 1 \text{ cm}^3$ ) of guinea pigs using a helium pycnometer ( $n=1$ ) as well as by the method of water displacement ( $n=3$ ). For the measurement with the pycnometer the sample (0.9042 g) was placed in the measurement chamber of known volume and one helium washing cycle was performed at  $22^\circ\text{C}$ . In result of the experiment by means of water displacement 1.15 g of SB corresponded to approximately 1 mL water. This was corroborated by the measurement with the pycnometer assessing a sample volume of  $0.8649 \text{ cm}^3$ , and, hence, a density value of  $1.05 \text{ g}/\text{cm}^3$ . Thus, concentrations of  $\mu\text{g}/\text{g}$  might be considered as concentrations in  $\mu\text{g}/\text{mL}$  providing the basis for comparison to the other matrices investigated.

In whole blood, voriconazole reached a low variable geometric mean  $C_{SS,max}$  of  $7.6 \mu\text{g}/\text{mL}$  (CV: 1.2%). The geometric mean AUC was calculated to be  $14.6 \mu\text{g}\cdot\text{h}/\text{mL}$  (CV: 5.4%) (see Tab. 3-10, Fig. 3-12). The increase of concentration of voriconazole at the end of the sampling time seemed to be not finished yet (see Fig. 3-11, right panel). Hence, in either of the two compartments – blood or skin – the true  $C_{SS,max}$  did not seem to have been reached during the 3 h sampling period ( $C_{SS,max}$  at  $t_{SS,max}$  180 min, see Tab. 3-10) since concentrations were still increasing after multiple doses have been administered over eleven days. Unbound concentrations in blood (geometric mean  $C_{SS,max}$   $1.8 \mu\text{g}/\text{mL}$ , CV: 1.2%, at  $t_{SS,max}$  180 min) amounted to a geometric mean AUC of  $3.4 \mu\text{g}\cdot\text{h}/\text{mL}$  (CV: 5.4%) (see Tab. 3-10, Fig. 3-12) substantiating the consistency between blood<sub>u</sub> and ISF.

In general and according to the individual results, AUC ratios were in comparable ranges in all guinea pigs and reflected the high distribution of voriconazole into tissue. With the 20 mg/kg once daily dose SB concentrations exceeded (unbound) whole blood approximately threefold (twelfold) and  $ISF_H$  and  $ISF_{IN}$  concentrations approximately tenfold and elevenfold, respectively, during the entire sampling period (see Tab. 3-11). Blood concentrations were approximately fourfold above ISF concentrations (see Tab. 3-11) whereas the unbound portion of blood approximately equalled the ISF concentrations.

## **3.4 IV – Clinical long-term microdialysis pilot study with voriconazole in healthy volunteers**

### **3.4.1 Feasibility of long-term application of clinical microdialysis**

During the pilot part of the study (February/March 2009) all three healthy volunteers adhered to the study protocol demonstrated by no exclusions (drop-outs) and replacements, respectively. Moreover, the conduction took place according to the protocol in terms of voriconazole administration and sampling.



In all healthy volunteers blood donation was uncomplicated and tolerated during the trial. Local irritations by the blood catheter were met by changing the application site on the forearm for the next study visit. Apart from time deviations (see 3.4.5), all blood samples planned were obtained and subjected to plasma preparation. The total blood loss of approximately 250 mL over a period of 4 days in addition to the screening visit, final examination and genotype sample was well tolerated by all healthy volunteers.

The experiences with the long-term applications of the concentric and linear microdialysis catheters were as follows: The tolerability of the procedure in the healthy volunteers was well, consistent, and remarkable as they stated long-term microdialysis to be even more convenient than the blood donation. An explanation for that apparent contradiction was found to be the repeating insertion of the venous blood catheters every study visit involving blood donation compared to the one-time application of the microdialysis catheter at the beginning of the study. Additionally, the acceptance of and positive attitude towards the catheters resulted from their sufficient fixation and protection implying only marginal restrictions for the daily life of the volunteers, and permitted the observation of the catheter sites. The reliable and sophisticated fixation of all components (see 2.6.2) involved in the clinical study setting ensured the easy and fast exchange of the pumps, the pump syringes and microvials, and guaranteed nearly complete mobility of the volunteers at any time. The dialysate samples were obtained even during sleep without any disturbances of the individual. These results observed and documented during the conduction of the trial should be substantiated by the results of extensive RR investigations (see 3.4.4). Barring one leakage problem due to a disjuncture within one linear catheter tubing (see 3.4.4), the microdialysis device and membranes of the catheters, respectively, kept their function over the entire study duration (~87 h) and microdialysates were continuously obtained in the volume the chosen flow rate allowed for except few exceptions (see below). Since the premature displacement of none of the catheters was indicated in one individual, microdialysate samples could be obtained from one catheter over the entire study duration according to the ESS (see 2.6.1).

If no (once happened) or less dialysate volume (five times of 210) was achieved, reasons were found to be sourced not in the catheter but in the position of the healthy volunteer leading to a back-flow of microdialysate when volunteers moved to an upright position and the tubing slipped out of the sample vial holder. An additional fixation of the tubing at the outlet tubing guide channel accounted for and quickly resolved that event. However, samples with less dialysate were analysed and commented in the data set regarding the sample volume (see 3.4.5). Microdialysis pumps worked reliable apart from battery problems resulting in discontinuation of perfusate flow (once possibly up to 10 h). Managing both the leakage (via fixation by two tubing connectors) as well as the battery problem (usage of new batteries and proper handling during insertion of batteries) led to the continuation in all volunteers until the planned end of the trial. Once the microdialysis catheters were withdrawn after ~87 h, they were complete and sites of implantations were normal except of one small haematoma at the site of insertion of one catheter.

### 3.4.2 Bioanalysis of the study samples

Quality assessment during the study sample measurements was realised by QC samples covering the entire analytical run. All runs – three UF and six microdialysate runs – met the criteria for precision and accuracy set in the international FDA guideline for bioanalytical methods [101] and could therefore be accepted. The results for accuracy and interday precision supported the results regarding the robustness and ruggedness of the method and are summarised in chapter 3.1.1.7.

During HPLC analysis a peak form slightly different from bell-shape occurred in some of the dialysates (see Fig. 3-1, left blue and red chromatogram). To investigate a possible influence of the pH value on elution, pH values of selected microdialysis samples were measured with pH measuring sticks (see 2.6.7). Several other ruggedness parameters have been investigated during ruggedness analysis (see 2.3.1.8). As a result, all of the selected samples were alkaline (pH values between 8.0 and 8.5 of study samples measured (10 h – 11 h visit 1 and 10 h – 11 h visit 7 of a representative study individual, 103)). The other solutions used during analysis (ACN, calibration working solutions, and calibration samples) had a pH value of ~5.0. Therefore, buffer solutions with pH values of 6, 8, and higher were produced using a pH meter and ammonium dihydrogen phosphate, adjusted with ammonia solution (30%). HPLC analysis of the samples containing buffer with alkaline pH value instead of Ringer's solution showed no peak shape comparable with the shape of the study samples. However, elution abnormalities were regarded to be due to the study samples since QCs, calibrators, and recovery solutions produced in the study centre showed normal peak shapes all the time.

Finally, variations of the mobile phase – leading to a shift of the  $t_R$  of voriconazole to higher values (~7.5 min) – revealed a co-eluent (~5 min) being responsible for the peak form (see 3.1.1.3), i.e., voriconazole has been overlaid with another eluent of unknown origin at a  $t_R$  of ~3 min. Since intake of concomitant medication has been precluded, exogenous substances could be ruled out, i.e., the interfering substance (or substance mixture) had to be of endogenous origin. Samples were reanalysed under adequate chromatographic conditions (see 3.1.1.3).

### 3.4.3 Genotype analysis

DNA was successfully purified from blood samples of the pilot study individuals with concentrations ranging from 52.9 ng/ $\mu$ L to 80.7 ng/ $\mu$ L. The ratio of absorptions at 260 nm (absorption of nucleic acids) versus 280 nm (absorption of protein) in order to assess the purity of DNA with respect to protein contamination (260/280 quotient) was 1.93 and, hence, in the recommended range of 1.8 to 2.0 [120]. Amplified DNA sequences were sufficiently yielded by PCR indicated by the 455 bp fragment for CYP2C9\*2, the 155 bp fragment for CYP2C9\*3, and the 323 bp fragment for CYP2C19\*2 as result of gel electrophoresis. The pyrosequencing analysis with regard to the SNPs of isoenzymes CYP2C9 and CYP2C19 predominantly identified homozygous wild types (see Tab. 3-12 and Tab. 3-18). For ID 101 a

heterozygous genotype was revealed for CYP2C9\*3 and a homozygous one for isoenzyme CYP2C19\*2 in ID 102. A representative pyrogram<sup>®</sup> is shown in Fig. 7-5.

**Tab. 3-12:** Genotype results of pilot study individuals (n=3).

ID	----- Isoenzymes -----		
	CYP2C9*2	CYP2C9*3	CYP2C19*2
101	C/C (G/G) <sup>1</sup>	T/G (A/C) <sup>2</sup>	C/C (G/G) <sup>1</sup>
102	C/C (G/G) <sup>1</sup>	T/T (A/A) <sup>1</sup>	T/T (A/A) <sup>3</sup>
103	C/C (G/G) <sup>1</sup>	T/T (A/A) <sup>1</sup>	C/C (G/G) <sup>1</sup>

<sup>1</sup>Homozygous wild type.

<sup>2</sup>Heterozygous for CYP2C9\*3.

<sup>3</sup>Homozygous for CYP2C19\*2.

### 3.4.4 *In vivo* relative recovery

Since this was a long-term application of a microdialysis catheter, extensive RR investigations were possible and performed, respectively, leading to an overall number of 93 RR samples including the RP samples. For the three study volunteers 48 values should be obtained for RR. Due to flow problems or insufficient volume two values were lacking (ID 102 visit 3, CMA60<sup>®</sup>; ID 103, visit 5, CMA66<sup>®</sup>). RR and RP samples were measured via HPLC and RR were calculated using Eq. 1-1 (see 1.2.3). Retrospectively, in all individuals ISF<sub>c</sub> and ISF<sub>f</sub> concentrations were below 7.29 µg/mL when retrodialysis started. Thus, the perfusate concentration used for the calibration after multiple dosing (see 2.6.6) widely exceeded ISF concentrations (>twentyfold). In conclusion, perfusate concentrations were sufficient for calibration on all study visits.

The RR results for each catheter (concentric: RR<sub>c</sub> and linear: RR<sub>l</sub>) in each individual (ID) per study day, study visit, and RR sample 1 and 2 are shown in Fig. 3-13 and listed in Tab. 7-8 and Tab. 7-9. The tables include the concentrations of the RP samples (C<sub>RP</sub>, with R of CV: 3.2% – 16.9%).

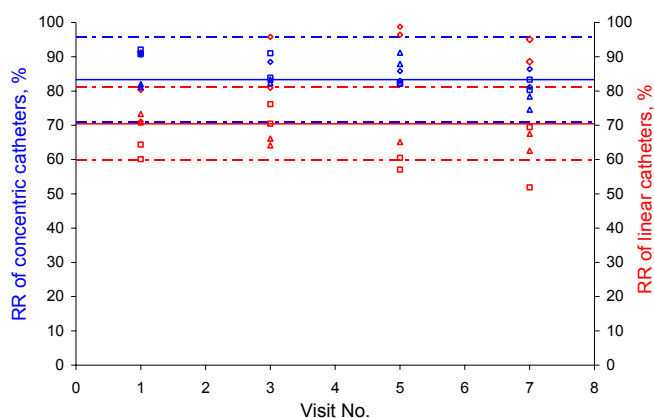


**Fig. 3-13:** Relative recoveries of concentric (RR<sub>c</sub>, blue symbols and lines) and linear catheters (RR<sub>l</sub>, red symbols and lines). Squares: ID 101, diamonds: ID 102, triangles: ID 103. Line: Overall median for catheter type; dotted line: ±15% of the median.

Overall,  $RR_c$  ranged from 74.6% to 92.1% for both subsequently taken samples (separate for RR1: 74.6% – 91.2%; separate for RR2: 78.4% – 92.1%). Mean  $RR_c$  ranged from 82.3% to 86.8% for the first RR sample and from 82.9% to 87.8% for the second one. This narrow range for each RR sample without significant differences between the IDs ( $p=0.212$ , Kruskal-Wallis test) was supported by low SDs and CVs predominantly in the single digit magnitude and in general less than 8.3% demonstrating a high consistency of  $RR_c$ .

Overall,  $RR_i$  values ranged from 51.9% to 98.8% for both subsequently taken samples (for RR1: 57.0% – 98.8%; for RR2: 51.9% – 96.4%). Mean  $RR_i$  ranged from 65.7% to 92.5% for the first RR sample and from 61.8% to 84.2% for the second one. However, since one leakage (broken inlet tubing) occurred in individual 102 on study day 1/visit 2 over night, the results, i.e., the larger range with significant differences ( $p=0.009$ , Kruskal-Wallis test) shown by these linear catheters than by the concentric ones, have further been differentiated ( $p=0.199$ , Kruskal-Wallis test, without the RR values of visit 3, 5, 7 for ID 102). On the subsequent study visit 3 this leakage was successfully managed using a tubing connector (see 2.2.4.1) which joined both parts together. In consequence, there was one missing sample caused by missing fluid directly after the reconnection and one subsequent sample with a larger volume than the nominal one. The latter one resulted from the additionally manual flush of the catheter realised by an external syringe filled with Ringer's solution. In consequence,  $RR_i$  yielded afterwards by the catheter (only seen via HPLC analysis in retrospect) were elevated up to 98.8% (Tab. 7-9, Fig. 3-13). The elevation of  $RR_i$  in this individual was responsible for the reversed results concerning the ratio of  $RR_c$  and  $RR_i$  in comparison to the results in the other individuals (Fig. 7-6).

But the results (if visit 1 was evaluated separately from visit 3-5-7) showed reproducible RR even after the leakage (RR1: Mean $\pm$ SD (CV): 96.5% $\pm$ 1.98% (2.0%), visit 3-5-7); RR2: Mean $\pm$ SD (CV): 88.6% $\pm$ 7.74% (8.7%), visit 3-5-7).

Statistically significantly lower RR were predominantly determined for linear catheters ( $RR_i$ ) ( $p=0.002$  for all IDs;  $p\leq 0.018$  for ID 101,103;  $p=0.499$  for ID 102, Wilcoxon test) represented by a ratio of  $RR_c$  and  $RR_i$  primarily higher than 1 (Fig. 7-6). In total,  $RR_i$  results were comparable to the  $RR_c$  results in terms of low SDs as well as CVs which were predominantly in the single digit magnitude, and in general less than 13.3% demonstrating a high consistency in  $RR_i$ .

Compared to RR1, the RR2 samples consistently showed lower or highly comparable coefficients of variation except for  $RR_i$  for ID 102. The exceptional behaviour might be explained by the leakage event in individual 102. In spite of this exception, it was suggested and realised, respectively, to correct voriconazole concentrations in the dialysate for the RR obtained by RR2 samples and not RR1 or a mean value from both of the samples. More explicitly, voriconazole concentrations in the dialysate obtained during visit 1 and 2 were transformed with RR2 obtained at the beginning of visit 1, dialysate concentrations of visit 3 and 4 with RR2 obtained during visit 3, dialysate concentrations of visit 5 and 6 with RR2 obtained during visit 5 and dialysate concentrations of visit 7 with RR2 obtained at the end of visit 7. The RR1 value was seen as a backup value for RR2 as Tab. 3-13 shows: The

variability between the RR1 and RR2 sample was low. In general, lower variability (intra-visit variability) was found for  $RR_c$  (CV:  $\leq 5.8\%$ ) than for  $RR_i$  (CV:  $\leq 20.5\%$ ).

**Tab. 3-13:** Variability of relative recovery ( $RR_c$  and  $RR_i$ ) for RR samples 1 and 2 within one visit and one individual (n=2; n=1 for visit 3 ID 102 for  $RR_c$  and visit 5 ID 103 for  $RR_i$ ).

Individual	Visit	$RR_c$			$RR_i$		
		$\bar{x}$ , %	SD, %	CV, %	$\bar{x}$ , %	SD, %	CV, %
101	1	91.4	0.93	1.0	62.2	2.99	4.8
101	3	87.4	5.09	5.8	73.3	4.05	5.5
101	5	82.2	0.20	0.2	58.8	2.46	4.2
101	7	81.8	2.16	2.6	60.6	12.43	20.5
102	1	91.0	0.41	0.4	75.7	6.57	8.7
102	3	88.5	-	-	88.4	10.51	11.9
102	5	84.4	2.04	2.4	97.6	1.68	1.7
102	7	83.8	3.67	4.4	91.8	4.57	5.0
103	1	81.5	0.64	0.8	72.1	1.73	2.4
103	3	82.9	0.72	0.9	65.1	1.38	2.1
103	5	89.5	2.34	2.6	65.1	-	-
103	7	76.5	2.71	3.5	65.1	3.49	5.4

Considering the leakage event – differentiated evaluation of visit 1 and visit 3-5-7 for individual 102 - intraindividual intervisit variability (CV: 4.4% – 12.5%, Tab. 3-14) and inter-individual variability (CV: 4.3% – 12.5%, Tab. 3-15) were low as well, across all samples and catheters over the four-day-period.

**Tab. 3-14:** Relative recovery ( $RR_c$  and  $RR_i$ ) for all study visits per individual during the whole study duration.

Individual	Visit	$n_{RR}$ samples/visit	$n_{total}$	$\bar{x}$ RR, %	SD, %	CV, %
----- $RR_c$ -----						
101	1, 3, 5, 7	2	8	85.7	4.75	5.5
102	1, 3, 5, 7	2 (1)	7	86.7	3.77	4.4
103	1, 3, 5, 7	2	8	82.6	5.16	6.3
----- $RR_i$ -----						
101	1, 3, 5, 7	2	8	63.7	7.96	12.5
102	1, 3, 5, 7	2	8	88.4	9.95	11.3
103	1, 3, 5, 7	2 (1)	7	67.1	3.79	5.6
----- $RR_i$ for individual 102 subdivided in visit 1 and visits 3, 5, 7 -----						
102	1	2	2	75.7	6.57	8.7
102	3, 5, 7	2	6	92.6	6.65	7.2

**Tab. 3-15:** Relative recovery ( $RR_c$  and  $RR_i$ ) for all study individuals at study visit 1, 3, 5, and 7.

Visit	$n_{volunteers}$	$n_{RR\ samples/visit}$	$n_{total}$	$\bar{x} RR_c, \% (CV, \%)$	$\bar{x} RR_i, \% (CV, \%)$
1	3	2	6	88.0 (5.7)	70.0 (10.1)
3	3 [2]	2 (1)	6 (5) [4]	85.8 (4.4)	75.6 (15.5) [69.2 (7.7)]
5	3 [2]	2 (1)	6 (5) [3]	85.4 (4.3)	75.6 (26.9) [60.9 (6.7)]
7	3 [2]	2	6 [4]	80.7 (5.0)	72.5 (22.5) [62.8 (12.5)]

Values in square brackets indicate the differential evaluation (exclusion of ID 102 in study visits  $\geq 3$ ) due to the leakage of the linear catheter in ID 102 (i.e., only IDs 101 and 103 for study visits 3, 5, and 7).

In some cases, RR obtained at study visit 1 (prior the drug administration) were higher than the RR obtained for the following ones (Tab. 3-13, Fig. 3-13). In accordance with the results mentioned so far, a calculation of the overall recovery value for all visits and individuals revealed a mean recovery of 84.9% with a CV of 5.6% for  $RR_c$ . The higher variability for  $RR_i$  (CV: 18.5%) was explained by the leakage event and could be reduced by a differentiated evaluation (without visits 3-5-7 in ID 102) leading to a CV of 10.7% with a mean recovery of 66.5% ( $n=17$ ). Mean recovery for both catheters resulted in 79.1% and 77.1% including the leakage, respectively, with variability values in comparable range (14.7% and 14.1%, respectively, Tab. 3-16).

**Tab. 3-16:** Overall relative recovery (RR): Mean RR for CMA60<sup>®</sup>, CMA66<sup>®</sup>, and both catheters for all RR samples obtained during the study.

Catheter	$n_{total}$	$\bar{x} RR_{c,i}, \%$	SD, %	CV, %
CMA60 <sup>®</sup>	23	84.9	4.76	5.6
CMA66 <sup>®</sup>	23 [17]	73.3 [66.5]	13.55 [7.09]	18.5 [10.7]
CMA60 <sup>®</sup> +CMA66 <sup>®</sup>	46 [40]	79.1 [77.1]	11.63 [10.88]	14.7 [14.1]

Values in square brackets indicate the results when considering the leakage of the linear catheter in ID 102.

### 3.4.5 Dataset and dataset checkout

The final dataset contained voriconazole UF,  $ISF_c$ , and  $ISF_i$  concentration data of three healthy, male individuals as well as their characteristics, dosing history, and other study characteristics and documentation.

**Tab. 3-17:** Distribution of the observations for the matrices studied (available samples at the end of the study).

Matrix	No. of samples planned	No. of samples obtained	Samples obtained, %
UF	174	174	100.0
$ISF_c$	186	184	98.9
$ISF_i$	186	181	97.3
Total	546	539	98.7

98.7% (539) of all samples planned were available from the observation period of 84 h – deriving from the different matrices shown in Tab. 3-17. Missing samples within the microdialysates were due to the problems mentioned in 3.4.1. Due to double analysis of the microdialysis samples (see 3.1.1.3 and 3.4.2) three additional missing samples had to be

recorded. Ultimately, 536 samples (98.2%) were available for PK analysis.

40 (7.3%) of the 546 samples planned had comments, recorded in the CRF, primarily concerning sample volume obtained or time deviations (5.1%). Unavoidable time deviations due to the study protocol were not included in this calculation. Two events of all dosing events had a comment resulting from disturbances during infusion. All exact sampling time points were documented and deviations to time planned noted in the CRF. These deviations were low and ranged from -2% to +0.6%. Therefore, the time planned value could be used to calculate, e.g., mean concentration and construction of mean voriconazole concentration-time profiles since a deviation of time lower than 10% from the time planned is considered as not relevant in terms of PK disposition process time scale.

The dataset (in total 609 rows) was built and checked by the same person. Mistakes were rare and of minimal extent. The small number of individuals renders the dataset clear and manageable. Single column check overall revealed plausible values. Cells without values were set to -99 for the dependent variable (i.e., drug concentration) indicated by Fig. 7-7. In conclusion no cell existed without any value.

The check for minimum and maximum values revealed reasonable values (ID: 101 – 103; TIME: 0.00 – 84.03 h; TIPL: 0.00 – 84.00 h; TALD: 0.00 – 12.00 h; AMT: 0 – 498 mg; RATE: 0 – 293.73 mg/h; DV: 0 – 7.29 µg/mL; CMT: 1 – 3; EVID: 0,1; ADMA: 0 – 2; FLDV: 0,1; FLCA: 0, 60, 66; FLAM: 0,1; VISI: 1 – 7; DAY: 1 – 4; OCC=VISI; DOS1: 2161 – 2260 mg; DOS2: 200 – 498 mg; AGE: 34 – 46 years; HT: 1.76 – 1.83 m; WT: 77.9 – 83.1 kg; BMI: 24.49 – 25.89 kg/m<sup>2</sup>; COME: 0,1; OID: 1 – 3; COM1: 0,1; COM2: 0,1,2; COM3: 0,1,2; COM4: 0,1; COM5: Text). In general, check for plausible values within all columns revealed correctness. The DOS1 column only contained values summed for each individual (2161, 2200, 2260 mg, cumulative), the DOS2 column the individual ones per visit (200, 320, 328, 332, 413, 480, 492, 498 mg, per visit). The following cross-column-check identified only conditional combinations in one row (e.g., for TIME=0: AMT>0, EVID=1 (indicating a dosing event), DV=0, RATE>0). This procedure revealed at time 0 (baseline, T=0) a concentration probably due to the retrodialysis process (see 3.4.9).

### 3.4.6 Demographic data and genetic characteristics

The demographic data are shown in Tab. 3-18. According to the study protocol AGE and HT were determined once and WT four times per participant. Analysis of the latter cardinally scaled parameter, and the parameter derived from it (BMI), demonstrated a low intraindividual variability during the entire observation period for all individuals. Interindividual variability among all individuals was low as well. For calculations of WT-related parameters within visit 1 to 4 the WT determined in visit 1 and for calculations within visit 5 to 7 the WT determined in visit 5 was employed according to the LOCF method (last observation carried forward) since the periods for which the observation was applied was very short ( $\leq 2$  days). Genetic characteristics are listed according to the results presented in section 3.4.3. All laboratory values were within the reference ranges. Hence, study individuals were young/middle aged, healthy volunteers with merely little variabilities.

**Tab. 3-18:** Individual characteristics: demographics and genetic variations for isoenzymes CYP2C9 and CYP2C19 within the individuals 101 – 103.

ID	AGE [years]	HT <sup>a</sup> [cm]	WT <sup>b</sup> [kg] x̄ (Min-Max)	BMI [kg/m <sup>2</sup> ] x̄ (Min-Max)	CYP2C9 genotype	CYP2C19 genotype
101	43	181	83 (82-84)	25.3 (25.1-25.5)	1*/3*	1*/1*
102	46	176	78 (77-80)	25.3 (24.9-25.9)	1*/1*	2*/2*
103	34	183	82 (82-82)	24.5 (24.5-24.5)	1*/1*	1*/1*
x̄ (R)	43 (34-46)	181 (176-183)	82 (77-84)	25.1 (24.5-25.9)	-	-

<sup>a</sup>Once determined at screening visit.

<sup>b</sup>Four times determined (at screening visit, at visit 1 and 5, and at final examination).

### 3.4.7 Dose characteristics

Apart from one event, due to disturbances during an infusion (see below), seven doses were very accurately administered in each individual in terms of time points and amount (Tab. 3-19) according to the study protocol. This is graphically shown in Fig. 7-8.

**Tab. 3-19:** Dosing characteristics.

ID	<i>Intravenous dosing</i>				<i>Oral dosing</i>		
	6 mg/kg WT		4 mg/kg WT		Independent from WT – 200 mg		
	Visit 1	Visit 2	Visit 3	Visit 4	Visit 5	Visit 6	Visit 7
	----- <i>Time [h]</i> -----						
101-103	0.00	12.00	24.00	36.00	48.00	60.00	72.00
	----- <i>Dose amount [mg]</i> -----						
101	498	498	332	332	200	200	200
102	480	480	320	320	200	200	200
103	492	413	328	328	200	200	200
	----- <i>Total dose iv [mg]</i> -----				----- <i>Total dose po [mg]</i> -----		
101		1660				600	
102		1600				600	
103		1561				600	
	----- <i>Total dose [mg]</i> -----						
101				2260			
102				2200			
103				2161			

Tab. 3-19 clearly shows the discrepancy between iv and oral administration. After the switch from one to the other administration route, the dose was reduced by about 40% (37.5 – 39.8%). All individuals received voriconazole without any loss except for one individual (103) where air bubbles at the beginning of the second infusion led to a difference of the infused solution of about 40 mL accounting for 79 mg voriconazole (16.1% of the dose planned, see Tab. 7-10). Tab. 7-10 demonstrates the interindividual variability among the amount given within the 6 mg/kg WT, 4 mg/kg WT, and oral administration period which was low and merely a result of the influence of the WT on the amount administered. The comparatively



high CV for visit 2 expressed the deviation (-16.1%) of the amount administered in individual 103. Due to the nature of an administration of a tablet and fixed absolute dose, respectively, no noticeable problems leading to variability occurred after the switch.

According to the study protocol, voriconazole was administered intravenously until the switch. As the duration and infusion rate of infusion should have been equal in all volunteers, the different doses were achieved by different concentrations and not by the total volume of the infusion solution. Deviations regarding the infusion end and, thus, duration of the infusions were low but occurred probably due to a slightly variability among the infusomates used (Tab. 7-11). Since the tubing system of the volunteer 103 contained air bubbles the volume of the infusion solution was discharged which led to a faster end of infusion and higher variability within visit 2 across the individuals (CV: 8.9%).

The variability in one infusomate was low as shown in Tab. 7-12. The CV (9.2%) for study visits 1 and 2 in individual 103 was found to be explained as before. However, the CV for study visits 3 and 4 (8.0%) in individual 103 was elevated, too. Since diffusion disturbances occurred in this infusomate one might conclude that this infusomate was the source of the deviations mentioned. Actual infusion durations were considered in the dataset.

#### **3.4.8 Safety assessment during the clinical trial**

Safety of study participants was monitored during the whole study duration by frequent examinations according to the study protocol.

There were no study drug discontinuations or dose reductions due to AEs. An AE, which was considered not related to voriconazole treatment, occurred in individual 101 and appeared as a small haematoma (diameter 1 cm) at a catheter insertion site. Treatment-emergent AEs (with probable (1), possible (4), and certain (4) relationship to treatment) were reported by each of the individuals (see Tab. 3-20). None of the events were classified as serious. The severity was mild to moderate. All AEs were completely recovered within or at the end of the study time, respectively. One AE in ID 102 was treated with concomitant medication (mefenamic acid) due to headache. As most frequent, AEs of the eyes were reported by all volunteers and led to a special additional examination in one of the individuals (ID102) since he reported eye disturbances of such a relevance that they were considered to be further investigated (see Tab. 3-20).

**Tab. 3-20:** Adverse events (AEs) with certain, probable, or possible relationship to treatment.

ID	AE	AE onset/end	Relationship to treatment	Seriousness	Severity	Action taken	Outcome
101	Impaired vision when eyes closed	Intermittent	Certain	Not serious	Moderate	No	Recovered/Resolved
101	Burning sensation at infusion site	Intermittent during drug administration	Certain	Not serious	Mild	No <sup>1</sup>	Recovered/Resolved
102	Headache	once, ~10 h after last drug administration	Possible	Not serious	Mild	Pharmaceutical treatment <sup>2</sup>	Recovered/Resolved
102	Impaired vision when eyes closed	Intermittent	Certain	Not serious	Moderate	No <sup>3</sup>	Recovered/Resolved
102	Nausea	Once, ~3 h after last drug administration	Probable	Not serious	Moderate	No	Recovered/Resolved
103	Impaired vision when eyes closed	Intermittent	Certain	Not serious	Mild	No	Recovered/Resolved
103	Headache	Once, ~3 h after last drug administration	Possible	Not serious	Mild	No	Recovered/Resolved
103	Slight dizziness	Once, ~1 h after last drug administration	Possible	Not serious	Mild	No	Recovered/Resolved
103	Slight drowsiness (asthenia)	Once, ~1/2 h after last drug administration	Possible	Not serious	Mild	No	Recovered/Resolved

<sup>1</sup>Once, infusion was stopped and the cannula was flushed with saline.

<sup>2</sup>PARKEMED<sup>®</sup> once orally (500 mg mefenamic acid).

<sup>3</sup>Ophthalmological examination without abnormalities.

### 3.4.9 Range of concentrations and individual concentration-time profiles of voriconazole

Overall, the concentrations ranged from 0.13 µg/mL (<LLOQ; if >LLOQ: from 0.16 µg/mL) to 3.27 µg/mL for UF concentrations and from 0.21 µg/mL to 7.29 µg/mL for voriconazole ISF concentrations obtained via linear catheters. ISF concentrations obtained via concentric catheters were in the range between 0.19 µg/mL and 3.13 µg/mL. Median concentrations in the ISF (1.10 µg/mL) were in the range of the UF concentrations ( $C_{UF}$ ) expressed by a median ratio of 1.0 for  $ISF_c$  and  $ISF_l$ .

**Tab. 3-21:** Concentration characteristics of voriconazole in UF and  $ISF_{c,l}$  during the entire study time.

	$C_{UF}$ [µg/mL]	$C_{ISF,c}$ [µg/mL]	$C_{ISF,l}$ [µg/mL]
Min	0.13 <sup>1</sup>	0.19	0.21
Max	3.27	3.13	7.29
Median	1.05	1.02	1.18
Median $C_{ISF}/C_{UF}$		1.0	1.1

<sup>1</sup>Baseline sample <LLOQ; two samples <LLOQ in ID 101: 0.13 and 0.14 µg/mL (considered for evaluation); if >LLOQ: 0.16 µg/mL.

The time planned (TIPL) has been utilised when concentration-time profiles are shown (see 3.4.5). For explorative graphical analysis some profiles implement dose-normalised concentrations (per 1 mg dose amount) or dose-, WT-normalised concentrations (1 mg dose amount and per 1 kg WT) since the concentrations were triggered by different doses for each individual as a consequence of 1) the applied dosing schedule (intraindividual dose de-escalation during maintenance iv dosing and by the switch from an iv to a fixed oral administration) and 2) the WT-based iv dose administration (see Tab. 3-19).

Overall concentration-time profiles are shown in Fig. 3-14 which were visually and statistically inspected in the following. In general, the order of individuals remained unchanged over the entire investigational period (see Fig. 3-14).

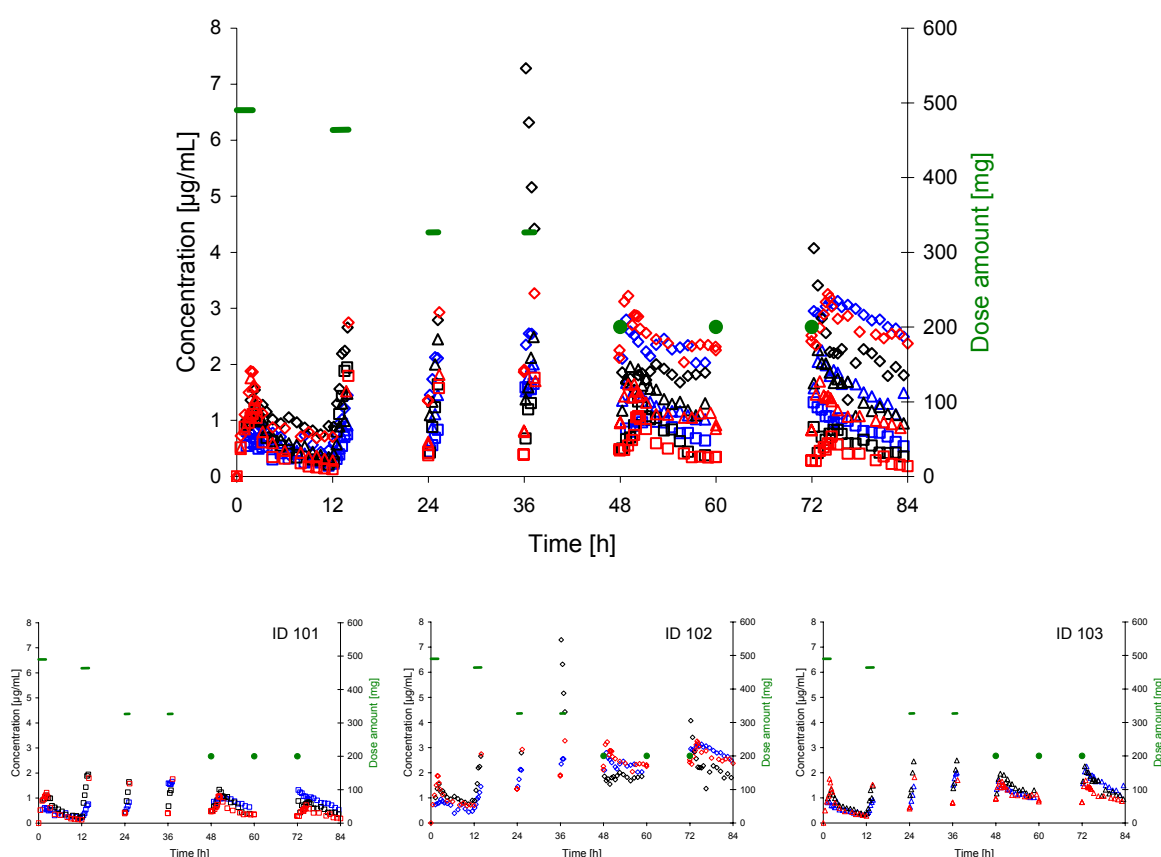


**Fig. 3-14:** Unbound plasma (UF (red colour)) and interstitial space fluid (ISF<sub>C</sub> (blue colour), ISF<sub>I</sub> (black colour)) concentration-time profile of voriconazole in ID 101 (squares), ID 102 (diamonds), ID 103 (triangles). Mean dose amounts: green bars for infusion; green dots for tablets. Baseline and next two ISF samples excluded (see Fig. 3-17).

The UF (unbound plasma) concentration-time profile of voriconazole is shown in Fig. 3-15 (left panel). After single iv loading dose concentrations appeared very similar among all individuals, however, this could not be statistically confirmed ( $p=0.040$ , Kruskal-Wallis test). This behaviour successively changed after multiple iv maintenance and oral dosing: Variability increased expressed by higher SDs and CVs (R: visit 2 31.8% – 67.1%, visit 3 34.3% – 76.2%, visit 4 39.5% – 75.0%, visit 5 49.0% – 87.1% and visit 7 68.8% – 101.9%)

caused by statistically significantly different reactions by the individuals to multiple doses of voriconazole. Nevertheless, concentration-time profile and, hence, the variability appeared similar within the visits of oral administration (Fig. 3-15, right panel, 48 h – 60 h and 72 h – 84 h) visible as a plateau-like phase and comparable to a steady state.

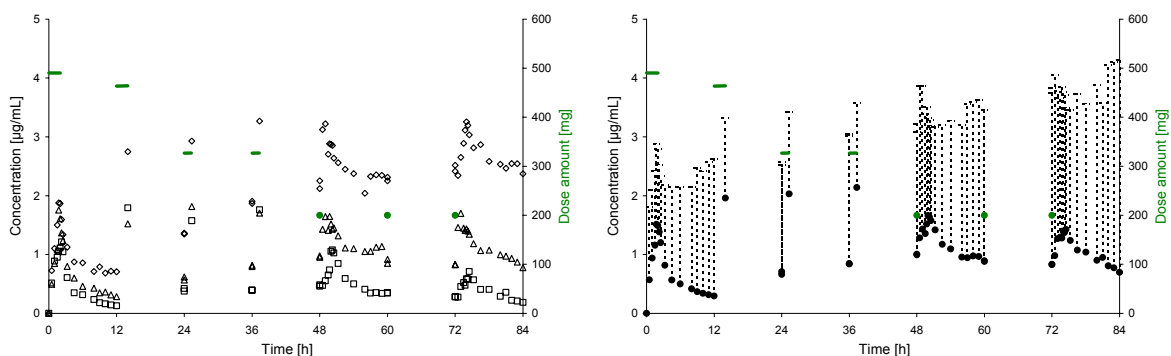


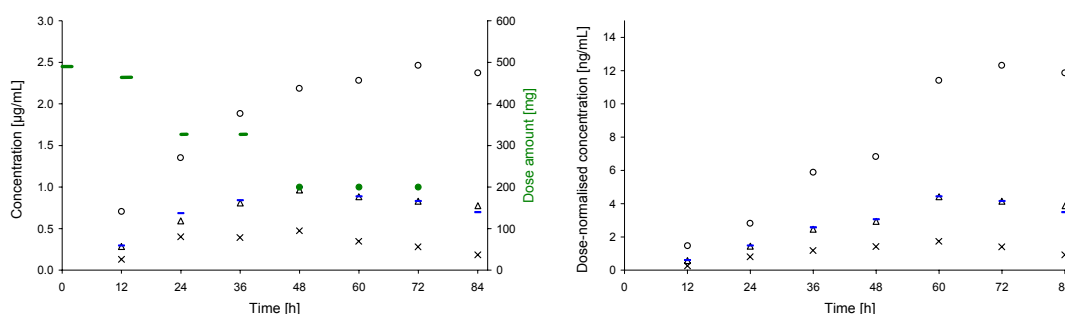
**Fig. 3-15:** UF concentration-time profiles of voriconazole in ID 101 (squares), ID 102 (diamonds), and ID 103 (triangles) (left panel). Geometric mean (+SD) concentrations (black filled circles) (right panel). Mean amount of doses: green lines for infusion; green dots for tablets.

The dose-normalisation of the data allowed to explore the concentration-time course independent from the total amount administered which differed in the sequence therapy scheme. While geometric mean values of the measured concentrations decreased after the switch to oral dose of nearly half of the iv dosing amount (Tab. 3-19) the normalised data showed a further increase of the concentrations and variability (Fig. 7-9, left panel). Dose-normalised data did not show differences to dose-, WT-normalised data (Fig. 7-9, right panel) since the WT values of the individuals were highly comparable in the sampling period of the study ( $81 \text{ kg} \pm 2 \text{ kg}$ , Tab. 3-18) and no considerable difference in variability occurred: The CVs of the dose-normalised data ranged from 14.01% to 101.89% while dose-, WT-normalised were in range of 15.73% to 104.38%. Hence, dose-, WT-normalised data were not further analysed when further evaluating the data.

At the end of study visits 2 to 6 two plasma samples, instead of one, were taken (tandem samples at  $C_{\min}$ , Fig. 7-10). The small coefficients of variation, ranging from 0.8% to 8.3% of each two concentrations reflect the high quality and reproducibility during the conduction of the study as well as the accuracy of the analytical method (Tab. 7-13). Referring to the work of JONSSON et al. the addition of one more sample at each study occasion can improve quality and quantity of the information obtained via population analysis [121]. For the study presented in this thesis, this was found to be important especially for the sparse sampling study visits (2, 3, 4, 6) since the data are planned to undergo further PK analysis when the main part is completed.

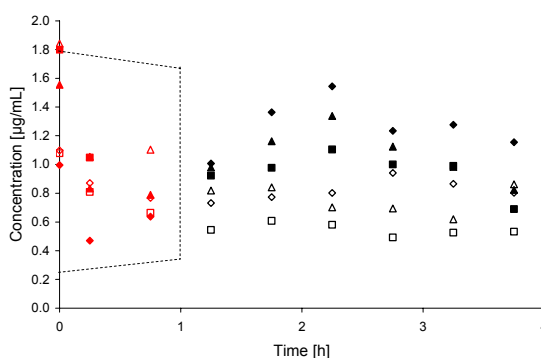
Geometric minimal unbound plasma concentrations increased within the study visits 1 to 4 about 3.4-fold – for ID 102 in factor 3.1 and more pronounced for ID 101 in factor 3.6 and

ID 103 in factor 3.4. Concentrations decreased after the switch to oral administration (Fig. 3-16, left panel). Individually seen, this was in accordance with ID 101 and 103 but for individual 102 a plateau phase seemed to have been reached. From the first oral dose on interindividual variability achieved a maximal range. Fig. 3-16 (right panel) demonstrates dose-normalised individual and the referring geometric minimal unbound plasma concentrations. An increase of concentrations could be noticed within the study visits 1 to 5, including the switch, for ID 102 in factor 7.8 and for ID 103 in factor 7.7 and more slightly for ID 101 in factor 6.6 indicating an accumulation of voriconazole. After the second oral dose concentrations tended to decrease (ID 101, ID 103).



**Fig. 3-16:** Minimal UF concentration-time profile (left panel) and dose-normalised profile (right panel) in ID 101 (crosses), ID 102 (circles), and ID 103 (triangles). Median values for tandem samples for visit 2-6. Geometric mean: blue bars. Mean amount of doses: green lines for infusion; green dots for tablets.

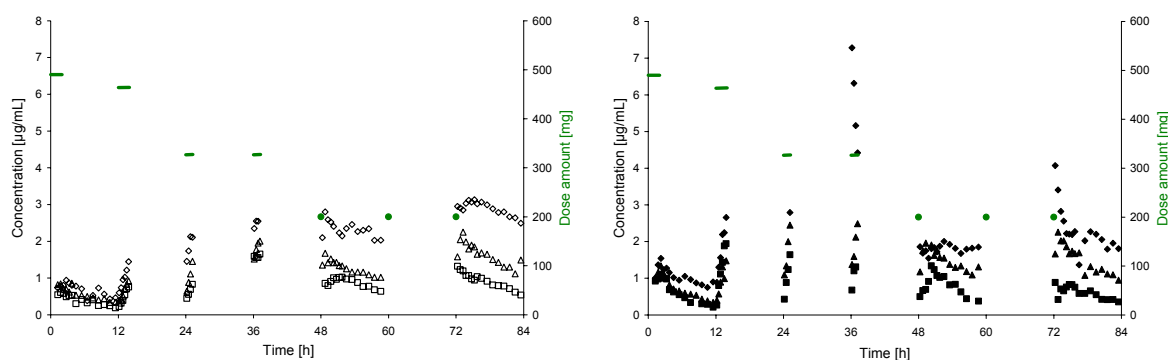
The visual inspection of the  $ISF_{c,l}$  concentration-time profiles demonstrated an implausible course within the early taken samples: The microdialysate baseline samples which were directly taken before the first infusion of voriconazole exhibited concentrations of voriconazole in the range of 1.00 µg/mL to 1.84 µg/mL (Fig. 3-17). In most instances, the subsequently taken samples decreased in concentration although an increase was expected as a result of the continuous voriconazole infusion (Fig. 3-17).



**Fig. 3-17:** Early individual microdialysate concentration-time data (first, second, and third ISF samples (red symbols)) in ID 101 (squares), ID 102 (diamonds), and ID 103 (triangles). Open symbols: concentric catheters, filled symbols: linear catheters.

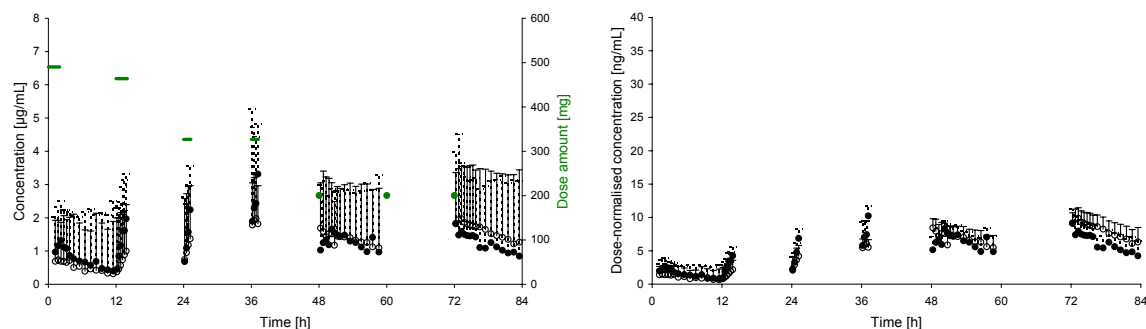
This observable fact was explained by the calibration of the individual catheters prior the first administration of voriconazole and will be discussed later (see 4.4.3). Therefore, the baseline as well as the next two samples were regarded to be implausible and were excluded from further graphical explorations or data analysis.

In general and as expected, concentration-time profiles of voriconazole in ISF<sub>c</sub> and ISF<sub>I</sub> were highly comparable ( $p=0.173$  all IDs;  $p=0.907$  ID 101;  $p=0.639$  ID 102;  $p=0.001$  ID 103, Wilcoxon test) in each individual (Fig. 3-18) visually illustrated by the geometric mean courses in Fig. 3-19 (left panel). A very small difference appeared in visit 7 ( $\Delta$ : 0.2  $\mu\text{g}/\text{mL}$ ). After single dose (in visit 1), a relatively low interindividual variability, comparable to the one among UF concentrations, was expressed by a range of  $CV_{\text{geom}}$  from 13.1% to 53.2% for ISF<sub>c</sub> (not statistically confirmed:  $p=0.004$ , for all IDs, Kruskal-Wallis test) and from 4.4% to 75.4% for ISF<sub>I</sub> (not statistically confirmed:  $p=0.006$ , for all IDs, Kruskal-Wallis test). After multiple dosing the individual courses behaved different leading to significantly different and increasing variability resembled by, in most cases, rising coefficients of variation (R for ISF<sub>c</sub>: visit 2: 29.3% – 48.2%, visit 3: 43.6% – 63.0%, visit 4: 13.6% – 26.6%, visit 5: 27.2% – 59.0% and visit 7: 39.9% – 72.5% and R for ISF<sub>I</sub>: visit 2: 28.6% – 63.2%, visit 3: 25.8% – 62.2%, visit 4: 39.5% – 116.6%, visit 5: 18.1% – 63.2% and visit 7: 43.9% – 75.4%).

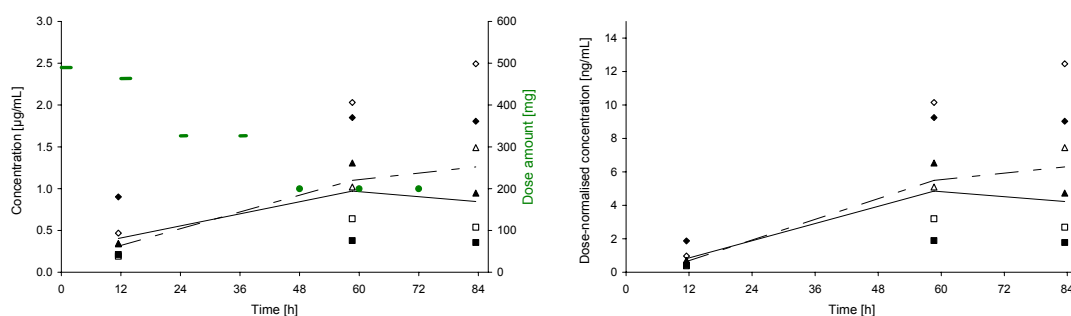


**Fig. 3-18:** Concentration-time profiles of voriconazole in ISF of ID 101 (squares), ID 102 (diamonds), and ID 103 (triangles). Left panel:  $C_{\text{ISF},c}$  (open symbols). Right panel:  $C_{\text{ISF},I}$  (filled symbols). Mean amount of doses: green lines for infusion; green dots for tablets.

The dose-normalisation of the ISF concentration data (Fig. 7-11, Fig. 3-19, right panel) accounted for different amounts of the individual doses during sequence therapy elucidating accumulation of voriconazole from single to multiple dose administration until an approximate plateau phase was reached illustrated by  $C_{\text{min}}$  in ISF<sub>c</sub> and ISF<sub>I</sub> (Fig. 3-20).

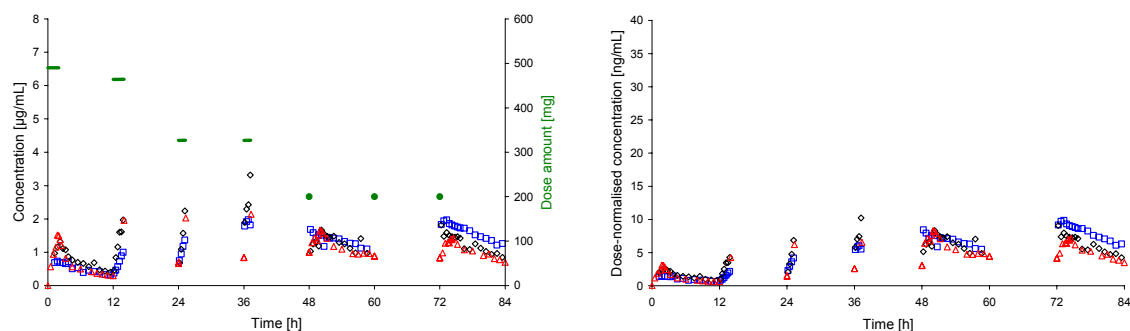


**Fig. 3-19:** Geometric mean  $\text{ISF}_c$  (+SD, open circles) and  $\text{ISF}_I$  (+SD, filled circles) concentrations (left panel, mean amount of doses: green lines for infusion; green dots for tablets) and dose-normalised geometric mean  $\text{ISF}_c$  (+SD, open circles) and  $\text{ISF}_I$  (+SD, filled circles) concentrations (right panel).



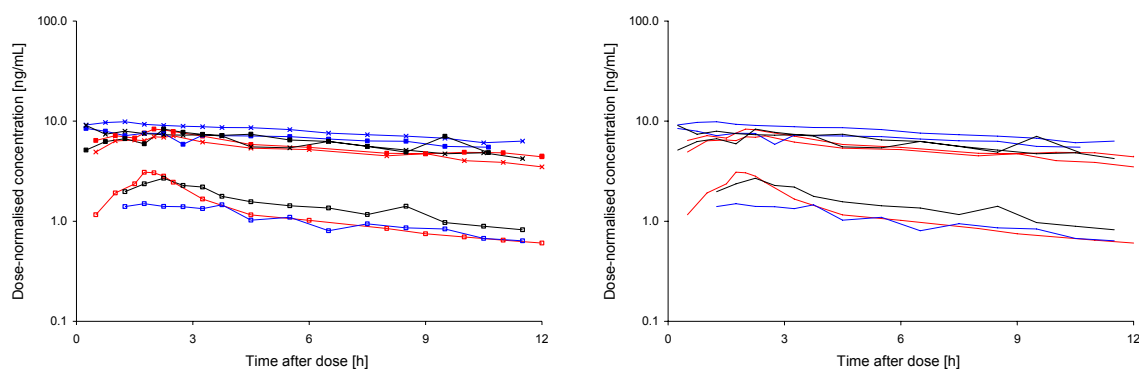
**Fig. 3-20:** Minimal  $\text{ISF}_c$  (open symbols) and  $\text{ISF}_I$  (filled symbols) concentration-time data for ID 101 (squares), ID 102 (diamonds), and ID 103 (triangles) including geometric mean of  $\text{ISF}_c$  (dashed line) and  $\text{ISF}_I$  (solid line) concentrations (left panel). Mean amount of doses: green lines for infusion; green dots for tablets. Right panel: dose-normalised data and geometric mean.

Fig. 3-21 illustrates the geometric mean concentration- (left panel) and dose-normalised concentration- (right panel) time profiles of voriconazole in all matrices studied allowing a direct comparison among each other:  $\text{ISF}$  concentrations exhibited comparable values to unbound plasma concentration values.



**Fig. 3-21:** Geometric mean concentration-time profile of voriconazole in all matrices (UF (red triangles),  $\text{ISF}_I$  (black circles),  $\text{ISF}_c$  (blue squares) (left panel, mean amount of doses: green lines for infusion; green dots for tablets)). Dose-normalised geometric mean concentration-time profile of voriconazole in all matrices (right panel).

Certainly, these courses masked the individual ones as seen in Fig. 3-14 and more clearly in Fig. 7-12 while overlaying the profiles according the time elapsed after the last dose. The illustrations in a semi-logarithmic scale (Fig. 7-12, right panels) are predestined to elaborate the number of phases of the decline in concentration after dose: After iv single dose a predominantly biphasic decline, most pronounced in UF, was derived and supported by the semi-logarithmic courses of the individuals in Fig. 7-13 (right panels) and the geometric ones in Fig. 3-22 sorted by the matrices. In ISF, this biphasic decline was less distinctive and resembled a monophasic behaviour (ID 101, ID 102). After multiple dosing a predominantly monophasic shape was visible, however, in UF a slight biphasic shape was found in all IDs (visit 7). In some profiles (ID 102, visit 1, UF; ID 103, visit 1, UF) a slight triphasic shape might be elaborated and others (ISF, multiple dose) did not show an ascent or descent at all. Less distinctive differences hamper an exact classification, however, visually inspected terminal phases declined more or less parallel to each other within one ID (most pronounced in ID 101) (Fig. 3-22, right panel) indicating a PK behaviour different from strong nonlinearity in the concentration range investigated.



**Fig. 3-22:** Semi-logarithmic geometric mean concentration (dose-normalised)-time plots of voriconazole in UF (red colour), ISF<sub>c</sub> (blue colour), and ISF<sub>i</sub> (black colour). Visit 1 (open squares), visit 2 (filled squares), visit 3 (crosses) (left panel). Right panel: spaghetti plot.

### 3.4.10 Pharmacokinetic parameters

The calculation of the terminal slope  $\lambda_z$  (see Tab. 7-14, Tab. 3-22), including 6 to 14 data points (see Tab. 7-14), revealed a wide variability of values which was predominantly lower after single dose in comparison to multiple dose administration (visit 5) (UF: 90.6% to 138.0%, ISF<sub>c</sub>: 22.7% to 45.6%, ISF<sub>i</sub>: 59.9% to 196.2%) (see Tab. 3-22, Fig. 3-23). While the variability of the terminal slopes of the UF and ISF<sub>i</sub> courses decreased as determined for visit 7, terminal slopes for the ISF<sub>c</sub> courses resulted in a comparable value. However, in general no tendency to an ascent or descent was discovered. Behind these estimations was the assumption of a mono-exponential terminal phase in the concentration-time curves. For each of the performed regression an adjusted  $r^2$  value was calculated ranging from 0.0908



(ID 102, visit 5, CMA60<sup>®</sup>) to 0.9752 with a median value of 0.8503. In general,  $\lambda_z$  values decreased from single to multiple dose administration.

**Tab. 3-22:** Geometric mean [1/h], geometric SD [1/h], and geometric CV, % of terminal slope  $\lambda_z$ .

Matrix	----- Visit 1 -----			----- Visit 5 -----			----- Visit 7 -----		
	$\bar{x}_{geom}$	SD <sub>geom</sub>	CV <sub>geom</sub>	$\bar{x}_{geom}$	SD <sub>geom</sub>	CV <sub>geom</sub>	$\bar{x}_{geom}$	SD <sub>geom</sub>	CV <sub>geom</sub>
UF	0.0747	2.1687	90.6	0.0352	2.8089	138.0	0.0461	2.5060	115.1
ISF <sub>c</sub>	0.0818	1.2508	22.7	0.0441	1.5443	45.6	0.0408	1.5468	45.8
ISF <sub>I</sub>	0.0903	1.7398	59.9	0.0466	3.5133	196.2	0.0655	1.3670	32.0

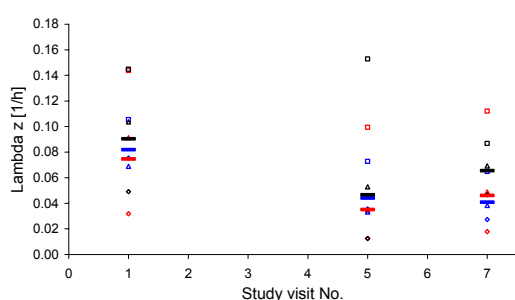


**Fig. 3-23:**  $\lambda_z$  after single (visit 1) and multiple dosing (visits 5, 7) in ID 101 (squares), ID 102 (diamonds), and ID 103 (triangles). UF (red colour), ISF<sub>c</sub> (blue colour), ISF<sub>I</sub> (black colour). Geometric means (bars).

**Tab. 3-23:** Geometric mean [h] of terminal half-life  $t_{1/2}$ .

Matrix	Visit 1	Visit 5	Visit 7
	$\bar{x}_{geom}$	$\bar{x}_{geom}$	$\bar{x}_{geom}$
UF	9.3	19.7	15.0
ISF <sub>c</sub>	8.5	15.7	17.0
ISF <sub>I</sub>	7.7	14.9	10.6

Under the assumption of no further phase in the terminal decline, the geometric mean terminal half-life was calculated to be 9.3 h for UF concentrations, 8.5 h for ISF<sub>c</sub>, and 7.7 h for ISF<sub>I</sub> after single dose (see Tab. 3-23). Following further administrations terminal half-lives increased. Both after single (visit 1) and after multiple dosing (visit 5, visit 7) geometric mean terminal half-lives were comparable between all matrices with about 9 h and 15 h, respectively, for  $t_{1/2}$ . Certainly, variability was as high as for  $\lambda_z$  (see Fig. 3-24).

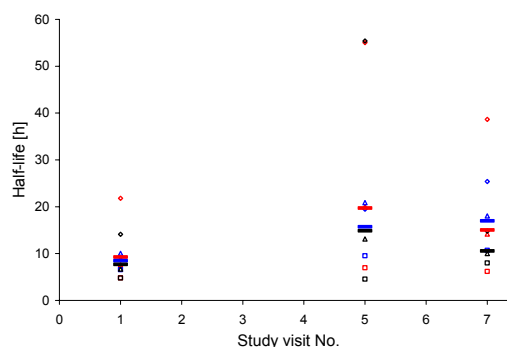


**Fig. 3-24:** Half-life  $t_{1/2}$  after single (visit 1) and multiple dosing (visits 5, 7) in ID 101 (squares), ID 102 (diamonds), and ID 103 (triangles). UF (red colour), ISF<sub>c</sub> (blue colour), ISF<sub>I</sub> (black colour). Geometric means (bars).

Tab. 7-15 summarises  $C_{max}$  and the related times ( $t_{max}$ ) of the UF and ISF concentration-time profiles. Both unbound plasma as well as ISF levels rapidly increased and  $C_{max}$  predominantly occurred within 2 h (median: 1.75 h, R: 0.25 h – 4.50 h) (Tab. 3-24, Fig. 3-25).

For UF in visit 1 this time span (median: 1.75 h) was close to the end of the infusion (2 h). For ISF,  $C_{max}$  was achieved at  $\sim 2.25$  h (ISF<sub>c</sub>, ISF<sub>i</sub>). After multiple dosing median  $t_{max}$  attained was predominantly lower than  $\sim 2.25$  h for all matrices (R: 0.25 h – 2.25 h). In more detail, median UF  $t_{max}$  was attained within  $\sim 2$  h and median ISF  $t_{max}$  within  $\sim 1$  h, respectively. In general, voriconazole was rapidly available after dosing and quickly absorbed after oral administration, respectively, but interindividual differences were elevated when comparing the time values over the entire study duration (see Fig. 3-25).

**Tab. 3-24:** Median [h] and range [h] of  $t_{max}$ .

Matrix	Visit 1 $\tilde{x}$ (R)	Visit 5 $\tilde{x}$ (R)	Visit 7 $\tilde{x}$ (R)
UF	1.75 (1.75-2.25)	1.75 (1.00-2.25)	2.00 (1.00-2.50)
ISF <sub>c</sub>	2.75 (1.75-3.75)	0.75 (0.75-3.75)	1.25 (0.25-3.25)
ISF <sub>i</sub>	2.25 (2.25-2.25)	2.25 (1.25-4.50)	0.25 (0.25-0.75)

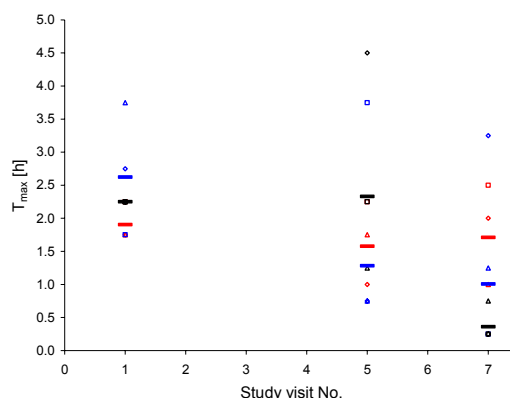


**Fig. 3-25:**  $T_{max}$  after single (visit 1) and multiple dosing (visits 5, 7) in ID 101 (squares), ID 102 (diamonds), and ID 103 (triangles). UF (red colour), ISF<sub>c</sub> (blue colour), ISF<sub>i</sub> (black colour). Geometric means (bars).

The visual analysis of the determined  $C_{max}$  data (Tab. 7-15, Fig. 3-26 upper left panel) after single dose in comparison to multiple dose administration revealed an increase of  $C_{max}$  for all IDs in ISF whereas  $C_{max}$  in UF either showed an increase (ID 102) or a decrease (ID 101) or approximately comparable values (ID 103). Geometric mean maximum unbound plasma concentrations of visit 1 (1.59  $\mu\text{g/mL}$ ) slightly increased by 12.6% in comparison to visit 5 (1.79  $\mu\text{g/mL}$ ) and remained static in comparison to visit 7 (1.58  $\mu\text{g/mL}$ ) indicating an almost comparable occurrence of this parameter during multiple dose administration (Tab. 3-25). The maximum ISF<sub>c</sub> concentrations of visit 1 (0.79  $\mu\text{g/mL}$ ) strongly increased by 113.9% in comparison to visit 5 (1.69  $\mu\text{g/mL}$ ) and by 167.1% in comparison to visit 7 (2.11  $\mu\text{g/mL}$ ), and maximum ISF<sub>i</sub> concentrations of visit 1 (1.32  $\mu\text{g/mL}$ ) moderately increased by 31.8% in comparison to visit 5 (1.74  $\mu\text{g/mL}$ ) and by 52.3% in comparison to visit 7 (2.01  $\mu\text{g/mL}$ ). Hence, after multiple dosing the mean parameters were more or less comparable within the matrices but variability strongly increased (Tab. 3-25). Dose-normalised  $C_{max}$  values and plots are

shown in Tab. 7-16 and in Fig. 3-26 (upper right panel), respectively. The normalised data clearly show an increase of  $C_{\max}$  after multiple dosing (visit 5) and a further slight increase compared to visit 7. The interindividual variability increased. Dose-normalised data did not show differences to dose-, WT-normalised data and no considerable difference in variability occurred. Hence, dose-, WT-normalised data were set aside when further evaluating the data, analogues to the concentration-time profile data.

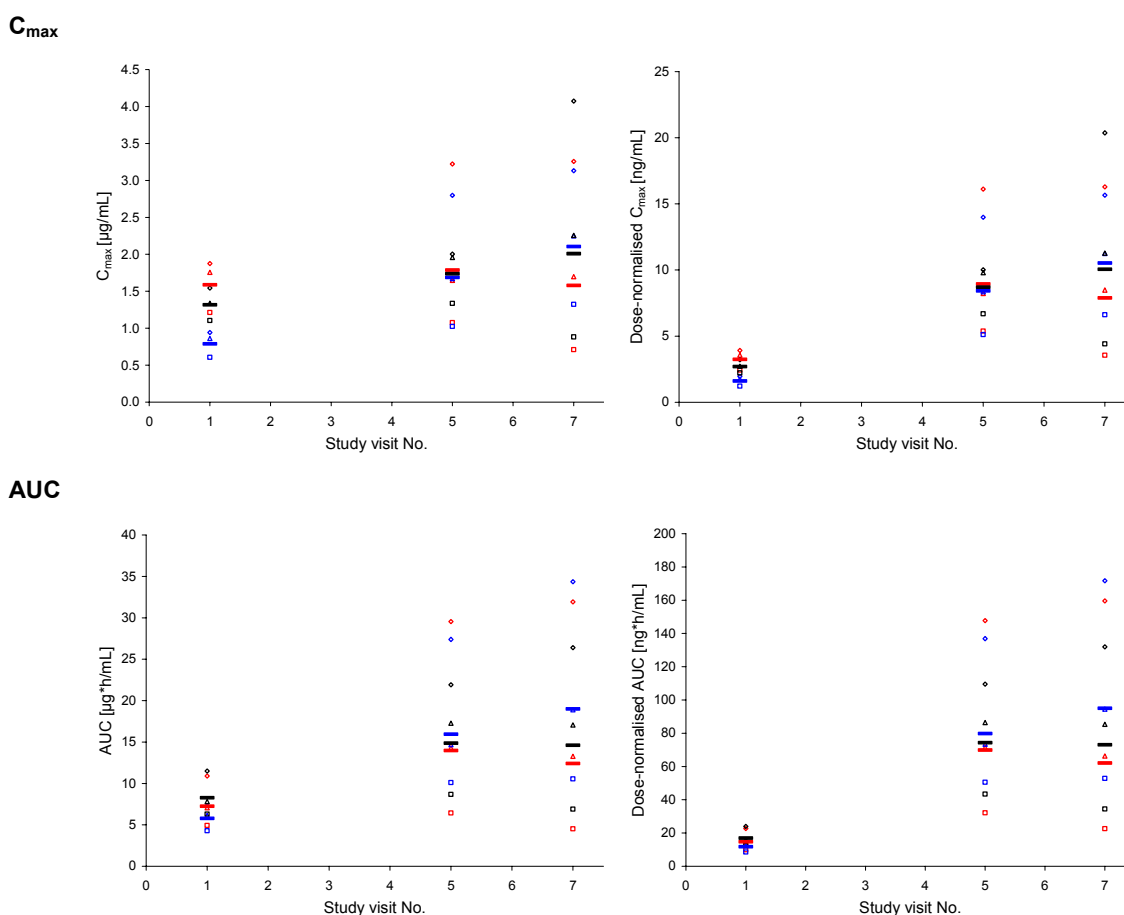


**Fig. 3-26:**  $C_{\max}$  and AUC after single (visit 1) and multiple dosing (visits 5, 7) in ID 101 (squares), ID 102 (diamonds), ID 103 (triangles). UF (red colour), ISF<sub>c</sub> (blue colour), ISF<sub>1</sub> (black colour). Determined parameters: left panel, dose-normalised parameters: right panel. Geometric means (bars).

**Tab. 3-25:** Geometric mean, geometric SD, and geometric CV, % of determined  $C_{max}$  [ $\mu\text{g/mL}$ ] and dose-normalised  $C_{max}$  [ $\text{ng/mL}$ ].

Matrix	----- Single dose -----			----- Multiple dose -----					
	----- Visit 1 -----			----- Visit 5 -----			----- Visit 7 -----		
	$\bar{X}_{geom}$	$SD_{geom}$	$CV_{geom}$	$\bar{X}_{geom}$	$SD_{geom}$	$CV_{geom}$	$\bar{X}_{geom}$	$SD_{geom}$	$CV_{geom}$
	----- Determined $C_{max}$ -----								
UF	1.59	1.27	23.8	1.79	1.74	59.8	1.58	2.15	89.0
ISF <sub>c</sub>	0.79	1.26	23.5	1.69	1.65	53.6	2.11	1.54	45.5
ISF <sub>f</sub>	1.32	1.18	16.9	1.74	1.25	23.0	2.01	2.16	90.1
	----- Dose-normalised $C_{max}$ -----								
UF	3.24	1.29	25.5	8.94	1.74	59.8	7.89	2.15	89.0
ISF <sub>c</sub>	1.61	1.28	25.2	8.43	1.65	53.6	10.53	1.54	45.5
ISF <sub>f</sub>	2.69	1.20	18.8	8.69	1.25	23.0	10.05	2.16	90.1

Regarding increasing variability, the analysis of the partial AUC values, as a measure of voriconazole exposure, almost led to the same pattern and conclusions as the ones of  $C_{max}$  (see Tab. 7-17, Tab. 3-26, Fig. 3-26 lower panels). The determined AUC values after multiple dose administration were higher compared to the values after single dose administration (visit 1) (UF: increase of 92.6% in visit 5 and of 71.3% in visit 7; ISF<sub>c</sub>: increase of 176.0% in visit 5 and of 228.5% in visit 7; ISF<sub>f</sub>: increase of 79.8% in visit 5 and 76.5% in visit 7) even after the reduced amount administered orally. For both parameters,  $C_{max}$  and AUC, no tendency towards lower or higher values in visit 7 was observable. Variability in plasma was generally higher than in the other matrices investigated. Within the parameters for ISF no tendency regarding lower or higher variability in ISF<sub>c</sub> and ISF<sub>f</sub>, respectively, could be observed.

**Tab. 3-26:** Geometric mean, geometric SD, and geometric CV, % of determined partial AUC [ $\mu\text{g}\cdot\text{h/mL}$ ] and dose-normalised partial AUC [ $\text{ng}\cdot\text{h/mL}$ ].

Matrix	----- Single dose -----			----- Multiple dose -----					
	----- AUC <sub>0-12h</sub> -----			----- AUC <sub>48-60h</sub> -----			----- AUC <sub>72-84h</sub> -----		
	$\bar{X}_{geom}$	$SD_{geom}$	$CV_{geom}$	$\bar{X}_{geom}$	$SD_{geom}$	$CV_{geom}$	$\bar{X}_{geom}$	$SD_{geom}$	$CV_{geom}$
	----- Determined AUC -----								
UF	7.25	1.49	41.3	13.96	2.14	88.7	12.42	2.66	126.7
ISF <sub>c</sub>	5.78	1.32	28.0	15.95	1.66	53.8	18.99	1.80	64.5
ISF <sub>f</sub>	8.27	1.36	31.2	14.87	1.62	51.1	14.60	1.98	77.2
	----- Dose-normalised AUC -----								
UF	14.80	1.52	43.4	69.81	2.14	88.7	62.11	2.66	126.7
ISF <sub>c</sub>	11.80	1.34	29.9	79.77	1.66	53.8	94.97	1.80	64.5
ISF <sub>f</sub>	16.88	1.38	33.3	74.33	1.62	51.1	73.00	1.98	77.2

In order to quantify the extent of tissue distribution, AUC ratios of unbound tissue and unbound plasma concentrations were calculated (Tab. 3-27). Both after single and multiple dosing ratios were at least 0.7 illustrated in Fig. 3-27. After the switch from iv to oral administration of voriconazole, AUC ratios increased from 0.87 to 1.57 (80.8%, ID 101), 0.67 to

0.93 (37.8%, ID 102), and 0.87 to 1.03 (18.2%, ID 103) for ISF<sub>c</sub> and for ISF<sub>I</sub> AUC ratios increased from 1.28 to 1.35 (5.5%, ID 101) and 1.10 to 1.21 (9.7%, ID 103), except for ID 102 for ISF<sub>I</sub> (decrease of AUC ratio from 1.05 to 0.74, i.e., by 29.7%). Since higher UF concentrations were obtained for ID 102 lower AUC ratios resulted. Maximum AUC ratios have been reached in ID 101 followed by ID 103. Compared to ISF<sub>I</sub>, the increase of the ISF<sub>c</sub> ratios from single dose to multiple dose administration was always higher. After the third oral application of voriconazole AUC ratios (AUC<sub>72-84h</sub>) further increased, most pronounced for ISF<sub>c</sub> ratios (most distinctive in ID 101 and ID 103).

**Tab. 3-27:** AUC ratios (AUC<sub>ISF</sub>/AUC<sub>UF</sub>).

ID	Matrix	----- AUC <sub>ISF</sub> /AUC <sub>UF</sub> -----				
		-- Single dose --		----- Multiple dose -----		
		Visit 1	Visit 5	Visit 7	Δ, %	
		AUC <sub>0-12h</sub>	AUC <sub>48-60h</sub>	AUC <sub>72-84h</sub>	Visit 1→Visit 5	Visit 5→Visit 7
101	ISF <sub>c</sub>	0.87	1.57	2.33	+80.8	+48.9
	ISF <sub>I</sub>	1.28	1.35	1.53	+5.5	+13.3
102	ISF <sub>c</sub>	0.67	0.93	1.08	+37.8	+16.1
	ISF <sub>I</sub>	1.05	0.74	0.83	-29.7	+11.5
103	ISF <sub>c</sub>	0.87	1.03	1.42	+18.2	+38.7
	ISF <sub>I</sub>	1.10	1.21	1.29	+9.7	+6.5
<i>Summary statistics</i>						
<i>ISF<sub>c</sub></i>						
	$\bar{X}_{\text{geom}}$	0.80	1.14	1.53		
	SD <sub>geom</sub>	1.158	1.322	1.480		
	CV, %	14.8	28.4	40.8		
<i>ISF<sub>I</sub></i>						
	$\bar{X}_{\text{geom}}$	1.14	1.06	1.18		
	SD <sub>geom</sub>	1.105	1.375	1.372		
	CV, %	10.0	32.6	32.5		

Δ, % indicates the difference between visit 5(7) and visit 1(5) relative to visit 1(5).

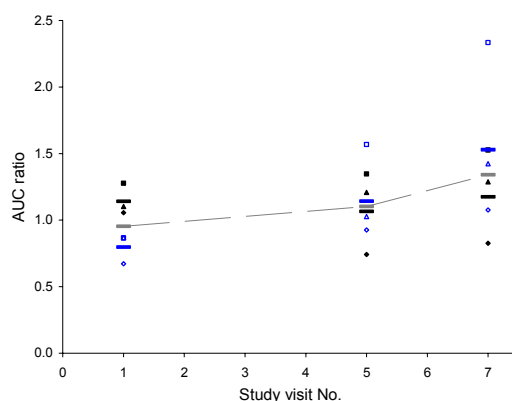


**Fig. 3-27:** AUC ratios ( $AUC_{ISF}/AUC_{UF}$ ) after single (visit 1) and multiple dosing (visits 5, 7) in ID 101 (squares), ID 102 (diamonds), and ID 103 (triangles).  $ISF_C$  (blue, open symbols),  $ISF_I$  (black, filled symbols). Geometric means ( $ISF_C$ : blue bars,  $ISF_I$ : black bars,  $ISF_C$  and  $ISF_I$ : grey bars and line).

Under the assumption that the plateau-phase could be regarded as steady state, the accumulation factors for visit 5 and 7 were calculated to be  $\sim 1.8$  for unbound plasma concentrations,  $\sim 3.0$  for  $ISF_C$  concentrations, and  $\sim 1.8$  for  $ISF_I$  concentrations (Tab. 3-28, Fig. 3-28). In addition, the accumulation could be substantiated when analysing dose-normalised concentrations: AUCs after multiple dosing were approximately fourfold higher for UF and  $ISF_I$  whereas the factor for  $ISF_C$  was calculated to be  $\sim 7$ . In UF drug accumulation factors predominantly decreased in visit 7 compared to visit 5 (except of ID 102).

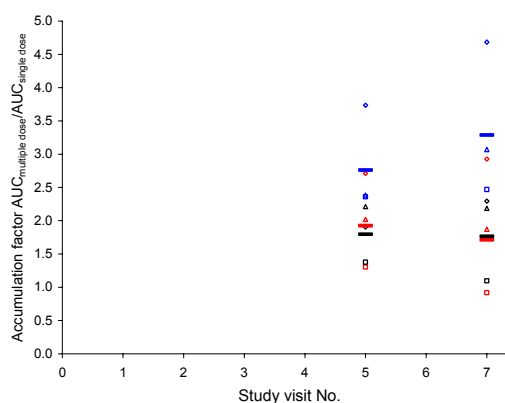


**Fig. 3-28:** Drug accumulation factors ( $AUC_{multiple\ dose}/AUC_{single\ dose}$ ) ( $AUC_{multiple\ dose}$  of visit 5 and visit 7,  $AUC_{single\ dose}$  of visit 1). ID 101 (squares), ID 102 (diamonds), ID 103 (triangles). UF (red colour),  $ISF_C$  (blue colour),  $ISF_I$  (black colour). Geometric means (bars).

**Tab. 3-28:** Drug accumulation factors ( $AUC_{multiple\ dose}/AUC_{single\ dose}$ ) ( $AUC_{multiple\ dose}$  of visit 5 and visit 7,  $AUC_{single\ dose}$  of visit 1).

	----- Visit 5 -----			----- Visit 7 -----		
	$\bar{X}_{geom}$	$SD_{geom}$	$CV_{geom}, \%$	$\bar{X}_{geom}$	$SD_{geom}$	$CV_{geom}, \%$
	----- <i>Determined <math>AUC_{multiple\ dose}/AUC_{single\ dose}</math></i> -----					
UF	1.9	1.44	38.0	1.7	1.80	64.0
$ISF_C$	2.8	1.30	26.6	3.3	1.38	33.4
$ISF_I$	1.8	1.27	24.6	1.8	1.51	43.1
	----- <i>Dose-normalised <math>AUC_{multiple\ dose}/AUC_{single\ dose}</math></i> -----					
UF	4.7	1.42	36.1	4.2	1.76	61.7
$ISF_C$	6.8	1.28	24.8	8.1	1.36	31.4
$ISF_I$	4.4	1.26	23.7	4.3	1.49	41.5

Relating the identified homozygous genotype for CYP2C19\*2 in ID 102 (Tab. 3-12, Tab. 3-18) to the PK analysis led to Fig. 3-29 for the AUC and AUC ratios. In ID 102 the geometric mean AUC after multiple dose administration was elevated more than sevenfold (7.0), hence, the differences between single and multiple dose administration within the AUC were more distinctive than for the other genotypes (4.5). The AUC ratios were slightly decreased for ID 102 after single dose since higher unbound plasma concentrations were measured in that individual. After multiple dosing highly comparable AUC ratios were calculated for ID 102 (+5%) whereas ratios for the other genotype (wild type) increased (+41%). For CYP2C9\*3 AUCs and AUC ratios behaved conversely. In ID 101 the geometric mean AUC after multiple dosing was decreased about 3.7-fold, for the wild type 5.6-fold. The ratios after single dose were comparable between the genotypes. After multiple dosing AUC ratios increased for the mutant (57%) as well as, to a lesser extent, for the wild type (26%). Hence, both differences between single dose and multiple dose administration within one genotype and differences within single dose and multiple dose administration, respectively, among the genotypes were found after analyses.

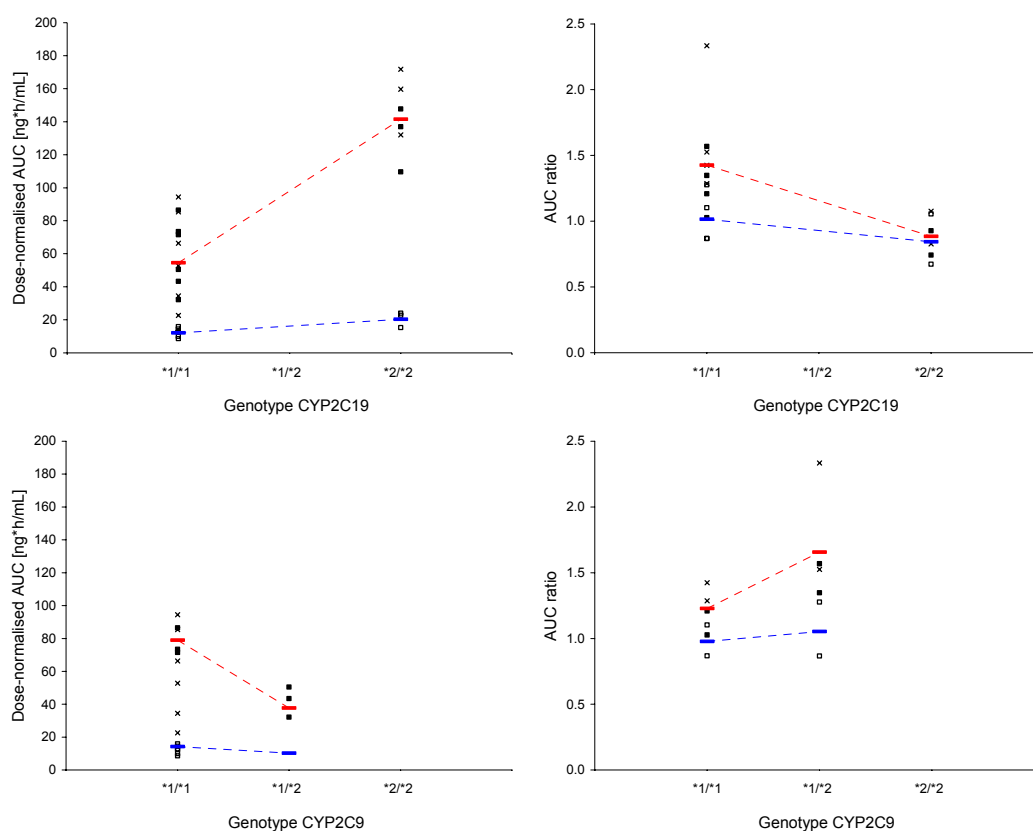


**Fig. 3-29:** AUC and AUC ratios in different genotypes. Single dose: visit 1 (open squares, blue colour); Multiple dose: visit 5 (filled squares, red colour) and visit 7 (crosses, red colour). Geometric means (bars).

---

## 4 DISCUSSION

### 4.1 I – Bioanalytical methods for quantification of voriconazole

The development of an analytical method for the quantification of voriconazole in different biological and biologically-mimicking fluids was the elementary prerequisite for the entire investigations dealt with in this thesis. The experiments and studies applied within the projects II to IV resulted in a variety of solutions containing voriconazole in either physiological concentrations or non-physiological concentrations, e.g., during the *in vivo* calibration procedure. In the first instance, the aim of the method development process was to establish an analytical assay capable of validly quantifying voriconazole from small sample volumes as those obtained during, e.g., microdialysis research and, at the same time, requiring minor laboratory expenditures and simple sample preparation enabling its implementation in the clinical routine. The criteria applied to assess the method validity were taken from international guidelines released by the FDA and International Conference on Harmonisation (ICH) [101, 102].

As a result, a rapid HPLC method with UV detection for microdialysate using common equipment has been developed and validated. Moreover, the method development process comprised the matrices plasma, UF, whole blood, and SB samples in order to have the ability to compare ISF concentrations with other biological fluids within preclinical and clinical trials. At the end, valid assays were available for all matrices important for human or animal disposition analysis of voriconazole.

For voriconazole bioanalytical methods have already been reported. Most of them determined its concentration in plasma and/or serum samples by liquid chromatography using either UV [86, 122-134], tandem mass spectrometry [135-138], or a bioassay [129, 132] as detection method. For plasma the LLOQ was in a range comparable with those for other LLOQs reported for voriconazole in HPLC assays [124, 132, 135]. However, assays implementing tandem mass spectrometry detection yielded LLOQs of 0.05 µg/mL – 0.1 µg/mL [135-138]. ZHOU et al. even determined voriconazole concentration down to 5 ng/mL in aqueous humour by liquid chromatography-electrospray ionisation-mass spectrometry [139]. Both the applicability to any laboratory performing drug analysis, usually equipped with common systems, and the analytical equipment available at the Department itself led to the development of a voriconazole quantifying method based on HPLC with UV detection.

Apart from the detection methods, the HPLC methods found in the literature mainly differed in instrumental equipment and sample preparation procedures. The method developed within this thesis implemented neither a separate extraction column/solid phase extraction (SPE) [128, 130, 131, 136, 138]/packed fiber SPE [125] nor liquid-liquid extraction (LLE) procedures [126, 127, 134] with subsequent evaporation of the extract [123]. Instead, the assay relied on a plasma sample preparation procedure which stipulated a protein precipitation with ACN and a subsequent centrifugation step [122, 124, 132, 135, 137] without further



evaporation of the sample [129]. For protein-free aqueous microdialysate samples a simple one-step dilution with ACN was sufficient. Similarly, ZHOU et al. proceeded with aqueous humour samples which contained very little amounts of protein, i.e., aliquots were directly injected onto the column [139]. The underlying mechanism of the developed method leading to recovery values above one hundred percent is yet unclear and should be further investigated. The use of an internal standard as UK-115794 [128, 131, 134], fenbuconazole [138], or ketoconazole [126, 135, 137] was not necessary being in line with PEREA et al. [132] and GAGE et al. [124] and included some disadvantages as, e.g., long  $t_R$  values (ketoconazole) and non-availability (UK-115794).

The well-used LLE technique is a multi-stage operation, which is both time-consuming and labour-intensive. Each step can introduce errors and solvent disposal causes additional costs and pollution to the environment. The usage of SPE cartridges circumvents the problems of the conventional LLE methods to some extent but the procedure still requires multiple steps. The volume of desorbing solvent needs several millilitres since the volume of packing material is relatively large and, thus, a concentration via solvent evaporation is often necessary, which results in a loss of volatile components. Own solvent evaporation processes performed during method development for quantification of voriconazole led to unreproducible results, probably due to problematic dissolving/volatility of the molecule under elevated temperature, and was not further pursued. More recently, a method based on the use of an electrospun polymer nanofiber as a SPE adsorbent with a larger specific surface has been published [125]. Miniaturisation of conventional packed SPE cartridges is enabled by the effective interaction of the target compound with a number of fine nanofibers, and, hence, the volume of both solid phase and desorption solvent could be significantly reduced. The evaporation of solvent and reconstitution of target analytes could be avoided since the sample preparation method delivered the target analyte in a sufficiently small volume of solvent, suitable for direct injection into the analytical instrument. KANG et al. realised this approach designing a mini-column by packing nanofibers into a pipette tip (packed-fiber SPE (PFSPE) column) [125]. However, the practical experience with PFSPE is limited and the implementation of PFSPE in the analytical routine remains to be awaited. When entering the analytical routine extraction columns within column switching HPLC systems might be the most convenient alternative to off-line sample preparation techniques since the biological (plasma) sample could directly be injected onto the HPLC system using an integrated specially designed extraction column. A number of restricted access media (RAM) columns has been designed and is currently commercially available. PINKERTON and HAGESTAM invented the internal surface reversed phase (ISRP) and, thus, provided a performance for RAM columns [140, 141]. Using this approach the sample could be analysed without any preparation operation and, hence, one could analyse the sample even more rapidly [128, 136]. An automation of the procedure using the column switching system could increase the throughput [142].

Prior to method development the principal drawback of reported methods using UV detection and conventional sample preparation resulted from the sample volume needed for the

preanalytical preparation ranging from 100  $\mu\text{L}$  to even 1000  $\mu\text{L}$ . Analytical combinations with tandem mass spectrometry [136, 137] or the utilisation of ISRP columns [130] were able to reduce the sample volume to 5  $\mu\text{L}$  – 10  $\mu\text{L}$  demanding expensive expenditures in material and analytical equipment still uncommon in clinical routine. For microdialysis samples, usually only a few microlitres are obtainable depending on the flow rates used in investigations, e.g., in this investigation at least 30  $\mu\text{L}$ . Hence, previously reported methods were inadequate for high-throughput, routine microdialysate investigations.

Overall, the method developed in this thesis was characterised by simple sample preparation and used common HPLC equipment, rendering the method applicable as high-throughput assay for any laboratory performing biomedical analyses. Voriconazole was stable in microdialysate and plasma while all conditions used in the stability experiments reflected situations likely to be encountered during actual sample collection, storage, preparation, and analysis [101]. This was in line with the stability results found by PÉHOURCQ et al. [130]. The required plasma volume input of 50  $\mu\text{L}$  will considerably reduce the sampling burden on study individuals while still maintaining the ability to quantify even small drug amounts emphasising the expedient application in clinical and preclinical studies of the developed method. Worth mentioning is the small sample volume available in microdialysis sampling while achieving the same LLOQ value. Voriconazole concentrations could be validly measured between 0.15  $\mu\text{g}/\text{mL}$  and 10  $\mu\text{g}/\text{mL}$  which was in accordance with the ranges already reported [123, 124, 128, 131]. Accuracy and precision were both good with all RE and CV values below +7.0% and 6.1%, respectively, for both matrices and all conditions investigated. The LLOQs will allow the measurement of antifungal concentrations in small sample volumes in plasma and tissue down to the MIC of the most relevant fungal pathogens [143, 144]. Investigations on robustness and ruggedness, respectively, showed the reliability of the assay with respect to deliberate variations in method parameters and to operational and environmental variables of the method, i.e., to variation in conditions normally expected from laboratory to laboratory and from analyst to analyst.

The assay developed for microdialysate was applied to UF, too, due to similar characteristics of both matrices. Prior, investigations demonstrated that voriconazole did not adsorb to any component of the ultrafiltration device and a calibrator analysed in UF as well as microdialysate yielded highly comparable results. A final centrifugation step introduced during the sample preparation accounting for the higher accuracy within the centrifuged sample batch was explained as follows: Protein separation might not be complete during the ultrafiltration process and small peptides <30 kDa (oligo-, polypeptides) might still be present in the UF available for reversible protein binding of voriconazole. A centrifugation step was scheduled to avoid protein binding again after precipitation with ACN within the time in the autosampler until analysis. Otherwise protein-bound voriconazole might evade the UV detection when assuming that protein-bound voriconazole cannot be detected. Although the results for the centrifuged and non-centrifuged batch did not differ largely among each other and were both in accordance with the limits set in international guidelines, the final centrifugation step was introduced for reliability reasons.

The composition of whole blood can be compared to plasma, except of additional blood cells. Consequently, a preparation procedure was applied similar to the one for plasma. This proceeding was in line with other methods subjected to both plasma and whole blood [145-148]. In preexaminations, preparation of plasma from whole blood was complicated when using blank blood samples after freezing irrespective of the anticoagulant. In order to avoid the same problem with study specimens, samples were treated as plasma: For whole blood specimens in this thesis a protein precipitation was performed with subsequent centrifugation separating protein as well as cells. A precolumn was used in order to account for possible impurities of the samples and deterioration in column performance. A drawback of this sample proceeding for this matrix might be the difficulties during pipetting when a slight clotting is recognised. Weighing of the samples could account for that phenomenon. Unexpectedly, the net weight was highly accurate (RE R: -1.0% – +6.1%, n=21) and precise (mean weight 102.8 mg, CV: 1.9%, n=21) among study specimens when applying the assay to a preclinical study (see 2.5). For the application of this method to a larger sample batch the omission of the time-consuming weighing step can be recommended but a further method validation will be required in order to check for appropriate accuracy and precision especially at the LLOQ. The hypothesis that if voriconazole accumulated in the clotted areas, which were accidentally transferred into the test vial, would result in higher total concentrations than anticipated was rejected since repeated measurements yielded acceptable values for accuracy. Alternative methods line up to the ones already mentioned for plasma using, e.g., LLE [146] on an EXtrelut<sup>®</sup> column containing wide-pore diatomaceous earth acting as a holder for the sample [148] or protein precipitation using other agents than ACN, e.g., perchloric acid [147].

A novel method has been developed for the analysis of SB samples since no method has been published regarding the quantification of voriconazole in this matrix. In contrast to other groups investigating skin tissue, this approach required neither additional equipment such as a Mikro-Dismembrator<sup>®</sup>, an Ultra-Turrax<sup>®</sup>, or a tissue homogeniser [149-152] nor digestives [153] or extra reagents such as NaOH [154, 155]/NaHCO<sub>3</sub> [152] or labour-intensive cleaning steps [153-155]. All methods published homogenised the skin before further proceeding with the sample. LAUGIER et al. extracted acitretin from skin with a mixture of diethylether and ethylacetate after homogenisation with an Ultra-Turrax<sup>®</sup> [150] requiring the washing of the apparatus and its dismounting after each sample [149]. For small sample volumes, this method led to a loss of tissue which was not properly homogenised [151]. PANUS et al. used a tissue homogeniser in combination with NaHCO<sub>3</sub> to extract ketoprofen from skin resulting in multiple isolation steps [152]. Grinding the deep-frozen skin tissues with a Mikro-Dismembrator<sup>®</sup> avoided loss of skin tissue and allowed obtaining very fine particles of skin, which promoted the efficient extraction of compounds by solvents [149, 151]. In general, the recoveries reported were high or almost complete, however, all methods required special apparatuses and purification steps. The main advantage of the method presented in this thesis was the purity of the extract demanding almost no cleaning step. In case of extracted protein which might have been precipitated by the solvent a centrifugation step was included

within the preparation procedure. The method developed in this thesis merely exhibited a moderate drug recovery due to less damaged skin tissue and required a time-consuming but very simple extraction procedure. The determination of the extraction recovery employed a spiking procedure of blank biopsy sample prior to extraction. An adhesion of the spike-sol solution  $C_{\text{spike-sol } 1}$  on the sample itself could not be excluded eventually leading to an overestimation of the recovery. Hence, concentrations in the preclinical and clinical setting might be underestimated. An increase in the recovery value could probably have been obtained using longer extraction times at an elevated temperature after the freeze-thaw cycles. Due to the small number of SB samples available for method development it was not possible to fully validate the sample preparation procedure. Furthermore, as it would not be feasible to prepare calibration samples from SBs in a routine clinical setting and, additionally, such an approach would not be justifiable from an ethical and practical point of view, the measurements against extraction solvent calibration samples was chosen as an appropriate alternative. To check for repeatability only one concentration was repeatedly examined instead of investigating a concentration range. Thus, the validity of this approach was not demonstrated for concentrations lower or higher than 0.3  $\mu\text{g/mL}$  (R: 0.2  $\mu\text{g/mL}$  – 0.34  $\mu\text{g/mL}$ ). This should be an issue for future method optimisation studies. The assay has been applied to nine study specimens originating from a preclinical study (see 2.5) yielding interindividually comparable voriconazole concentrations in the SBs of the study animals.

In conclusion, a rapid and reliable HPLC assay for the determination of voriconazole in different matrices was developed and fully validated for the matrices microdialysate and plasma. The chromatographic conditions of the method are suitable for analysing voriconazole in these matrices in one batch without changing any parameter. The method is characterised by the usage of minimal sample volumes, an in most instances (except of SB) fast and simple sample preparation requiring minor laboratory expenditures, and complied with the requirements to be applicable for target site monitoring of voriconazole during preclinical and clinical applications.

## 4.2 II – *In vitro* microdialysis

A robust system (IVMS) was developed in order to be able to perform *in vitro* microdialysis investigations regarding the questions arisen in this thesis in an easy, clearly arranged, and efficient way. Moreover, the system should provide a reliable basis for various future investigations to characterise, e.g., a drug or endogenous compound in context with a microdialysis catheter *in vitro*. Those investigations are essential to determine if it is possible to explore a drug or a physiological compound by microdialysis *in vivo*. The investigations in this thesis included voriconazole and its drug product Vfend<sup>®</sup> since the drug was planned to be researched in a preclinical and a clinical study as well as two other anti-infectives, linezolid and daptomycin. The latter were analysed to compare their transfer behaviour via the membrane of the catheter to voriconazole.

#### 4.2.1 *In vitro* microdialysis system

The design and, consequently, the capability of the IVMS with regard to *in vitro* microdialysis investigations have been described in section 3.2.1.2. Frequently, authors waived the information about the technical details of the *in vitro* microdialysis settings used (e.g., [156-158]). This situation, the available alternative at the Department (MLU, Freie Universität Berlin), and the insufficient commercial options were the decisive motivation for the development of the IVMS. So far, *in vitro* microdialysis investigations had been performed using a very simple and fragile setting. A test tube rack had been used for positioning the liquid (medium) containers to which the catheters had been provisorily attached with tape often leading to contact with the sides of the glass container. Moreover, a lid for covering to protect from contaminations was not on hand and the setting has been, at best, covered with a piece of parafilm<sup>®</sup> which was impractical and uneconomical. Furthermore, that setting did not provide options for elevating the temperature or moderate stirring in the medium container [48, 106, 107]. If properly adjusted both latter factors can contribute to reflect the *in vivo* situation more properly. Commercially available opportunities hold several additional disadvantages: The clinical microdialysis catheters of interest in this thesis could hardly be analysed using these stations since those systems were designed for catheters used in basic research. Options for elevating the temperature, moderate stirring in the liquid (medium) container, or for safely positioning the microdialysis pumps are not provided. These stations maximally offer place for three parallel determinations and the liquid (medium) containers have to be separately supplied. Hence, those stations are rather employed for storage of already used or intended to use catheters.

In summary, the developed IVMS is applicable for the intended experiments: The easy-to-handle and compact system offers the opportunity to cleanly, simply, reliably, and rapidly investigate *in vitro* microdialysis issues applying different concentrations, flow rates, directions of diffusion, or temperatures.

#### 4.2.2 *In vitro* microdialysis investigations

A comprehensive characterisation of the permeation behaviour of the moderately lipophilic drug voriconazole investigated in *in vitro* microdialysis experiments using clinically approved concentric and linear catheters was performed. The hypothesis for these *in vitro* experiments that RR is sufficient, concentration-independent, flow rate-dependent, and reproducible was confirmed. Furthermore, flow rate, sampling intervals, and *in vivo* catheter calibration solution concentration of voriconazole were optimised for subsequent *in vivo* sampling situations, also at steady state.

In order to mimic the temperature of the living tissue, and taking the temperature dependence of the diffusion coefficients into consideration [43], all *in vitro* experiments were conducted at 37 °C in the developed system (IVMS, see 2.4.1). As previously reported, fluid boundary layers exist in microdialysis sampling and affect the RR (extraction efficiency) [159]. The impact of the fluid boundary layer can be reduced by increasing the fluid move-

ment [160]. Hence, in order to prevent an unstirred water layer in the medium constant stirring, appropriately provided in the IVMS, was employed according to GROTH et al. [161]. The application of the microdialysis technique to lipophilic compounds has controversially been discussed. Several attempts to measure highly lipophilic compounds have more or less failed. There are some reports on the successful measurement of lipophilic compounds [162]. Docetaxel has been reported to be very suitable for microdialysis despite its lipophilicity and high molecular mass [163], however, contradictory results have been found by LOOS et al. [164]. Recovery experiments suggested non-specific binding of docetaxel to currently available microdialysis catheters that might be managed by using polysorbate 80 as a non-ionic surfactant effecting the recovery of docetaxel at the same time [164]. Due to low recoveries attributed to the (poor) solubility observed for lipophilic compounds, lipophilic perfusates have been proposed [165]. The *in vitro* results revealed that microdialysis experiments for voriconazole can be carried out using Ringer's solution as a physiologically-based perfusate that has very often been used for other drugs [106, 166-170]. Usage of lipophilic perfusion medium [165] or lipid emulsion as perfusate [171] in order to improve recovery of voriconazole as a lipophilic compound could be disregarded.

Barring the lipophilicity, it was expected that voriconazole (molecular mass: 349 Da) would pass the microdialysis membrane in quantifiable amounts since sufficient RR will be obtained with substances having a molecular mass lower than approximately one-fourth of the membrane cut-off (20 kDa) [43]. The *in vitro* investigations revealed that voriconazole concentrations achieved in the dialysate would be sufficient for *in vivo* sampling.

However, a prerequisite for conducting microdialysis experiments is a concentration independence of RR. This basic requirement was demonstrated over a range covering potential ISF concentrations *in vivo* (1.0 µg/mL – 50.0 µg/mL) (see 3.2.2.2). The experiments with concentric catheters resulted in consistent RR (overall mean RR: 96.9%, CV: 1.3%) over the whole investigated concentration range with CVs below 1.5% and 0.9%, respectively, for recovery and delivery experiments corresponding to the values yielded for intraday variability of the bioanalytical assay. The latter conclusion was as well true for results obtained with linear catheters: The overall mean RR amounted to 93.0%, CV: 5.2% over the whole investigated concentration range with CVs below 8.1% and 6.4%, respectively, for recovery and delivery experiment. This concentration independence was assumed for *in vivo* conditions, too. The marginal difference in RR between the concentric and the linear catheters has been attributed to the slightly higher flow rate of the perfusate of the linear catheters (2.0 µL/min) in comparison to the one perfusing the concentric catheters (1.5 µL/min). Moreover, from the results it can be concluded that the permeation process was quantitatively equal in both directions through the semipermeable membrane and, therefore, retrodialysis is suitable for catheter calibration in future *in vivo* microdialysis studies. For the latter ones flow rates below or even better equal to 2.0 µL/min were recommended in order to retain adequate recoveries as well as sufficient sample volumes for HPLC analysis with an acceptable time resolution.

The usage of CMA60<sup>®</sup> as well as CMA66<sup>®</sup> catheters should be emphasised. These types of catheters are both approved for clinical application and consequently commonly applied in humans (CMA60<sup>®</sup>). The recently developed linear catheters CMA66<sup>®</sup> allow for simple application in scientific investigations as well as in clinical routine. So far, they have been rarely deployed in pre-/clinical investigations. In contrast to other microdialysis CMA catheters, materials of clinical CMA catheters (CMA60<sup>®</sup> – 64<sup>®</sup>, CMA66<sup>®</sup>, CMA70<sup>®</sup>) do not differ among each other (membrane: predominantly PAES, PA in CMA60<sup>®</sup> (today: PAES) and CMA70<sup>®</sup>; tubing: PU). Therefore, feasibility and reproducibility results of the investigations reported here for CMA60<sup>®</sup> (PA) and CMA66<sup>®</sup> (PAES) might be well transferable to other clinical CMA catheters as, e.g., CMA70<sup>®</sup> (PA, implemented in the preclinical investigation in this thesis, see 2.5.1.1).

The studies presented in this thesis demonstrated reproducible and comparable recoveries of different settings (gain and loss). Investigations published by ARAUJO et al. [172] revealed conflicting results: This group investigated *in vitro* probes (CMA20<sup>®</sup>; not applicable to human *in vivo* studies) showing higher recoveries by retrodialysis compared to dialysis after 1 h equilibration concluding the necessity of a mathematical consideration of drug binding to the probe. Although, binding of voriconazole to parts of the microdialysis system cannot totally be excluded, possibly disguised by obligatory system equilibration following any change (e.g. flow rate, concentration of the solute in the perfusate, *in vitro* or *in vivo*), the results presented in this thesis allowed for disregarding a mathematical correction. Additionally, LINDBERGER et al. investigated, both *in vitro* and *in vivo*, the adsorption of carbamazepine, phenytoin, and phenobarbital to the microdialysis sampling device (CMA60<sup>®</sup>) differentiating between whole catheters and separate parts of the catheters in order to estimate drug binding and to propose a mathematical model to calculate drug binding and recovery itself [157]. As log P of voriconazole is comparable, or more precisely slightly higher, to phenobarbital (log P 1.47 [173]) results may be compared as well. The binding to the outlet PU tubing was limited and predictable for phenobarbital, while binding to the hard internal tubing was not recorded. Phenobarbital did not bind to the dialysis membrane. The authors stated that microdialysis can be used for reliable estimations of phenobarbital concentrations if drug binding to the plastic tubing is considered [157]. Although the log P value of voriconazole is slightly higher adsorption to none of the constituent parts of the microdialysis device could be concluded in the present study suggesting that other properties than lipophilicity and protein binding of the other (drug) molecules investigated may be responsible for adsorption processes, e.g., specific interactions with PU.

Up to now, *in vitro* [174, 175] and *in vivo* [174-177] microdialysis investigations among antifungal triazoles have only been carried out for fluconazole being an ideal candidate for microdialysis due to the low lipophilicity and the low plasma protein binding. In summary and according to the *in vitro* results in this thesis voriconazole seems to be as well suitable as fluconazole for valid clinical microdialysis investigations despite its moderate lipophilicity. The experiments revealed that voriconazole concentrations achieved in the dialysate should be sufficient for further *in vivo* investigation. Based on the results the optimal conditions for the

*in vivo* microdialysis procedure were determined (see 3.2.2.1 and 3.2.2.2). Steady state investigations were performed and led to recommendations for the *in vivo* catheter calibration solution concentration of voriconazole (see 3.2.2.3).

Due to the tortuosity of the sample matrix *in vivo* recovery has been shown being lower than *in vitro* recovery [178-180]. This could be as well confirmed when comparing the results of the *in vitro* experiments with the mean RR values of voriconazole obtained in animals or humans (see 0, 3.3.1, and 3.4.4). The underlying mechanism can be explained by several factors influencing the diffusion. *In vitro* the diffusion and RR, respectively, are characterised by the diffusion coefficient which is a characteristic of a substance dependent on temperature, viscosity, and the hydrodynamic radius of the molecule. But, *in vivo* the peripheral medium of the catheter can be evaluated as the restricting factor of the diffusion [181]. There, tortuosity and microviscosity can occur in varying extents. The tortuosity is based on the structure of the biological tissue. Due to the complex composition of the tissues the length of the diffusion path is considerably altered in comparison to aqueous solutions. With increasing cellular portions the extracellular space available for diffusion of, e.g., small molecules (drugs), proteins, or macromolecules decreases. The microviscosity in ISF is higher than in water caused by the structural macromolecules such as collagen fibers, forming the framework, glycosaminoglycans, and proteins [181, 182]. Thus, smaller *in vivo* RR values can be explained by the structure of the tissue being different from an aqueous solution and, thus, limiting the diffusion of molecules. Therefore, it is important that *in vitro* recovery of voriconazole should not be used for the calculations of the actual concentrations in the peripheral medium. Rather it should provide evidence of feasibility and validity of the microdialysis technique for voriconazole using clinically approved catheters. Future investigations on *in vitro* recovery might implement a medium which is more comparable to the catheter surrounding medium of the catheter *in vivo*. This setting might reflect the *in vivo* recovery somewhat more properly than the usage of an aqueous solution and might enlighten possible influences on the recovery not yet seen with the aqueous medium. The imitation of the tortuosity remains a challenge requiring a complete reproduction of the living tissue of interest. However, this approach might reflect the true *in vivo* recovery ideally allowing to omit the *in vivo* recovery determination during a clinical microdialysis investigation.

The observed flow rate dependence was in accordance with other investigations [106, 107, 156]. Furthermore, the mathematical relation between flow rate, membrane area, and mass transfer has been described. The method of flow rate variation has been introduced in 1985 and realised calibration by varying the perfusate flow rate [43, 45]. Equilibrium conditions will be reached at a flow rate of zero yielding the intrinsic sample concentration ( $C_0$ ). However, this method only leads to an estimate of the actual recovery. The mass transfer coefficient  $r$  estimation was achieved by utilisation of recoveries obtained from the conventional retrodialysis recovery calculation. The coefficient  $r$  is unique to the analyte, the membrane



properties [160], and setting. Therefore, the coefficient might become a well-suited reference parameter for *in vitro* experiments being able to control the whole *in vitro* setting.

Referring to the studies with voriconazole the hypothesis emerged that the coefficient  $r$  might be unique for the system and setting (specific flow rate, temperature, stirring rate) independent from the drug applied, certainly provided that the molecular mass is below one-fourth of the membrane cut-off (see above). This hypothesis was strengthened when evaluating the results attained for linezolid. Linezolid (337 Da) has been chosen since the molecule is well suitable for microdialysis and the bioanalytical assay for its valid quantification had already been established at the Department [106]. Both voriconazole and linezolid demonstrated almost the same RR dependence on flow rate indicated by a nearly identical value of  $r$  and, hence, the shape of the curve when plotting the predicted RR versus flow rate (see 3.2.2.1). Besides, the RR of linezolid, yielded with IVMS under body temperature and moderate agitation of the medium, were compared to those attained on the previously described way without heating and stirring [106]. In this previous work, RR were decreased by 10% to 20% and, consequently, the value of  $r$  lower than the value obtained with the IVMS (0.053 mm/min, SE: 0.002 mm/min, CV: 2.9%) clearly indicating the influence of the temperature and fluid agitation on the viscosity and the gradient of diffusion and, hence, on the diffusion coefficient of the molecule. To further investigate the hypothesis of a unique coefficient  $r$  another drug substance was analysed. Daptomycin was already subjected to microdialysis by KIM et al. [183]. A previously at the Department established assay for the quantification of this drug in Mueller-Hinton broth was successfully adapted to microdialysate. The molecular mass of daptomycin (1620 Da) was more than tenfold lower than the cut-off of the microdialysis membrane. However, in comparison to voriconazole and linezolid a smaller mass transfer coefficient was revealed when curve-fitting was performed. An explanation might derive from a view to the molecule dimension. The molecule is more stretched than the two other and, thus, has a larger radius which decreases the diffusion coefficient. In conclusion, the coefficient  $r$  does not reflect a system parameter for the IVMS but might serve as a well-suited reference parameter for the system developed enabling to control the setting when investigating molecules of certain molecular masses or ranges of molecular masses, respectively. To systematically investigate the various factors (physicochemical properties; system parameters, e.g., temperature, stirring velocity) might ultimately lead to a (multivariate) relationship.

Since the conduction of retrodialysis *in vivo* requires the local application of the drug via perfusing the microdialysis catheter it is of importance that the utilised perfusate is clinically approved or positively evaluated by the ethics committee when the solution is self-prepared using the drug substance. Very frequently, the drug substance provided by the manufacturing company is not intended for human use. A convenient option is to apply the clinically approved drug product. If so, it is essential to ensure no impact of the additionally contained excipients on RR. The drug product of voriconazole (Vfend<sup>®</sup>) contains SBECD (160 mg/mL) [72]. Cyclodextrins (CD) are used as solubilising agents, e.g., for hardly soluble drugs in pharmaceutical formulations.

Systematic chemical variations led to a polyanionic variably substituted sulphobutyl ether of  $\beta$ -cyclodextrin (SBECD) as a non-nephrotoxic derivative of  $\beta$ -CD [184]. Up to now, SBECDs are used in four products approved by the FDA [184]. SBECDs are cyclic oligosaccharides made up of seven dextrose units (Fig. 4-1). They can interact with drug molecules to form inclusion

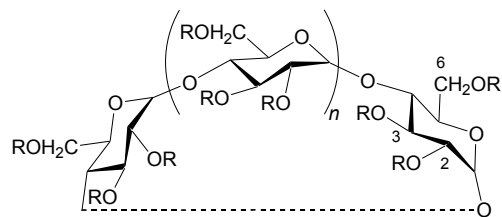


**Fig. 4-1:** Structure of sulphobutyl ether  $\beta$ -cyclodextrin sodium (SBECD) ( $n=5$ ,  $R=(CH_2)_4SO_3Na$  or H, derivatives may have differing degrees of substitution on the 2, 3, and 6 positions).

complexes. The major driving force for drug release from an inclusion complex is simple dilution [184, 185] with either body fluids *in vivo* or with artificial solutions (e.g., Ringer's solution) in *in vitro* experiments that would be sufficient to completely dissociate the drug from the CD. The results in this thesis demonstrated similar RR of both voriconazole in Vfend<sup>®</sup> with SBECD and voriconazole without SBECD. This was as well assumed for *in vivo* and, thus, Vfend<sup>®</sup> was implemented in the *in vivo* calibration procedures of the preclinical and clinical trials in this thesis (see 2.5.1.1 and 2.6.6). The analogous behaviour might be derived from the fact that after dissolving the stock solution of Vfend<sup>®</sup> with Ringer's solution *in vitro* drug release from the complex is forced by the high dilution. During microdialysis, it is assumed that both molecules, released voriconazole molecules and empty SBECDs, separately pass over the membrane where a second dilution step occurs in the medium. Thus, voriconazole transfer over the membrane would be equal to the one of voriconazole originating from the solution merely containing voriconazole. The same is supposed for the *in vivo* situation with the extracellular fluid being in place of the medium. Controversially, KHRAMOV et al. reported an enhanced RR by using a perfusate enriched with 2-hydroxypropyl- $\beta$ -CD or  $\beta$ -CD during microdialysis with a polycarbonate-polyether membrane [186]. However, the vice versa situation has not been investigated yet. In case of an influence of the SBECDs in Vfend<sup>®</sup> perfusate, RR would be enhanced and, consequently, ISF concentrations would be underestimated.

In summary, the presented results regarding the microdialysis experiments for voriconazole formed the basis for investigating the ISF PK of voriconazole in an *in vivo* setting.

### 4.3 III – Influence of disease state on target site exposure

The preclinical microdialysis pilot study mainly focused on the investigation of the influence of an infection on the availability of voriconazole at the site of infection. For this purpose, the microdialysis technique was applied to both healthy and infected subcutaneous adipose tissue of three guinea pigs. Besides the investigation of the feasibility of this approach, the penetration of voriconazole into the ISF was evaluated to be sufficient or inadequate regarding the treatment of dermatophytosis and fungal infections, respectively. In addition to microdialysate, SB and (unbound) whole blood specimens were analysed employing the

developed analytical assays presented in this thesis. Finally, the exposure of voriconazole in ISF was compared to the results in SB and (unbound) whole blood specimens.

#### 4.3.1 Applicability of microdialysis to healthy and inflamed subcutaneous adipose tissue

The study procedures were completely accomplished and feasibility to apply the microdialysis catheter to the infected skin areas was comparable to that in healthy skin. In accordance with that and recently published, application of microdialysis to inflamed lung in rats was performed even though the information about RR determination or RR results was lacking [187]. Moreover, microdialysis has been applied to the kidney cortex in infected (*Candida* species) Wistar rats [188]. Finally, research groups reported successful implementation of microdialysis to inflamed subcutaneous adipose tissue in patients [189, 190]. The suitability of the microdialysis approach for the preclinical investigation presented here was reflected by very consistent and sufficient RR results based on two subsequent recovery measurements using different  $C_{RP}$ . Moreover, microdialysate concentrations were highly consistent, too and, hence, no variability due to possible methodological or PK issues was revealed. A considerable concentration of voriconazole (geometric mean 1.8  $\mu\text{g/mL}$ ) was found in the baseline samples of the study which might have originated in both the multiple dose administration prior to the sampling procedure and a slight carry-over of  $RP_{\text{high}}$  used during the second calibration. However, an influence of the latter reason on the concentrations of the ISF samples during the present study was assessed to be less probable since the concentration of the baseline sample was close to the range of the  $T_{30}$  samples and no descending trend after the baseline sample has been observed. In any case, for future investigations the calibration should be performed at the end of the sampling periods, especially for short-time investigations, to eliminate any potential influence of the procedure on the PK samples. For consistency to the other matrices, SB (no baseline sample concentration available) and whole blood (two concentrations below the LLOQ and, hence, set to zero), the  $T_0$  value of the microdialysates were set to zero. However, this was not in accordance with the multiple doses administered before and should be considered when discussing the absolute values. Due to the lack of later samples, precluding the use of the elimination rate constant, extrapolation to infinity, when calculating the AUC, was not performed. Instead of that partial AUC from  $T_0$  to  $T_{180}$  ( $AUC_{\text{SS},0-3h}$ ) was calculated.

#### 4.3.2 Pharmacokinetics of voriconazole at the target site

The availability of voriconazole in ISF obtained by means of cutaneous microdialysis was evaluated in healthy and infected skin areas aiming at the question whether the free fraction of the drug in the ISF is influenced by infections or not. The differences in tissue penetration are associated with many factors, e.g., protein binding and lipophilicity, and can be influenced by the infection process and inflammation [191, 192]. For instance, *Candida* species infections lead to secretion of lytic enzymes, such as phospholipases and proteinases,

playing an important role in endothelial cell invasion causing change of physiological conditions in tissue and induction of inflammatory response by macrophages [193]. Infections with *Microsporium canis* might have comparable outcome. But, the results yielded from the study showed similar unbound concentrations of voriconazole in tissue ISF in healthy and infected skin, leading to the hypothesis that drug penetration was not influenced by the inflammatory response. Recently, ARAUJO et al. supported this assumption by investigating free renal concentrations of voriconazole in healthy and *Candida* species-infected Wistar rats [188]. However, another reason that penetration remained unaffected might probably be due to the fact that the infection was almost healed at the time of sampling (day 12). Thus, an influence of an ongoing infection with inflammation on voriconazole concentration in ISF could not be ruled out. A possible difference might have been found if sampling would have been performed at an earlier stage of infection [99].

When assuming a plasma protein binding of 45%, determined in guinea pigs by ROFFEY et al. [86], the geometric mean penetration factor of voriconazole ( $AUC_{ISF,H,IN}/AUC_{blood,u}$ ) was calculated to be 0.5 (CV: 7.8%). This value accounts only for protein binding. Intracellular uptake of voriconazole has been described to be high within human polymorphonuclear leucocytes [194]. By omitting calculation, ultrafiltration of the blood samples enabled the elucidation of the true relation between unbound concentrations in blood and in ISF separating both cells and proteins. Performing this was not possible for all blood samples due to clotting and limited sample volume. A direct comparison of neither blood concentrations nor blood concentrations corrected for plasma protein binding from the literature with ISF concentrations leads to a reliable determination of the extent of penetration of voriconazole into the ISF compartment. Therefore, concentration results of four (seven, see 3.3.2) ultrafiltrated blood samples were used to calculate the unbound fraction of voriconazole in blood in order to apply this fraction to the other blood samples not accessible to ultrafiltration. Due to low variability in  $f_u$  determination, this procedure seemed to be acceptable. The geometric mean penetration factor of voriconazole ( $AUC_{ISF,H,IN}/AUC_{blood,u}$ ) was calculated to be 1.1 (CV: 7.8%) suggesting equilibration between the matrices at steady state. This finding was in line with results of ARAUJO et al. This group revealed a kidney to plasma penetration ratio of 0.34 which was similar to the free plasma fraction of voriconazole in rats [188]. LUTSAR et al. studied the penetration of voriconazole in CSF in guinea pigs elaborating a mean ratio of CSF/plasma concentration of 0.68 [84] indicating an accumulation in that compartment, when considering protein binding of 45%. A further analysis in animals or even better in humans is needed to confirm or to question the results derived from the kidney and CSF (see sections 2.6, 3.4, and 0).

Multiple dose administration and continuous permeation of voriconazole from the blood into the ISF and accumulation in the surrounding tissue might be plausible explanations for the low fluctuation of ISF concentrations elaborated during this study setting. In contrast, concentrations of voriconazole in whole blood and SB specimens were still increasing 3 h after dosing, indicating that the maximum concentration has not been reached yet. This is in line with a study by ROFFEY et al., who showed increasing voriconazole blood concentrations

in guinea pigs reaching  $C_{\max}$  8 h ( $t_{\max}$ ) after a single oral dose (10 mg/kg) [86]. Hence, if a single dose was given, absorption process of voriconazole is most likely not finished after the sampling period applied here. In the present study, multiple doses were given and  $t_{\max}$  did not seem to have been reached yet, too. In humans the maximum plasma concentration is typically achieved earlier than 2 h after administration [195]. This discrepancy might partly be due to decreased gastrointestinal absorption during anaesthesia of the animals. The hypothesis that metabolites of voriconazole might contribute to the unexpected high values after 3 h was refused since the main metabolite, the N-oxid of voriconazole, would probably elute earlier than the parent molecule when using the analytical method developed (see 2.3.3). A chromatographic investigation on that issue has not been performed since reference standard material of the metabolites of voriconazole was not available.

The concentrations in SB specimens were remarkably high, as illustrated by an overall geometric mean concentration of 16.6  $\mu\text{g/g}$ . Although these concentrations cannot be directly compared to other matrices, the data demonstrate an accumulation in the skin that cannot be solely explained by protein binding (45% [86]). Experimental design and sample preparation led to values obtained for SB tissue in the unit  $\mu\text{g/g}$ . Consequently, concentration values in  $\mu\text{g/g}$  should be converted to the unit  $\mu\text{g/mL}$  enabling a comparison among the other matrices. But it needs to be kept in mind that skin is not one homogenous, solid mass, and, hence, density determination without differentiating between all components merely led to an estimation of the value. An overall density of blank skin biopsies of guinea pigs was estimated using two different approaches yielding comparable values of approximately 1  $\text{g/cm}^3$ . Measurement by means of water displacement could be considered as less reliable because of difficulties in visually metering the exact volume of water in the used measuring cylinder. Due to the limitation in blank sample size and necessary blank sample dimension the value measured by the helium pycnometer relates to only one sample. However and in conclusion,  $\mu\text{g/g}$ -concentrations found in the skin biopsies might be assumed to be equal to  $\mu\text{g/mL}$ -concentrations. In case of biopsy density over 1  $\text{g/cm}^3$  SB sample concentrations would be higher than the actual values and vice versa. Yet, an increase of voriconazole in the skin over the examined time could be seen and a large difference between SB and ISF could be observed. Under the assumption of a density of 1  $\text{g/mL}$  for the SB, the comparison led to a twelve-fold higher concentration in SB than in ISF. Those SB concentrations were in line with other compounds of this drug class indicating an accumulation [154, 155]. Itraconazole and fluconazole have been shown to accumulate in stratum corneum of the skin and, additionally, fluconazole has been shown to be incorporated into the keratin structures of epidermal adnexa, where it can be detected months after the end of treatment [154, 155, 196]. This behaviour of itraconazole and fluconazole is thought to contribute to the eradication of dermatophyte infections and to the fact that pulse therapy including weeks without treatment is effective. Future studies are warranted to elucidate the nature and time course of the voriconazole accumulation in the skin by systematic investigations on the contributing factors and mechanisms. One might hypothesise that biomolecule binding of voriconazole to certain structures, which are comparable to the drug target only available intracellularly, could

be plausible reasons for the observed phenomenon. Additionally, the behaviour might refer to the chemical structure of voriconazole. The moderate lipophilic characteristic of the molecule may be the reason for high permeation and, therefore, for high voriconazole concentrations in skin biopsies. Among the animals, variability was highest in this matrix. Skin biopsies represent a complex matrix. Apart from skin cells and subcellular organelles, SB samples also contain ISF and blood vessels. Thus, in order to become available in skin, voriconazole has to penetrate into various tissues influenced by the tortuosity of the tissue. Cellular structures and the connectivity of the spaces increase the diffusion length [197]. In consequence, the capability of a drug to reach the skin might differ according to the differences in the tissue structure of each subject. Methodologically, the extraction of voriconazole from SB was laborious and might have been not complete leading to another reason for interindividual variability. Since the trend of the SB concentration-time courses was comparable in all animals investigated and recovery yielded by the method developed was reproducible (CV: 11.9%, n=3) analytical errors were ruled out.

As already revealed in this subsection, the biopsy sampling approach holds several shortcomings. When sampling and analysing a SB, neither differentiation between intra- and extracellular concentrations nor between skin and blood cells, i.e., between distinctive compartments, is possible and, therefore, the usage of concentrations derived from tissue homogenates to determine exposure-response relationships and drawing conclusions with respect to clinical use are not recommended [198]. The present study involved the microdialysis approach to sample the unbound fraction of voriconazole in order to determine its availability at the site of infection. For PD discussion only those concentrations will be considered.

Besides PK analysis, a significant clinical efficacy of oral voriconazole against *M. canis* dermatophytosis has been demonstrated during the present study [99]. Skin redness and lesion severity scores were significantly reduced and continued to decline in contrast to the progressive infection observed in untreated animals throughout a 17-day observation period [99]. This effect was confirmed by mycological examination since only one animal (12.5%) in the treatment group (n=8) was culture positive at the end of the study. Finally, there was no recurrence of the dermatophytosis three days after the last dose of voriconazole treatment [99]. This is in accordance with previous *in vitro* reports in which voriconazole has been demonstrated to possess *in vitro* activity against dermatophytes [199, 200], with MICs for *Microsporum* species in general (*M. canis*, *M. gypseum*, *M. cookei*, *M. distortum*, *M. audouinii*, and *M. nanum*) between 0.01 µg/mL and 2 µg/mL [199, 200] and specifically for *M. canis* in the range of 0.01 µg/mL to 0.5 µg/mL. The concentration of unbound voriconazole in ISF after multiple dose administration, on the 12<sup>th</sup> day of treatment, in this study ranged between 0.9 µg/mL to 2.0 µg/mL with a geometric mean concentration of 1.4 µg/mL during the 3 h observation period uninterruptedly being above the MIC of the *M. canis* isolate (0.25 µg/mL [99]). Voriconazole concentrations in all specimens were in the range or higher than the MICs previously published for *M. canis* and, therefore, indicate that voriconazole may be a future alternative to griseofulvin for the treatment of tinea capitis in humans [99]. However, the ISF concentrations not only were well above the MIC for the pathogen involved

in the inflammation but also for other fungal pathogens involved in IFIs [201]. In this respect, it has to be noted that a 2.5-fold higher dose (compared to iv maintenance dose) was administered to the guinea pigs. Due to the lack of prior knowledge of the *in vivo* situation this higher dose had been chosen in order to be able to detect voriconazole in the tissue matrices investigated. Consequently, correlating the concentrations with the MIC has to be regarded with caution. *In vivo* studies investigating the PD characteristics of voriconazole demonstrated that the 24 h fAUC/MIC ratio is the critical PK/PD parameter associated with triazole treatment efficacy against *Candida albicans* [202-204]. Further analyses from these *in vivo* studies have demonstrated that a triazole (unbound) drug 24 h fAUC/MIC of 20 to 25 is predictive of a successful treatment [202, 203, 205-207]. The voriconazole unbound drug fAUC/MIC ratios ranged from 11 to 58 with a mean ratio of 24 (SD  $\pm$ 17) [208]. The present study elaborated  $AUC_{SS,0-3h}$  values. For an estimation of the 24 h fAUC/MIC ratio the  $AUC_{0-24h}$  would be necessary to calculate but those extrapolation is not advised [115]. When relating the  $AUC_{SS,0-3h}$  to PD applying the  $AUC_{SS,0-3h}/MIC$  ratio at a MIC of 0.25  $\mu$ g/mL, values of 16.0 and 14.8 were calculated for healthy and infected areas, respectively. These values alone would be within the desired limits. A further multiplying, i.e., octuplicating, in order to account for the time interval which might be an over- or underestimation of the  $AUC_{0-24h}$  would exceed the value for the 24 h AUC/MIC ratio about 5-fold. This result indicated that the dose given in the present study was appropriate for the treatment of the pathogen involved in the inflammation and led to the hypothesis that the lower dose as recommended for voriconazole in human use might be sufficient for treatment, too. Further *in vivo* studies, preferentially involving microdialysis, should focus on this subject substantiating this hypothesis.

#### **4.4 IV – Clinical long-term microdialysis pilot study with voriconazole in healthy volunteers**

The pilot study was designed to combine two main objectives (Fig. 4-2): The feasibility approach aimed at elucidating the applicability of long-term microdialysis in humans during a clinical trial and the second one, termed as PK approach, should preliminary examine the PK of voriconazole at the target site including a novel microdialysis catheter type during sequence dosing. Hence, this proof-of-principle investigation combined both a methodological and a PK study of a drug of major importance. In this chapter, both items and the positive results obtained will be discussed with respect to a continuation of the pilot trial (part II).

**Clinical long-term microdialysis pilot study with voriconazole in healthy volunteers**

- Prerequisites
- Bioanalytical assay for voriconazole quantification from small microdialysate sample volumes and ultrafiltrate (see 2.3, 3.1)
  - Determination of optimal conditions (flow rate, influence of cyclodextrines, RP concentrations) for voriconazole microdialysis *in vivo* (see 2.4, 3.2)
  - Suitable setting for *in vivo* long-term microdialysis involving linear and concentric probes (Feasibility approach) (see 2.6.2)

**Feasibility approach of long-term microdialysis**

- Challenges and claims**
- Catheter performance over 87 h → handling, reproducibility of RR (perpendicular to body axis, horizontal catheter application)
  - Linear vs. concentric catheters → handling (guide cannulas), reproducibility of RR
  - Catheter fixation → protection and fixation of catheters, mobility for individual (medicinal tape)
  - Risk of infection of catheter sites → preventing infection, observation of catheter sites (transparent medicinal tape)
  - Pump performance → long-term pump work (battery life-span as weak point)
  - Pump fixation → protection and fixation of pumps, easy and fast change of pump syringes, mobility for individual (modified medicinal belt)
  - Microvial fixation → safe microdialysate sampling, easy and fast change of microvials, mobility for individual (guide channels with connections for microvials)

**PK (Pharmacokinetic) approach**

- Aspects and scopes**
- Male healthy volunteers defined by inclusion and exclusion criterias
  - Single dose vs. multiple dose (3.5 days, 7 visits)
  - Sequence therapy: switch from WT-based iv to fixed-dosed po administration
  - ISF concentrations vs. unbound plasma concentrations
  - Comparison of ISF<sub>c</sub> vs. ISF<sub>i</sub> concentrations
  - Screening for isoenzymes CYP2C9 (\*2-, \*3-allele) and CYP2C19 (\*2-allele)

**Fig. 4-2:** Feasibility and PK approach of the clinical trial presented in this thesis.

**4.4.1 Feasibility of long-term application of clinical microdialysis**

The aim of the explorative, sequentially designed, pilot study (part I) was to apply microdialysis over several days to subcutaneous ISF of healthy volunteers in order to further investigate the long-term feasibility of the technique. The pilot study should investigate whether the inserted microdialysis catheter with sampling from it over an ~87 h insertion period was feasible, i.e., with regard to tolerability for healthy volunteers, and for reliable sampling until the last sample after multiple dosing. Technically, it should be investigated if the catheter maintained its functionality and sufficient drug diffusion occurred across the membrane. Based on the results of part I, the decision for part II (main study) regarding the best sampling schedule should have been made. In case of unfeasibility, one catheter should have been inserted at study day 1 and removed thereafter and another catheter should have been inserted at study day 4. Hence, microdialysis sampling would only have taken place at these days according to the RSS. Three facts should be emphasised: 1) the period of insertion of the CMA60<sup>®</sup>/CMA66<sup>®</sup> catheter is guaranteed to be 5 days (personal communication by CMA Microdialysis AB, Solna, Sweden) but knowledge of this long-term insertion is very limited and has very scarcely been employed in clinical drug investigations, 2) a clinical comparison between CMA60<sup>®</sup> and CMA66<sup>®</sup> has not been reported, and 3) clinical microdialysis in humans with the moderately lipophilic drug voriconazole has never



been performed. So far, first experiences concerning microdialysis of voriconazole resulted from own *in vitro* investigations (see sections 2.4, 3.2, and 0) and preclinical research [99] (see sections 2.5, 3.3, and 4.3) as well as from the literature [172, 187, 188]. However, all these explorations had not been performed in humans. Previously, authors elaborated problems with the *in vivo* measurement of lipophilic substances using microdialysis (see also 0). This work suggested voriconazole being suitable for *in vivo* microdialysis.

Prolonged microdialysis sampling over several days has been used for endogenous compounds in humans as glucose [209-219], glycerol [209, 213, 215, 220], glutamate [219, 221], lactate [213, 215, 219, 221, 222], pyruvate [213, 219], ASAT and troponin T [223], aspartate [219], and hypoxanthine [219] in neonatal [210, 216, 217] and adult [211, 212, 214, 218] diabetic patients, in patients admitted for breast reconstruction with transverse rectus abdominis muscle flaps after mastectomy [213], in patients with ischemic heart disease [223], and in patients for neurochemical monitoring or on the neurosurgical ICU [219-222], respectively. The duration of the catheter insertion ranged from 1.5 to 21 days. All investigators revealed microdialysis being a well suited tool for continuous endogenous compound monitoring in patients. Some problems were reported, e.g., accidental withdrawals in agile infants [210, 216], disturbances in perfusion flow [210], minor bleeding around the microdialysis catheter during microdialysis in one child [210], discontinuation because of obstruction of the inlet tubing of the catheter [212], or removal of a catheter because of a puncture of a small vein [216].

However, less investigations than for endogenous compounds have been published for xenobiotics in clinical (PK) studies [224-226]. STÄHLE et al. monitored free extracellular valproic acid by microdialysis in epileptic patients in which one individual was subjected to continuous microdialysis for three days [226]. In a subsequently conducted study in three healthy volunteers, LINDBERGER determined RR of valproic acid on day two of a three-day-period, whereas the insertion of the catheter was on day one and microdialysate sampling on day three [227]. No RR determination was performed after the sampling in order to check for consistency of RR over time. KOPACZ et al. did not assess RR at all [225]. This group studied the PK of bupivacaine and dexamethasone released from microcapsules at a subcutaneous injection site in healthy volunteers [225]. Here, the reliability of the microdialysis approach was seen in the similarity of the tissue fluid PK obtained at different sites using identical doses of bupivacaine. Recently, KONINGS et al. reported a prolonged microdialysis sampling over 47 h in carboplatin-treated cancer patients [224]. Microdialysis catheters were inserted at the tumour site and into healthy abdominal subcutaneous tissue. *In vivo* RR was performed by retrodialysis on day one of the study. However, this group elaborated two technical problems with microdialysis, i.e., one leakage of a microdialysis catheter leading to inadequate sampling and removal of both catheters and highly variable and decreasing recovery in one patient exemplifying the challenge of this technique. Moreover, a relatively low, over-time decreasing and highly fluctuating RR in the healthy adipose tissue was revealed in comparison to malignant tissue. In conclusion, the group demanded for "...further research [...] to evaluate the definite role of microdialysis in subcutaneous normal tissue..." [224].

The study presented in this thesis successfully implemented long-term microdialysis over ~87 h in healthy subcutaneous ISF in a PK study. Clinical drug investigations, aiming at analysing the PK after single dose as well as during steady state conditions, usually employ the microdialysis technique in two or more subsequent steps, i.e., requiring at least two catheter insertions [168, 228-232]. Via long-term insertion of one catheter and sampling from it data can be obtained with only one catheter in situ for several days.

Studies of endogenous compounds or the studies mentioned examining xenobiotics did not indicate further equipment than the microdialysis device. Here, the setting developed (Fig. 2-7, 2.6.2) for the conduction of the pilot trial aimed at 1) convenient and easy procedures for the study personnel using low-priced additional equipment, 2) good clinical practice (GCP) during the trial, and at the same time 3) a maximum of mobility for the individual to be able to transfer the setting in the future in the clinical routine to patients requiring nursery. The unproblematic and easy handling resulting from this setting, enabling, e.g., safe sample collection and fast and easy sample vial exchange (see 3.4.1), resulted in low time deviations being highly important for PK studies. Subcutaneous periumbilical adipose tissue was easily accessible for catheter implantation and disruption/alteration of the membrane by the abdominal fat (preliminary investigation, data not shown) was prevented by a perpendicular to the body axis and horizontal application of the catheter (see Fig. 2-7).

To circumstantiate the results about feasibility observed and documented during the conduction of the study, retrodialysis investigations were extensively performed: In conclusion, long-term microdialysis application over ~3.5 days was appraised as feasible (proof-of-principle) determined by reliable multiple RR over the whole study duration permitting appropriate transformation of dialysate drug concentrations. Results indicate a potential benefit from an overall recovery value determined for one individual and one catheter type or even of a once-determined value for one catheter type assessed in only one individual due to low intra- and interindividual variability of RR. With regard to the intraindividual results for the RR determination at study visit 1 (prior the drug administration) this was in accordance with the findings by KONINGS et al. in tumor tissue but further determinations of RR during and after the sampling time have not been performed [224]. Intraindividual variability in adipocytic normal tissue was comparable in only three of six patients. In the remaining three cases problems occurred due to leakage problems, incorrect flow settings or extremely decrease in recovery. In contrast to the study in this thesis, the leakage problem could not be managed and led to the removal of the catheter. During the pilot phase leakage of one linear catheter was successfully managed using a tubing connector (see 3.4.1 and 3.4.4) and RR<sub>i</sub> yielded afterwards by the catheter were elevated up to 98.8% probably due to the long duration without perfusate flow within the catheter as a result of the leakage and subsequent manually flush of the catheter. Assuming these reasons the catheter was seen as affected in membrane performance which might have led to a more facilitated passage of voriconazole molecules expressed in the RR<sub>i</sub> value. However, the results showed reproducible RR even after the leakage and, thus, were considered in the calculation of the study samples for this individual. Voriconazole concentrations in the dialysates were corrected for the RR obtained

by RR2 samples and not RR1 or a mean value from both of the samples. This was found to be justified due to the lower or highly comparable variability in the RR2 samples, respectively, which might be originated in the longer equilibrated retrodialysis setting after the first sample (RR1). The RR1 sample was, in contrast, immediately followed by an equilibration phase after changing the dialysis perfusate into the RP solutions. Nevertheless, the RR1 value was seen as a well usable backup value for RR2 (for ID 102, visit 3, CMA60<sup>®</sup>). RR values were highly consistent over the ~87 h-period. Cases of RR values of visit 1 being lower than the RR values of the following visit might be explained with the insertion and subsequent adaptation to the environment which might have taken about one study day since the following recovery values at the subsequent study visit were more comparable. KONINGS et al. implanted the catheter the day before drug infusion in order to allow enough time to let adverse tissue reactions (inflammatory effects [162]) subside [224]. Moreover, they allowed for the drug being washed out from the peripheral medium while not starting with drug infusion until 2 h after the recovery determination by retrodialysis. In this study microdialysate baseline samples have shown significant voriconazole amounts after retrodialysis indicating a wash-out phase of 30 min being insufficient (Fig. 3-17). For the subsequent main part of the study (part II), it is strongly suggested to waive the retrodialysis on study visit 1 and to invest the ~2 h time spent for a longer equilibration period consisting of the former equilibration period of 30 min, the *in vivo* catheter calibration procedure (40 min), the wash-out phase (30 min) and the baseline sampling (15 min). RR determinations on study visits 3 and 5 allowed a wash-out period of 10 h – 12 h.

Interindividual variability in the study of KONINGS et al. was much more different than in the present study (mean RR: 44.8% – 75.8% in tumor tissue, n=6; mean RR: 10.8% – 62.9% in normal tissue, n=5) although the correct positioning of the catheters was determined by ultrasound than in the study presented in this thesis [224]. So far, examinations using both the concentric and the linear catheters, allowing a direct comparison between them, have not been published yet. Lower RR (median: -20.2%, R: -35.4% – -9.5%, leakage considered) were predominantly determined for linear catheters (RR<sub>l</sub>) probably due to the slightly smaller lateral surface area of the linear catheter membrane (47.12 mm<sup>2</sup>; concentric catheter membrane: 56.55 mm<sup>2</sup>) caused by a shorter diameter (0.5 mm linear catheters, 0.6 mm concentric catheters) and/or possibly due to the different membrane materials (PA in concentric catheters, PAES in linear catheters). However, in *in vitro* experiments both catheters revealed similar RR values (see 3.2.2.1 and 3.2.2.2). The stable performance of the catheters demonstrated by consistent RR in the present study was well in line with BOLINDER et al. [212] and BAUMEISTER et al. [210]. They published unchanged recovery of glucose across the microdialysis membrane after 3, 6, and 7 days [212] and after 8 and 9 days [210]. Voriconazole as moderately lipophilic drug has proven suitable for *in vivo* microdialysis as already suggested by own *in vitro* microdialysis (see 3.2.2.1 and 3.2.2.2) which has extensively characterised the microdialysis catheters CMA60<sup>®</sup> and CMA66<sup>®</sup>. However, due to tissue tortuosity and limited volume fraction of ISF *in vivo*, the diffusion path length is well known to be increased and subsequently the effective drug diffusion coefficient

in tissue to be decreased compared to *in vitro*. Hence, the *in vivo* feasibility is impossible to be predicted from the *in vitro* experiments. Here, this conclusion is confirmed by *in vivo* RR being predominantly lower than *in vitro* (see 3.2.2.1 and Tab. 4-1). The comparable RR values of the preclinical study (see 3.3.1) to the ones obtained during the clinical investigation (see 3.4.4) although the implemented catheters had different membrane areas might be explained by the lower flow rate applied.

**Tab. 4-1:** Relative recovery (RR) results presented in this thesis.

	<i>In vitro</i> In IVMS (see 3.2.2.1)	<i>In vivo</i> In guinea pigs (see 3.3.1)	<i>In vivo</i> In humans (see 3.4.4)
Flow rate	2 µL/min	1 µL/min	2 µL/min
Surrounding of catheters	Ringer's solution <sup>a</sup>	Subcutaneous ISF	Subcutaneous ISF
<i>Concentric CMA60<sup>®</sup> catheters (30 mm<sup>b</sup>)</i>			
Mean RR (CV, %)	91.5 (1.8)	-	84.9 (5.6)
<i>Linear CMA66<sup>®</sup> catheters (30 mm<sup>b</sup>)</i>			
Mean RR (CV, %)	90.8 (4.6)	-	66.5 (10.7)
<i>Concentric CMA70<sup>®</sup> catheters (10 mm<sup>b</sup>)</i>			
Mean RR (CV, %)	-	72.4 (12.5)	-

<sup>a</sup>Stirred up, at 37 °C.

<sup>b</sup>Catheter membrane length.

Perfusate concentrations were sufficient for calibration on all study visits. Taken this fact into account as well as the *in vitro* results, it was assumed, that the diffusion of voriconazole was unhindered and led to unaffected accurate recovery results.

Long-term microdialysis was well tolerated without any local complication/inflammation at the site of implantation and reduced the burden in humans due to avoidance of several catheter insertions allowing at the same time to monitor drug concentration-time courses. Further investigations corroborating the following hypotheses will be performed during the main part of the trial: 1) For the determination of RR a one-time/twice (instead of four times) measured value for each individual (despite the low intra- and interindividual variability) and each catheter ideally at the end of the study duration is sufficient to achieve an adequate conversion factor. In consequence, this reduction will lead to a 75% saving of the retrodialysate samples, perfusate samples, and the time spent for the recovery procedure. Waiving the recovery determination on study visit 1 will avoid voriconazole concentrations in the baseline and subsequent samples. 2) Provided that the appropriate RP solution will be employed, a once determined RP1/RP2 concentration via HPLC is sufficient. 3) Concentric catheters appeared to be more adequate to be employed for the subsequent part II of the study: However, apart from the leakage event in one of the linear catheters, performance of all the catheters was consistent over the entire study duration as demonstrated by the RR results. Nevertheless, it should be mentioned that microdialysis is still subject to some technical

challenge to avoid any preventable disturbances. In summary, three facts favour employing the concentric catheters for the following study part: i) Higher recoveries, ii) leakage problems are considered to be less possible than for the linear catheters since the disruption of the inlet tubing occurred exactly at the position where the tubing from the syringe is joined to the inlet tubing leading to the membrane, and iii) the linear catheters hold the risk of infection when the outlet tubing has to be removed, even though the outlet tubing has directly been cut at the position where the catheter leaves the investigated skin area.

In conclusion, long-term microdialysis was assessed to be feasible, reliable, and mature to be unchangedly applied in the main part of the study (part II). Microdialysate concentrations as well as calculated ISF concentrations based on RR were regarded as highly accurate and therefore – together with the concentrations of the UFs – incorporated into the dataset for PK evaluation.

#### **4.4.2 Dataset, dataset checkout, demographic data and genetic characteristics**

Mistakes due to the transfer of the samples and data from the study centre to the institutes where the data were processed could be kept minimal since the study team members in fact were the analysts performing HPLC analysis of the samples as well as evaluation of the data. Compared to drug monitoring (patient) studies on the ward (alternating study personnel) this was highly advantageous concerning the quality of the entire data evaluation. In conclusion of the dataset checkout, the dataset input was plausible and consistent; a low number of implausible and missing values were identified and corrected.

The WT of the IDs was only marginally differing over the entire observation period. Since the time span of the study (3.5 days) was short, the nutrition of the individuals normally balanced, and no influence of voriconazole on the WT is known from the literature, the results were plausible and in accordance with the expectations. For the continuation of the main study (part II) it is justifiable to renounce the determination of WT in visit 5 in order to spare this additional step for both the ID and study personnel. Regarding the typical demographical data IDs were reasonably comparable.

In this pilot investigation, genotypes of the isoenzyme CYP2C19 of all IDs were additionally determined since this P450 isoenzyme is primarily discussed to be responsible for the metabolism of voriconazole [87, 88]. CYP2C19 is a protein of 490 amino acids encoded by the CYP2C19 gene, which has nine exons and is mapped to chromosome 10 [233, 234]. DE MORAIS et al. identified two genetic defects in CYP2C19 that are responsible for the majority of the poor metabolisers (PM) of this enzyme [235, 236]. These variants are two null alleles, which include a splice defect in exon 5 (CYP2C19\*2, trivial name: m1, single base change G→A) [236] (Tab. 4-2) and a premature stop codon at position 636 of exon 4 (CYP2C19\*3, trivial name: m2, single base change G→A) [235], while CYP2C19\*1 represents the wild type allele (Tab. 4-2). In both variants, a premature stop codon is produced resulting in truncated and inactive enzyme or a truncated protein that is unable to bind to the haem moiety. The distribution of these common alleles is different among different populations reviewed by XIE

et al.: The frequency of CYP2C19\*2 has been reported to be ~30%, ~17%, and ~15% in Chinese, African-Americans and Caucasians, respectively, and the CYP2C19\*3 allele was shown to be more frequent in Chinese (~5%) than in Blacks (0.4%) and Caucasians (0.04%) [237]. The main defective allele is CYP2C19\*2 accounting for 75 – 85% of CYP2C19 alleles responsible for PMs in Caucasians [236]. CYP2C19\*3 is extremely rare in Caucasian populations. But the CYP2C19\*2 allele does not explain all PMs in Caucasians. WEDLUND et al. reviewed additional variant alleles, which affect either expression of the protein or catalytic activity, identifying ~99.74% of defective alleles [238]: CYP2C19\*4 (a variant of the initiation codon) [239], CYP2C19\*5 (Arg433→Trp, affecting structure and stability) [240], CYP2C19\*6 (Arg132→Gln, affecting structure and stability) [241], CYP2C19\*7 (intron 5 splicing defect) [242], and CYP2C19\*8 (Trp120→Arg, affecting structure and stability) [242]. Hence, the seven variant alleles leading to inactivating mutations (CYP2C19\*2 to CYP2C19\*8) explain almost all PMs of CYP2C19. PMs of CYP2C19 represent approximately 2.2%(3%) – 5% of Caucasians [243, 244]. Recently, further variant alleles have been identified: CYP2C19\*9 – \*26 [245-252], whereby one mutation, CYP2C19\*17, caused ultra-rapid (UM) instead of poor (PM) drug metabolism [250, 251] expressing a metabolism activity even more pronounced compared to extensive metaboliser (EM, wild type).

For the study in this thesis, genetic polymorphism screening for CYP2C19 only comprised the allele CYP2C19\*2 due to lack of established methods or collaborations providing them. Therefore, the occurrence of other defective alleles in the IDs leading to misclassifications cannot be ruled out and have to be discussed. However, the CYP2C19\*2 allele is the main defective allele in Caucasian individuals [236, 253].

The genotype of CYP2C9 was determined as well although this enzyme is involved in the metabolism of voriconazole to a lesser extent than CYP2C19 [87] and the incidence of functional polymorphisms is much lower than for CYP2C19 (~1/250 in Caucasians) [243]. Among the variant alleles for CYP2C9 identified so far (CYP2C9\*2 – \*34, [254]), CYP2C9\*2 and CYP2C9\*3 have been determined for the study in this thesis. CYP2C9\*1 represents the wild type (Tab. 4-2). The CYP2C9\*2 allele is characterised by an Arg144→Cys substitution (single base change C→T) and the effect on catalytic activity has been attributed to an impaired ability of CYP2C9\*2 to associate with reductase (Tab. 4-2) [255] leading to a markedly reduced enzyme activity of 20% in comparison to the wild type [256]. Its frequency is approximately 8% in Caucasians [257]. The other mutant allele, CYP2C9\*3, has a frequency of 6% in Caucasians, whereby frequency of homozygous CYP2C9\*3 is 0.3% [257]. In general, homozygous PMs of CYP2C9 are very uncommon in Caucasians with 0.2 to 1% [258]. The molecular basis for the mutation of CYP2C9\*3 is an Ile359→Leu mutation (single base change A→C) (Tab. 4-2) [257] leading to a markedly reduced enzyme activity of less than 10% in comparison to the wild type [256].

Although CYP3A4 is involved in the metabolism of voriconazole, too, if only to a lesser extent [259] (see 1.4.2), the genotype for this isoenzyme has not been examined since, to date, no significant polymorphism has been identified for CYP3A4 [260, 261]. In spite of that, variability of CYP3A4 expression is widely documented and may contribute to interindividual

variability in voriconazole PK to some degree [261]. Ritonavir interaction studies have shown that there is a significant contribution of CYP3A4 to the overall elimination of voriconazole *in vivo* (so far no explicit fraction reported) [262], but the effect of the CYP3A4 gene mutation on the kinetics of voriconazole still remains unknown, possibly because of the rare functional variation of this isoenzyme and its extremely low frequencies.

Meaningful differences among the IDs regarding their genotype have been revealed during the study: Whereas ID 103 showed the wild type (\*1/\*1) for both isoenzymes CYP2C9 and CYP2C19, ID 101 and ID 102 exhibited SNPs leading to a heterozygous non-wild type situation (mutant) in ID 101 for CYP2C9 (\*1/\*3) and a homozygous non-wild type situation (mutant) in ID 102 (\*2/\*2) for CYP2C19. Due to the pilot character and, hence, the limited number of individuals investigated the frequency of CYP2C19\*2 and CYP2C9\*3 was higher than reported. The consequences, reported in the literature, arising from these polymorphisms investigated are summarised in Tab. 4-2 [236, 255, 257, 260].

**Tab. 4-2:** Nucleotide changes, effects, and resulting enzyme activity for isoenzymes CYP2C9\*2, CYP2C9\*3, and CYP2C19\*2 (determined during the pilot study (see 2.6.8)).

Alleles	Nucleotide changes	Effect	Enzyme activity
<i>CYP2C9*1</i>	-	-	Normal (wild type)
<i>CYP2C9*2</i>	430C→T	Arg144→Cys	Decreased <sup>1</sup>
<i>CYP2C9*3</i>	1075A→C	Ile359→Leu	Decreased <sup>2</sup>
<i>CYP2C19*1</i>	-	-	Normal (wild type)
<i>CYP2C19*2</i>	681G→A	Splicing defect	None <sup>3</sup>

C-Cytosine, T-Thymine, A-Adenine, G-Guanine; 430, 1075, 681 indicate the mRNA position; Arg-Arginine, Cys-Cysteine, Ile-Isoleucine, Leu-Leucine; 144, 359 indicate the amino acid position).

<sup>1</sup>Enzyme activity *in vitro*.

<sup>2</sup>Enzyme activity *in vitro* and *in vivo*.

<sup>3</sup>Enzyme activity *in vivo*.

In general, the genetic polymorphisms of CYP2C9 and CYP2C19 investigated influence the concentrations (e.g., plasma) of an administered drug (e.g., voriconazole) and cause variability: Voriconazole concentrations were approximately three times higher in homozygous CYP2C19 PMs compared with homozygous CYP2C19 EMs, with intermediate concentrations in heterozygous CYP2C19 EMs, in plasma in healthy Japanese individuals after repeated oral voriconazole administration [90]. By contrast, a homozygous CYP2C9 PM (\*2/\*2) did not alter plasma PK parameters in comparison to homozygous EMs for CYP2C9 supporting the minor role for CYP2C9 in the metabolism and elimination, respectively, of voriconazole [263]. Furthermore, WEISS et al. also discussed CYP2C9 PM genotype might not be of PK relevance [264], suggesting CYP2C9 PMs without impairment of CYP2C19 have unchanged voriconazole PK. Moreover, in the human liver microsome, sulfaphenazole (an inhibitor of CYP2C9) had no effect on voriconazole metabolism [87]. MURAYAMA et al. suggest that the CYP2C19 genotype, but not CYP2C9 genotype, should be evaluated as a key factor in the PK of voriconazole and that 4-hydroxyvoriconazole formation, produced by

CYP3A4, may become an important pathway for voriconazole metabolism in IDs with poor CYP2C19 catalytic function [88] and not CYP2C9. Based on this data, genotype of CYP2C9 among individuals in the present study was less considered for interpretation of the pilot study results and it is suggested to waive the determination of SNPs for isoenzyme CYP2C9 for individuals recruited for the main part of the study (part II). The potential influence of the genotypes revealed being different from the wild type, mainly for CYP2C19, on the PK of voriconazole will be discussed throughout the next chapter.

#### **4.4.3 Target site pharmacokinetics of voriconazole assessed by microdialysis**

##### *Data base and data analysis*

The second objective of the pilot study was the preliminary examination of the PK of voriconazole at the potential site of infection reflected by ISF<sub>c</sub> and ISF<sub>i</sub> in comparison to the unbound voriconazole concentrations in plasma (UF) (see Fig. 4-2).

Due to the explorative nature and design of the pilot study, unbound voriconazole concentrations in plasma and ISF obtained over ~87 h in merely three male healthy volunteers were available for PK analysis. The individuals were examined after single and multiple voriconazole sequence administration, applying an intensive sampling schedule after single iv and during multiple oral administration, i.e., after first and third oral dose, for both blood and ISF, and sparse sampling in between. The limitation of the pilot study to a small number of individuals but the rich data situation within each individual with 58 blood samples and 61 microdialysate samples per ID accounted for the chosen NCA approach for PK analysis of voriconazole concentrations. For important PK parameter 12-18 samples are recommended by the FDA [115] which has been met for the intensive sampling periods of the present study. Determination of the mono-exponential terminal elimination phase was manually performed according to the recommendations of SCHEERANS et al. [114] without using the automatic r-based algorithm which iteratively select the appropriate n concentrations by the software used.

##### *Sequence therapy*

The sequence dosing scheme administered is a possible alternative to an iv therapy with voriconazole due to the availability of both iv and oral formulations of the drug. Since the timeframe of the treatment of fungal infections can last up to several weeks (e.g., up to six weeks [265] and much longer) five main advantages result from the practical implementation of a sequence dosing scheme [266]: 1) The period of hospitalisation might be shortened, 2) AEs owing to the iv therapy, e.g., line infections or phlebitis, might be reduced, and comfort and mobility of the patient might increase, 3) the need for supplementary equipment might be eliminated, 4) pharmacy and nursing time might be reduced since oral formulations are easier to administer than iv preparations and require less time to prepare, and 5) considerably decreased expenditures for the oral drug product (health care cost for oral voriconazole therapy  $\approx$  ~20% of iv therapy).

However, two main criteria have to be met when using this dosing approach:



1) The availability of an oral formulation with equal effectiveness in comparison to the iv formulation. In case of voriconazole, this goal is met expressed by an estimated high oral bioavailability  $F$  of 96% [267]. Voriconazole is rapidly and almost completely absorbed following oral administration, with maximum plasma concentrations achieved 1 h to 2 h after dosing in the fasted state. Multiple dosing with the commercial tablet formulation of voriconazole with high-fat meals reduced the  $AUC_{\tau}$  by 22% – 24%, compared with administration in the fasted state [267, 268]. It is recommended that voriconazole should be given at least 1 h before or 1 h following a meal which was adhered to during the pilot study in this thesis.

The absorption of voriconazole was not affected by changes in gastric pH induced by treatment with a histamine  $H_2$  receptor antagonist (ranitidine, cimetidine, omeprazole) [267] which is of high importance for the sequence therapy administered in patients. Moreover, crushed voriconazole tablets have been shown to be bioequivalent to whole-tablet administration being the prerequisite when administering the drug via enteral feeding tubes [269].

2) For patients, it has to be elicited if an oral intake or enteral administration is appropriate and possible, i.e., absence of gastrointestinal abnormalities altering the drug absorption or of specific disease states leading to poor penetration behaviour of the drug [266].

The conversion from iv to po anti-infective therapy is indicated as soon as the patient's clinical condition allows decreasing both the resources being utilised and the length of hospital stay leading to reducing hospital expenditures without compromising clinical outcome. Several examples of conversions from iv to po administration of antibiotics leading to the same or altered drug exposure exist [266]. The feasibility of sequence therapy for voriconazole has already been demonstrated by several groups, e.g., by PURKINS et al. in healthy volunteers assessed by total plasma concentrations [270]. Own investigations revealed sequence therapy of voriconazole being practicable in critically ill patients ( $n=23$ ) but a high interindividual variability in total plasma concentrations and AUC values, respectively, has been observed during the trial which compared merely iv administration ( $n=11$ ) with sequentially administered voriconazole ( $n=12$ ) (variability in AUC of all patients after the 1<sup>st</sup> dose: 55.9% CV, after the 7<sup>th</sup> dose: 77.2% CV, and 77.6% CV after the 21<sup>st</sup> dose) without major differences between the iv therapy and sequence therapy group (21. dose: iv therapy group: 89.0% CV and sequence therapy group: 66.6% CV) [265]. With regard to the high interindividual variability, various studies investigating the PK of voriconazole after merely iv or merely oral administration came to the same conclusion and attributed the highly variable behaviour to genetic and non-genetic factors which include: age, sex, liver disease, and drug-drug interactions since the drug is metabolised by the CYP enzyme system and, therefore, has potential drug interactions [262, 271-277].

So far, neither a clinical trial is available to support the conversion from the iv route to oral administration of voriconazole by unbound plasma concentrations nor target site investigations have been conducted during this sequential dosing scheme or any other dosing scheme. Both items, leading to information about the pharmacologically active fraction in

blood and in the tissue interstitium (ISF), have been demonstrated to be able to evaluate an anti-infective therapy as appropriate or not [168]. To characterise the unbound plasma (UF) and interstitial (ISF) concentration-time profiles and PK of voriconazole independent from the complex situation in patients the clinical trial was performed in healthy volunteers. Further PK influencing factors as age, sex, and concomitant medication were excluded by the inclusion and exclusion criteria defining only young healthy male volunteers to be eligible for the investigation.

The sequential dosing scheme applied in this trial is a currently applied one at the ICU of the University Clinic for Anaesthesiology and Surgical Intensive Medicine, MLU, adhering to the dose recommendations in the summary product characteristics (SPC) of voriconazole [267] which state the switch from 4 mg/kg WT iv to 200 mg oral dosing leading to a lower dose in IDs with WT values above 50 kg.

#### *Unbound plasma concentration-time profiles*

PURKINS et al. suggested that steady state conditions have been reached on day three after two loading dose infusions of 6 mg/kg WT/12 h and maintenance dose infusions of 3 mg/kg WT (which correspond to ~200 mg) every 12 h from day two onwards [278]. This group visually inspected  $C_{\min}$  data, i.e., geometric mean and individual plasma values. However, a few individuals showed an increase of  $C_{\min}$  values after day two being in line with the results for ID 102, and to some extent for ID 103 regarding dose-normalised concentrations. ID 101 showed nearly steady state like conditions over the entire study time with a decreasing trend which was more pronounced in ID 103 regarding the determined concentrations. Considering also the genotypes the variability in the concentration-time profiles (up to ~102%) appeared plausible since ID 102 was assessed to be a homogenous PM for CYP2C19. Conversely, in view of the fact that ID 101 was determined to be a heterozygous PM for CYP2C9 and ID 103 showed the wild type for all alleles of CYP2C19 and CYP2C9 investigated the concentration profiles seemed to behave reversely. The plausible reasons for that may result from the limited number of isoenzymes of CYP2C19 (and CYP2C9) being examined. A misspecification of the individuals cannot be ruled out as derived in the subsection before. Thus, ID 103 might express other polymorphisms leading to higher concentrations than in ID 101. Alternatively, ID 101 might be an UM (CYP2C19\*17 allele, [279]) giving rise to lower concentrations than in ID 103. For a reliable characterisation of an individual with regard to genotype it is demandable to explore the entire, possibly defective alleles of CYP2C19 (and CYP2C9).

#### *Pharmacokinetic-Pharmacodynamic relationship for unbound voriconazole in plasma*

Despite the lower dose after the switch and the different genotypes, minimal UF concentration-time profiles were above or almost equal to the clinical MIC breakpoint values for voriconazole which recently have been stated by the Subcommittee on Antifungal Susceptibility Testing (AFST) of the ESCMID European Committee for Antimicrobial Susceptibility testing (EUCAST) [201] for the species most frequently involved in causing human infections: *Candida albicans*, *Candida tropicalis*, and *Candida parapsilosis*

( $\leq 0.125$  mg/L). MICs for *Candida glabrata* and *Candida krusei* are higher (commonly  $\leq 1$  mg/L) but clinical MIC breakpoints have not been set since less data for analysis are available. Hypothetically, for these species ID 101 ( $C_{\min} \geq 0.28$ ) and, for a large time frame, ID 103 ( $C_{\min} \geq 0.59$ ) would not have been treated appropriately. Due to variable PK of voriconazole and scarce clinical data on species other than *Candida albicans*, *Candida tropicalis* and *Candida parapsilosis*, and on isolates with higher MIC, non-species related breakpoints have not been set either. Clinical response of 76% has been achieved for infections due to *Candida albicans*, *Candida tropicalis*, and *Candida parapsilosis* when MICs were lower than, or equal to, the epidemiological cut-offs. Therefore, the wild type populations of these species were considered to be susceptible to voriconazole. Insufficient information exists on the response to voriconazole treatment in infections caused by *Candida* isolates with higher MICs. Clinical studies of invasive candidosis caused by *Candida glabrata* have shown lower response to voriconazole (insufficient evidence was found for any correlation between MIC and clinical outcome) whereas response of infections caused by *Candida krusei* were similar to those infections caused by *Candida albicans*, *Candida tropicalis*, and *Candida parapsilosis*, respectively. Although the data are limited, it has been shown that there is a decrease in the clinical response of patients when voriconazole plasma  $C_{\min}$  are below 1 mg/L [280]. SMITH et al. reported a favourable response when voriconazole serum concentrations in randomly taken samples exceeded 2.05 mg/L [281]. A strong relationship between voriconazole exposure and treatment efficacy in invasive aspergillosis was suggested with optimal  $C_{\min}$  of 0.5 mg/L by DENNING et al. [282].

Conversely, voriconazole plasma  $C_{\min}$  above 5.5 mg/L have been associated with an increase in toxicity by PASCUAL et al. [280] which have been further strengthened by a population PK analysis, PK effect relationship analysis, and simulations of voriconazole concentration-time profiles [283]. A  $C_{\min}$  of  $>5.5$  mg/L has not been achieved in any of the ID 101 – 103. However, all studies cited analysed total plasma concentrations. Considering a protein binding of 58% [75], plasma concentrations after multiple dose administration (fourth dose) in ID 102 ( $C_{\min} \geq 2.19$  after fourth dose) were near or above this threshold. In this ID the AE of the eyes was found to be most expressed since further examinations of the eyes were indicated. Moreover, ID 102 needed treatment owing to headache. The correlation of the elevated unbound voriconazole plasma concentration and the severity of the AEs was obvious. The wide interindividual variability of the PK of voriconazole after multiple dosing can probably be explained by the genetic variability. Non-genetic factors such as enzyme inhibition and induction, old age, and liver cirrhosis can also modulate, e.g., CYP2C19 activity but can be excluded to be the determinants for the results in the present study. However, it has to be mentioned that in one case an AE (headache) in ID 102 led to an unintentional, pharmacological intervention with mefenamic acid at study visit 2 (once orally, 500 mg). This compound is metabolised by CYP2C9 [284] and might interfere with the metabolism of voriconazole. Owing to less relevance of CYP2C9 for metabolism of voriconazole and inhibition of CYP2C9 by voriconazole [285], leading to an influenced metabolism of

mefenamic acid but not of the one of voriconazole, the influence of co-administered mefenamic acid was evaluated as not relevant with regard to PK.

#### *Pharmacokinetic parameters of unbound voriconazole in plasma*

A predominantly biphasic decline of maximum UF voriconazole concentrations was observed assuming a (rapid) distribution phase for voriconazole pursuant to PURKINS et al. [278]. This biphasic behaviour was distinctive after single dose for all IDs, leading to low variability, and continued for UF concentrations after multiple doses in ID 101. For the two remaining IDs the decline converged to a more monophasic manner after multiple dosing indicating an accumulation (by superposition/increase of voriconazole concentrations) possibly due to limited metabolic processes and, therefore, a further shallow decline of the concentrations was demonstrated. Moreover, the ascent part was not as pronounced in these two IDs, ID 102 and 103, and most probably resulted from previous (less metabolised (according to genotype, e.g., homozygous PM, ID 102)) drug administrations further supported by increasing half-lives and concentrations higher than the single dose ones after further (multiple dose) administrations (although with lower dose). This cannot be assumed for ID 101 since half-lives were similar after multiple dose administration eventually due to EM (or UM), to superposition compensating the lower dose, or to distribution into the tissue. The half-life for the homozygous carrier of the CYP2C19 mutant allele reached about more than twice the value of the CYP2C19 EMs after single dose (PM: 21.8 h (ID 102); EMs: 4.8 h (ID 101), 7.6 h (ID 103)) which was in line with MIKUS et al. and WEISS et al. [262, 264]. Moreover, the magnitude of  $t_{1/2}$  was comparable to other studies [262, 264, 286]. An increase in mean half-life after multiple dosing was previously found by authors investigating oral PK of voriconazole generally associated with a higher accumulation of voriconazole [195] without differentiating between certain genotypes and representing distribution parameters accounting for variability. The terminal half-life of voriconazole is concentration-dependent and, therefore, there is limited predictability of voriconazole accumulation or elimination as a result of nonlinear PK [267]. However, a recently performed population PK analysis by CSAJKA et al. implemented a linear one-compartment model with first-order absorption and elimination on log-transformed data of adult patients [283]. From the inspection of terminal phases in the present study some IDs supported (non)linearity and some did not.

$T_{max}$  was achieved near the end of the 2 h infusion after single dose whereas after multiple dosing  $t_{max}$  attained was more variable ranging from 1.0 h to 2.5 h. However, the values indicated a rapid absorption of oral administered voriconazole matching with previously reports [195]. In general, high and over time increasing interindividual variability was demonstrated for AUC and  $C_{max}$  (up to 126.7% and 89.0%, respectively). Data published so far indicate that voriconazole AUC and  $C_{max}$  are approximately 5.8 times and three times, respectively, higher in CYP2C19 PMs as compared with homozygous EMs on day ten after multiple administration (200 mg) matching with the dose-normalised data of ID 101 of the present study [90] confirming ID 101 as wild type for CYP2C19. But, ID 103 represented AUC and  $C_{max}$  being approximately two times lower compared with the homozygous PM

(ID 102). For the AUC, this difference is reported by publicly available EMA and FDA documents for heterozygous EMs [75, 287]. Since pyrosequencing<sup>®</sup> is seen as a highly reliable procedure to detect defective alleles by analysing the surrounding genetic information as in-built control, a misspecification of ID 103 as wild type for CYP2C19 can rather be excluded. However, there is considerable variability in voriconazole exposure within each genotype and overlap in exposure across genotypes [75, 264]. This might be one explanation for the 'intermittent behaviour' of ID 103 between wild type (ID 101) and homozygous mutant (ID 102). But, several other constellations are thinkable since merely one important variation in CYP2C19 has been studied. For the measurement of direct response and extent of mutations phenotype determinations can be recommended. However, the phenotype status has not been examined for the IDs in the present study by, e.g., omeprazole, a compound often used as a probe to determine CYP2C19 phenotype status [288] which would have been matched with the genotype determinations<sup>®</sup> and may reveal the actual metabolism activity regarding this enzyme. This could be seen as a promising alternative when genotyping of all isoenzymes is not possible. However, an exact classification cannot be achieved via phenotype determinations.

Drug accumulation factors determined for UF (merely seen as a hint since  $C_{\min}$  concentrations showed a decreasing trend) lined up with the results discussed so far demonstrating high interindividual variability (up to 64%) among the IDs with higher accumulation for the PM (ID 102) followed by the two wild types (ID 101, ID 103). Drug accumulation occurs under multiple dosing regimens owing to the addition of each dose to the residual amount of drug still in the body (i.e., not yet eliminated) from the previous doses. Since steady state seemed to have not been reached in some IDs it would be of interest to sample one or two  $C_{\min}$  sample(s) in one or two additional visit(s) to determine those factors more accurate.

In summary, highly variable PK of voriconazole unbound plasma concentrations between individuals was observed with wide ranging CVs, depending on the PK parameter. Typically, high variability in PK is mainly observed in drugs with low bioavailability owing to substantial first-pass metabolism, e.g., for felodipine [289]. One would have expected from *in vitro* data that the CYP2C19 genotype might be of major importance for the PK of voriconazole but merely a few of the numerous publications on voriconazole PK, mainly interaction studies (e.g., [271-276]), reported genotype specific data [90, 262, 264, 277, 279] predominantly after single dose. The results presented here once more demonstrate the association between the CYP2C19 genotype and voriconazole exposure. Genotypes other than CYP2C19 probably may have a further contribution. CYP2C19 genotype could not totally explain the variability in voriconazole exposure being in line with others investigating the influence of polymorphisms on the PK [290, 291]. Even higher variability of voriconazole exposure might occur due to underlying diseases, co-administered drugs leading to interactions, age, and sex. One limitation of this work is that only voriconazole concentrations have been determined due to lack of metabolite reference material and missing capacities for synthesising the main metabolites, respectively. Analysis of the metabolites might provide for more insight in the distribution and elimination of voriconazole.

*Investigation at the target site – concentration-time profiles*

Besides the issues discussed so far, the present study allowed to pursue the voriconazole concentrations at the potential site of an IFI and, thus, the distribution of voriconazole in humans. Unbound tissue concentrations (ISF) of voriconazole were highly comparable to or exceeded (ID 101, ID 103) the unbound plasma (UF) concentrations. This phenomenon was reflected by the concentration-time profiles themselves, particularly by the (geometric) minimal concentration-time profiles (ID 101, ID 103, except ID 102: minimal ISF concentrations were predominantly below the UF concentrations) as well as by the median ratio of ISF and UF concentrations of 1.0 demonstrating the  $C_{ISF}$  being in the the same range as the  $C_{UF}$  which was further shown by the geometric mean AUC ratios ( $AUC_{ISF}/AUC_{UF} \sim 1.1$ ). However, variability was high (~30%). A continuous increase of this ratio starting from ID 102 (mean: 0.9) followed by ID 103 (mean: 1.2) and ID 101 (mean: 1.5) mirrored the different extent of the ascent of unbound plasma concentrations (ID 102 > ID103 > ID101) leading to the assumption of a tissue uptake to a certain degree. The longitudinal increase in the ratios after multiple dose administration (except for ID 102 ISF<sub>i</sub>) might be explained by increasing ISF concentrations or by a decreasing drug accumulation after oral dose. The ISF<sub>c</sub> and ISF<sub>i</sub> data were highly comparable over the entire investigational period. Different RR values for both catheter types resulted in well comparable ISF concentrations in each ID. This fact might be seen as a kind of proof-of-principle for the microdialysis procedure. Certainly, a method independent from the microdialysis setting (see section 1.1) would be more appropriate to corroborate accuracy of the method. The comparatively low interindividual variability after single dose increased after multiple dose administration leading to a wide concentration range. As it has already been proposed from the feasibility results to waive some of the RR determinations, it should be once more emphasised to waive at least the first RR determination in order to avoid voriconazole exposure before administration, and to allow the system to equilibrate longer (~2 h): The microdialysate baseline samples which were directly taken before the first infusion of voriconazole exhibited a concentration of voriconazole and, in most instances, the subsequently taken samples decreased in concentration although an increase was expected as a result of the continuous voriconazole infusion. This phenomenon was explained by the calibration of the individual catheters prior the first administration of voriconazole. Locally administered voriconazole via the catheters was still available in the ISF after the washout phase of 30 min which was performed immediately after the retrodialysis. Even after the first two samples (1. 0 h – 0.5 h, 2. 0.5 h – 1 h) 'local' voriconazole added to the concentration provided by the infusion. With the third sample (3. 1 h – 1.5 h) a slight increase of the concentration was recognised resembling the typical concentration behaviour during an infusion. Hence, the baseline as well as the next two samples were regarded to be implausible and were excluded from data evaluation. Further influence of the exposure of voriconazole by RR determinations during the entire study time can most probably be ruled out since washout periods were much longer than for the first retrodialysis and implausible courses could not be revealed. However, to avoid any influence of local administered voriconazole by the RR determination on the measurements

of the *in vivo* PK exposure of voriconazole, it is suggested to omit retrodialysis during the entire sampling period and instead to examine the RR after the last taken sample according to the ESS. This modification of the study protocol has its justification from the stable and reproducible RR results demonstrated and discussed in this thesis. However, this procedure carries a risk since no ISF concentrations would be available at all when a catheter will lose its function before RR determination. According to the study protocol the pilot study should prove the feasibility of the long-term sampling from both concentric and linear catheters whereas the main part (part II) stipulated the continuation with merely one, the more suitable one, microdialysis catheter. According to the feasibility section (see 4.4.1), several reasons prefer to continue the main part using the concentric catheter. However, both catheters could be used since the visits showed comparable profiles and results, respectively.

#### *Investigation at the target site – sampling phenomenon*

The longer equilibration period prior to visit 1 would allow a) vascular reactions of the needle insertion trauma (e.g., increase of skin blood flow, skin redness, and erythema) to stabilise [292] and b) mediators, provoked by the insertion of the microdialysis catheter, to definitely return to their baseline levels in the interstitium: Histamine was rapidly eliminated in the skin and returned to baseline within 40 min [293] to 2 h [294, 295]; eicosanoids have been found to remain stable [296] or to return to baseline within 2 h [294, 297] after needle insertion. Recently, IL-1 $\beta$ , IL-6, and IL-8 were seen in healthy subjects at all time points after the first hour after insertion of a concentric microdialysis catheter (100 kDa) [298]. Of these cyto- and chemokines, IL-8 has also been recovered using a 20 kDa catheter as utilised in the present study [299]. The maximum concentrations were reached after 5 h to 8 h and equilibrated to lower concentrations at 24 hours [298]. During analysis of the microdialysis samples of the study presented in this thesis an unknown substance (or substance mixture), (exponentially-like) decreasing directly after catheter insertion to a baseline value approximately after 52 hours, was detected during the HPLC analysis of voriconazole (see 3.1.1.3). According to the facts regarding their (dis)appearance mentioned for the mediators and molecular mass (IL-1 $\beta$ , IL-6 >20 kDa) these substances can probably be excluded as interference. By the initial trauma, cellular damage and physical damage to blood vessels might have led to secretion of certain substances (intracellular, e.g., sodium glycerophosphate) and their decrease due to clearance by distribution or metabolism. Voriconazole itself might have triggered the release or production of the substance, however, no reports have been found in the literature. Since intake of concomitant medication has been precluded, exogenous substances could be ruled out. Metabolites emerge not before drug administration and, hence, could be excluded. The same is assumed for analytical artefacts due to reproducible results independent from the sequence of measurements of the interference. SBECDs would have been detected during the *in vitro* measurements, too, and might therefore be excluded. The colourant of the disinfectant applied prior to catheter insertion might be a further possibility. However, this dye is high water soluble and penetration into skin was not expected. It is obvious that this over time decreasing substance (or substance mixture) was related to one of the study proce-

dures (e.g., catheter insertion trauma, voriconazole administration via retrodialysis, infusion, or oral intake). Future investigations should focus on the elucidation of substance identity a) to reveal an influence of that substance on the local situation, e.g., local blood flow and, hence, on recovery of the compound of (PK) interest and b) to include the substance within the investigations regarding specificity of the bioanalytical method.

#### *Investigation at the target site – pharmacokinetic parameters*

A rapid increase of  $C_{ISF}$  within the infusion period could be observed although the first two ISF samples after administration had to be disregarded. A minor initial delay to unbound plasma concentration could be defined (~0.5 h). After multiple oral dosing  $t_{max}$  was attained sooner probably due to faster available and, hence, higher amounts after oral intake and rapid absorption realisable by the high bioavailability. The accumulation was similar ( $ISF_1$ ) or slightly higher ( $ISF_c$ ) compared to unbound plasma concentrations and variability, ranging from 24.6% to 43.1%, was not as pronounced as in UF probably due to a limited passage in the tissue ISF. However, the profiles paralleled the unbound plasma concentrations with a small but considerable absolute difference after multiple dosing. Drug distribution in the interstitium of soft tissues such as muscle or lung is governed by passive diffusion that allows unbound drug to diffuse across membranes from the vascular compartment to tissues (ISF), and an equilibrium of unbound drug should occur rapidly between plasma and tissue ISF [300, 301], without existing significant barriers as well as influx or efflux mechanisms. Therefore, unbound concentrations in blood and tissue ISF should be identical at equilibrium [302]. Neither an analytical error of the validated HPLC assay (see 2.3, [100]) nor errors in RR determination have to be considered. At first sight one idea to reflect the accumulation results might be as follows: SBECDs which were locally administered via the first retrodialysis procedure might have been caught systemic administered voriconazole during the entire study. Due to the hydrophilic nature of these molecules it was assumed that they have been washed out during the subsequent wash-out period. Experiences in the preclinical study (III) did not support this consideration, too. Moreover, results of visit 1 would have shown the same results since RR determinations have been performed prior to single dose of voriconazole.

Studies employing microdialysis to determine unbound tissue concentrations of antifungal agents are rare in the literature. So far, SASONGKO et al. was the only group studying the time course of fluconazole concentrations in subcutaneous ISF (CMA60®) in five healthy volunteers [177]. Interestingly, in three of five IDs the  $ISF_c$  exceeded the unbound plasma concentrations during an eight-hour period after a single dose of fluconazole (200 mg). AUC ratios ( $AUC_{ISF,0-8h}/AUC_{UF,0-8h}$ ) were calculated to be 0.9, 1.02, 1.12, 1.28, and 1.47, respectively, for the five IDs with a mean ratio of 1.16 (CV: 19.0%). These results were in line with the pilot study ones for both catheters. Another study, supporting the good penetration of voriconazole, was recently published by CRANDON et al. [303]. This group determined bronchopulmonary disposition of iv administered voriconazole at steady state in twenty healthy volunteers revealing penetration ratios into ELF (epithelial lining fluid, extracellular



compartment) and alveolar macrophages (intracellular compartment) of 7.1 and 4.5, respectively, demonstrating a good penetration, concentrations exceeding those in plasma, and high drug exposure of the drug in these matrices. The results of CRANDON et al. confirmed the findings in patients of CAPITANO et al., by publishing a comparable range of penetration ratios of voriconazole into ELF [304]. For voriconazole it might be concluded that unbound plasma concentrations may not be a good surrogate of unbound tissue ISF concentrations of antifungals and may underestimate the actual tissue ISF concentrations after multiple dosing since AUC ratios predominantly exceeded the value 1. However, after single dose, UF concentrations seemed to reflect the ISF concentrations. Studies in the interstitial space of the kidneys [172, 188], of the lungs and skeletal muscle tissue [187] of healthy and infected rats elaborated unbound tissue ISF concentrations similar to the unbound plasma fraction of voriconazole after single dose. Both study data derived from a preclinical experimental setting in rats and compared observed (tissue) and estimated (unbound plasma) voriconazole concentrations. Furthermore, voriconazole was detectable in CSF indicating a permeation across the blood-brain-barrier [305]. LUTSAR et al. reported concentrations in randomly collected samples ranging from 0.08 µg/mL to 3.93 µg/mL 1 h to 10 h after intake of voriconazole, with a CSF/plasma ratio of voriconazole concentration of 0.22-1.0 (median 0.46) [84].

#### *Investigation at the target site – Pharmacokinetic-Pharmacodynamic relationship*

The different study measure sites of voriconazole (drug) concentrations foreshadow the ignorance of the exact site of infection, i.e., the location of the pathogen, a question which is not always easily answered [306]. It is generally accepted that the ISF of tissue and other body fluids represents the actual target space for the vast majority of infections [28]. The indications for voriconazole are systemic fungal infections characterised by an overall infection of the (human) body, in fact, demanding all ISFs of all tissues of the body have potentially to be investigated. However, the prerequisites for microdialysis investigations are well accessible sites for catheter application, e.g., subcutaneous adipose tissue or muscles. For long-term microdialysis the site also depends on the duration of the application of the linear and concentric catheters. Sampling from the skeletal muscle is not feasible over days using concentric catheters (no movement of ID is possible), whereas linear catheters are not applicable in muscles due to the catheter design. The further rationale choosing the interstitium of soft tissues, i.e., ISF, as appropriate and clinically relevant site for microdialysis measurement is discussed as follows. The lungs are the most common site of primary infection in cases of invasive aspergillosis [307, 308]. An overwhelming part of the infected patients is immuno-compromised often requiring mechanic ventilation, the most important source of *Aspergillus* infections. This is not the case for infections caused by *Candida* species, whose most hosts (>80%), developing disseminated candidiasis, are not neutropenic or immuno-compromised. Instead, these patients are characterised by, e.g., alterations in anatomical barrier function or commensal organism burden due to, e.g., central venous catheterisation, parenteral nutrition, surgical manipulation of the intestines, receipt of

broad spectrum antibacterial agents, and/or overgrowth of commensal *Candida* [65]. For these patients soft tissue infections outside the lung are much more frequent than lung infections [309] outlining the importance of adequate voriconazole concentrations in those tissues. In case of invasive candidiasis the fungi are located in the ISF between the cells, as evidenced by histopathological investigations [310], then spreading into blood vessels. *Aspergillus* species are one of the major opportunistic fungal pathogens causing invasive pulmonary infections which rarely involve extrapulmonary organs. As soon as *Aspergillus* starts to leave lung alveoli and to invade lung tissue again fungi are located within the interstitial space, as confirmed by histopathological investigations [310]. The ELF concentration of an antibacterial agent is considered to be a good estimate of the concentration at the site of extrapulmonary bacterial infection [311, 312]. However, the site of intrapulmonary infection of *Aspergillus* species is not well defined, and the clinical relevance of antifungal ELF concentrations is unknown. Besides, ELF investigations are laborious and methodically problematic (e.g., the degree of dilution of ELF during the method of determination (bronchoalveolar lavage) is not known, the exact sampling location remains unknown and not only alveolar space but also bronchioles and conducting airways are lavaged, and some components may be sampled inadequately due to incomplete mixing [313]). *In vitro* studies demonstrated a propensity for the conidia and hyphae of *Aspergillus fumigatus* to invade and to germinate in human pneumocytes [314, 315]. Thus, the sites of pulmonary aspergillosis likely include not only the ELF but also alveolar macrophages, pulmonary epithelial cells, and the ISF of lung tissue. Several microdialysis studies on different antimicrobials have shown that concentrations in the interstitium of peripheral soft tissues, even though solely in skeletal muscle tissue, can be used as surrogate for the ISF of lung tissue [316]. One study investigating levofloxacin showed lower concentrations in lung ISF than in the ISF of skeletal muscle or adipose tissue [317]. Nevertheless, the microdialysis approach used in the pilot study may provide an important insight into expected concentrations of voriconazole in the human lung. Although pulmonary involvement is the main presentation of *Aspergillus*, cases of invasive extrapulmonary aspergillosis (disseminative aspergillosis) have markedly increased during the last decade, probably owing to the increasing number of organ transplantations [318-320]. In rare cases not the lung but the skin might be the initial place of *Aspergillus* infection, leading to consecutive spread of fungi from this site throughout the body [321].

However, with regard to the MIC, the present results for tissue ISF concentrations underline the conclusions drawn for unbound plasma concentrations and can be seen as even more important since they reflect the situation at the potential target site of infection.  $C_{ISF}$  concentrations were ranked in the same order to the  $C_{UF}$  expressing high interindividual variability. For voriconazole, lower exposure in tissue ISF might not be expected when unbound plasma concentrations are determined to be above a certain breakpoint. In cases of well tolerated drugs a higher exposure in ISF would be completely advantageous. For drugs showing an unfavourable AE profile, as voriconazole, this would lead to consequences demonstrated by, e.g., more severe AEs.

*Adverse events and therapeutic drug monitoring*

Although AEs and laboratory test data indicated that the study drug was well tolerated, without serious AEs, and AEs resolved predominantly without the need for treatment, visual AEs occurred in all IDs with different severity (mild to moderate). This visual disturbance has been recognised as the most frequent AE reaction to voriconazole and is related to transient electric changes in the retina but without detection of permanent damage [91]. Moreover, ID 102 expressed headache. These AE results were in accordance with other recently performed studies in healthy volunteers [262, 277]. In general, AEs have been reported by every research group conducting a clinical trial with voriconazole. Since an optimal individual drug therapy should be tailored to achieve the desired drug effect and to avoid AEs as much as possible, and a relationship between exposure of voriconazole and response as well as between exposure and toxicity [280] has been elaborated, most of the groups concluded a therapeutic drug monitoring (TDM) for the therapy with voriconazole [129, 280, 281, 322-335]. In contrast, others elaborated individual plasma concentrations of voriconazole being not predictive of, e.g., abnormal liver function tests or treatment outcomes [336, 337]. However, a definite therapeutic range for voriconazole has not been defined so far. Very recently, MOUTON summarised the appropriateness of TDM for voriconazole [338] and provided results of CART analysis of the already published data of PASCUAL et al. [280] indicating that voriconazole  $C_{\min}$  should exceed 1.15 mg/L to be effective. Since this thesis supported the findings regarding the high variability in PK of voriconazole and, additionally, concluded high variability of target site PK, too, it is strongly suggested to perform TDM studies in patients implementing microdialysis and genotype determinations. These studies have to define or corroborate a therapeutic range for voriconazole concentrations and should consider unbound plasma concentrations and the difference between unbound plasma and ISF concentrations. Although the influence of SNPs in the metabolising enzymes on the PK of voriconazole has been elaborated and published none of the research groups dealing with voriconazole recommend a PG-oriented TDM. Even then, in 2001, ENSOM et al. asked the question “Pharmacogenetics: The Therapeutic Drug Monitoring of the Future?” [339]. This thesis hypothesised the correlation of the severity of the AEs and elevated unbound voriconazole plasma concentration due to a genotype responsible for a poor metabolism of the drug. Although the present study was conducted in healthy volunteers and the results may not be directly extrapolated to critically ill patients, it seems reasonable to conclude that care should be exercised if a PM patient has been detected. According to the documents of the EMA and therefore, e.g., to the German summary of product characteristics (SPC) for voriconazole (Pfizer, Germany, Februar 2009), the recommended voriconazole dosage is still independent of the genotype (e.g., CYP2C19 genotype). Future studies should elaborate genotype-dependent dose recommendations which should be considered for dose adjustments and should be directly incorporated in the dose, dose adjustment, and warning sections of the SPC of voriconazole.

### *Perspective*

In perspective, the PK analysis presented here should be regarded as a preliminary examination of voriconazole target site and unbound plasma concentrations and, indeed, should be an indication for how to go further with the pilot data and future data of the subsequent part of the pilot study (main study, part II) since the long-term microdialysis study has been proven suitable and a continuation of the trial is strongly recommended. The pilot analysis is certainly not able to lead to definite dose recommendations for voriconazole but should serve as basis for several tasks after including further individuals (main study): 1) An individual PK analysis using a compartmental approach (one- or two-compartment model), 2) a population PK analysis investigating, e.g., the influences of the genotype or WT, 3) a physiology-based PK analysis (PBPK approach) leading to a more physiological interpretation of the PK model, or 4) optimal design investigations eventually leading to a reduced number of necessary study samples without any loss of information but with significantly reduced burden on the study individuals (especially patients) and facilitated conduction of the clinical study. First beginnings have already been operated. Moreover, investigations regarding the problem that the ISF concentrations represent an integrated measure of a drug in tissue during the sampling period and the impact of this eventual misrepresentation are under way. These more advanced evaluations of the pilot and main study data might lead to an adequate description of the PK of voriconazole using mathematical equations in the form of mechanistic PK model and covariate relations. A further inclusion of individuals or further trials might confirm those results and might examine the differences in the PK of merely iv administered voriconazole to oral administered voriconazole with regard to variability. However, voriconazole has been developed for patients as an answer to the need of a broad-spectrum antimycotic agent [81]. Therefore, target site investigations in critically ill individuals are strongly indicated to enlighten non-genetic covariates responsible for the strong variability of the PK of voriconazole and to assess the influence of the disease state on the concentrations of tissue ISF. Long-term application of microdialysis has been proven suitable within the pilot study of this thesis and it is suggested to adapt this approach to a clinical trial to patients requiring voriconazole therapy. This patient investigation might implement the description of the relation between PK and PD of voriconazole, realisable by PK/PD indices such as AUC/MIC [340, 341] or, more progressive, by applying time-kill curve methodology [342-344], deducing un-/successful treatment of an infection. Even more progressive seems the consideration of the active drug concentrations that are measured at the site of infection and to use this data for simulating the PK of the drug in the *in vitro* PD models [300, 345]. In this context, the data used should be preferably based on a population PK approach which further improves the PK input and quantifies and accounts for inter- and intraindividual variability. PK/PD considerations are not only important for optimising the antiinfective activity, but also and of similar importance, for preventing the development of resistance and for rationally designing dosing regimens that suppress or delay the emergence of resistance [346-348]. Comparable to the limited occurrence of *in vitro* PD analysis relying on target site concentrations is the

limited experience with PD models describing the activity against resistant strains by simulating exposure at extravascular sites.

But, antiinfectives may affect not only microorganisms but also innate host immunity. BALTCH et al. studied the effects of voriconazole, alone and in combination with anidulafungin, on the production of cytokines *in vitro* [349]. For this purpose, the concentrations of eight cytokines (TNF- $\alpha$ , MIP-1 $\beta$ , IL-1ra, IL-6, IL-1 $\beta$ , IL-10, IL-8, and MCP-1) in the supernatants of monocyte-derived macrophages monolayers were determined before, after infection with *Candida glabrata*, and during treatment with anidulafungin and voriconazole in different concentrations for 18 h. In result, both agents modulated cytokine production mostly by down-regulation, especially with drug combination at high concentrations indicating an important effect of voriconazole (and anidulafungin) on secretory functions of infected monocyte-derived macrophages. Since cytokines emerged as clinically useful biomarkers of disease and have also been successfully recovered by microdialysis [350, 351], a combination of a PK analysis via determination of unbound plasma and ISF concentration of voriconazole with a PD analysis a) via *in vitro* pathogen/infection model analysis and b) via microdialysis cytokine sampling analysing the relation of PK and PD would be a possible and fascinating approach enabling dose individualisation preferentially regarding the minimisation of AEs. However, this idea is still subjected to some technical challenges of both the PD analysis using *in vitro* infection models (e.g., clogging of filters by the pathogens or tightness of the infection model) and cytokine sampling by microdialysis (e.g., ultrafiltration due to higher cut-off values of the microdialysis membrane or adhesion of the molecules to the microdialysis device) but a justified challenge for upholding the effect of one of the potent drugs in the pharmacological armamentarium for IFIs.

---

## 5 SUMMARY

The majority of infections is localised extracellularly, i.e., in the interstitial space fluid (ISF). Microdialysis is the method of choice to facilitate the direct access to the ISF and the target space, respectively, in order to determine local, unbound and, hence, pharmacodynamically active drug concentrations. For *in vitro* and *in vivo* application this thesis laid the necessary foundations required by the microdialysis approach. In order to combine both this methodological investigation and a clinical research issue of current concern all investigations were accomplished with voriconazole, a second-generation antifungal agent of major importance primarily intended for the critically ill suffering from invasive aspergillosis and candidiasis. Information about its target site availability is lacking yet, making voriconazole a candidate for microdialysis investigations.

For *in vitro* and *in vivo* investigations the basic prerequisite is the reliable and efficient quantification of the drug of concern. Therefore, an analytical HPLC assay for voriconazole was developed and validated in terms of stability, specificity, linearity, precision, accuracy, recovery, as well as robustness and ruggedness permitting its reliable quantification from small microdialysate sample volumes. Moreover, the analytical repertoire was extended to the matrices plasma, whole blood, ultrafiltrate, and skin biopsy allowing for comparison of the concentrations found in the interstitium with the ones in the other compartments investigated. The reliable HPLC method is characterised by a fast and simple sample preparation requiring minor laboratory expenditures. These assays were successfully applied to samples obtained in the *in vitro* experiments and (pre)clinical trials presented in this thesis reflected by the adherence to the limits for accuracy and precision set in international guidelines. After providing the analytical basis, the development and optimisation of methods enabling reproducible microdialysis investigations *in vitro* and *in vivo* were performed.

For *in vitro* purposes, an *in vitro* microdialysis system (IVMS) has been developed. The easy-to-handle and compact system offers the opportunity to cleanly, simply, reliably, and rapidly investigate *in vitro* microdialysis issues for every compound and setting of interest using both concentric and linear catheters. Following the development, this system was successfully subjected to several *in vitro* investigations. For voriconazole a general suitability for the microdialysis approach was demonstrated for both concentric and linear catheters. A concentration independence and flow rate dependence were elaborated. Moreover, experiments with the drug product of voriconazole (Vfend®) revealed its applicability for calibration purposes in *in vivo* investigations as an (approved) alternative to the drug substance. For the determination of system suitability and specifications the *in vitro* experiments were extended to other anti-infectives. Applicability of the chosen drugs was as feasible as for voriconazole. Mass transfer through the catheter membrane depended on each substance and was of the same magnitude in drugs of comparable size. Preliminary results should be confirmed and perpetuated in further experiments. The results regarding the microdialysis experiments for voriconazole formed the basis for investigating the ISF pharmacokinetics of voriconazole in *in vivo* settings.

As a next step microdialysis was applied to healthy and infected skin using concentric catheters in three guinea pigs after twelve days of multiple oral administration of voriconazole. This approach was assessed to be feasible affirmed by highly reproducible *in vivo* relative recovery results among all inserted catheters independent from the surrounding, i.e., healthy or infected area. The investigation revealed no significant differences between the ISF concentrations obtained in both healthy and infected skin leading to the hypothesis that the disease state, i.e., an inflammation, did not alter the pharmacokinetics of voriconazole in this matrix. The comparison to unbound concentrations in blood indicated that voriconazole penetrated well into ISF.  $C_{\max}$  and AUC values in ISF were determined to be highly comparable to the unbound fraction of voriconazole in blood and substantially below the concentrations in skin biopsy samples. However, the ISF concentrations were well above the MIC for the pathogen involved in the inflammation (*M. canis*) and other fungal pathogens.

For reproducible microdialysis *in vivo* measurements over several days in humans a special setting for long-term microdialysis implementing both concentric and linear catheters has been developed. The application of the setting and devices developed could be demonstrated to be feasible and tolerable for healthy volunteers in a pilot study (part I) allowing, in a further step, to characterise the data and results obtained from a statistical and pharmacokinetic point of view. The investigation was designed as a prospective, two part, open-labelled, uncontrolled trial and applied voriconazole as multiple sequence dosing. As this was the first human study of voriconazole employing the microdialysis technique determining the target site concentrations over several days the trial has been divided into two subsequent parts: An observational pilot study (part I) with two microdialysis catheters (linear and concentric design) and an extensive sampling schedule to determine the feasibility of the long-term *in vivo* microdialysis catheter insertion and entire sampling schedule for single and multiple dose investigations. The main study (part II) will be based on the results of part I considering the feasibility results of the pilot phase (long-term insertion, choice of catheter). Obvious feasibility recognised during the study procedures was confirmed by reproducible relative recovery values within each catheter and catheter type longitudinally received over the entire study period of ~87 h. Different relative recovery values between both catheter types resulted in well comparable ISF concentrations in each individual over the entire investigational time. A continuation of the trial (as part II) will profit from the concluded optimised study design derived from the pilot study which should employ concentric catheters and be, e.g., characterised by a reduction of recovery determinations and, hence, reduced expenditures in time and for the equipment spent for calibration procedure. The successful conduction of the pilot study enabled the evaluation of the pharmacokinetics of voriconazole in three healthy volunteers after single and multiple sequence dosing. As a consequence of the applied dosing schedule – intraindividual dose de-escalation during maintenance iv dosing and by the switch from an iv to a fixed oral administration – and the weight-based iv dose administration, the concentrations were triggered by different doses for each individual. Unbound voriconazole concentrations in ISF of subcutaneous adipose tissue and plasma were available for analysis which revealed favourable penetration capabilities of

voriconazole into ISF and, hence, distribution to and availability at the potential target site demonstrated by ISF concentrations primarily higher or equal to unbound plasma concentrations and AUC ratios predominantly increasing over the investigational time. The high and over time increasing interindividual variability in the pharmacokinetics elaborated for both matrices, target site ISF and plasma (more pronounced), could partially be explained when considering the genotype for the main metabolising cytochrome P450 (CYP) enzymes for voriconazole for each individual investigated. Genotypes for the polymorphic isoenzymes CYP2C9 and CYP2C19 have been determined via pyrosequencing identifying, e.g., a homozygous non-wild type for CYP2C19\*2 in one individual. The occurrence of this genotype was associated with an increase of adverse events. Follow-up investigations in healthy volunteers (part II) and in patients are needed to confirm the influence of the genotype on target site concentrations of voriconazole. Concepts for data evaluation and more advanced settings are outlined in the perspective section. Pharmacokinetic analysis of those trials will further contribute to characterise voriconazole and its distribution and might guide future dose recommendations eventually according to the specific genotype in order to individualise and improve the therapy regarding the balance between toxicity and effect.

In summary, the results of this thesis yielded a decisive contribution to the development, optimisation, and application of methods enabling reproducible *in vitro* and clinical microdialysis investigations contributing to pharmacokinetically characterise drug (voriconazole) disposition processes.



---

## 6 REFERENCES

- [1] G.J. Veal, S.A. Coulthard, A.V. Boddy. Chemotherapy individualization. *Invest New Drugs*, 21: 149-156 (2003).
- [2] J.H. Song. What's new on the antimicrobial horizon? *Int J Antimicrob Agents*, 32 Suppl 4: S207-213 (2008).
- [3] M. Ruhnke, K. Hartwig, G. Kofla. New options for treatment of candidaemia in critically ill patients. *Clin Microbiol Infect*, 14 Suppl 4: 46-54 (2008).
- [4] U. Jaehde, R. Radziwill, S. Mühlebach, W. Schunack (Eds.). *Lehrbuch der Klinischen Pharmazie*. 2 ed. Wissenschaftliche Verlagsgesellschaft, Stuttgart (2003).
- [5] D.I. Jodrell, M.J. Egorin, R.M. Canetta, P. Langenberg, E.P. Goldbloom, J.N. Burroughs, J.L. Goodlow, S. Tan, E. Wiltshaw. Relationships between carboplatin exposure and tumor response and toxicity in patients with ovarian cancer. *J Clin Oncol*, 10: 520-528 (1992).
- [6] S.P. Joel, P. Ellis, K. O'Byrne, D. Papamichael, M. Hall, R. Penson, S. Nicholls, C. O'Donnell, A. Constantinou, J. Woodhull, M. Nicholson, I. Smith, D. Talbot, M. Slevin. Therapeutic monitoring of continuous infusion etoposide in small-cell lung cancer. *J Clin Oncol*, 14: 1903-1912 (1996).
- [7] A.H. Calvert, D.R. Newell, L.A. Gumbrell, S. O'Reilly, M. Burnell, F.E. Boxall, Z.H. Siddik, I.R. Judson, M.E. Gore, E. Wiltshaw. Carboplatin dosage: prospective evaluation of a simple formula based on renal function. *J Clin Oncol*, 7: 1748-1756 (1989).
- [8] L.P. Rivory, K. Slaviero, J.P. Seale, J.M. Hoskins, M. Boyer, P.J. Beale, M.J. Millward, J.F. Bishop, S.J. Clarke. Optimizing the erythromycin breath test for use in cancer patients. *Clin Cancer Res*, 6: 3480-3485 (2000).
- [9] R.B. Diasio, M.R. Johnson. The role of pharmacogenetics and pharmacogenomics in cancer chemotherapy with 5-fluorouracil. *Pharmacology*, 61: 199-203 (2000).
- [10] M.E. Burton, L.M. Shaw, J.J. Schentag, W.E. Evans (Eds.). *Applied Pharmacokinetics and Pharmacodynamics*. 4 ed. Lippincott Williams & Williams, Baltimore, Philadelphia (2006).
- [11] W.E. Evans, J.A. Johnson. Pharmacogenomics: the inherited basis for interindividual differences in drug response. *Annu Rev Genomics Hum Genet*, 2: 9-39 (2001).
- [12] W.E. Evans, M.V. Relling. Pharmacogenomics: translating functional genomics into rational therapeutics. *Science*, 286: 487-491 (1999).
- [13] H.L. McLeod, W.E. Evans. Pharmacogenomics: unlocking the human genome for better drug therapy. *Annu Rev Pharmacol Toxicol*, 41: 101-121 (2001).
- [14] M. Eichelbaum, M. Ingelman-Sundberg, W.E. Evans. Pharmacogenomics and individualized drug therapy. *Annu Rev Med*, 57: 119-137 (2006).
- [15] E.Y. Krynetski, W.E. Evans. Pharmacogenetics of cancer therapy: getting personal. *Am J Hum Genet*, 63: 11-16 (1998).
- [16] Y. Ando, H. Saka, G. Asai, S. Sugiura, K. Shimokata, T. Kamataki. UGT1A1 genotypes and glucuronidation of SN-38, the active metabolite of irinotecan. *Ann Oncol*, 9: 845-847 (1998).
- [17] L. Iyer, C.D. King, P.F. Whittington, M.D. Green, S.K. Roy, T.R. Tephly, B.L. Coffman, M.J. Ratain. Genetic predisposition to the metabolism of irinotecan (CPT-11). Role of uridine diphosphate glucuronosyltransferase isoform 1A1 in the glucuronidation of its active metabolite (SN-38) in human liver microsomes. *J Clin Invest*, 101: 847-854 (1998).
- [18] L. Bertilsson. Metabolism of antidepressant and neuroleptic drugs by cytochrome p450s: clinical and interethnic aspects. *Clin Pharmacol Ther*, 82: 606-609 (2007).
- [19] G.P. Aithal, C.P. Day, P.J. Kesteven, A.K. Daly. Association of polymorphisms in the cytochrome P450 CYP2C9 with warfarin dose requirement and risk of bleeding complications. *Lancet*, 353: 717-719 (1999).
- [20] H. Furuya, P. Fernandez-Salguero, W. Gregory, H. Taber, A. Steward, F.J. Gonzalez, J.R. Idle. Genetic polymorphism of CYP2C9 and its effect on warfarin maintenance dose requirement in patients undergoing anticoagulation therapy. *Pharmacogenetics*, 5: 389-392 (1995).

- [21] H.G. Eichler, M. Muller. Drug distribution. The forgotten relative in clinical pharmacokinetics. *Clin Pharmacokinet*, 34: 95-99 (1998).
- [22] M. Muller, A. dela Pena, H. Derendorf. Issues in pharmacokinetics and pharmacodynamics of anti-infective agents: distribution in tissue. *Antimicrob Agents Chemother*, 48: 1441-1453 (2004).
- [23] B.H.C. Westerink, T.I.F.H. Cremers (Eds.). *Handbook of Microdialysis Methods, Applications and Perspectives*. 1 ed. Elsevier (Academic Press), London (2007).
- [24] C. Joukhadar, H. Derendorf, M. Muller. Microdialysis. A novel tool for clinical studies of anti-infective agents. *Eur J Clin Pharmacol*, 57: 211-219. (2001).
- [25] W.A. Craig, S.C. Ebert. Protein binding and its significance in antibacterial therapy. *Infect Dis Clin North Am*, 3: 407-414 (1989).
- [26] C.M. Kunin, W.A. Craig, M. Kornguth, R. Monson. Influence of binding on the pharmacologic activity of antibiotics. *Ann N Y Acad Sci*, 226: 214-224 (1973).
- [27] D.J. Merrikin, J. Briant, G.N. Rolinson. Effect of protein binding on antibiotic activity in vivo. *J Antimicrob Chemother*, 11: 233-238 (1983).
- [28] D.M. Ryan. Pharmacokinetics of antibiotics in natural and experimental superficial compartments in animals and humans. *J Antimicrob Chemother*, 31 Suppl D: 1-16 (1993).
- [29] European Medicines Agency (EMA). Evaluation of medicines for human use. Points to consider on pharmacokinetics and pharmacodynamics in the development of antibacterial medicinal products. (2000); available at <http://www.emea.europa.eu/pdfs/human/ewp/265599en.pdf> [accessed 05 January 2010].
- [30] Food and Drug Administration (FDA). Guidance for Industry. Developing antimicrobial drugs - general considerations for clinical trials. Draft guidance (1998); available at <http://www.fda.gov/downloads/Drugs/GuidanceComplianceRegulatoryInformation/Guidances/ucm070983.pdf> [accessed 05 January 2010].
- [31] M. Brunner, H. Derendorf, M. Muller. Microdialysis for in vivo pharmacokinetic/pharmacodynamic characterization of anti-infective drugs. *Curr Opin Pharmacol*, 5: 495-499 (2005).
- [32] M. Brunner, A. Schmiedberger, R. Schmid, D. Jager, E. Piegler, H.G. Eichler, M. Muller. Direct assessment of peripheral pharmacokinetics in humans: comparison between cantharides blister fluid sampling, in vivo microdialysis and saliva sampling. *Br J Clin Pharmacol*, 46: 425-431 (1998).
- [33] M. Muller, M. Brunner, R. Schmid, E.M. Putz, A. Schmiedberger, I. Wallner, H.G. Eichler. Comparison of three different experimental methods for the assessment of peripheral compartment pharmacokinetics in humans. *Life Sci*, 62: PL227-234 (1998).
- [34] J. Blaser, H.L. Rieder, R. Luthy. Interface-area-to-volume ratio of interstitial fluid in humans determined by pharmacokinetic analysis of netilmicin in small and large skin blisters. *Antimicrob Agents Chemother*, 35: 837-839 (1991).
- [35] C. Clerc, M. Pibouin, A. Ruelland, B. Legras, J. Chevrant-Breton, L. Cloarec. Cutaneous interstitial fluid protein concentrations in the inflammatory syndrome: pharmacological consequences. *Clin Chim Acta*, 189: 181-189 (1990).
- [36] F. Philip-Joet, B. Bruguerolle, M. Reynaud, A. Arnaud. Correlations between theophylline concentrations in plasma, erythrocytes and cantharides-induced blister fluid and peak expiratory flow in asthma patients. *Eur J Clin Pharmacol*, 43: 563-565 (1992).
- [37] A.J. Fischman, N.M. Alpert, J.W. Babich, R.H. Rubin. The role of positron emission tomography in pharmacokinetic analysis. *Drug Metab Rev*, 29: 923-956 (1997).
- [38] M.E. Phelps. PET: the merging of biology and imaging into molecular imaging. *J Nucl Med*, 41: 661-681 (2000).
- [39] Committee for Proprietary Medicinal Products (CPMP). Points to consider on pharmacokinetics and pharmacodynamics in the development of antibacterial medicinal products, CPMP/EWP/2655/99 (2000); available at <http://www.ema.europa.eu/pdfs/human/ewp/265599en.pdf> [accessed 07 January 2010].

- [40] Committee for Proprietary Medicinal Products (CPMP). Note for guidance on evaluation of new anti-bacterial medicinal products, CPMP/EWP/558/95 rev 1 (2004); available at <http://www.ema.europa.eu/pdfs/human/ewp/055895en.pdf> [accessed 07 January 2010].
- [41] Food and Drug Administration (FDA). Anti-Infective Drugs Advisory Committee Meeting, 64th Meeting (1998); available at [www.fda.gov/cder/present/anti-infective798/073198.pdf](http://www.fda.gov/cder/present/anti-infective798/073198.pdf) [accessed 25 October 2006].
- [42] U. Ungerstedt, C. Pycock. Functional correlates of dopamine neurotransmission. *Bull Schweiz Akad Med Wiss*, 30: 44-55 (1974).
- [43] N. Plock, C. Kloft. Microdialysis - theoretical background and recent implementation in applied life-sciences. *Eur J Pharm Sci*, 25: 1-24 (2005).
- [44] C. Joukhadar, M. Muller. Microdialysis: current applications in clinical pharmacokinetic studies and its potential role in the future. *Clin Pharmacokinet*, 44: 895-913 (2005).
- [45] I. Jacobson, M. Sandberg, A. Hamberger. Mass transfer in brain dialysis devices-a new method for the estimation of extracellular amino acids concentration. *J Neurosci Methods*, 15: 263-268. (1985).
- [46] P. Lonroth, P.A. Jansson, U. Smith. A microdialysis method allowing characterization of intercellular water space in humans. *Am J Physiol*, 253: E228-231 (1987).
- [47] R.J. Olson, J.B. Justice, Jr. Quantitative microdialysis under transient conditions. *Anal Chem*, 65: 1017-1022 (1993).
- [48] O. Schwalbe, C. Buerger, N. Plock, C. Joukhadar, C. Kloft. Urea as an endogenous surrogate in human microdialysis to determine relative recovery of drugs: analytics and applications. *J Pharm Biomed Anal*, 41: 233-239 (2006).
- [49] L. Stahle, P. Arner, U. Ungerstedt. Drug distribution studies with microdialysis. III: Extracellular concentration of caffeine in adipose tissue in man. *Life Sci*, 49: 1853-1858 (1991).
- [50] C.I. Larsson. The use of an "internal standard" for control of the recovery in microdialysis. *Life Sci*, 49: L73-L78. (1991).
- [51] L. Stahle. Drug distribution studies with microdialysis: I. Tissue dependent difference in recovery between caffeine and theophylline. *Life Sci*, 49: 1835-1842 (1991).
- [52] M. Muller. Science, medicine, and the future: Microdialysis. *BMJ*, 324: 588-591 (2002).
- [53] M.A. Pfaller, D.J. Diekema. Epidemiology of invasive candidiasis: a persistent public health problem. *Clin Microbiol Rev*, 20: 133-163 (2007).
- [54] G.S. Martin, D.M. Mannino, S. Eaton, M. Moss. The epidemiology of sepsis in the United States from 1979 through 2000. *N Engl J Med*, 348: 1546-1554 (2003).
- [55] H. Wisplinghoff, T. Bischoff, S.M. Tallent, H. Seifert, R.P. Wenzel, M.B. Edmond. Nosocomial bloodstream infections in US hospitals: analysis of 24,179 cases from a prospective nationwide surveillance study. *Clin Infect Dis*, 39: 309-317 (2004).
- [56] C. Engel, F.M. Brunkhorst, H.G. Bone, R. Brunkhorst, H. Gerlach, S. Grond, M. Gruendling, G. Huhle, U. Jaschinski, S. John, K. Mayer, M. Oppert, D. Olthoff, M. Quintel, M. Ragaller, R. Rossaint, F. Stuber, N. Weiler, T. Welte, H. Bogatsch, C. Hartog, M. Loeffler, K. Reinhart. Epidemiology of sepsis in Germany: results from a national prospective multicenter study. *Intensive Care Med*, 33: 606-618 (2007).
- [57] S.J. Lin, J. Schranz, S.M. Teutsch. Aspergillosis case-fatality rate: systematic review of the literature. *Clin Infect Dis*, 32: 358-366 (2001).
- [58] M.M. McNeil, S.L. Nash, R.A. Hajjeh, M.A. Phelan, L.A. Conn, B.D. Plikaytis, D.W. Warnock. Trends in mortality due to invasive mycotic diseases in the United States, 1980-1997. *Clin Infect Dis*, 33: 641-647 (2001).
- [59] M. Borg-von Zepelin, L. Kunz, R. Ruchel, U. Reichard, M. Weig, U. Gross. Epidemiology and antifungal susceptibilities of *Candida* spp. to six antifungal agents: results from a surveillance study on fungaemia in Germany from July 2004 to August 2005. *J Antimicrob Chemother*, 60: 424-428 (2007).

- [60] A.M. Tortorano, J. Peman, H. Bernhardt, L. Klingspor, C.C. Kibbler, O. Faure, E. Biraghi, E. Canton, K. Zimmermann, S. Seaton, R. Grillot. Epidemiology of candidaemia in Europe: results of 28-month European Confederation of Medical Mycology (ECMM) hospital-based surveillance study. *Eur J Clin Microbiol Infect Dis*, 23: 317-322 (2004).
- [61] A. Upton, K.A. Kirby, P. Carpenter, M. Boeckh, K.A. Marr. Invasive aspergillosis following hematopoietic cell transplantation: outcomes and prognostic factors associated with mortality. *Clin Infect Dis*, 44: 531-540 (2007).
- [62] A.H. Groll, T.J. Walsh. Uncommon opportunistic fungi: new nosocomial threats. *Clin Microbiol Infect*, 7 Suppl 2: 8-24 (2001).
- [63] Z. Erjavec, H. Kluin-Nelemans, P.E. Verweij. Trends in invasive fungal infections, with emphasis on invasive aspergillosis. *Clin Microbiol Infect*, 15: 625-633 (2009).
- [64] M. Michallet, J.I. Ito. Approaches to the management of invasive fungal infections in hematologic malignancy and hematopoietic cell transplantation. *J Clin Oncol*, 27: 3398-3409 (2009).
- [65] M.J. Ruping, J.J. Vehreschild, O.A. Cornely. Patients at high risk of invasive fungal infections: when and how to treat. *Drugs*, 68: 1941-1962 (2008).
- [66] B. De Pauw, T.J. Walsh, J.P. Donnelly, D.A. Stevens, J.E. Edwards, T. Calandra, P.G. Pappas, J. Maertens, O. Lortholary, C.A. Kauffman, D.W. Denning, T.F. Patterson, G. Maschmeyer, J. Bille, W.E. Dismukes, R. Herbrecht, W.W. Hope, C.C. Kibbler, B.J. Kullberg, K.A. Marr, P. Munoz, F.C. Odds, J.R. Perfect, A. Restrepo, M. Ruhnke, B.H. Segal, J.D. Sobel, T.C. Sorrell, C. Viscoli, J.R. Wingard, T. Zaoutis, J.E. Bennett. Revised definitions of invasive fungal disease from the European Organization for Research and Treatment of Cancer/Invasive Fungal Infections Cooperative Group and the National Institute of Allergy and Infectious Diseases Mycoses Study Group (EORTC/MSG) Consensus Group. *Clin Infect Dis*, 46: 1813-1821 (2008).
- [67] A. Bohme, M. Ruhnke, D. Buchheidt, O.A. Cornely, H. Einsele, R. Enzensberger, H. Hebart, W. Heinz, C. Junghanss, M. Karthaus, W. Kruger, U. Krug, T. Kubin, O. Penack, D. Reichert, S. Reuter, G. Silling, T. Sudhoff, A.J. Ullmann, G. Maschmeyer. Treatment of invasive fungal infections in cancer patients - recommendations of the Infectious Diseases Working Party (AGIHO) of the German Society of Hematology and Oncology (DGHO). *Ann Hematol*, 88: 97-110 (2009).
- [68] Y. Koltin, C.A. Hitchcock. The search for new triazole antifungal agents. *Curr Opin Chem Biol*, 1: 176-182 (1997).
- [69] H.W. Boucher, A.H. Groll, C.C. Chiou, T.J. Walsh. Newer systemic antifungal agents: pharmacokinetics, safety and efficacy. *Drugs*, 64: 1997-2020 (2004).
- [70] J.L. Davis, D. Little, A.T. Bliklager, M.G. Papich. Mucosal permeability of water-soluble drugs in the equine jejunum: a preliminary investigation. *J Vet Pharmacol Ther*, 29: 379-385 (2006).
- [71] J.L. Davis, J.H. Salmon, M.G. Papich. Pharmacokinetics of voriconazole after oral and intravenous administration to horses. *Am J Vet Res*, 67: 1070-1075 (2006).
- [72] European Medicines Agency (EMA). EPARs for authorised medicinal products for human use: Voriconazole. (2007); available at <http://www.emea.europa.eu/humandocs/PDFs/EPAR/vfend/404901en6.pdf> [accessed 05 January 2010].
- [73] M. Schäfer-Korting, U. Holzgrabe. Neue Antimykotika: Ein Silberstreif am Horizont. *Pharm Unserer Zeit*, 32: 154-156 (2003).
- [74] E. Mutschler, G. Geisslinger, H. Kroemer, P. Ruth, M. Schäfer-Korting. *Mutschler Arzneimittelwirkungen*. 9 ed. Wissenschaftliche Verlagsgesellschaft, Stuttgart (2008).
- [75] Food and Drug Administration (FDA). Briefing Document for Voriconazole (2001); available at [http://www.fda.gov/ohrms/dockets/ac/01/briefing/3792b2\\_01\\_Pfizer.pdf](http://www.fda.gov/ohrms/dockets/ac/01/briefing/3792b2_01_Pfizer.pdf) [accessed 01 September 2009].
- [76] M. Ruhnke. *Pilzinfektionen bei immunsupprimierten Patienten*. 2 ed. Uni-Med Verlag, Bremen (2007).
- [77] M. Schaeffer-Kurepkat, H.C. Korting. *Voriconazol*. 2 ed. ABW Wissenschaftsverlag, Berlin (2006).

- [78] N.L. Varanasi, I. Baskaran, G.J. Alangaden, P.H. Chandrasekar, E.K. Manavathu. Novel effect of voriconazole on conidiation of *Aspergillus* species. *Int J Antimicrob Agents*, 23: 72-79 (2004).
- [79] P.E. Verweij, S.J. Howard, W.J. Melchers, D.W. Denning. Azole-resistance in *Aspergillus*: proposed nomenclature and breakpoints. *Drug Resist Updat*, 12: 141-147 (2009).
- [80] Pfizer Inc. Label. Voriconazole for injection, tablets, oral suspension: LAB-0311-5.0 (Revision 2008); available at [http://www.pfizer.com/files/products/uspi\\_vfend.pdf](http://www.pfizer.com/files/products/uspi_vfend.pdf) [accessed 27 October 2009].
- [81] U. Theuretzbacher, F. Ihle, H. Derendorf. Pharmacokinetic/pharmacodynamic profile of voriconazole. *Clin Pharmacokinet*, 45: 649-663 (2006).
- [82] E. Denes, A. Boumediene, H. Durox, A. Oksman, F. Saint-Marcoux, M.L. Darde, J.M. Gaulier. Voriconazole concentrations in synovial fluid and bone tissues. *J Antimicrob Chemother*, 59: 818-819 (2007).
- [83] E. Denes, N. Pichon, M. Debette-Gratien, B. Bouteille, J.M. Gaulier. Pharmacokinetics of voriconazole in the cerebrospinal fluid of an immunocompromised patient with a brain abscess due to *Aspergillus fumigatus*. *Clin Infect Dis*, 39: 603-604 (2004).
- [84] I. Lutsar, S. Roffey, P. Troke. Voriconazole concentrations in the cerebrospinal fluid and brain tissue of guinea pigs and immunocompromised patients. *Clin Infect Dis*, 37: 728-732 (2003).
- [85] T. Elter, M. Sieniawski, A. Gossmann, C. Wickenhauser, U. Schroder, H. Seifert, J. Kuchta, J. Burhenne, K.D. Riedel, G. Fatkenheuer, O.A. Cornely. Voriconazole brain tissue levels in rhinocerebral aspergillosis in a successfully treated young woman. *Int J Antimicrob Agents*, 28: 262-265 (2006).
- [86] S.J. Roffey, S. Cole, P. Comby, D. Gibson, S.G. Jezequel, A.N. Nedderman, D.A. Smith, D.K. Walker, N. Wood. The disposition of voriconazole in mouse, rat, rabbit, guinea pig, dog, and human. *Drug Metab Dispos*, 31: 731-741 (2003).
- [87] R. Hyland, B.C. Jones, D.A. Smith. Identification of the cytochrome P450 enzymes involved in the N-oxidation of voriconazole. *Drug Metab Dispos*, 31: 540-547 (2003).
- [88] N. Murayama, N. Imai, T. Nakane, M. Shimizu, H. Yamazaki. Roles of CYP3A4 and CYP2C19 in methyl hydroxylated and N-oxidized metabolite formation from voriconazole, a new anti-fungal agent, in human liver microsomes. *Biochem Pharmacol*, 73: 2020-2026 (2007).
- [89] S.B. Yanni, P.P. Annaert, P. Augustijns, A. Bridges, Y. Gao, D.K. Benjamin, Jr., D.R. Thakker. Role of flavin-containing monooxygenase in oxidative metabolism of voriconazole by human liver microsomes. *Drug Metab Dispos*, 36: 1119-1125 (2008).
- [90] Y. Ikeda, K. Umemura, K. Kondo, K. Sekiguchi, S. Miyoshi, M. Nakashima. Pharmacokinetics of voriconazole and cytochrome P450 2C19 genetic status. *Clin Pharmacol Ther*, 75: 587-588 (2004).
- [91] L.B. Johnson, C.A. Kauffman. Voriconazole: a new triazole antifungal agent. *Clin Infect Dis*, 36: 630-637 (2003).
- [92] Central Research Division Pfizer Inc. Compound data sheet. Voriconazole (2006).
- [93] Tepnel Scientific Services. Certificate of analysis. Daptomycin (2006).
- [94] Central Research Division Pfizer Inc. Compound data sheet. Linezolid (2006).
- [95] CMA Microdialysis AB. Product note CMA 60 (2005); available at [http://www.microdialysis.se/public/file.php?REF=f9b902fc3289af4dd08de5d1de54f68f&art=325&FILE\\_ID=20070627160256\\_1\\_1.pdf](http://www.microdialysis.se/public/file.php?REF=f9b902fc3289af4dd08de5d1de54f68f&art=325&FILE_ID=20070627160256_1_1.pdf) [accessed 08 October 2009].
- [96] CMA Microdialysis AB. Product note CMA 70 (2005); available at [http://www.microdialysis.se/public/file.php?REF=b3967a0e938dc2a6340e258630febd5a&art=334&FILE\\_ID=20070628093649\\_1\\_1.pdf](http://www.microdialysis.se/public/file.php?REF=b3967a0e938dc2a6340e258630febd5a&art=334&FILE_ID=20070628093649_1_1.pdf) [accessed 08 October 2009].
- [97] CMA Microdialysis AB. Product note CMA 66 (2007); available at [http://www.microdialysis.se/public/file.php?REF=3ad7c2ebb96fcb7cda0cf54a2e802f5&art=333&FILE\\_ID=20071029135928\\_1\\_2.pdf](http://www.microdialysis.se/public/file.php?REF=3ad7c2ebb96fcb7cda0cf54a2e802f5&art=333&FILE_ID=20071029135928_1_2.pdf) [accessed 08 October 2009].
- [98] H. Fakhrai-Rad, N. Pourmand, M. Ronaghi. Pyrosequencing: an accurate detection platform for single nucleotide polymorphisms. *Hum Mutat*, 19: 479-485 (2002).

- [99] D.M. Saunte, F. Simmel, N. Frimodt-Moller, L.B. Stolle, E.L. Svejgaard, M. Haedersdal, C. Kloft, M.C. Arendrup. In vivo efficacy and pharmacokinetics of voriconazole in an animal model of dermatophytosis. *Antimicrob Agents Chemother*, 51: 3317-3321 (2007).
- [100] F. Simmel, J. Soukup, A. Zoerner, J. Radke, C. Kloft. Development and validation of an efficient HPLC method for quantification of voriconazole in plasma and microdialysate reflecting an important target site. *Anal Bioanal Chem*, 392: 479-488 (2008).
- [101] Food and Drug Administration (FDA). Guidance for Industry. Bioanalytical Method Validation (2001); available at <http://www.fda.gov/downloads/Drugs/GuidanceComplianceRegulatoryInformation/Guidances/UCM070107.pdf> [accessed 27 October 2009].
- [102] International Conference on Harmonisation (ICH). ICH Harmonised Tripartite Guideline: Validation of Analytical Procedures: Text and Methodology Q2(R1) (2005); available at <http://www.ich.org/LOB/media/MEDIA417.pdf> [accessed 30 October 2009].
- [103] V.P. Shah, K.K. Midha, J.W. Findlay, H.M. Hill, J.D. Hulse, I.J. McGilveray, G. McKay, K.J. Miller, R.N. Patnaik, M.L. Powell, A. Tonelli, C.T. Viswanathan, A. Yacobi. Bioanalytical method validation - a revisit with a decade of progress. *Pharm Res*, 17: 1551-1557 (2000).
- [104] R.L. Bertholf, R.E. Winecker (Eds.). *Chromatographic methods in clinical chemistry and toxicology*. 1 ed. John Wiley & Sons, Ltd, West Sussex (2007).
- [105] *United States Pharmacopeia (USP)*. 26 ed. United States Pharmacopeial Convention, Rockville (2003).
- [106] C. Buerger, C. Joukhadar, M. Muller, C. Kloft. Development of a liquid chromatography method for the determination of linezolid and its application to in vitro and human microdialysis samples. *J Chromatogr B Analyt Technol Biomed Life Sci*, 796: 155-164. (2003).
- [107] N. Plock, C. Buerger, C. Kloft. Successful management of discovered pH dependence in vancomycin recovery studies: novel HPLC method for microdialysis and plasma samples. *Biomed Chromatogr*, 19: 237-244 (2005).
- [108] World Medical Association. Declaration of Helsinki - Ethical Principles for Medical Research Involving Human Subjects (1964, amended October 2008 in Seoul by the 59th WMA General Assembly); available at <http://www.wma.net/en/30publications/10policies/b3/index.html> [accessed 27 October 2009].
- [109] S. Beal, L. Sheiner. *NONMEM Users Guides*. University of California, San Francisco (1998).
- [110] J. Gabrielsson, D. Weiner. *Pharmacokinetic and Pharmacodynamic Data Analysis: Concepts and Applications*. Apotekarsocieteten (Swedish Pharmaceutical Society), Stockholm (2000).
- [111] *WinNonlin help guide*. Pharsight Corporation, (2008).
- [112] M. Brett, H.J. Weimann, W. Cawello, H. Zimmermann, G. Pabst, B. Sierakowski, R. Gieschke, A. Baumann. *Parameters for Compartment-free Pharmacokinetics-Standardisation of Study Design, Data Analysis and Reporting*. Shaker-Verlag, Aachen (1999).
- [113] S. Pfeifer, P. Pfliegel, H.H. Borchert. *Biopharmazie: Pharmakokinetik, Bioverfügbarkeit, Biotransformation*. 3 ed. Ullstein/Mosby, Berlin/Wiesbaden (1995).
- [114] C. Scheerans, H. Derendorf, C. Kloft. Proposal for a standardised identification of the mono-exponential terminal phase for orally administered drugs. *Biopharm Drug Dispos*, 29: 145-157 (2008).
- [115] Food and Drug Administration (FDA). Guidance for Industry - Bioavailability and Bioequivalence Studies for Orally Administered Drug Products - General Considerations (2003); available at <http://www.fda.gov/downloads/Drugs/GuidanceComplianceRegulatoryInformation/Guidances/UCM070124.pdf> [accessed 27 October 2009].
- [116] J. Werner. *Biomathematik und Medizinische Statistik*. 2 ed. Urban und Schwarzenberg, München (1992).
- [117] N. Jonsson, M.O. Karlsson. *Xpose 2.0 User's Manual*. Department of Pharmacy, Uppsala University, Sweden, (1998).

- [118] A.M. Almeida, M.M. Castel-Branco, A.C. Falcao. Linear regression for calibration lines revisited: weighting schemes for bioanalytical methods. *J Chromatogr B Analyt Technol Biomed Life Sci*, 774: 215-222 (2002).
- [119] *Wissenschaftliche Tabellen Geigy: Physikalische Chemie, Blut, Humangenetik, Stoffwechsel von Xenobiotika*. 8 ed. CIBA-GEIGY AG, Basel (1979).
- [120] G. Schrimpf (Ed.). *Gentechnische Methoden*. 3 ed. Spektrum, Akad. Verl., Heidelberg (2002).
- [121] E.N. Jonsson, J.R. Wade, M.O. Karlsson. Comparison of some practical sampling strategies for population pharmacokinetic studies. *J Pharmacokinet Biopharm*, 24: 245-263 (1996).
- [122] S. Cheng, F. Qiu, J. Huang, J. He. Development and validation of a simple and rapid HPLC method for the quantitative determination of voriconazole in rat and beagle dog plasma. *J Chromatogr Sci*, 45: 409-414 (2007).
- [123] S. Chhun, E. Rey, A. Tran, O. Lortholary, G. Pons, V. Jullien. Simultaneous quantification of voriconazole and posaconazole in human plasma by high-performance liquid chromatography with ultra-violet detection. *J Chromatogr B Analyt Technol Biomed Life Sci*, 852: 223-228 (2007).
- [124] R. Gage, D.A. Stopher. A rapid HPLC assay for voriconazole in human plasma. *J Pharm Biomed Anal*, 17: 1449-1453 (1998).
- [125] X.J. Kang, L.Q. Chen, Y.Y. Zhang, Y.W. Liu, Z.Z. Gu. Performance of electrospun nanofibers for SPE of drugs from aqueous solutions. *J Sep Sci*, 31: 3272-3278 (2008).
- [126] G. Khoschsorur, F. Fruehwirth, S. Zelzer. Isocratic high-performance liquid chromatographic method with ultraviolet detection for simultaneous determination of levels of voriconazole and itraconazole and its hydroxy metabolite in human serum. *Antimicrob Agents Chemother*, 49: 3569-3571 (2005).
- [127] L.J. Langman, F. Boakye-Agyeman. Measurement of voriconazole in serum and plasma. *Clin Biochem*, 40: 1378-1385 (2007).
- [128] S. Nakagawa, R. Suzuki, R. Yamazaki, Y. Kusuhara, S. Mitsumoto, H. Kobayashi, S. Shimoeda, S. Ohta, S. Yamato. Determination of the antifungal agent voriconazole in human plasma using a simple column-switching high-performance liquid chromatography and its application to a pharmacokinetic study. *Chem Pharm Bull (Tokyo)*, 56: 328-331 (2008).
- [129] A. Pascual, V. Nieth, T. Calandra, J. Bille, S. Bolay, L.A. Decosterd, T. Buclin, P.A. Majcherczyk, D. Sanglard, O. Marchetti. Variability of voriconazole plasma levels measured by new high-performance liquid chromatography and bioassay methods. *Antimicrob Agents Chemother*, 51: 137-143 (2007).
- [130] F. Pehourcq, C. Jarry, B. Bannwarth. Direct injection HPLC micro method for the determination of voriconazole in plasma using an internal surface reversed-phase column. *Biomed Chromatogr*, 18: 719-722 (2004).
- [131] G.J. Pennick, M. Clark, D.A. Sutton, M.G. Rinaldi. Development and validation of a high-performance liquid chromatography assay for voriconazole. *Antimicrob Agents Chemother*, 47: 2348-2350 (2003).
- [132] S. Perea, G.J. Pennick, A. Modak, A.W. Fothergill, D.A. Sutton, D.J. Sheehan, M.G. Rinaldi. Comparison of high-performance liquid chromatographic and microbiological methods for determination of voriconazole levels in plasma. *Antimicrob Agents Chemother*, 44: 1209-1213 (2000).
- [133] D.A. Stopher, R. Gage. Determination of a new antifungal agent, voriconazole, by multi-dimensional high-performance liquid chromatography with direct plasma injection onto a size-exclusion column. *J Chromatogr B Biomed Sci Appl*, 691: 441-448 (1997).
- [134] M. Wenk, A. Droll, S. Krahenbuhl. Fast and reliable determination of the antifungal drug voriconazole in plasma using monolithic silica rod liquid chromatography. *J Chromatogr B Analyt Technol Biomed Life Sci*, 832: 313-316 (2006).
- [135] B.V. Araujo, D.J. Conrado, E.C. Palma, T. Dalla Costa. Validation of rapid and simple LC-MS/MS method for determination of voriconazole in rat plasma. *J Pharm Biomed Anal*, 44: 985-990 (2007).

- [136] H. Egle, R. Trittler, A. Konig, K. Kummerer. Fast, fully automated analysis of voriconazole from serum by LC-LC-ESI-MS-MS with parallel column-switching technique. *J Chromatogr B Analyt Technol Biomed Life Sci*, 814: 361-367 (2005).
- [137] B.G. Keevil, S. Newman, S. Lockhart, S.J. Howard, C.B. Moore, D.W. Denning. Validation of an assay for voriconazole in serum samples using liquid chromatography-tandem mass spectrometry. *Ther Drug Monit*, 26: 650-657 (2004).
- [138] M. Vogeser, X. Schiel, U. Spohrer. Quantification of voriconazole in plasma by liquid chromatography-tandem mass spectrometry. *Clin Chem Lab Med*, 43: 730-734 (2005).
- [139] L. Zhou, R.D. Glickman, N. Chen, W.E. Sponsel, J.R. Graybill, K.W. Lam. Determination of voriconazole in aqueous humor by liquid chromatography-electrospray ionization-mass spectrometry. *J Chromatogr B Analyt Technol Biomed Life Sci*, 776: 213-220 (2002).
- [140] S.E. Cook, T.C. Pinkerton. Characterization of internal surface reversed-phase silica supports for liquid chromatography. *J Chromatogr*, 368: 233-248 (1986).
- [141] I.H. Hagestam, T.C. Pinkerton. Production of "internal surface reversed-phase" supports: the hydrolysis of selected substrates from silica using chymotrypsin. *J Chromatogr*, 368: 77-84 (1986).
- [142] E. Yamamoto, K. Murata, Y. Ishihama, N. Asakawa. Methylcellulose-immobilized reversed-phase precolumn for direct analysis of drugs in plasma by HPLC. *Anal Sci*, 17: 1155-1159 (2001).
- [143] A. Espinel-Ingroff, E. Johnson, H. Hockey, P. Troke. Activities of voriconazole, itraconazole and amphotericin B in vitro against 590 moulds from 323 patients in the voriconazole Phase III clinical studies. *J Antimicrob Chemother*, 61: 616-620 (2008).
- [144] F. Sabatelli, R. Patel, P.A. Mann, C.A. Mendrick, C.C. Norris, R. Hare, D. Loebenberg, T.A. Black, P.M. McNicholas. In vitro activities of posaconazole, fluconazole, itraconazole, voriconazole, and amphotericin B against a large collection of clinically important molds and yeasts. *Antimicrob Agents Chemother*, 50: 2009-2015 (2006).
- [145] C.A. Griffith, L.J. Owen, R. Body, G. McDowell, B.G. Keevil. Development of a method to measure plasma and whole blood choline by liquid chromatography tandem mass spectrometry. *Ann Clin Biochem*, 47: 56-61 (2010).
- [146] Y.X. Huang, G.H. Xie, Z.M. Zhou, X.M. Sun, Y.L. Wang. Determination of artemether in plasma and whole blood using HPLC with flow-through polarographic detection. *Biomed Chromatogr*, 2: 53-56 (1987).
- [147] E. Pussard, N. Guigueno, O. Adam, J.F. Giudicelli. Validation of HPLC-amperometric detection to measure serotonin in plasma, platelets, whole blood, and urine. *Clin Chem*, 42: 1086-1091 (1996).
- [148] P.P. Rop, M. Bresson, J. Antoine, J. Spinazzola, M. Fornaris, A. Viala. Quantitation and ultraviolet spectrum identification of buflomedil in whole blood and plasma by HPLC. *J Anal Toxicol*, 14: 18-21 (1990).
- [149] S. Henry de Hassonville, P. Chiap, J.F. Liegeois, B. Evrard, L. Delattre, J. Crommen, G. Piel, P. Hubert. Development and validation of a high-performance liquid chromatographic method for the determination of cyproterone acetate in human skin. *J Pharm Biomed Anal*, 36: 133-143 (2004).
- [150] J.P. Laugier, C. Surber, H. Bun, J.M. Geiger, K.P. Wilhelm, A. Durand, H.I. Maibach. Determination of acitretin in the skin, in the suction blister, and in plasma of human volunteers after multiple oral dosing. *J Pharm Sci*, 83: 623-628 (1994).
- [151] T.E. Murdter, B. Sperker, K. Bosslet, P. Fritz, H.K. Kroemer. Simultaneous high-performance liquid chromatographic determination of a glucuronyl prodrug of doxorubicin, doxorubicin and its metabolites in human lung tissue. *J Chromatogr B Biomed Sci Appl*, 709: 289-295 (1998).
- [152] P.C. Panus, B. Tober-Meyer, K.E. Ferslew. Tissue extraction and high-performance liquid chromatographic determination of ketoprofen enantiomers. *J Chromatogr B Biomed Sci Appl*, 705: 295-302 (1998).



- [153] G. De Groot, B.C. Tepas, G. Storm. High-performance liquid chromatographic determination of doxorubicin in tissues after solid phase extraction. *J Pharm Biomed Anal*, 6: 927-932 (1988).
- [154] J. Faergemann, H. Laufen. Levels of fluconazole in serum, stratum corneum, epidermis-dermis (without stratum corneum) and eccrine sweat. *Clin Exp Dermatol*, 18: 102-106 (1993).
- [155] S. Sobue, K. Sekiguchi, T. Nabeshima. Intracutaneous distributions of fluconazole, itraconazole, and griseofulvin in Guinea pigs and binding to human stratum corneum. *Antimicrob Agents Chemother*, 48: 216-223 (2004).
- [156] P. Abrahamsson, O. Winso. An assessment of calibration and performance of the microdialysis system. *J Pharm Biomed Anal*, 39: 730-734 (2005).
- [157] M. Lindberger, T. Tomson, S. Lars. Microdialysis sampling of carbamazepine, phenytoin and phenobarbital in subcutaneous extracellular fluid and subdural cerebrospinal fluid in humans: an in vitro and in vivo study of adsorption to the sampling device. *Pharmacol Toxicol*, 91: 158-165 (2002).
- [158] H. Zheng, L.F. Shi, J.H. Hu. Assessment of in vitro and in vivo recovery of sinomenine using microdialysis. *Skin Res Technol*, 13: 323-329 (2007).
- [159] J.A. Stenken, E.M. Topp, M.Z. Southard, C.E. Lunte. Examination of microdialysis sampling in a well-characterized hydrodynamic system. *Anal Chem*, 65: 2324-2328 (1993).
- [160] J.A. Stenken. Methods and issues in microdialysis calibration. *Anal Chim Acta*, 379: 337-358 (1999).
- [161] L. Groth. Cutaneous microdialysis. Methodology and validation. *Acta Derm Venereol Suppl (Stockh)*, 197: 1-61 (1996).
- [162] C.S. Chaurasia, M. Muller, E.D. Bashaw, E. Benfeldt, J. Bolinder, R. Bullock, P.M. Bungay, E.C. DeLange, H. Derendorf, W.F. Elmquist, M. Hammarlund-Udenaes, C. Joukhadar, D.L. Kellogg, Jr., C.E. Lunte, C.H. Nordstrom, H. Rollema, R.J. Sawchuk, B.W. Cheung, V.P. Shah, L. Stahle, U. Ungerstedt, D.F. Welty, H. Yeo. AAPS-FDA Workshop White Paper: microdialysis principles, application, and regulatory perspectives. *J Clin Pharmacol*, 47: 589-603 (2007).
- [163] V.J. Schuck, I. Rinas, H. Derendorf. In vitro microdialysis sampling of docetaxel. *J Pharm Biomed Anal*, 36: 807-813 (2004).
- [164] W.J. Loos, W.C. Zamboni, F.K. Engels, P. de Bruijn, M.H. Lam, R. de Wit, J. Verweij, E.A. Wiemer. Pitfalls of the application of microdialysis in clinical oncology: controversial findings with docetaxel. *J Pharm Biomed Anal*, 45: 288-294 (2007).
- [165] C. Carneheim, L. Stahle. Microdialysis of lipophilic compounds: a methodological study. *Pharmacol Toxicol*, 69: 378-380 (1991).
- [166] S. Bielecka-Grzela, A. Klimowicz. Application of cutaneous microdialysis to evaluate metronidazole and its main metabolite concentrations in the skin after a single oral dose. *J Clin Pharm Ther*, 28: 465-469 (2003).
- [167] S. Bielecka-Grzela, A. Klimowicz. Penetration of ciprofloxacin and its desethylenemetabolite into skin in humans after a single oral dose of the parent drug assessed by cutaneous microdialysis. *J Clin Pharm Ther*, 30: 383-390 (2005).
- [168] C. Buerger, N. Plock, P. Dehghanyar, C. Joukhadar, C. Kloft. Pharmacokinetics of unbound linezolid in plasma and tissue interstitium of critically ill patients after multiple dosing using microdialysis. *Antimicrob Agents Chemother*, 50: 2455-2463 (2006).
- [169] B.X. Mayer, M. Petsch, E.M. Tschernko, M. Muller. Strategies for the determination of cefazolin in plasma and microdialysis samples by short-end capillary zone electrophoresis. *Electrophoresis*, 24: 1215-1220 (2003).
- [170] M. Petsch, B.X. Mayer-Helm, R. Sauermann, C. Joukhadar, E. Kenndler. Capillary electrophoresis analysis of fosfomicin in biological fluids for clinical pharmacokinetic studies. *Electrophoresis*, 25: 2292-2298 (2004).
- [171] Y. Kurosaki, S. Nakamura, Y. Shiojiri, H. Kawasaki. Lipo-microdialysis: a new microdialysis method for studying the pharmacokinetics of lipophilic substances. *Biol Pharm Bull*, 21: 194-196 (1998).

- [172] B.V. Araujo, C.F. Silva, S.E. Haas, T. Dalla Costa. Microdialysis as a tool to determine free kidney levels of voriconazole in rodents: a model to study the technique feasibility for a moderately lipophilic drug. *J Pharm Biomed Anal*, 47: 876-881 (2008).
- [173] P. Kallinteri, S.G. Antimisiaris. Solubility of drugs in the presence of gelatin: effect of drug lipophilicity and degree of ionization. *Int J Pharm*, 221: 219-226 (2001).
- [174] F.X. Mathy, D. Ntivunwa, R.K. Verbeeck, V. Preat. Fluconazole distribution in rat dermis following intravenous and topical application: a microdialysis study. *J Pharm Sci*, 94: 770-780 (2005).
- [175] H. Yang, Q. Wang, W.F. Elmquist. Fluconazole distribution to the brain: a crossover study in freely-moving rats using in vivo microdialysis. *Pharm Res*, 13: 1570-1575 (1996).
- [176] C.H. Lee, P.H. Yeh, T.H. Tsai. Hepatobiliary excretion of fluconazole and its interaction with cyclosporin A in rat blood and bile using microdialysis. *Int J Pharm*, 241: 367-373 (2002).
- [177] L. Sasongko, K.M. Williams, R.O. Day, A.J. McLachlan. Human subcutaneous tissue distribution of fluconazole: comparison of microdialysis and suction blister techniques. *Br J Clin Pharmacol*, 56: 551-561 (2003).
- [178] H. Benveniste, A.J. Hansen, N.S. Ottosen. Determination of brain interstitial concentrations by microdialysis. *J Neurochem*, 52: 1741-1750 (1989).
- [179] H. Benveniste, P.C. Huttemeier. Microdialysis - theory and application. *Prog Neurobiol*, 35: 195-215 (1990).
- [180] L. Groth, A. Jorgensen. In vitro microdialysis of hydrophilic and lipophilic compounds. *Anal Chim Acta*, 355: 75-83 (1997).
- [181] W.F. Elmquist, R.J. Sawchuk. Application of microdialysis in pharmacokinetic studies. *Pharm Res*, 14: 267-288 (1997).
- [182] H. Wiig, R.K. Reed, O. Tenstad. Interstitial fluid pressure, composition of interstitium, and interstitial exclusion of albumin in hypothyroid rats. *Am J Physiol Heart Circ Physiol*, 278: H1627-1639 (2000).
- [183] A. Kim, L.A. Suecof, C.A. Sutherland, L. Gao, J.L. Kutl, D.P. Nicolau. In vivo microdialysis study of the penetration of daptomycin into soft tissues in diabetic versus healthy volunteers. *Antimicrob Agents Chemother*, 52: 3941-3946 (2008).
- [184] V.J. Stella, Q. He. Cyclodextrins. *Toxicol Pathol*, 36: 30-42 (2008).
- [185] R.A. Rajewski, V.J. Stella. Pharmaceutical applications of cyclodextrins. 2. In vivo drug delivery. *J Pharm Sci*, 85: 1142-1169 (1996).
- [186] A.N. Khramov, J.A. Stenzen. Enhanced microdialysis recovery of some tricyclic antidepressants and structurally related drugs by cyclodextrin-mediated transport. *Analyst*, 124: 1027-1033 (1999).
- [187] C. Joukhadar, C. Thallinger, W. Poppl, F. Kovar, K.H. Konz, S.M. Joukhadar, F. Traunmuller. Concentrations of voriconazole in healthy and inflamed lung in rats. *Antimicrob Agents Chemother*, 53: 2684-2686 (2009).
- [188] B.V. de Araujo, C.F. da Silva, S.E. Haas, T. Dalla Costa. Free renal levels of voriconazole determined by microdialysis in healthy and *Candida* sp.-infected Wistar rats. *Int J Antimicrob Agents*, 33: 154-159 (2009).
- [189] R. Bellmann, G. Kuchling, P. Dehghanyar, M. Zeitlinger, E. Minar, B.X. Mayer, M. Muller, C. Joukhadar. Tissue pharmacokinetics of levofloxacin in human soft tissue infections. *Br J Clin Pharmacol*, 57: 563-568 (2004).
- [190] C. Joukhadar, H. Stass, U. Muller-Zellenberg, E. Lackner, F. Kovar, E. Minar, M. Muller. Penetration of moxifloxacin into healthy and inflamed subcutaneous adipose tissues in humans. *Antimicrob Agents Chemother*, 47: 3099-3103 (2003).
- [191] R. Sauermann, G. Delle-Karth, C. Marsik, I. Steiner, M. Zeitlinger, B.X. Mayer-Helm, A. Georgopoulos, M. Muller, C. Joukhadar. Pharmacokinetics and pharmacodynamics of cefpirome in subcutaneous adipose tissue of septic patients. *Antimicrob Agents Chemother*, 49: 650-655 (2005).

- [192] R. Sauermann, M. Müller, C. Joukhadar. Penetration von Antibiotika in das schwer erreichbare Kompartiment. *Chemotherapie Journal*, 3: 74-78 (2005).
- [193] L. Romani, F. Bistoni, P. Puccetti. Adaptation of *Candida albicans* to the host environment: the role of morphogenesis in virulence and survival in mammalian hosts. *Curr Opin Microbiol*, 6: 338-343 (2003).
- [194] S. Ballesta, I. Garcia, E.J. Perea, A. Pascual. Uptake and intracellular activity of voriconazole in human polymorphonuclear leucocytes. *J Antimicrob Chemother*, 55: 785-787 (2005).
- [195] L. Purkins, N. Wood, K. Greenhalgh, M.J. Allen, S.D. Oliver. Voriconazole, a novel wide-spectrum triazole: oral pharmacokinetics and safety. *Br J Clin Pharmacol*, 56 Suppl 1: 10-16 (2003).
- [196] A. Wildfeuer, J. Faergemann, H. Laufen, G. Pfaff, T. Zimmermann, H.P. Seidl, P. Lach. Bio-availability of fluconazole in the skin after oral medication. *Mycoses*, 37: 127-130 (1994).
- [197] C. Nicholson, E. Sykova. Extracellular space structure revealed by diffusion analysis. *Trends Neurosci*, 21: 207-215 (1998).
- [198] J.W. Mouton, U. Theuretzbacher, W.A. Craig, P.M. Tulkens, H. Derendorf, O. Cars. Tissue concentrations: do we ever learn? *J Antimicrob Chemother*, 61: 235-237 (2008).
- [199] B. Fernandez-Torres, A.J. Carrillo, E. Martin, A. Del Palacio, M.K. Moore, A. Valverde, M. Serrano, J. Guarro. In vitro activities of 10 antifungal drugs against 508 dermatophyte strains. *Antimicrob Agents Chemother*, 45: 2524-2528 (2001).
- [200] S. Perea, A.W. Fothergill, D.A. Sutton, M.G. Rinaldi. Comparison of in vitro activities of voriconazole and five established antifungal agents against different species of dermatophytes using a broth macrodilution method. *J Clin Microbiol*, 39: 385-388 (2001).
- [201] EUCAST Technical Note on voriconazole. *Clin Microbiol Infect*, 14: 985-987 (2008).
- [202] D. Andes, K. Marchillo, T. Stamstad, R. Conklin. In vivo pharmacodynamics of a new triazole, ravuconazole, in a murine candidiasis model. *Antimicrob Agents Chemother*, 47: 1193-1199 (2003).
- [203] D. Andes, M. van Ogtrop. Characterization and quantitation of the pharmacodynamics of fluconazole in a neutropenic murine disseminated candidiasis infection model. *Antimicrob Agents Chemother*, 43: 2116-2120 (1999).
- [204] A. Louie, G.L. Drusano, P. Banerjee, Q.F. Liu, W. Liu, P. Kaw, M. Shayegani, H. Taber, M.H. Miller. Pharmacodynamics of fluconazole in a murine model of systemic candidiasis. *Antimicrob Agents Chemother*, 42: 1105-1109 (1998).
- [205] J.H. Rex, M.A. Pfaller, J.N. Galgiani, M.S. Bartlett, A. Espinel-Ingroff, M.A. Ghannoum, M. Lancaster, F.C. Odds, M.G. Rinaldi, T.J. Walsh, A.L. Barry. Development of interpretive breakpoints for antifungal susceptibility testing: conceptual framework and analysis of in vitro-in vivo correlation data for fluconazole, itraconazole, and candida infections. Subcommittee on Antifungal Susceptibility Testing of the National Committee for Clinical Laboratory Standards. *Clin Infect Dis*, 24: 235-247 (1997).
- [206] T.E. Rogers, J.N. Galgiani. Activity of fluconazole (UK 49,858) and ketoconazole against *Candida albicans* in vitro and in vivo. *Antimicrob Agents Chemother*, 30: 418-422 (1986).
- [207] J.W. Van t Wout, H. Mattie, R. van Furth. Comparison of the efficacies of amphotericin B, fluconazole, and itraconazole against a systemic *Candida albicans* infection in normal and neutropenic mice. *Antimicrob Agents Chemother*, 33: 147-151 (1989).
- [208] D. Andes, K. Marchillo, T. Stamstad, R. Conklin. In vivo pharmacokinetics and pharmacodynamics of a new triazole, voriconazole, in a murine candidiasis model. *Antimicrob Agents Chemother*, 47: 3165-3169 (2003).
- [209] P. Arner, J. Bolinder. Microdialysis of adipose tissue. *J Intern Med*, 230: 381-386 (1991).
- [210] F.A. Baumeister, B. Rolinski, R. Busch, P. Emmrich. Glucose monitoring with long-term subcutaneous microdialysis in neonates. *Pediatrics*, 108: 1187-1192 (2001).

- [211] J. Bolinder, U. Ungerstedt, P. Arner. Microdialysis measurement of the absolute glucose concentration in subcutaneous adipose tissue allowing glucose monitoring in diabetic patients. *Diabetologia*, 35: 1177-1180 (1992).
- [212] J. Bolinder, U. Ungerstedt, P. Arner. Long-term continuous glucose monitoring with microdialysis in ambulatory insulin-dependent diabetic patients. *Lancet*, 342: 1080-1085 (1993).
- [213] A. Edsander-Nord, J. Rojdmarm, M. Wickman. Metabolism in pedicled and free TRAM flaps: a comparison using the microdialysis technique. *Plast Reconstr Surg*, 109: 664-673 (2002).
- [214] Y. Hashiguchi, M. Sakakida, K. Nishida, T. Uemura, K. Kajiwara, M. Shichiri. Development of a miniaturized glucose monitoring system by combining a needle-type glucose sensor with microdialysis sampling method. Long-term subcutaneous tissue glucose monitoring in ambulatory diabetic patients. *Diabetes Care*, 17: 387-396 (1994).
- [215] U. Hildingsson, H. Sellden, U. Ungerstedt, C. Marcus. Microdialysis for metabolic monitoring in neonates after surgery. *Acta Paediatr*, 85: 589-594 (1996).
- [216] A. Holzinger, W. Bonfig, B. Kusser, T. Eggermann, H. Muller, H.G. Munch. Use of long-term microdialysis subcutaneous glucose monitoring in the management of neonatal diabetes. A first case report. *Biol Neonate*, 89: 88-91 (2006).
- [217] M. Horal, U. Ungerstedt, B. Persson, M. Westgren, C. Marcus. Metabolic adaptation in IUGR neonates determined with microdialysis - a pilot study. *Early Hum Dev*, 42: 1-14 (1995).
- [218] H.L. Lutgers, L.M. Hullegie, K. Hoogenberg, W.J. Sluiter, R.P. Dullaart, K.J. Wientjes, A.J. Schoonen. Microdialysis measurement of glucose in subcutaneous adipose tissue up to three weeks in type 1 diabetic patients. *Neth J Med*, 57: 7-12 (2000).
- [219] L. Persson, J. Valtysson, P. Enblad, P.E. Warme, K. Cesarini, A. Lewen, L. Hillered. Neurochemical monitoring using intracerebral microdialysis in patients with subarachnoid hemorrhage. *J Neurosurg*, 84: 606-616 (1996).
- [220] L. Hillered, J. Valtysson, P. Enblad, L. Persson. Interstitial glycerol as a marker for membrane phospholipid degradation in the acutely injured human brain. *J Neurol Neurosurg Psychiatry*, 64: 486-491 (1998).
- [221] P.J. Hutchinson, M.T. O'Connell, L.B. Maskell, J.D. Pickard. Monitoring by subcutaneous microdialysis in neurosurgical intensive care. *Acta Neurochir Suppl*, 75: 57-59 (1999).
- [222] M.J. During, I. Fried, P. Leone, A. Katz, D.D. Spencer. Direct measurement of extracellular lactate in the human hippocampus during spontaneous seizures. *J Neurochem*, 62: 2356-2361 (1994).
- [223] C. Kennergren, V. Mantovani, P. Lonroth, B. Nystrom, E. Berglin, A. Hamberger. Monitoring of extracellular aspartate aminotransferase and troponin T by microdialysis during and after cardioplegic heart arrest. *Cardiology*, 92: 162-170 (1999).
- [224] I.R. Konings, F.K. Engels, S. Sleijfer, J. Verweij, E.A. Wiemer, W.J. Loos. Application of prolonged microdialysis sampling in carboplatin-treated cancer patients. *Cancer Chemother Pharmacol*, 64: 509-516 (2009).
- [225] D.J. Kopacz, C.M. Bernards, H.W. Allen, C. Landau, P. Nandy, D. Wu, P.G. Lacouture. A model to evaluate the pharmacokinetic and pharmacodynamic variables of extended-release products using in vivo tissue microdialysis in humans: bupivacaine-loaded microcapsules. *Anesth Analg*, 97: 124-131 (2003).
- [226] L. Stahle, C. Alm, B. Ekquist, B. Lundquist, T. Tomson. Monitoring free extracellular valproic acid by microdialysis in epileptic patients. *Ther Drug Monit*, 18: 14-18 (1996).
- [227] M. Lindberger, T. Tomson, L. Stahle. Validation of microdialysis sampling for subcutaneous extracellular valproic acid in humans. *Ther Drug Monit*, 20: 358-362 (1998).
- [228] P. Dehghanyar, C. Burger, M. Zeitlinger, F. Islinger, F. Kovar, M. Muller, C. Kloft, C. Joukhadar. Penetration of linezolid into soft tissues of healthy volunteers after single and multiple doses. *Antimicrob Agents Chemother*, 49: 2367-2371 (2005).
- [229] R. Gattringer, E. Urbauer, F. Traunmuller, M. Zeitlinger, P. Dehghanyar, P. Zeleny, W. Graninger, M. Muller, C. Joukhadar. Pharmacokinetics of telithromycin in plasma and soft tissues after

- single-dose administration to healthy volunteers. *Antimicrob Agents Chemother*, 48: 4650-4653 (2004).
- [230] A.M. Persky, M. Muller, H. Derendorf, M. Grant, G.A. Brazeau, G. Hochhaus. Single- and multiple-dose pharmacokinetics of oral creatine. *J Clin Pharmacol*, 43: 29-37 (2003).
- [231] F. Traunmuller, M. Fille, C. Thallinger, C. Joukhadar. Multiple-dose pharmacokinetics of telithromycin in peripheral soft tissues. *Int J Antimicrob Agents*, 34: 72-75 (2009).
- [232] F. Traunmuller, M. Zeitlinger, P. Zeleny, M. Muller, C. Joukhadar. Pharmacokinetics of single- and multiple-dose oral clarithromycin in soft tissues determined by microdialysis. *Antimicrob Agents Chemother*, 51: 3185-3189 (2007).
- [233] M. Romkes, M.B. Faletto, J.A. Blaisdell, J.L. Raucy, J.A. Goldstein. Cloning and expression of complementary DNAs for multiple members of the human cytochrome P450IIC subfamily. *Biochemistry*, 30: 3247-3255 (1991).
- [234] P.G. Zaphiropoulos. RNA molecules containing exons originating from different members of the cytochrome P450 2C gene subfamily (CYP2C) in human epidermis and liver. *Nucleic Acids Res*, 27: 2585-2590 (1999).
- [235] S.M. De Morais, G.R. Wilkinson, J. Blaisdell, U.A. Meyer, K. Nakamura, J.A. Goldstein. Identification of a new genetic defect responsible for the polymorphism of (S)-mephenytoin metabolism in Japanese. *Mol Pharmacol*, 46: 594-598 (1994).
- [236] S.M. de Morais, G.R. Wilkinson, J. Blaisdell, K. Nakamura, U.A. Meyer, J.A. Goldstein. The major genetic defect responsible for the polymorphism of S-mephenytoin metabolism in humans. *J Biol Chem*, 269: 15419-15422 (1994).
- [237] H.G. Xie, R.B. Kim, A.J. Wood, C.M. Stein. Molecular basis of ethnic differences in drug disposition and response. *Annu Rev Pharmacol Toxicol*, 41: 815-850 (2001).
- [238] P.J. Wedlund. The CYP2C19 enzyme polymorphism. *Pharmacology*, 61: 174-183 (2000).
- [239] R.J. Ferguson, S.M. De Morais, S. Benhamou, C. Bouchardy, J. Blaisdell, G. Ibeanu, G.R. Wilkinson, T.C. Sarich, J.M. Wright, P. Dayer, J.A. Goldstein. A new genetic defect in human CYP2C19: mutation of the initiation codon is responsible for poor metabolism of S-mephenytoin. *J Pharmacol Exp Ther*, 284: 356-361 (1998).
- [240] G.C. Ibeanu, J. Blaisdell, B.I. Ghanayem, C. Beyeler, S. Benhamou, C. Bouchardy, G.R. Wilkinson, P. Dayer, A.K. Daly, J.A. Goldstein. An additional defective allele, CYP2C19\*5, contributes to the S-mephenytoin poor metabolizer phenotype in Caucasians. *Pharmacogenetics*, 8: 129-135 (1998).
- [241] G.C. Ibeanu, J.A. Goldstein, U. Meyer, S. Benhamou, C. Bouchardy, P. Dayer, B.I. Ghanayem, J. Blaisdell. Identification of new human CYP2C19 alleles (CYP2C19\*6 and CYP2C19\*2B) in a Caucasian poor metabolizer of mephenytoin. *J Pharmacol Exp Ther*, 286: 1490-1495 (1998).
- [242] G.C. Ibeanu, J. Blaisdell, R.J. Ferguson, B.I. Ghanayem, K. Brosen, S. Benhamou, C. Bouchardy, G.R. Wilkinson, P. Dayer, J.A. Goldstein. A novel transversion in the intron 5 donor splice junction of CYP2C19 and a sequence polymorphism in exon 3 contribute to the poor metabolizer phenotype for the anticonvulsant drug S-mephenytoin. *J Pharmacol Exp Ther*, 290: 635-640 (1999).
- [243] J.A. Goldstein. Clinical relevance of genetic polymorphisms in the human CYP2C subfamily. *Br J Clin Pharmacol*, 52: 349-355 (2001).
- [244] T. Shimizu, H. Ochiai, F. Asell, H. Shimizu, R. Saitoh, Y. Hama, J. Katada, M. Hashimoto, H. Matsui, K. Taki, T. Kaminuma, M. Yamamoto, Y. Aida, A. Ohashi, N. Ozawa. Bioinformatics research on inter-racial difference in drug metabolism I. Analysis on frequencies of mutant alleles and poor metabolizers on CYP2D6 and CYP2C19. *Drug Metab Pharmacokinet*, 18: 48-70 (2003).
- [245] J. Blaisdell, H. Mohrenweiser, J. Jackson, S. Ferguson, S. Coulter, B. Chanas, T. Xi, B. Ghanayem, J.A. Goldstein. Identification and functional characterization of new potentially defective alleles of human CYP2C19. *Pharmacogenetics*, 12: 703-711 (2002).

- [246] H. Fukushima-Uesaka, Y. Saito, K. Maekawa, S. Ozawa, R. Hasegawa, H. Kajio, N. Kuzuya, K. Yasuda, M. Kawamoto, N. Kamatani, K. Suzuki, T. Yanagawa, M. Tohkin, J. Sawada. Genetic variations and haplotypes of CYP2C19 in a Japanese population. *Drug Metab Pharmacokinet*, 20: 300-307 (2005).
- [247] S.J. Lee, W.Y. Kim, H. Kim, J.H. Shon, S.S. Lee, J.G. Shin. Identification of new CYP2C19 variants exhibiting decreased enzyme activity in the metabolism of S-mephenytoin and omeprazole. *Drug Metab Dispos*, 37: 2262-2269 (2009).
- [248] A. Matimba, J. Del-Favero, C. Van Broeckhoven, C. Masimirembwa. Novel variants of major drug-metabolising enzyme genes in diverse African populations and their predicted functional effects. *Hum Genomics*, 3: 169-190 (2009).
- [249] J. Morita, K. Kobayashi, A. Wanibuchi, M. Kimura, S. Irie, T. Ishizaki, K. Chiba. A novel single nucleotide polymorphism (SNP) of the CYP2C19 gene in a Japanese subject with lowered capacity of mephobarbital 4'-hydroxylation. *Drug Metab Pharmacokinet*, 19: 236-238 (2004).
- [250] I. Rudberg, B. Mohebi, M. Hermann, H. Refsum, E. Molden. Impact of the ultrarapid CYP2C19\*17 allele on serum concentration of escitalopram in psychiatric patients. *Clin Pharmacol Ther*, 83: 322-327 (2008).
- [251] S.C. Sim, C. Risinger, M.L. Dahl, E. Aklillu, M. Christensen, L. Bertilsson, M. Ingelman-Sundberg. A common novel CYP2C19 gene variant causes ultrarapid drug metabolism relevant for the drug response to proton pump inhibitors and antidepressants. *Clin Pharmacol Ther*, 79: 103-113 (2006).
- [252] Q. Zhou, X.M. Yu, H.B. Lin, L. Wang, Q.Z. Yun, S.N. Hu, D.M. Wang. Genetic polymorphism, linkage disequilibrium, haplotype structure and novel allele analysis of CYP2C19 and CYP2D6 in Han Chinese. *Pharmacogenomics J*, 9: 380-394 (2009).
- [253] Z. Desta, X. Zhao, J.G. Shin, D.A. Flockhart. Clinical significance of the cytochrome P450 2C19 genetic polymorphism. *Clin Pharmacokinet*, 41: 913-958 (2002).
- [254] Human Cytochrome P450 (CYP) Allele Nomenclature Committee. CYP2C9 allele nomenclature (2009); available at <http://www.cypalleles.ki.se/cyp2c9.htm> [accessed 31 August 2009].
- [255] C.L. Crespi, V.P. Miller. The R144C change in the CYP2C9\*2 allele alters interaction of the cytochrome P450 with NADPH: cytochrome P450 oxidoreductase. *Pharmacogenetics*, 7: 203-210 (1997).
- [256] C.R. Lee, J.A. Goldstein, J.A. Pieper. Cytochrome P450 2C9 polymorphisms: a comprehensive review of the in-vitro and human data. *Pharmacogenetics*, 12: 251-263 (2002).
- [257] T.H. Sullivan-Klose, B.I. Ghanayem, D.A. Bell, Z.Y. Zhang, L.S. Kaminsky, G.M. Shenfield, J.O. Miners, D.J. Birkett, J.A. Goldstein. The role of the CYP2C9-Leu359 allelic variant in the tolbutamide polymorphism. *Pharmacogenetics*, 6: 341-349 (1996).
- [258] G.R. Wilkinson. Drug metabolism and variability among patients in drug response. *N Engl J Med*, 352: 2211-2221 (2005).
- [259] L. Purkins, N. Wood, P. Ghahramani, D. Kleinermans, G. Layton, D. Nichols. No clinically significant effect of erythromycin or azithromycin on the pharmacokinetics of voriconazole in healthy male volunteers. *Br J Clin Pharmacol*, 56 Suppl 1: 30-36 (2003).
- [260] Human Cytochrome P450 (CYP) Allele Nomenclature Committee. Allele nomenclature for Cytochrome P450 enzymes (2009); available at <http://www.cypalleles.ki.se/> [accessed 31 August 2009].
- [261] Y. Nivoix, D. Leveque, R. Herbrecht, J.C. Koffel, L. Beretz, G. Ubeaud-Sequier. The enzymatic basis of drug-drug interactions with systemic triazole antifungals. *Clin Pharmacokinet*, 47: 779-792 (2008).
- [262] G. Mikus, V. Schowel, M. Drzewinska, J. Rengelshausen, R. Ding, K.D. Riedel, J. Burhenne, J. Weiss, T. Thomsen, W.E. Haefeli. Potent cytochrome P450 2C19 genotype-related interaction between voriconazole and the cytochrome P450 3A4 inhibitor ritonavir. *Clin Pharmacol Ther*, 80: 126-135 (2006).

- [263] M.J. Geist, G. Egerer, J. Burhenne, G. Mikus. Safety of voriconazole in a patient with CYP2C9\*2/CYP2C9\*2 genotype. *Antimicrob Agents Chemother*, 50: 3227-3228 (2006).
- [264] J. Weiss, M.M. Ten Hoevel, J. Burhenne, I. Walter-Sack, M.M. Hoffmann, J. Rengelshausen, W.E. Haefeli, G. Mikus. CYP2C19 genotype is a major factor contributing to the highly variable pharmacokinetics of voriconazole. *J Clin Pharmacol*, 49: 196-204 (2009).
- [265] J. Soukup, F. Simmel, U. Götze, S. Schneider, C. Kloft. „Therapeutic Drug Monitoring“ während Voriconazol-Sequenztherapie - Eine prospektive Studie bei intensivmedizinischen Patienten. 9. Deutscher Interdisziplinärer Kongress für Intensivmedizin und Notfallrettung (DIVI). Hamburg (2008).
- [266] G.A. Wetzstein. Intravenous to oral (iv:po) anti-infective conversion therapy. *Cancer Control*, 7: 170-176 (2000).
- [267] Pfizer Inc. Label. Voriconazole for injection, tablets, oral suspension: LAB-0271-12 (2005); available at [http://www.pfizer.com/files/products/uspi\\_vfend.pdf](http://www.pfizer.com/files/products/uspi_vfend.pdf) [accessed 19 February 2008].
- [268] L. Purkins, N. Wood, D. Kleinermans, K. Greenhalgh, D. Nichols. Effect of food on the pharmacokinetics of multiple-dose oral voriconazole. *Br J Clin Pharmacol*, 56 Suppl 1: 17-23 (2003).
- [269] E.S. Dodds Ashley, A.K. Zaas, A.F. Fang, B. Damle, J.R. Perfect. Comparative pharmacokinetics of voriconazole administered orally as either crushed or whole tablets. *Antimicrob Agents Chemother*, 51: 877-880 (2007).
- [270] L. Purkins, N. Wood, P. Ghahramani, K. Greenhalgh, M.J. Allen, D. Kleinermans. Pharmacokinetics and safety of voriconazole following intravenous- to oral-dose escalation regimens. *Antimicrob Agents Chemother*, 46: 2546-2553 (2002).
- [271] P. Liu, G. Foster, K. Gandelman, R.R. LaBadie, M.J. Allison, M.J. Gutierrez, A. Sharma. Steady-state pharmacokinetic and safety profiles of voriconazole and ritonavir in healthy male subjects. *Antimicrob Agents Chemother*, 51: 3617-3626 (2007).
- [272] P. Liu, G. Foster, R. Labadie, E. Somoza, A. Sharma. Pharmacokinetic interaction between voriconazole and methadone at steady state in patients on methadone therapy. *Antimicrob Agents Chemother*, 51: 110-118 (2007).
- [273] P. Liu, G. Foster, R.R. LaBadie, M.J. Gutierrez, A. Sharma. Pharmacokinetic interaction between voriconazole and efavirenz at steady state in healthy male subjects. *J Clin Pharmacol*, 48: 73-84 (2008).
- [274] L. Purkins, N. Wood, P. Ghahramani, E.R. Love, M.D. Eve, A. Fielding. Coadministration of voriconazole and phenytoin: pharmacokinetic interaction, safety, and toleration. *Br J Clin Pharmacol*, 56 Suppl 1: 37-44 (2003).
- [275] L. Purkins, N. Wood, D. Kleinermans, E.R. Love. No clinically significant pharmacokinetic interactions between voriconazole and indinavir in healthy volunteers. *Br J Clin Pharmacol*, 56 Suppl 1: 62-68 (2003).
- [276] L. Purkins, N. Wood, D. Kleinermans, D. Nichols. Histamine H<sub>2</sub>-receptor antagonists have no clinically significant effect on the steady-state pharmacokinetics of voriconazole. *Br J Clin Pharmacol*, 56 Suppl 1: 51-55 (2003).
- [277] J. Rengelshausen, M. Banfield, K.D. Riedel, J. Burhenne, J. Weiss, T. Thomsen, I. Walter-Sack, W.E. Haefeli, G. Mikus. Opposite effects of short-term and long-term St John's wort intake on voriconazole pharmacokinetics. *Clin Pharmacol Ther*, 78: 25-33 (2005).
- [278] L. Purkins, N. Wood, K. Greenhalgh, M.D. Eve, S.D. Oliver, D. Nichols. The pharmacokinetics and safety of intravenous voriconazole - a novel wide-spectrum antifungal agent. *Br J Clin Pharmacol*, 56 Suppl 1: 2-9 (2003).
- [279] G. Wang, H.P. Lei, Z. Li, Z.R. Tan, D. Guo, L. Fan, Y. Chen, D.L. Hu, D. Wang, H.H. Zhou. The CYP2C19 ultra-rapid metabolizer genotype influences the pharmacokinetics of voriconazole in healthy male volunteers. *Eur J Clin Pharmacol*, 65: 281-285 (2009).
- [280] A. Pascual, T. Calandra, S. Bolay, T. Buclin, J. Bille, O. Marchetti. Voriconazole therapeutic drug monitoring in patients with invasive mycoses improves efficacy and safety outcomes. *Clin Infect Dis*, 46: 201-211 (2008).

- [281] J. Smith, N. Safdar, V. Knasinski, W. Simmons, S.M. Bhavnani, P.G. Ambrose, D. Andes. Voriconazole therapeutic drug monitoring. *Antimicrob Agents Chemother*, 50: 1570-1572 (2006).
- [282] D.W. Denning, P. Ribaud, N. Milpied, D. Caillot, R. Herbrecht, E. Thiel, A. Haas, M. Ruhnke, H. Lode. Efficacy and safety of voriconazole in the treatment of acute invasive aspergillosis. *Clin Infect Dis*, 34: 563-571 (2002).
- [283] C. Csajka, A. Pascual, S. Bolay S, J. Bille, T. Calandra, O. Marchetti, T. Buclin. Population Pharmacokinetics and Effect of Voriconazole in Adults Patients for Concentrations Profile Optimization. Meeting of the Population Approach Group in Europe (PAGE). St. Petersburg, Russia (2009).
- [284] J.A. Goldstein, S.M. de Morais. Biochemistry and molecular biology of the human CYP2C subfamily. *Pharmacogenetics*, 4: 285-299 (1994).
- [285] T. Niwa, T. Shiraga, A. Takagi. Effect of antifungal drugs on cytochrome P450 (CYP) 2C9, CYP2C19, and CYP3A4 activities in human liver microsomes. *Biol Pharm Bull*, 28: 1805-1808 (2005).
- [286] V.V. Hynninen, K.T. Olkkola, L. Bertilsson, K.J. Kurkinen, T. Korhonen, P.J. Neuvonen, K. Laine. Voriconazole increases while itraconazole decreases plasma meloxicam concentrations. *Antimicrob Agents Chemother*, 53: 587-592 (2009).
- [287] European Medicines Agency (EMA). EPARs for authorised medicinal products for human use: Voriconazole (2007); available at <http://www.emea.europa.eu/humandocs/PDFs/EPAR/vfend/404901en6.pdf> [accessed 01 September 2009].
- [288] P.J. Wedlund, G.R. Wilkinson. In vivo and in vitro measurement of CYP2C19 activity. *Methods Enzymol*, 272: 105-114 (1996).
- [289] P.H. Dunselman, B. Edgar. Felodipine clinical pharmacokinetics. *Clin Pharmacokinet*, 21: 418-430 (1991).
- [290] C. Ekhardt, V.D. Doodeman, S. Rodenhuis, P.H. Smits, J.H. Beijnen, A.D. Huitema. Influence of polymorphisms of drug metabolizing enzymes (CYP2B6, CYP2C9, CYP2C19, CYP3A4, CYP3A5, GSTA1, GSTP1, ALDH1A1 and ALDH3A1) on the pharmacokinetics of cyclophosphamide and 4-hydroxycyclophosphamide. *Pharmacogenet Genomics*, 18: 515-523 (2008).
- [291] A. Henningsson, S. Marsh, W.J. Loos, M.O. Karlsson, A. Garsa, K. Mross, S. Mielke, L. Vigano, A. Locatelli, J. Verweij, A. Sparreboom, H.L. McLeod. Association of CYP2C8, CYP3A4, CYP3A5, and ABCB1 polymorphisms with the pharmacokinetics of paclitaxel. *Clin Cancer Res*, 11: 8097-8104 (2005).
- [292] L. Groth, J. Serup. Cutaneous microdialysis in man: effects of needle insertion trauma and anaesthesia on skin perfusion, erythema and skin thickness. *Acta Derm Venereol*, 78: 5-9 (1998).
- [293] C. Anderson, T. Andersson, R.G. Andersson. In vivo microdialysis estimation of histamine in human skin. *Skin Pharmacol*, 5: 177-183 (1992).
- [294] M.K. Church, T.J. Griffiths, S. Jeffery, L.C. Ravell, A.S. Cowburn, A.P. Sampson, G.F. Clough. Are cysteinyl leukotrienes involved in allergic responses in human skin? *Clin Exp Allergy*, 32: 1013-1019 (2002).
- [295] L.J. Petersen, P.S. Skov, C. Bindslev-Jensen, J. Sondergaard. Histamine release in immediate-type hypersensitivity reactions in intact human skin measured by microdialysis. A preliminary study. *Allergy*, 47: 635-637 (1992).
- [296] P.C. Huttemeier, Y. Kamiyama, M. Su, W.D. Watkins, H. Benveniste. Microdialysis measurements of PGD<sub>2</sub>, TXB<sub>2</sub> and 6-KETO-PGF<sub>1</sub> alpha in rat CA1 hippocampus during transient cerebral ischemia. *Prostaglandins*, 45: 177-187 (1993).
- [297] H. Langberg, D. Skovgaard, M. Karamouzis, J. Bulow, M. Kjaer. Metabolism and inflammatory mediators in the peritendinous space measured by microdialysis during intermittent isometric exercise in humans. *J Physiol*, 515: 919-927 (1999).
- [298] F. Sjogren, C. Anderson. Sterile trauma to normal human dermis invariably induces IL1beta, IL6 and IL8 in an innate response to "danger". *Acta Derm Venereol*, 89: 459-465 (2009).



- [299] L. Waelgaard, A. Pharo, T.I. Tonnessen, T.E. Mollnes. Microdialysis for monitoring inflammation: efficient recovery of cytokines and anaphylotoxins provided optimal catheter pore size and fluid velocity conditions. *Scand J Immunol*, 64: 345-352 (2006).
- [300] J.H. Lin. Tissue distribution and pharmacodynamics: a complicated relationship. *Curr Drug Metab*, 7: 39-65 (2006).
- [301] S. Marchand, M. Chenel, I. Lamarche, W. Couet. Pharmacokinetic modeling of free amoxicillin concentrations in rat muscle extracellular fluids determined by microdialysis. *Antimicrob Agents Chemother*, 49: 3702-3706 (2005).
- [302] C. Dahyot, S. Marchand, G.L. Pessini, C. Pariat, B. Debaene, W. Couet, O. Mimoz. Microdialysis study of imipenem distribution in skeletal muscle and lung extracellular fluids of *Acinetobacter baumannii*-infected rats. *Antimicrob Agents Chemother*, 50: 2265-2267 (2006).
- [303] J.L. Crandon, M.A. Banevicus, A.F. Fang, P.H. Crownover, R.F. Knauft, J.S. Pope, J.H. Russomanno, E. Shore, D.P. Nicolau, J.L. Kuti. Bronchopulmonary Disposition of Intravenous Voriconazole and Anidulafungin Given in Combination to Healthy Adults. *Antimicrob Agents Chemother*, 53: 5102-5107 (2009).
- [304] B. Capitano, B.A. Potoski, S. Husain, S. Zhang, D.L. Paterson, S.M. Studer, K.R. McCurry, R. Venkataramanan. Intrapulmonary penetration of voriconazole in patients receiving an oral prophylactic regimen. *Antimicrob Agents Chemother*, 50: 1878-1880 (2006).
- [305] S. Schwartz, E. Thiel. Update on the treatment of cerebral aspergillosis. *Ann Hematol*, 83 Suppl 1: S42-44 (2004).
- [306] U. Theuretzbacher. Tissue penetration of antibacterial agents: how should this be incorporated into pharmacodynamic analyses? *Curr Opin Pharmacol*, 7: 498-504 (2007).
- [307] T.F. Patterson, W.R. Kirkpatrick, M. White, J.W. Hiemenz, J.R. Wingard, B. Dupont, M.G. Rinaldi, D.A. Stevens, J.R. Graybill. Invasive aspergillosis. Disease spectrum, treatment practices, and outcomes. I3 Aspergillus Study Group. *Medicine (Baltimore)*, 79: 250-260 (2000).
- [308] N. Singh, D.L. Paterson. Aspergillus infections in transplant recipients. *Clin Microbiol Rev*, 18: 44-69 (2005).
- [309] B. Spellberg. Novel insights into disseminated candidiasis: pathogenesis research and clinical experience converge. *PLoS Pathog*, 4: e38 (2008).
- [310] The Geraldine Kaminski Medical Mycology Library/Doctorfungus Corporation. The Fungi. Image Bank: *Candida albicans* and *Aspergillus fumigatus* (2003); available at <http://www.doctorfungus.org/imageban/> [accessed 27 October 2009].
- [311] D. Honeybourne. Antibiotic penetration in the respiratory tract and implications for the selection of antimicrobial therapy. *Curr Opin Pulm Med*, 3: 170-174 (1997).
- [312] D.E. Nix. Intrapulmonary concentrations of antimicrobial agents. *Infect Dis Clin North Am*, 12: 631-646 (1998).
- [313] P.L. Haslam, R.P. Baughman. Report of ERS Task Force: guidelines for measurement of acellular components and standardization of BAL. *Eur Respir J*, 14: 245-248 (1999).
- [314] O. Ibrahim-Granet, B. Philippe, H. Boleti, E. Boisvieux-Ulrich, D. Grenet, M. Stern, J.P. Latge. Phagocytosis and intracellular fate of *Aspergillus fumigatus* conidia in alveolar macrophages. *Infect Immun*, 71: 891-903 (2003).
- [315] J.A. Wasylnka, A.H. Hissen, A.N. Wan, M.M. Moore. Intracellular and extracellular growth of *Aspergillus fumigatus*. *Med Mycol*, 43 Suppl 1: S27-30 (2005).
- [316] M. Zeitlinger, M. Muller, C. Joukhadar. Lung microdialysis - a powerful tool for the determination of exogenous and endogenous compounds in the lower respiratory tract (mini-review). *AAPS J*, 7: E600-608 (2005).
- [317] M.A. Zeitlinger, F. Traunmuller, A. Abraham, M.R. Muller, Z. Erdogan, M. Muller, C. Joukhadar. A pilot study testing whether concentrations of levofloxacin in interstitial space fluid of soft tissues may serve as a surrogate for predicting its pharmacokinetics in lung. *Int J Antimicrob Agents*, 29: 44-50 (2007).

- [318] G. Dimopoulos, M. Piagnerelli, J. Berre, B. Eddafali, I. Salmon, J.L. Vincent. Disseminated aspergillosis in intensive care unit patients: an autopsy study. *J Chemother*, 15: 71-75 (2003).
- [319] K. Keven, S. Sengul, O. Memikoglu, Z. Soypacaci, E. Ustuner, A. Cakmak, B. Erbay. Fatal outcome of disseminated invasive aspergillosis in kidney allograft recipients. *Med Mycol*, 46: 713-717 (2008).
- [320] N.S. Raja, N.N. Singh. Disseminated invasive aspergillosis in an apparently immunocompetent host. *J Microbiol Immunol Infect*, 39: 73-77 (2006).
- [321] N.J. Barrios, M.E. Echevarria, R. Velez. Successful treatment of disseminated Aspergillosis in a leukemic child. *P R Health Sci J*, 24: 157-160 (2005).
- [322] A.E. Boyd, S. Modi, S.J. Howard, C.B. Moore, B.G. Keevil, D.W. Denning. Adverse reactions to voriconazole. *Clin Infect Dis*, 39: 1241-1244 (2004).
- [323] R.J. Bruggemann, J.P. Donnelly, R.E. Aarnoutse, A. Warris, N.M. Blijlevens, J.W. Mouton, P.E. Verweij, D.M. Burger. Therapeutic drug monitoring of voriconazole. *Ther Drug Monit*, 30: 403-411 (2008).
- [324] M.J. Geist, G. Egerer, J. Burhenne, K.D. Riedel, G. Mikus. Induction of voriconazole metabolism by rifampin in a patient with acute myeloid leukemia: importance of interdisciplinary communication to prevent treatment errors with complex medications. *Antimicrob Agents Chemother*, 51: 3455-3456 (2007).
- [325] M.L. Goodwin, R.H. Drew. Antifungal serum concentration monitoring: an update. *J Antimicrob Chemother*, 61: 17-25 (2008).
- [326] W.W. Hope, E.M. Billaud, J. Lestner, D.W. Denning. Therapeutic drug monitoring for triazoles. *Curr Opin Infect Dis*, 21: 580-586 (2008).
- [327] A. Imhof, D.J. Schaer, U. Schanz, U. Schwarz. Neurological adverse events to voriconazole: evidence for therapeutic drug monitoring. *Swiss Med Wkly*, 136: 739-742 (2006).
- [328] R.E. Lewis. What is the "therapeutic range" for voriconazole? *Clin Infect Dis*, 46: 212-214 (2008).
- [329] K. Matsumoto, K. Ikawa, K. Abematsu, N. Fukunaga, K. Nishida, T. Fukamizu, Y. Shimodozono, N. Morikawa, Y. Takeda, K. Yamada. Correlation between voriconazole trough plasma concentration and hepatotoxicity in patients with different CYP2C19 genotypes. *Int J Antimicrob Agents*, 34: 91-94 (2009).
- [330] F. Pea, P. Viale. Hallucinations during voriconazole therapy: who is at higher risk and could benefit from therapeutic drug monitoring? *Ther Drug Monit*, 31: 135-136 (2009).
- [331] B.A. Potoski, J. Brown. The safety of voriconazole. *Clin Infect Dis*, 35: 1273-1275 (2002).
- [332] S. Trifilio, R. Ortiz, G. Pennick, A. Verma, J. Pi, V. Stosor, T. Zembower, J. Mehta. Voriconazole therapeutic drug monitoring in allogeneic hematopoietic stem cell transplant recipients. *Bone Marrow Transplant*, 35: 509-513 (2005).
- [333] S. Trifilio, G. Pennick, J. Pi, J. Zook, M. Golf, K. Kaniecki, S. Singhal, S. Williams, J. Winter, M. Tallman, L. Gordon, O. Frankfurt, A. Evens, J. Mehta. Monitoring plasma voriconazole levels may be necessary to avoid subtherapeutic levels in hematopoietic stem cell transplant recipients. *Cancer*, 109: 1532-1535 (2007).
- [334] S.M. Trifilio, P.R. Yarnold, M.H. Scheetz, J. Pi, G. Pennick, J. Mehta. Serial plasma voriconazole concentrations after allogeneic hematopoietic stem cell transplantation. *Antimicrob Agents Chemother*, 53: 1793-1796 (2009).
- [335] D.I. Zonios, J. Gea-Banacloche, R. Childs, J.E. Bennett. Hallucinations during voriconazole therapy. *Clin Infect Dis*, 47: e7-e10 (2008).
- [336] I. Lutsar, M.R. Hodges, K. Tomaszewski, P.F. Troke, N.D. Wood. Safety of voriconazole and dose individualization. *Clin Infect Dis*, 36: 1087-1088 (2003).
- [337] K. Tan, N. Brayshaw, K. Tomaszewski, P. Troke, N. Wood. Investigation of the potential relationships between plasma voriconazole concentrations and visual adverse events or liver function test abnormalities. *J Clin Pharmacol*, 46: 235-243 (2006).

- [338] J.W. Mouton. *Use of Pharmacodynamics to Guide Therapeutic Drug Monitoring*. Interscience Conference on Antimicrobial Agents and Chemotherapy. San Francisco (2009).
- [339] M.H. Ensom, T.K. Chang, P. Patel. Pharmacogenetics: the therapeutic drug monitoring of the future? *Clin Pharmacokinet*, 40: 783-802 (2001).
- [340] W.A. Craig. Pharmacokinetic/pharmacodynamic parameters: rationale for antibacterial dosing of mice and men. *Clin Infect Dis*, 26: 1-10 (1998).
- [341] J.W. Mouton, M.N. Dudley, O. Cars, H. Derendorf, G.L. Drusano. Standardization of pharmacokinetic/pharmacodynamic (PK/PD) terminology for anti-infective drugs: an update. *J Antimicrob Chemother*, 55: 601-607 (2005).
- [342] A. Dalhoff. *What are the best antibacterial endpoints to use in pharmacokinetic/pharmacodynamic models?* Interscience Conference on Antimicrobial Agents and Chemotherapy. San Francisco (2009).
- [343] A. Dalhoff, P.G. Ambrose, J.W. Mouton. A long journey from minimum inhibitory concentration testing to clinically predictive breakpoints: deterministic and probabilistic approaches in deriving breakpoints. *Infection*, 37: 296-305 (2009).
- [344] J.W. Mouton, A.A. Vinks. Relationship between minimum inhibitory concentration and stationary concentration revisited: growth rates and minimum bactericidal concentrations. *Clin Pharmacokinet*, 44: 767-768 (2005).
- [345] C.H. Nightingale. Future in vitro and animal studies: development of pharmacokinetic and pharmacodynamic efficacy predictors for tissue-based antibiotics. *Pharmacotherapy*, 25: 146S-149S (2005).
- [346] L.M. Boak, J. Li, C.R. Rayner, R.L. Nation. Pharmacokinetic/pharmacodynamic factors influencing emergence of resistance to linezolid in an in vitro model. *Antimicrob Agents Chemother*, 51: 1287-1292 (2007).
- [347] V.H. Tam, M. Nikolaou. Mathematical modelling of resistance emergence. *J Antimicrob Chemother*, 56: 983 (2005).
- [348] V.H. Tam, A.N. Schilling, S. Neshat, K. Poole, D.A. Melnick, E.A. Coyle. Optimization of meropenem minimum concentration/MIC ratio to suppress in vitro resistance of *Pseudomonas aeruginosa*. *Antimicrob Agents Chemother*, 49: 4920-4927 (2005).
- [349] A. Baltch, D. Lawrence, W. Ritz, N. Andersen, L. Bopp, R. Smith. *Modulation by Anidulafungin and Voriconazole, Singly and in Combination, of Cytokine Production by Human Monocytes Infected with Candida glabrata and by Uninfected Monocytes*. Interscience Conference on Antimicrobial Agents and Chemotherapy. San Francisco (2009).
- [350] X. Ao, J.A. Stenken. Microdialysis sampling of cytokines. *Methods*, 38: 331-341 (2006).
- [351] G.F. Clough. Microdialysis of large molecules. *AAPS J*, 7: E686-692 (2005).



---

## 7 APPENDIX

### 7.1 Tables

**Tab. 7-1:** Inclusion criteria, exclusion criteria, and reasons for withdrawal for study volunteers.

---

#### **Inclusion criteria for healthy volunteers**

Healthy males aged between 18 and 50 years

Body mass index (BMI) between 20 and 28 kg/m<sup>2</sup>

No regular concomitant (topical or systemic) medication within the last four weeks prior to the start of the trial

Written informed consent given by volunteers, i.e., after being provided with detailed information about the nature, risks, and scope of the clinical study as well as the expected desirable and adverse effects of the drug

No legal incapacity and/or other circumstances rendering the individual unable to understand the nature, scope and possible consequences of the study

---

#### **Exclusion criteria for healthy volunteers**

Known allergy or hypersensitivity against study drug or drug class

Participation in another clinical study within the last six weeks prior to study

Blood donation within the last four weeks prior to study

Administration of live or killed virus or bacteria vaccines within 14 days prior to study

Alcohol or drug abuse

Abuse of nicotine

History of severe allergic or anaphylactic reactions to any medication

History of or ongoing optic dysfunction (all volunteers had to undergo mandatory testing at screening)

Ongoing bacterial, viral, fungal, or atypical mycobacterial infection

Presence of malignancy within the past five years, including lymphoproliferative disorders

History of or ongoing hepatic cirrhosis regardless of cause or severity

History of or ongoing hospital admission for cardiac disease, stroke, or pulmonary disease within the last five years

History of or ongoing symptoms for blood coagulation disorders

Seropositivity for human immunodeficiency virus (HIV), all volunteers had to undergo mandatory testing at screening

Seropositivity for hepatitis B or C virus (HepB antigen, HepC antibody), all volunteers had to undergo testing at screening

Clinically significant thrombocytopenia, bleeding disorders, or a platelet count < 50,000/ $\mu$ L

White blood count (WBC) count <3,000/L or >14,000/L, all volunteers had to undergo mandatory testing at screening

Hepatic enzymes (aspartate aminotransferase (ASAT), alanine aminotransferase (ALAT), alkaline phosphatase (AP), gamma-glutamyltranspeptidase ( $\gamma$ -GTP), lactate dehydrogenase (LDH)) and bilirubin three times the upper limit of normal, all volunteers had to undergo mandatory testing at screening

Serum creatinine two times the upper limit of normal, all volunteers had to undergo mandatory testing at screening

Abnormalities in electrocardiogram (ECG) that were considered clinically relevant, all volunteers had to undergo mandatory testing at screening

Unreliability and/or lack of cooperation

Other objections to participate in the study in the opinion of the investigator

---

#### **Reasons for withdrawal**

Unreliability and/or lack of cooperation

Signs of clinically relevant illness that might hamper the performance of the study according to the protocol or the evaluation of the primary and/or secondary outcome variables

Alcohol or drug abuse

Other objections to participate in the study in the opinion of the investigator

---

**Tab. 7-2:** Lifestyle restrictions.

---

**Lifestyle restrictions**

Consumption of any food or drinks (except water) for about 2 h before oral drug administration

Intake of concomitant medication except in case of emergency or treatment of AEs

Smoking

Intake of alcohol or grapefruit juice from 24 h before until end of the study

Excessive intake of coffee, tea and any other food containing xanthines (i.e., coke, chocolate etc.)

---

Tab. 7-3: Study schedule.

	Screening visit	Study day 1		Study day 2		Study day 3		Study day 4	Final examination
		Visit 1	Visit 2	Visit 3	Visit 4	Visit 5	Visit 6	Visit 7	
Written informed consent	X								
Demographics <sup>1</sup>	X								
Medical history, concomitant diseases	X								
Physical examination	X								X
ECG, eye examination	X								X
Genotype sample	X								
Weight, BMI	X	X <sup>17</sup>				X <sup>17</sup>			X <sup>17</sup>
Vital signs <sup>2</sup>	X	X		X		X		X	X
Drug history <sup>3</sup>	X	X							
Virology <sup>4</sup>	X								
Drug screening in urine	X								
Urinalysis	X								X
Coagulation test	X								X
Clinical chemistry/haematology	X								X
Inclusion/Exclusion criteria	X								
<b>Procedures before administration</b>									
Concomitant medication		X	X	X	X	X	X	X	
Food intake within 2 h prior to p.o. administration						X	X	X	
Insertion of catheters		X						X <sup>16</sup>	
<i>In vivo</i> calibration of catheters		X <sup>6</sup>		X <sup>7</sup>			X <sup>8,9</sup>	X <sup>8,10</sup>	
<b>Administration of Vfend<sup>®</sup> i.v.</b>		X <sup>11</sup>	X <sup>11</sup>	X <sup>12</sup>	X <sup>12</sup>				
<b>Administration of Vfend<sup>®</sup> p.o.</b>						X <sup>13</sup>	X <sup>13</sup>	X <sup>13</sup>	
<b>Plasma for PK</b>		X <sup>14</sup>	X <sup>15</sup>	X <sup>15</sup>	X <sup>15</sup>	X <sup>14</sup>		X <sup>14</sup>	
<b>Microdialysate for PK<sup>5</sup></b>		X <sup>14</sup>	X <sup>15</sup>	X <sup>15</sup>	X <sup>15</sup>	X <sup>14</sup>		X <sup>14</sup>	
<b>AE (adverse event) monitoring</b>		X	X	X	X	X	X	X	X

<sup>1</sup>Initials, birth date, height (HT). <sup>2</sup>Before drug administration: blood pressure (BP), heart rate (HR), temperature. <sup>3</sup>Volunteer must not have taken any drugs during the last 14 days (except paracetamol, max. 1.5 g/d). <sup>4</sup>Testing for HIV and Hepatitis B. <sup>5</sup>Also for potentially influencing local factors. <sup>6</sup>Pre-equilibration, RR Sampling, Post-equilibration. <sup>7</sup>RR Sampling, Post-equilibration. <sup>8</sup>RR Sampling. <sup>9</sup>before 6<sup>th</sup> administration. <sup>10</sup>12 h after 7<sup>th</sup> administration. <sup>11</sup>Vfend<sup>®</sup> Loading dose (iv): 6 mg/kg over 120 min. <sup>12</sup>Vfend<sup>®</sup> Maintenance dose (iv): 4 mg/kg over 80 min. <sup>13</sup>Vfend<sup>®</sup> Maintenance dose (po): 200 mg. <sup>14</sup>Extensive sampling (except RSS Visit 5: no sampling). <sup>15</sup>ESS: Sparse sampling; RSS: no sampling of  $\mu$ D (except Visit 2). <sup>16</sup>Only RSS. <sup>17</sup>Only weight.

**Tab. 7-4:** Data items in the dataset.

Data items	Unit	Item description
ID	-	Individual identification No.
OID	-	Original identification code for individual
CMT	-	Assignment of compartment
<i>Time related items</i>		
TIME	h	Relative time after start of first drug administration
TIPL	h	Relative time planned after start of first drug administration
TALD	h	Relative time planned after start of most recent drug administration
VISI	-	Study visit No.
OCC	-	Data belonging to one administration (dosing record and all observations)
DAY	day	Study day
<i>Dose related data items</i>		
AMT	mg	Administered amount of drug
RATE	mg/h	Infusion rate normalised to amount administered in 1 h
DOS1	mg	Total dose administered in one ID
DOS2	mg	Last dose administered in one ID
<i>Dependent variable item</i>		
DV	µg/mL	Dependent variable (measured or transformed voriconazole concentrations)
<i>Flags for data items</i>		
EVID	-	Identification No. of event (0: observation event (only DV observation), 1: dosing event)
ADMA	-	Administered formulation (0: no administration, 1: solution i.v. (infusion (6/4mg voriconazole/kgWT), 2: tablet p.o. (200 mg voriconazole))
FLDV	-	Identifier for different types of records (0: dosing record, 1: e.g. PK observations, parent compound)
FLCA	-	Identifier for different matrices (catheters) (60: dialysate from concentric catheter, 66: dialysate from linear catheter, 0: ultrafiltrate (unbound plasma concentration))
FLAM	-	Identifier for analytical method used (0: no analytical method, e.g., for dosing events, 1: HPLC (LLOQ=0.15 µg/mL plasma))
COME	-	Flag for co-medication (0: no co-medication given, 1: co-medication given)
COM1-5	-	Comments (flags) (0, 1, or text)
<i>Continuous covariates</i>		
AGE	year	Age
HT	m	Height
WT	kg	Weight
BMI	kg/m <sup>2</sup>	Body mass index <sup>1</sup>

<sup>1</sup>WT [kg] divided by squared HT [m].



**Tab. 7-5:** Within-day and between-day precision (expressed as coefficient of variation, CV, %) and accuracy (as mean percentage deviation, RE, %) of determined voriconazole concentrations [ $\mu\text{g/mL}$ ] in microdialysate calibrators.

$C_{\text{nom}}$ [ $\mu\text{g/mL}$ ]	$\bar{x}$ [ $\mu\text{g/mL}$ ] $\pm$ SD [ $\mu\text{g/mL}$ ]	CV, %	RE, %
<i>Within-day variability (n=3)</i>			
0.156	0.161 $\pm$ 0.001	0.3	+3.5
0.520	0.465 $\pm$ 0.005	1.2	-10.6
1.040	0.980 $\pm$ 0.003	0.3	-5.8
2.080	2.185 $\pm$ 0.011	0.5	+5.1
6.240	6.488 $\pm$ 0.109	1.7	+4.0
10.400	10.799 $\pm$ 0.065	0.6	+3.8
<i>Between-day variability (n=5)</i>			
0.156	0.160 $\pm$ 0.002	1.0	+2.8
0.520	0.474 $\pm$ 0.013	2.8	-8.9
1.040	1.000 $\pm$ 0.028	2.8	-3.8
2.080	2.184 $\pm$ 0.020	0.9	+5.0
6.240	6.424 $\pm$ 0.116	1.8	+3.0
10.400	10.612 $\pm$ 0.277	2.6	+2.0

**Tab. 7-6:** Within-day and between-day precision (expressed as coefficient of variation, CV, %) and accuracy (as mean percentage deviation, RE, %) of determined voriconazole concentrations [ $\mu\text{g/mL}$ ] in plasma calibrators.

$C_{\text{nom}}$ [ $\mu\text{g/mL}$ ]	$\bar{x}$ [ $\mu\text{g/mL}$ ] $\pm$ SD [ $\mu\text{g/mL}$ ]	CV, %	RE, %
<i>Within-day variability (n=3)</i>			
0.153	0.153 $\pm$ 0.007	4.7	+0.01
0.510	0.506 $\pm$ 0.007	1.5	-0.7
1.020	1.039 $\pm$ 0.052	5.0	+1.9
2.040	2.048 $\pm$ 0.023	1.1	+0.4
5.100	5.102 $\pm$ 0.147	2.9	+0.0
10.200	10.099 $\pm$ 0.690	6.8	-1.0
<i>Between-day variability (n=5)</i>			
0.153	0.154 $\pm$ 0.005	3.4	+0.5
0.510	0.498 $\pm$ 0.013	2.6	-2.4
1.020	1.035 $\pm$ 0.035	3.4	+1.5
2.040	2.076 $\pm$ 0.087	4.2	+1.8
5.100	4.999 $\pm$ 0.299	6.0	-2.0
10.200	10.295 $\pm$ 0.612	5.9	+0.9

**Tab. 7-7:** Calculation of recovery (n=3) of the method for the quantification of voriconazole in skin biopsy (SB) samples.

No. of blank biopsy		1	2	3
Origin		flank	flank	flank
Mass 1	[mg]	2.2	3.6	3.7
<i>Spiking procedure</i>				
V <sub>spike-sol 1</sub>	[μL]	100.00	100.00	100.00
C <sub>spike-sol 1</sub>	[μg/mL]	5.00	5.00	5.00
m <sub>spike-sol 1</sub>	[μg]	0.50	0.50	0.50
Mass 2	[mg]	4.1	7.0	6.2
Mass 2 - Mass 1	[mg]	1.9	3.4	2.5
V <sub>spike-sol 2</sub>	[μL]	98.10	96.60	97.50
C <sub>spike-sol 2</sub>	[μg/mL]	4.64	4.56	4.58
m <sub>spike-sol 2</sub>	[μg]	0.46	0.44	0.45
<i>Extraction procedure</i>				
C <sub>meas extract</sub>	[μg/mL]	0.20	0.34	0.29
m <sub>meas extract 1</sub>	[μg]	0.02	0.03	0.03
m <sub>nom extract 1</sub>	[μg]	0.04	0.06	0.05
m <sub>meas extract 2</sub>	[μg]	8.92	9.12	7.64
m <sub>nom extract 2</sub>	[μg]	20.37	16.53	14.45
Recovery	%	43.78	55.20	52.90
Mean recovery ± SD (CV, %)		50.63 ± 6.039 (11.9)		

Mass 1: mass of the blank skin biopsy samples before spiking procedure, Mass 2: mass of the blank skin biopsy samples after spiking procedure, Mass 2 – Mass 1: difference which expressed the spike solution absorbed by the sample ( $mg \approx \mu L$ ,  $\rho \sim 1$ ), V<sub>spike-sol 1</sub>: volume of the spiking solution (spike-sol) before spiking procedure, C<sub>spike-sol 1</sub>: voriconazole concentration of the spiking solution (spike-sol) before spiking procedure, m<sub>spike-sol 1</sub>: voriconazole mass of the spiking solution (spike-sol) before spiking procedure, V<sub>spike-sol 2</sub>: volume of the spiking solution (spike-sol) after spiking procedure, C<sub>spike-sol 2</sub>: voriconazole concentration of the spiking solution (spike-sol) after spiking procedure, m<sub>spike-sol 2</sub>: voriconazole mass of the spiking solution (spike-sol) after spiking procedure, C<sub>meas extract</sub>: calculated voriconazole concentration in the extract, m<sub>meas extract 1</sub>: calculated voriconazole mass in the extract, m<sub>nom extract 1</sub>: nominal voriconazole mass in the extract, m<sub>meas extract 2</sub>: calculated voriconazole mass in the extract referring to the biopsy mass (mass 1), m<sub>nom extract 2</sub>: nominal voriconazole mass in the extract referring to the biopsy mass (mass 1).

**Tab. 7-8:** Relative recoveries of concentric catheters (RR<sub>c</sub>): mean, standard deviation, and coefficient of variation.

Individual	Visit	RR sample	RR <sub>c</sub> <sup>1</sup> , %	$\bar{x}$ , % RR1,RR2	SD, % RR1,RR2	CV, % RR1,RR2
101	1	1	90.8			
101	3	1	91.0			
101	5	1	82.1			
101	7	1	83.3	86.8	4.77	5.5
101	1	2	92.1			
101	3	2	83.8			
101	5	2	82.4			
101	7	2	80.2	84.6	5.18	6.1
102	1	1	90.7			
102	3	1	88.5			
102	5	1	82.9			
102	7	1	81.2	85.8	4.50	5.2
102	1	2	91.3			
102	3	2	-			
102	5	2	85.8			
102	7	2	86.4	87.8	2.99	3.4
103	1	1	81.1			
103	3	1	82.3			
103	5	1	91.2			
103	7	1	74.6	82.3	6.83	8.3
103	1	2	82.0			
103	3	2	83.4			
103	5	2	87.9			
103	7	2	78.4	82.9	3.91	4.7

<sup>1</sup>Mean C<sub>RP</sub> within visit 1 (CV, %): 15.5 µg/mL (3.2) (n=6). Mean C<sub>RP</sub> within visit 3, 5 and 7 (CV, %): 155.8 µg/mL (8.2) (n=17).

**Tab. 7-9:** Relative recoveries of linear catheters (RR): mean, standard deviation, and coefficient of variation.

Individ.	Visit	RR sample	RR <sub>1</sub> <sup>1</sup> , %				$\bar{x}$ , % RR1,RR2	SD, % RR1,RR2	CV, % RR1,RR2
				$\bar{x}$ , %	SD, %	CV, %			
101	1	1	60.1						
101	3	1	76.2						
101	5	1	57.0						
101	7	1	69.4	65.7	8.77	13.3			
101	1	2	64.3						
101	3	2	70.5						
101	5	2	60.5						
101	7	2	51.9	61.8	7.79	12.6			
102	1	1	80.3						
102	3	1	95.8						
102	5	1	98.8						
102	7	1	95.0	92.5	8.26	8.9			
102	1	2	71.1						
102	3	2	80.9						
102	5	2	96.4						
102	7	2	88.6	84.2	10.83	12.9			
103	1	1	73.3						
103	3	1	66.1						
103	5	1	-						
103	7	1	67.5	69.0	3.79	5.5			
103	1	2	70.8						
103	3	2	64.2						
103	5	2	65.1						
103	7	2	62.6	65.7	3.59	5.5			

<sup>1</sup>Mean C<sub>RP</sub> within visit 1 (CV, %): 15.1 µg/mL (4.4) (n=6). Mean C<sub>RP</sub> within visit 3, 5 and 7 (CV, %): 141.3 µg/mL (16.9) (n=18).

**Tab. 7-10:** Interindividual variability among the amount of voriconazole given within the 6 mg/kg WT iv (visit 1, 2), 4 mg/kg WT iv (visit 3, 4), and 200 mg oral (visit 5, 6, 7) administration period.

Visit	$\bar{x}$ [mg]	Min [mg]	Max [mg]	CV, %	R of deviation from amount planned, %
<i>6 mg/kg WT iv administration</i>					
1	492	480	498	1.9	-
2	480	413	498	9.7	-16.1 – 0
<i>4 mg/kg WT iv administration</i>					
3	328	320	332	1.9	-
4	328	320	332	1.9	-
<i>200 mg oral administration</i>					
5-7	200	200	200	0	-

**Tab. 7-11:** Interindividual variability among the duration of infusion.

Visit	Duration of infusion planned [h]	$\tilde{x}$ [h]	Min [h]	Max [h]	CV, %	R of deviation from duration time planned, %
<i>6 mg/kg WT iv administration</i>						
1	2.00	1.92	1.87	1.98	3.1	-6.7 – -0.8
2	2.00	1.90	1.68	2.02	8.9	-15.8 – +0.8
<i>4 mg/kg WT iv administration</i>						
3	1.25	1.17	1.12	1.25	5.8	-10.7 – 0
4	1.25	1.25	1.15	1.25	4.6	-8.0 – 0

**Tab. 7-12:** Intraindividual variability among the duration of infusion.

ID	Visit 1, 2 (6 mg/kg WT) CV, %	Visit 3, 4 (4 mg/kg WT) CV, %
101	1.2	0
102	1.3	1.0
103	9.2	8.0

**Tab. 7-13:** Analysis of additionally obtained plasma samples at  $C_{min}$ .

ID	Visit	Time [h]	Time <sub>planned</sub> [h]	Concentration [ $\mu\text{g/mL}$ ]	Mean [ $\mu\text{g/mL}$ ]	SD [ $\mu\text{g/mL}$ ]	CV, %
101	2	23.95	24.00	0.42	0.40	0.033	8.3
		23.98	24.00	0.38			
	3	35.93	36.00	0.40	0.39	0.006	1.5
		35.97	36.00	0.39			
	4	47.93	48.00	0.49	0.47	0.018	3.8
		47.97	48.00	0.46			
	5	59.93	60.00	0.35	0.35	0.003	0.8
		59.97	60.00	0.35			
6	71.93	72.00	0.28	0.28	0.003	1.1	
	71.97	72.00	0.28				
102	2	23.92	24.00	1.36	1.35	0.013	0.9
		23.95	24.00	1.35			
	3	35.95	36.00	1.87	1.89	0.027	1.4
		35.98	36.00	1.90			
	4	47.90	48.00	2.12	2.19	0.094	4.3
		47.93	48.00	2.25			
	5	59.93	60.00	2.31	2.28	0.042	1.8
		59.97	60.00	2.25			
6	71.93	72.00	2.42	2.47	0.071	2.9	
	71.97	72.00	2.52				
103	2	23.97	24.00	0.62	0.59	0.035	6.0
		24.00	24.00	0.57			
	3	35.97	36.00	0.82	0.81	0.015	1.9
		36.00	36.00	0.80			
	4	47.97	48.00	0.95	0.96	0.017	1.7
		48.00	48.00	0.98			
	5	59.97	60.00	0.85	0.88	0.047	5.3
		60.00	60.00	0.92			
6	71.95	72.00	0.83	0.83	0.007	0.8	
	71.98	72.00	0.82				

**Tab. 7-14:** Terminal slope  $\lambda_z$  [1/h] (data points involved in the analysis of  $\lambda_z$ ).

ID	Matrix	Visit 1	Visit 5	Visit 7
101	UF	0.1438 (7)	0.0994 (8)	0.1121 (7)
	ISF <sub>c</sub>	0.1054 (13)	0.0728 (7)	0.0649 (14)
	ISF <sub>l</sub>	0.1448 (8)	0.1528 (9)	0.0868 (9)
102	UF	0.0318 (7)	0.0126 (10)	0.0179 (7)
	ISF <sub>c</sub>	0.0755 (11)	0.0356 (6)	0.0273 (8)
	ISF <sub>l</sub>	0.0491 (11)	0.0125 (7)	0.0468 (6)
103	UF	0.0913 (7)	0.0347 (10)	0.0489 (10)
	ISF <sub>c</sub>	0.0689 (8)	0.0332 (7)	0.0384 (9)
	ISF <sub>l</sub>	0.1037 (8)	0.0529 (11)	0.0693 (13)

**Tab. 7-15:** Maximum concentration  $C_{max}$  [ $\mu\text{g/mL}$ ] and related time  $t_{max}$  (time after dose) [h].

ID	Matrix	Visit 1	Visit 5	Visit 7	Visit 1	Visit 5	Visit 7
		$C_{max}$			$t_{max}$		
101	UF	1.21	1.08	0.71	2.25	50.25 (2.25)	74.50 (2.50)
	ISF <sub>c</sub>	0.61	1.02	1.32	1.75	51.75 (3.75)	72.25 (0.25)
	ISF <sub>l</sub>	1.10	1.34	0.88	2.25	50.25 (2.25)	72.25 (0.25)
102	UF	1.88	3.22	3.26	1.75	49.00 (1.00)	74.00 (2.00)
	ISF <sub>c</sub>	0.94	2.80	3.13	2.75	48.75 (0.75)	75.25 (3.25)
	ISF <sub>l</sub>	1.54	2.00	4.07	2.25	52.50 (4.50)	72.25 (0.25)
103	UF	1.76	1.65	1.70	1.75	49.75 (1.75)	73.00 (1.00)
	ISF <sub>c</sub>	0.86	1.67	2.25	3.75	48.75 (0.75)	73.25 (1.25)
	ISF <sub>l</sub>	1.34	1.96	2.26	2.25	49.25 (1.25)	72.75 (0.75)

**Tab. 7-16:** Dose-normalised  $C_{max}$  [ng/mL].

ID	Matrix	Visit 1	Visit 5	Visit 7
----- Dose-normalised $C_{max}$ -----				
101	UF	2.44	5.38	3.55
	ISF <sub>c</sub>	1.22	5.12	6.62
	ISF <sub>l</sub>	2.22	6.69	4.42
102	UF	3.91	16.11	16.28
	ISF <sub>c</sub>	1.96	13.99	15.65
	ISF <sub>l</sub>	3.22	10.01	20.36
103	UF	3.57	8.24	8.49
	ISF <sub>c</sub>	1.75	8.36	11.25
	ISF <sub>l</sub>	2.72	9.79	11.28

**Tab. 7-17:** Determined partial AUC [ $\mu\text{g}\cdot\text{h/mL}$ ] and dose-normalised partial AUC [ng·h/mL]. Visit 1: AUC<sub>0-12h</sub>, visit 5: AUC<sub>48-60h</sub>, visit 7: AUC<sub>72-84h</sub>.

ID	Matrix	Visit 1	Visit 5	Visit 7	Visit 1	Visit 5	Visit 7
		----- Determined partial AUC -----			----- Dose-normalised partial AUC -----		
101	UF	4.93	6.44	4.53	9.91	32.20	22.63
	ISF <sub>c</sub>	4.28	10.10	10.56	8.59	50.49	52.81
	ISF <sub>l</sub>	6.30	8.67	6.91	12.65	43.37	34.53
102	UF	10.90	29.55	31.93	22.72	147.77	159.65
	ISF <sub>c</sub>	7.33	27.39	34.35	15.28	136.95	171.74
	ISF <sub>l</sub>	11.50	21.91	26.40	23.96	109.56	131.98
103	UF	7.09	14.30	13.27	14.40	71.51	66.33
	ISF <sub>c</sub>	6.15	14.69	18.89	12.51	73.43	94.46
	ISF <sub>l</sub>	7.81	17.29	17.07	15.88	86.44	85.37

## 7.2 Figures

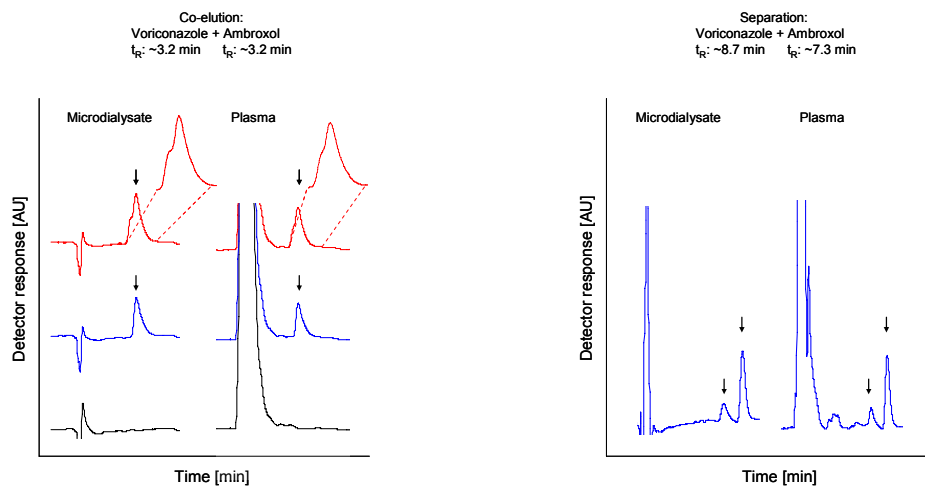


**Fig. 7-1:** Left panel: Chromatograms of microdialysate (left) and plasma (right): blank microdialysate and plasma (black lines), microdialysate (2.08  $\mu\text{g/mL}$ ) and plasma (2.04  $\mu\text{g/mL}$ ) calibrator (blue lines, retention time ( $t_R$ ) of voriconazole: 3.2 min), microdialysate and plasma calibrator with interfering co-eluting peak of ambroxol (red lines). Right panel: Peak separation of voriconazole and ambroxol: Chromatograms of microdialysate (left) and plasma (right) calibrator ( $t_R$  of voriconazole: 8.7 min) and ambroxol ( $t_R$ : 7.3 min). AU: arbitrary units.

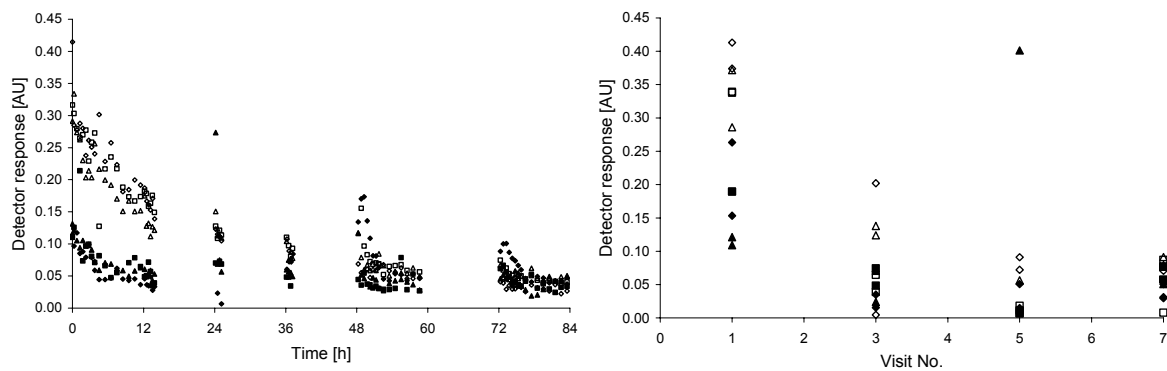


**Fig. 7-2:** Signal-time profile of the unknown endogenous substance or substance mixture in microdialysate (left panel) and retrodialysate (right panel) samples (CMA60<sup>®</sup>, open symbols; CMA66<sup>®</sup>, filled symbols) originating from healthy volunteers (ID 101, squares; ID 102, diamonds; ID 103, triangles) (see 2.6 and 3.4). AU: arbitrary units.



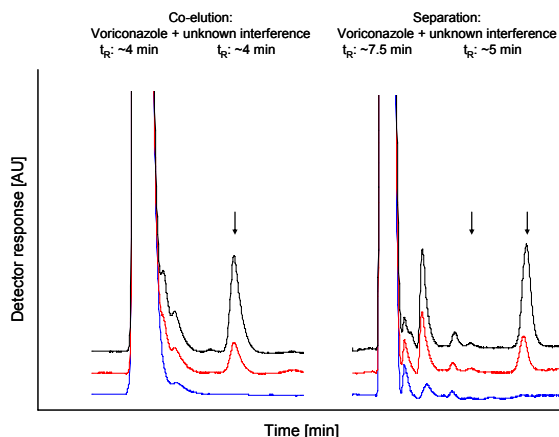


**Fig. 7-3:** Peak separation of voriconazole and an unknown endogenous substance or substance mixture in ultrafiltrate samples originating from a healthy volunteer (ID 102) (see 2.6 and 3.4): Chromatograms showing the interference (left) and the separation (right) in the baseline sample (blue line), visit 1 (red line), and in visit 7 (black line). AU: arbitrary units.

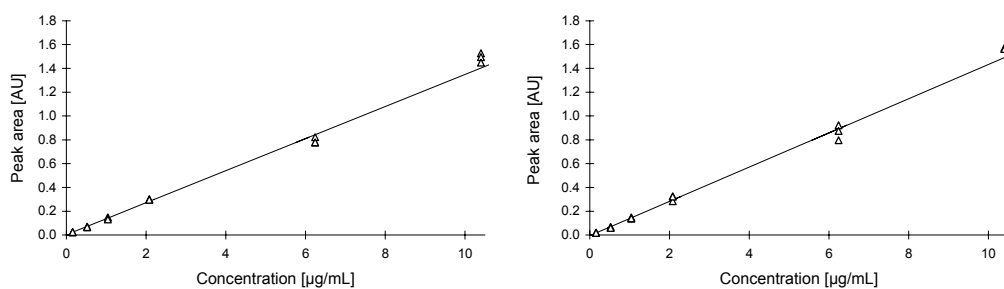


**Fig. 7-4:** Calibration curve of voriconazole microdialysate calibrators (each  $n=6$ ) from ruggedness experiments using different pH values of the mobile phase. Left panel: pH 5.4 (coefficient of determination: 0.997), right panel: pH 7.1 (coefficient of determination: 0.997). AU: arbitrary units.

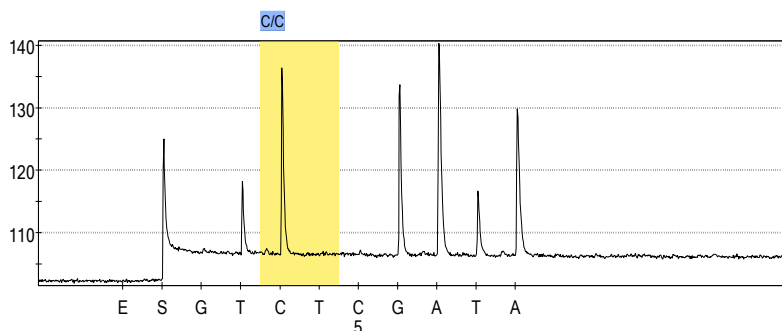


**Fig. 7-5:** Representative pyrogram<sup>®</sup>: Wild type for CYP2C19 (ID 101). X axis: chronologically dispensed nucleotides. Y axis: corresponding light signal. Highlighted area (yellow): polymorphic nucleotides.

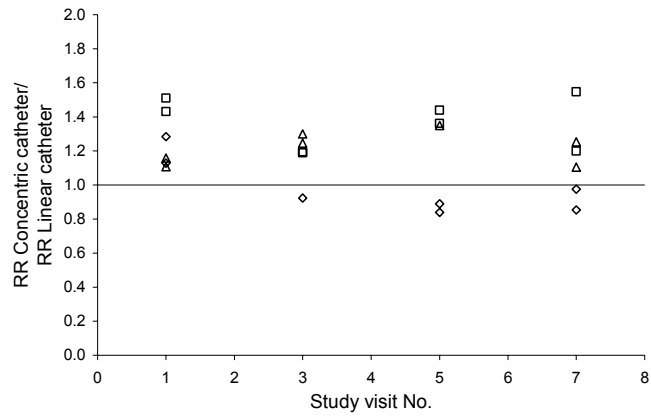


**Fig. 7-6:** Ratio of relative recoveries ( $RR_c$  and  $RR_l$ ). Squares: ID 101, Diamonds: ID 102, Triangles: ID 103); Line: ratio=1.

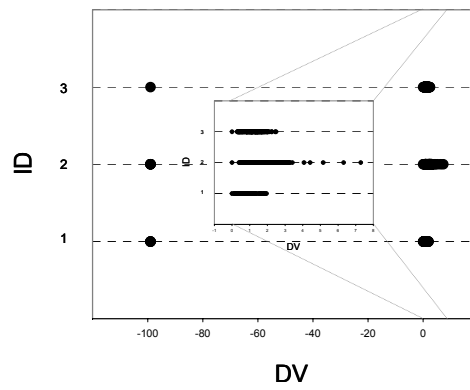


**Fig. 7-7:** Index plot of dependent variable DV (concentration).

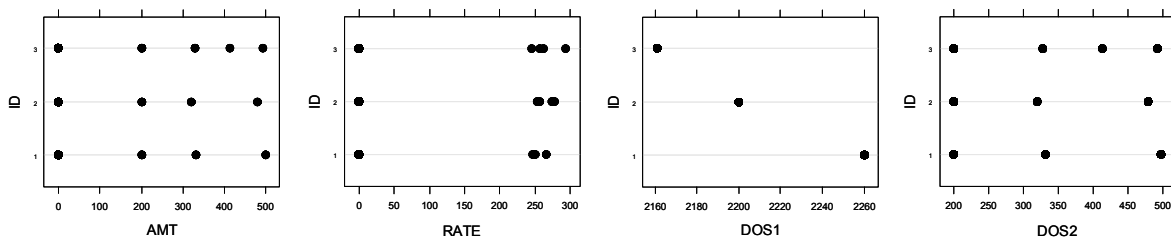


**Fig. 7-8:** Index plots for dosing related data items: amount (AMT), infusion rate (RATE), total dose within one individual (DOS1), and dose for each visit/occasion (DOS2).

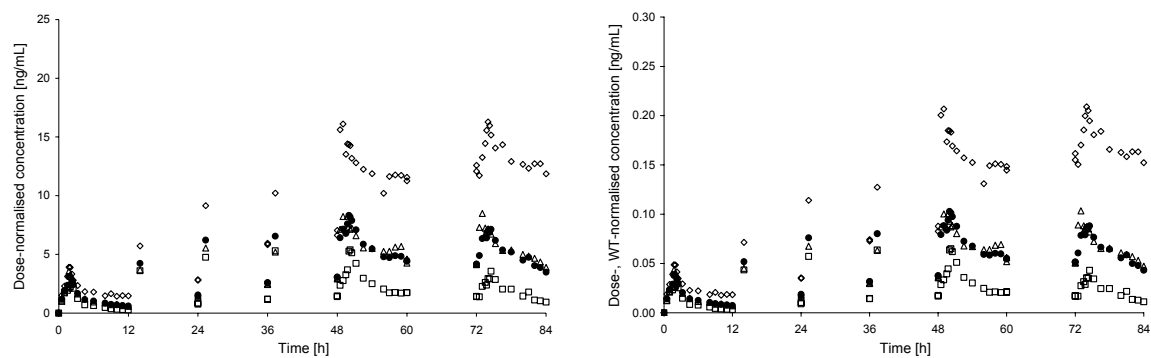


**Fig. 7-9:** Dose-normalised (left panel) and dose-, WT-normalised (right panel) concentration-time profile in UF in ID 101 (squares), ID 102 (diamonds), and ID 103 (triangles), geometric mean concentrations (filled circles).

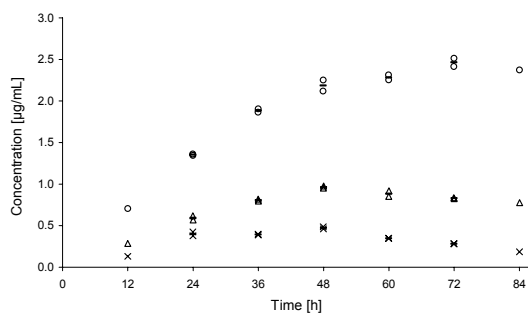


**Fig. 7-10:** Minimal UF concentration-time profile showing tandem samples for visits 2-6 in ID 101 (crosses), in ID 102 (circles), and in ID 103 (triangles). Lines show the median of tandem samples per ID.

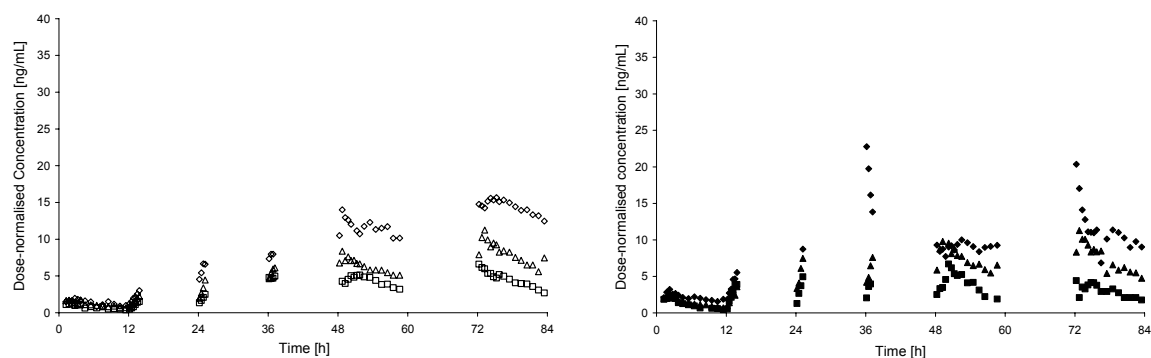
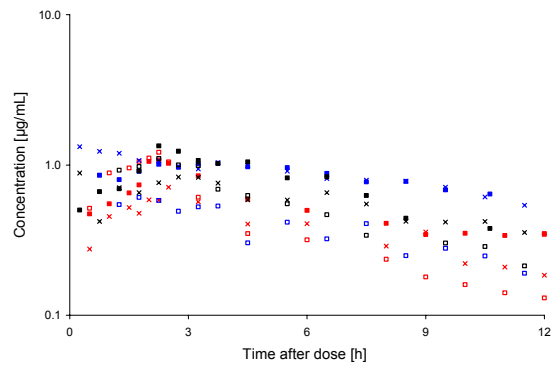
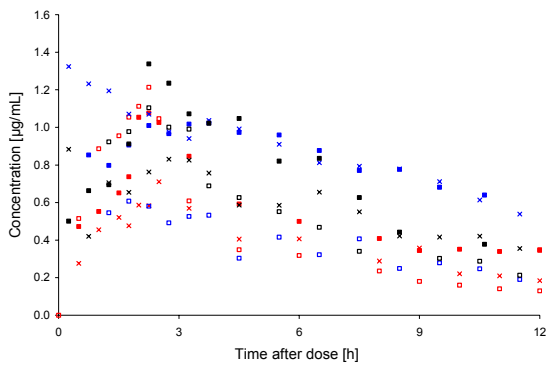
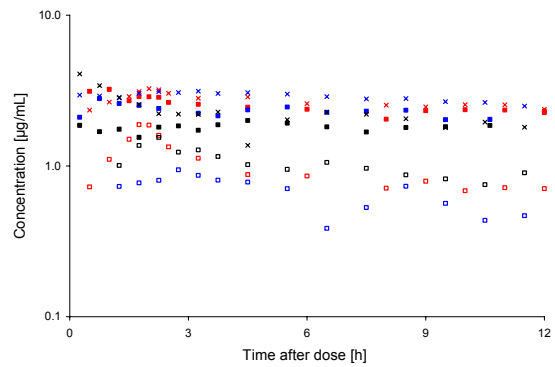
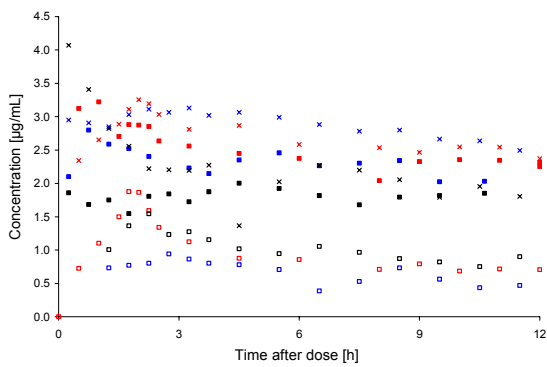


**Fig. 7-11:** Dose-normalised concentration-time profiles voriconazole in ISF of ID 101 (squares), ID 102 (diamonds), and ID 103 (triangles). Left panel:  $C_{\text{ISF},c}$  (open symbols). Right panel:  $C_{\text{ISF},f}$  (filled symbols).

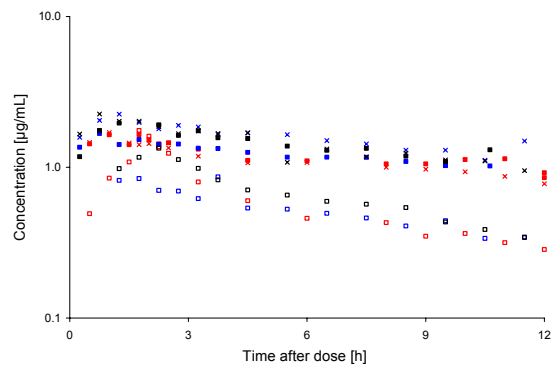
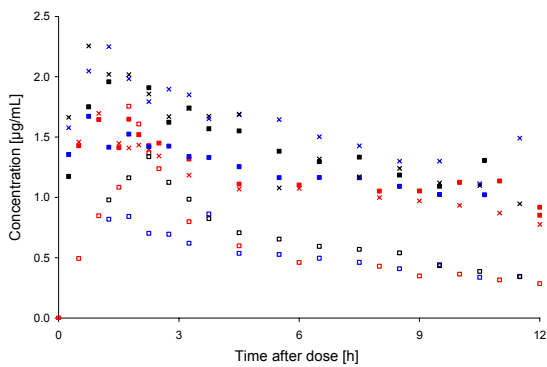
## ID 101



## ID 102

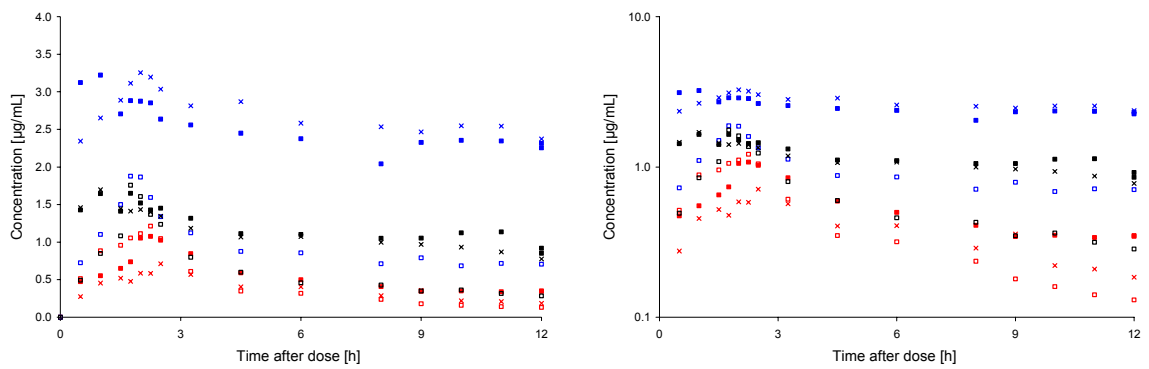
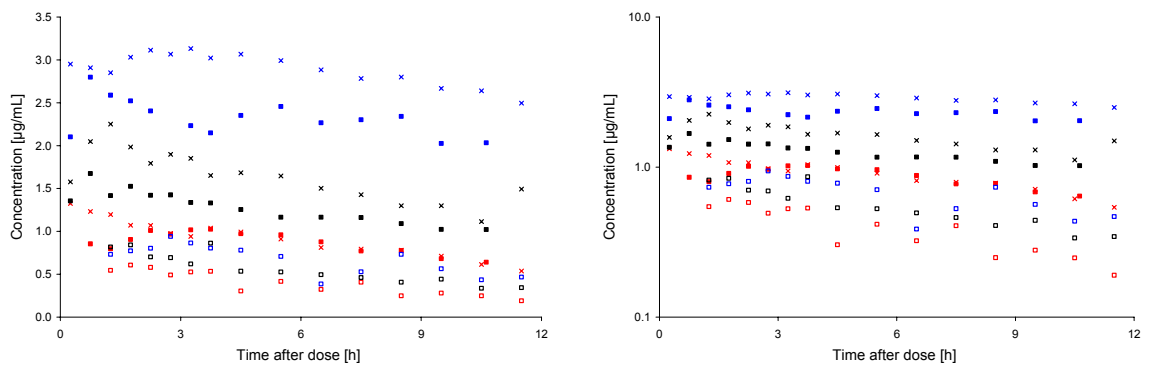
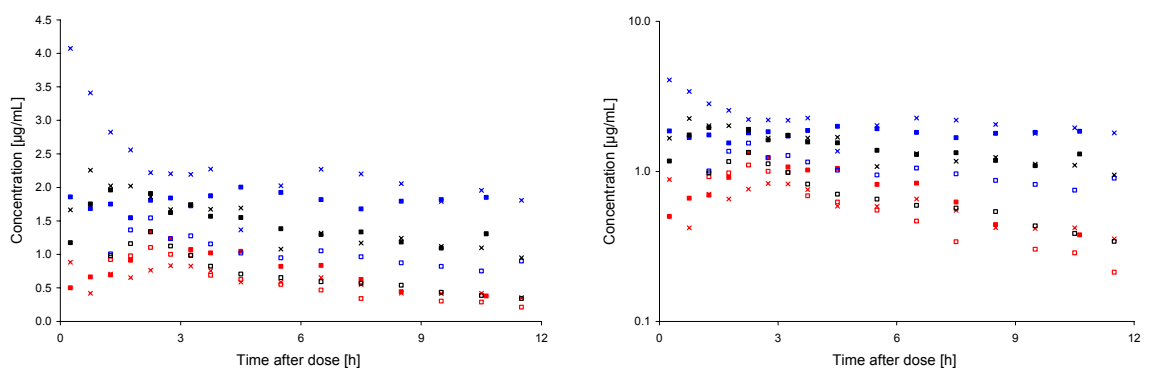


## ID 103



**Fig. 7-12:** Concentration-time plots of voriconazole (left panels; semi-logarithmic (right panels)) after single and multiple intravenous and oral voriconazole administration for all matrices: UF (red colour), ISF<sub>c</sub> (blue colour), and ISF<sub>i</sub> (black colour). Visit 1 (open squares), visit 5 (filled squares), and visit 7 (crosses).

## Ultrafiltrate

ISF<sub>c</sub>ISF<sub>i</sub>

**Fig. 7-13:** Concentration-time plots of voriconazole (left panels; semi-logarithmic (right panels)) after single and multiple intravenous and oral voriconazole administration for all individuals: ID 101 (red colour), ID 102 (blue colour), and ID 103 (black colour). Visit 1 (open squares), visit 5 (filled squares), and visit 7 (crosses).

# PUBLICATIONS

## Publications related to this thesis

### Original papers

D.M. Saunte, F. Simmel, N. Frimodt-Moller, L.B. Stolle, E.L. Svejgaard, M. Haedersdal, C. Kloft, M.C. Arendrup.  
In-vivo efficacy and pharmacokinetics of voriconazole in an animal model of dermatophytosis.  
*Antimicrob. Agents Chemother.*, 51: 3317-3321 (2007).

F. Simmel, J. Soukup, A. Zoerner, J. Radke, C. Kloft.  
Development and validation of an efficient HPLC method for quantification of voriconazole in plasma and microdialysate reflecting an important target site.  
*Anal Bioanal Chem.*, 392: 479-488 (2008).

F. Simmel, I. Zündorf, C. Kloft.  
Grundlagen rationaler Pharmakotherapie bei Intensivpatienten – Blickpunkt Antimykotika.  
*Intens Notfallbeh.*, 34: 60-69 (2009).

F. Simmel, C. Kloft.  
Microdialysis Feasibility Investigations with the Non-hydrophilic Antifungal Voriconazole for Potential Applications in Nonclinical and Clinical Settings.  
*Int J Clin Pharmacol Ther*, in revision (2010).

### Patents

F. Simmel, D. Reese, C. Kloft.  
*In-vitro*-Mikrodialyse-System, patent application, date of registration: 18.09.2008, application number: 10 2008 047 962.4 (submitted).

### Presentations

F. Simmel, C. Kloft.  
Impact of solubilizing excipients on the feasibility of *in vitro* and *in vivo* microdialysis investigations.  
4th International Conference on Clinical Microdialysis (ICCM) 2007, Cambridge, UK, 19.-21.09.2007. Proceedings, 125 (2007).

F. Simmel.  
Demonstration of the feasibility of the microdialysis approach for voriconazole and its drug product in (non)clinical settings.  
Berliner Mikrodialyse-Symposium 2008 (18.09.), Berlin (2008).

F. Simmel, C. Kloft.  
Microdialysis with moderately lipophilic drugs: what is essential to know for voriconazole and its drug product to be applicable in pre-/clinical microdialysis settings?  
Ehrlich II – 2<sup>nd</sup> World Conference on Magic Bullets, Nuremberg, 03.-05.10.2008. Proceedings online [[www.ehrlich-2008.org/scientificprogram.htm](http://www.ehrlich-2008.org/scientificprogram.htm)], A-297 (2008).

## Conference Abstracts

F. Simmel, D.M. Saunte, L.B. Stolle, M.C. Arendrup, C. Kloft.

Feasibility to determine *in vivo* voriconazole exposure in healthy versus inflamed skin by microdialysis.

Jahrestagung der Deutschen Pharmazeutischen Gesellschaft (DPhG) 2007, Erlangen, 10.-13.10.2007. Proceedings, 138 (2007).

J. Soukup, F. Simmel, U. Götze, S. Schneider, C. Kloft.

„Therapeutic Drug Monitoring“ während Voriconazol-Sequenztherapie - Eine prospektive Studie bei intensivmedizinischen Patienten.

9. Deutscher Interdisziplinärer Kongress für Intensivmedizin und Notfallrettung (DIVI) 2008, Hamburg, 03.-06.12.2008. Proceedings, P/10/02 (2008).

F. Simmel, M. Zeitlinger, Z. Erdogan, E. Lackner, C. Kloft.

Feasibility of Long-term Microdialysis with Moderately Lipophilic Voriconazole in Humans.

49th Interscience Conference on Antimicrobial Agents and Chemotherapy (ICAAC), San Francisco, USA, 12.-15.09.2009. Proceedings, A1-589 (2009).

## Further publications

S. R. Quist, F. Simmel, I. Wiswedel, R. Neubert, H. Gollnick.

Influence of green and black tea, Epigallocatechin-3-gallate and Theaflavin on prostanoid synthesis *in vitro* and *in vivo* using microdialysis.

Jahrestagung der Arbeitsgemeinschaft Dermatologische Forschung (ADF) 2006, Aachen, 23.-25.03.2006. Proceedings, P120 (2006).

F. Simmel.

Einfluss von grünem und schwarzem Tee, sowie der isolierten Reinstoffe –

Epigallocatechingallat und Theaflavin – auf oxidierte Arachidonsäurederivate *in vitro* und in der Haut. Diploma Thesis.

Faculty of Medicine, Otto-von-Guericke-Universität, Magdeburg, Germany and Institute of Pharmacy, Martin-Luther-Universität Halle-Wittenberg, Halle, Germany (2006).

## ACKNOWLEDGEMENTS

This thesis resulted from my work as Ph.D. student at the Department of Clinical Pharmacy, headed by Prof. Dr. rer. nat. habil. Charlotte Kloft, Institute of Pharmacy, Martin-Luther-Universität Halle-Wittenberg (MLU). Prof. Charlotte Kloft guided my research activity in the field of clinical pharmacy since 2006 and constantly supported my work as my supervisor during the entire time. I owe her special thanks for providing such an exciting interdisciplinary topic, many helpful suggestions, enthusiastic and motivating discussions, some unforgettable extraordinary situations, and the opportunity of getting in contact with the microdialysis research community. Besides, it was a special pleasure and challenge for me to actively participate in the development of the research group Clinical Pharmacy in Halle and to follow the way from its birth up to now.

My work would not have been successful without the support of several persons.

In particular, I am grateful to Assoc. Prof. Dr. Markus Zeitlinger, Edith Lackner, and Zeynep Erdogan from the Department of Clinical Pharmacology of the Medical University of Vienna for the rewarding cooperation, enabling me to apply laboratory results into clinical practice, and uncomplicated, enjoyable collaboration, and for the opportunity to attend such a professional (team-)working and the possibility to actively participate in. In this regard, my greatest debt of appreciation goes to the study participants.

I am grateful to Dr. Ditte Marie Saunte, Unit of Mycology and Parasitology, Statens Serum Institut, Denmark for the intensive cooperation during the preclinical study. Thanks are due to Dr. Ilona Schön, University Clinic and Polyclinic for Otorhinolaryngology, Head and Neck Surgery, Medical Faculty and Jenny Bienias, Department of Chemical Engineering, Institute of Chemistry, MLU for support regarding method development for preclinical study samples.

I wish to thank Dr. Christian Rimbach and Ingrid Geisslinger, Institute of Pharmacology, Medical Faculty, Ernst Moritz Arndt Universität Greifswald for the pleasant and quick integration and many explanations during the measurements in Greifswald.

My thanks also go to Dr. Jens Soukup, Ulrike Götze, and Annett Christel, University Clinic for Anaesthesiology and Surgical Intensive Medicine, Medical Faculty, MLU for the whole collaboration and the reliance on blood collections at short notice.

The collaboration with Dieter Reese and co-workers, fine mechanical laboratory, Institute of Pharmacy, MLU is deeply appreciated. I am indebted for the exciting time in the technical lab making me hardly able to wait until the next step of the *in vitro* microdialysis system. Pfizer is gratefully acknowledged for providing voriconazole substance. Thomas Zimmermann is acknowledged for his reliable support in PC matters.

I want to thank my colleagues and all other members of the Department of Pharmaceutical Chemistry and Clinical Pharmacy, Institute of Pharmacy, MLU for an interesting time and support of any kind contributing to this work and enjoyable times during teachings, whereas special thanks go to Angela Munk.

Heartfelt thanks go to Julia Michael for the enjoyable and, at the same time, efficient collaboration during the entire time.



Especially, I would like to express my heartfelt gratitude to Dorothea Frenzel for providing many useful hints and support regarding the work in the lab and her general support in many respects during this intensive time.

Heartly gratitude is devoted to Dr. Sandra Heuschkel being a constant reliable part of my scientific work after my university degree, for many true words in many respects, and final support of this work.

Finally, I want to thank my family, Susann and, especially, Simon for their invaluable support – in their own inimitable way – during the hard and difficult times and, more importantly, sharing my happiness during the great moments of this work.



# CURRICULUM VITAE

Name Franziska Simmel (Dipl. Pharm.)  
Date and place of birth 16 September 1981, Magdeburg  
Marital status unmarried  
Nationality German

## POSTGRADUATE EDUCATION

Since 03/2006 – 02/2010 Ph.D. student at the Department of Clinical Pharmacy, Institute of Pharmacy, Martin-Luther-Universität Halle-Wittenberg (MLU)  
05/2005 – 10/2005 Diploma thesis, Faculty of Medicine, Otto-von-Guericke-Universität Magdeburg and Institute of Pharmacy, MLU  
Title: „Einfluss von grünem und schwarzem Tee, sowie der isolierten Reinstoffe – Epigallocatechingallat und Theaflavin – auf oxidierte Arachidonsäurederivate *in vitro* und in der Haut“

## UNDERGRADUATE STUDIES AND PROFESSIONAL EXPERIENCE

12/2005 Registered Pharmacist  
11/2004 – 04/2005 Pre-registration pharmacist, Rheinapotheke, Cologne  
09/2004 Degree in Pharmacy (2. Staatsexamen)  
10/2000 – 09/2004 Undergraduate studies of Pharmacy at the MLU

## EDUCATION

09/1992 – 08/2000 Grammar school Albert-Einstein-Gymnasium, Magdeburg

## ACADEMIC ACTIVITIES

08/2003 - 09/2003 Industrial internship at RICOH Research & Development Center, Yokohama, Japan  
03/2003 Academic internship at the Institute of Pharmacology and Toxicology at the MLU  
02/2003 Academic internship at the Institute of Medicinal Chemistry at the MLU

## MEMBERSHIPS

Since 10/2007 Member of the chamber assembly (elected) of the Council of Pharmacists Saxony-Anhalt and member of the training committee  
Since 2005 German Pharmaceutical Society (DPHG)

Halle (Saale),





## ERKLÄRUNG

Hiermit erkläre ich, dass ich mich mit der vorliegenden Dissertation erstmals um die Erlangung eines Doktorgrades bewerbe. Ferner erkläre ich, dass ich die vorliegende Arbeit selbständig und ohne fremde Hilfe angefertigt, andere als die von mir angegebenen Quellen und Hilfsmittel nicht benutzt und die den verwendeten Werken wörtlich oder inhaltlich entnommenen Stellen als solche kenntlich gemacht habe.

## DECLARATION

Hereby I declare that this work was not handed in to any other doctorate committee. Furthermore I declare that I have prepared this thesis by myself and without the use of resources other than the ones indicated in this thesis. Quotations, verbatim or with regard to content, from other sources are marked as such.

Halle (Saale) in June 2010



Franziska Simmel